Impairment in Mitochondrial Oxidative Phosphorylation Alters Clock Gene Expression

by

Beverly Joan Baxter

A thesis submitted in partial fulfillment

of the requirements for the degree of

Doctor of Philosophy (PhD) in Biomolecular Sciences

The Faculty of Graduate Studies

Laurentian University

Sudbury, Ontario, Canada

THESIS DEFENCE COMMITTEE/COMITÉ DE SOUTENANCE DE THÈSE
Laurentian Université/Université Laurentienne
Faculty of Graduate Studies/Faculté des études supérieures

Title of Thesis
Titre de la thèse: Impairment in Mitochondrial Oxidative Phosphorylation Alters Clock Gene Expression

Name of Candidate
Nom du candidat: Baxter, Beverly

Degree
Diplôme: Doctor of Philosophy

Department/Program
Département/Programme: Biomolecular Sciences

Date of Defence
Date de la soutenance: October 21, 2020

APPROVED/APPROUVÉ

Thesis Examiners/Examinateurs de thèse:

Dr. Robert Lafrenie
(Supervisor/Directeur(trice) de thèse)

Dr. Carita Lanner
(Committee member/Membre du comité)

Dr. Frank Mallory
(Committee member/Membre du comité)

Dr. Tami Marconi
(External Examiner/Examinateur externe)

Approved for the Faculty of Graduate Studies
Approuvé pour la Faculté des études supérieures
Dr. Lace Marie Brogden
Madame Lace Marie Brogden
Acring Dean, Faculty of Graduate Studies
Doyenne Intérimaire, Faculté des études supérieures

ACCESSIBILITY CLAUSE AND PERMISSION TO USE

Abstract

Epidemiological studies provide evidence that workers who perform chronic night shift work are at significantly higher risk of a number of severe disease states including cancer. The perturbed activity/rest and feeding/fasting cycles, which occurs in persons performing shift work or who are subjected to jet lag, disrupt our normal 24- hour internal clock or circadian rhythm. The molecular mechanisms that link chronic circadian disruption to disease are not well understood. Since light exposure at night is known to decrease melatonin levels, some researchers have hypothesized that a reduction in the nocturnal levels of this pineal hormone predisposes individuals to disease. Animals that displayed atypical behaviours in their daily cycles, led to the identification of eight-key clock or circadian genes that are differentially expressed during the day and which determine normal internal timing. The expression of these genes was abnormal in a large number of human tumors including breast cancer. In this study, a temperature shift model was characterized and used as a means to synchronize the expression of these clock genes in a human breast cancer cell line. The model was compared to another cell synchronization protocol which utilizes serum shock and which showed differences in gene expression and cell cycle regulation between the two protocols. The temperature shift model was then used to study the impact of melatonin on clock gene expression and on the production of reactive oxygen species (ROS) in cells exposed to chemotherapeutic drugs. Melatonin influenced the cell cycle but did not cause significant differences in clock gene expression. Chemotherapeutic drugs differed in their effects on the production of intracellular ROS. A mitochondrial deficient (*Rhø)* cell line which exhibited impaired oxidative phosphorylation, was developed from MCF-7 cells.

The profile of clock gene expression in *Rhø* cells that were also subjected to the temperature shift protocol was different than that of the parental MCF-7 line. This suggests that impairment of mitochondrial function disrupts clock gene expression and may be a link to the oncogenic transformation of cells.

Keywords

Circadian disruption, Clock gene expression, Circadian cycle, Melatonin, Reactive Oxygen Species, Breast Cancer, Mitochondria, Oxidative Phosphorylation, *Rhø* cell

Acknowledgements

I want to thank my wonderful, patient, and kind supervisor, Dr. Robert Lafrenie. All graduate students should be so fortunate as to have a mentor such as Rob who is always accessible, and thoughtful and whose incredible wealth of knowledge makes it possible for him to ask the best questions which stimulate learning and thinking.

I want to thank the current members of my Supervisory Committee, Drs. Carita Lanner and Frank Mallory for their support, encouragement and time. I feel incredibly fortunate to have had superb guidance from two engaged researchers and teachers. I also want to acknowledge the *late* Dr. Michael Persinger, an original Committee member, and essentially the person who single handedly convinced me to pursue a doctoral program at Laurentian University.

I want to thank Dr. Carly Buckner, Dr. Lafrenie's Research Associate and our lab task master, for her time, assistance with experiments, support, training and trouble shooting. Carly helped to make me a better scientist.

I want to thank my friends and colleagues within the lab group, Danah Almnayan and Albatul Alharbi for their interest and support and Danah's gift of time in assisting me in pictures and figures. I am also indebted to Justin Boudreau for his technical support and endless interesting conversations and Dr James Knockleby for his technical assistance with temperamental equipment.

Finally, I wish to thank my three amazing sons, Jay, Owen and Scott, for their encouragement, patience and interest as I pursued my dream of graduate school and research.

Table of Contents

List of Tables

List of Figures

List of Appendices

Chapter 1

Chapter 1 Introduction

1.1 Biological rhythms

Nature is exhibits biological rhythms. There are annual cycles such as the orbiting of the earth around the sun; seasonal as evidenced by plant growth and the breeding cycles of animals; monthly lunar cycles; and, daily cycles, described as circadian from the latin; circa – around, diem – day that are organized by the earth's rotation on its own axis (Savvidis and Koutsilieris 2012). The primary driver of the circadian cycle is the light /dark cycle of the environment which imposes various cycles upon the organism including, behavioural manifestations such as activity/rest, feeding/fasting, and a large number of physiological processes that include blood pressure, hormonal regulation, core temperature control, and immune cell diurnal variations (Eclosion 2008). Evolution has prepared for a circadian response to anticipated environmental cues through complex regulatory systems and through on-demand mechanisms related to metabolism and movement (Takahashi 2017) (Panda, Hogenesch, and Kay 2002). Almost all organisms that have access to and can sense and process visible light are entrained or synchronized to circadian rhythms with light serving as the primary *zeitgeber*; a German language-derived word that translates as – time giver or external environmental cue (Oliva-Ramírez *et al.* 2014). The central organizing principle in the mammalian model refers to the processing of light cues by specialized retinal cells that project to a portion of the brain, called the suprachiasmatic nucleus (SCN), a paired structure in the ventral hypothalamus, which is responsible for coordinating daily body rhythms (Takahashi 2017).

There are three defining features of a circadian rhythm. First it must be maintained by the organism despite fluctuations in external temperature; a feature called temperature compensation; secondly, they are free-running, meaning that when the organisms are moved from the typical light/dark cycle to constant darkness, their behavioral and physiological cycles persist; and, finally the cycle must be entrainable or able to be synchronized (Wever 1986) . Zebrafish and *Drosophila sp.,* both translucent organisms, were used in early experiments to establish these fundamental principles (Ben-Moshe, Foulkes, and Gothilf 2014). The mechanistic model by which organisms manage to organize themselves around a fairly precise 24 hour period was established in *Drosophila sp.* (Panda, Hogenesch, and Kay 2002), for which the researchers, Jeffrey Hall, Michael Rosbach and Michael Young received the Nobel prize for Physiology or Medicine in 2017 (Van Laake, Luscher and Young 2018).

1.2 Circadian organization and clock gene expression

There has been a rapid translation of the molecular framework which governs the 24 hour internal clock from the fruit fly to mammals, illustrating the important underlying principles of how well these mechanisms are evolutionarily preserved (Takahashi 2017). The regulatory basis of the circadian rhythm consists of a transcriptional – translational feedback loop (**TTFL**) involving a positive arm controlled by two transcription factors (reviewed in Papagiannakopoulos *et al.* 2016), Circadian Locomotor Output Cycles Kaput (CLOCK (King *et al.* 1997, or Neuronal Protein domain shared by PER, ARNT and SIM (NPAS)(Shearman *et al.* 1997) in brain tissue) and Brain and Muscle Aryl Hydrocarbon Receptor Nuclear Translocator-like (Arntl, also known as BMAL1(Bunger *et al.* 2000). CLOCK and BMAL1 heterodimerize and bind to specific elements in the promoter regions of their target genes, identified as E boxes (Panda, Hogenesch, and Kay 2002). In mammals, the primary targets of the circadian regulatory

transcription factors, CLOCK:BMAL, are the period (PER) and cryptochrome (CRY) genes. Increased levels of the protein products of PER and CRY accumulate in the cytoplasm, form heterodimers, and then translocate to the nucleus where they can repress their own transcription representing the negative arm of the TTFL (Papagiannakopoulos *et al.* 2016). The core circadian clock genes are identified as CLOCK, BMAL, PER1, PER2, PER3, CRY1, and CRY2 in mammals (Takahashi 2017). There is a secondary loop that also appears to be essential in maintaining a 24 hour clock that involves two orphan nuclear receptors, REV-ERBα and a retinoid orphan receptor (ROR) α, β, γ which binds to the ROR gene promoter elements (RORE) (Zhao *et al.* 2014). BMAL contains RORE elements and REV-ERBα inhibits BMAL transcription (Preitner *et al.* 2002) while RORα binding activates BMAL expression (Zhao *et al.* 2014).

The observation of arrhythmic behaviour in *Drosophila sp.* was the key that unlocked the discovery of mutations in the PER genes that were responsible for the loss of circadian activity (Panda, Hogenesch, and Kay 2002). Adult *Drosophila sp.* display consistent behaviours from their early morning exit from the pupal cocoon (eclosion) to the diurnal rhythm of daytime activity and night time rest such that mutations in the PER gene resulted in completely aberrant eclosion and locomotor activity or an altered day period length (Hyuk *et al.* 2007). A similar observation was made in the Syrian hamster which exhibited a shortened circadian cycle and that led to the discovery of the *tau* mutation, a gain of function mutation in casein kinase 1δ, which phosphorylates the PER proteins and promotes their early degradation (Loudon *et al.* 2007). The other post translational modification that is important in the temporal regulation of the PER and CRY proteins is their degradation by ubiquitination due to tagging by E3 ligases (Takahashi 2017). In people, mutations in the PER2 genes are associated with familial advanced sleep

phase syndrome (FAPS) (Panda, Hogenesch, and Kay 2002) and variants in the clock genes are important determinants of chronotype, or what makes a person a "lark" versus a "night owl" (Jones *et al.* 2019).

SCN cells continue to generate circadian oscillations in cell culture for sustained periods of time (Panda, Hogenesch, and Kay 2002). Non-neuronal cells isolated from peripheral tissues are also able to maintain circadian cycles independently of the SCN (Balsalobre, Damiola, and Schibler 1998). The molecular TTFL loops that regulate the 24 hour rhythm centrally in the SCN are replicated in peripheral cells (Takahashi 2017). It is thought that the central hierarchy of the circadian rhythm controlled by the SCN pacemaker is able to regulate systemic functions such as activity and feeding by coordinating hormone and sympathetic nervous system outputs (Potter *et al.* 2016). However, peripheral circadian oscillators are not always subservient to central regulation and can be reset in tissue-specific ways: for example, food intake presents a powerful synchronizer (Mendoza 2007). Glucocorticoid hormones, both endogenous and exogenous, are also powerful peripheral synchronizers but do not appear to influence the SCN due to a lack of local glucocorticoid receptors in the SCN (Cuesta, Cermakian, and Boivin 2015). Transcriptome analysis reveals that up to 40% of peripheral cells oscillate in a circadian manner but that the distribution of gene expression is very tissue-specific such that the genes that oscillate tandemly in the liver are different from those that oscillate in cardiac tissue (Zhang *et al.* 2014). Some of the clock-controlled genes contain E boxes and therefore are direct targets of CLOCK:BMAL while others contain RORE elements and a third group, such as the D albumen binding protein (DBP), exhibit D boxes in their promoters that are targets of the core clock genes (Takahashi 2017).

DNA microarray analysis of the cell's transcriptome shows that the expression of specific circadian-regulated control genes is of core importance to the molecular framework that regulates circadian rhythms in either central or organ-specific tissues. Post transcriptional modifications of the core clock genes, including alternative splicing and mRNA nuclear export, are also under circadian influence (Preubner and Heyd 2016). PER2 protein translation is regulated by miRNA binding to the 3'-UTR and genetic modifications to the 3'-UTR of the PER2 gene in mice changes the length of their circadian cycle (Yoo *et al.* 2017). Protein degradation of PER and CRY through the casein kinase 1δ- or the ubiquitin-mediated degradation pathways are also key in maintaining tight timing control while phosphorylation and dephosphorylation by other kinases and phosphatases imparts additional post-translational modifications in a tissue-specific manner (Gallego and Virshup 2007).

1.3 Animal models and experiments involving disruption of circadian influence

Unravelling the impact of circadian dysregulation on animal health has involved experiments on SCN-lesioned animals, animals with a pinealectomy, animals exposed to manipulated light: dark (L:D) schedules, and clock gene knock-out, knock-in, and mutated models. To begin with the hierarchal arrangement, SCN-lesioned mice that were subsequently implanted with pancreatic adenocarcinoma or osteosarcoma cells demonstrated significantly quicker mortality, increased tumor growth, and body temperature dysregulation (Filipski *et al.* 2002). Pinealectomized Spraque- Dawley rats were significantly more likely to develop mammary tumors in a chemically-induced breast cancer model than rats with intact pineal glands. Melatonin injection reduced the risk of cancer development in pinealectomized mice slightly and those animals that had intact pineal glands and received exogenous melatonin, had the lowest incidence of tumor development (Tamarkin *et al.* 1981). Manipulating the L:D cycle

to establish a model of shift work or chronic circadian rhythm disruption (CRD) in cancer-prone p53-/- mutant mice, resulted in the CRD mice developing tumors earlier than controls, gaining significantly more weight, and having significantly different corticosterone hormone secretion patterns (Van Dycke *et al.* 2015). In a sophisticated series of experiments involving a genetically engineered mouse model of lung adenocarcinoma, mice subjected to a jet lag schedule of altered L:D cycles had an increased incidence of lung tumors, more rapid tumor progression, loss of BMAL- and PER2-increased tumor progression, and increased c-MYC expression in the tumors (Papagiannakopoulos *et al.* 2016). There appears to be quite a bit of redundancy within the network of genes that organize the circadian rhythm. While a deficiency or mutation in a single clock gene in mutant mice may demonstrate some altered rhythm activity or may increase the tendency to metabolic syndrome, there is no evidence that severe overt disease or lethality results unless there are double knock outs (Takahashi *et al.* 2008). However, Per2 mutant (m/m) mice are more prone to cancer after radiation exposure, their thymocytes demonstrated altered p53 expression, and their liver cells expressed increased levels of c-Myc and cyclin D_1 (Fu *et al.* 2002). Other than Per2 (m/m), it does not appear that clock gene mutations or a loss of gene function results in increased tumor initiation and progression, but rather these mutations may increase the risks of carcinogenesis which are related to hormone or nervous system influence and/or lifestyle and environmental exposure.

1.4 Circadian rhythm disruption and disease: Epidemiological evidence

The evidence that circadian rhythm disturbance (CRD) contributes to an increased risk of disease, including metabolic syndrome and cancer, is derived from numerous epidemiological reports particularly those involving shift workers (Schernhammer *et al.* 2001)(Hansen and Stevens 2012)(Grundy *et al.* 2013)(Papantoniou *et al.* 2015)(Salamanca-Fernández *et al*. 2018).

Known human clock gene mutations are not usually associated with increased cancer risk but rather are associated with sleep disorders (Rijo-Ferreira and Takahashi 2019) (Patke *et al*. 2017). A genetic variant in PER3 appears to predispose people to mood disorders (Zhang *et al.* 2016). People with specific variations in clock genes suggest a mechanism that predicts chronotype or preferred time of day for rising and activity (Jones *et al*. 2019). Chronotype may pose an increased risk for cancer in night shift workers but this could be due to a lifestyle choice based on individual preference (Papantoniou *et al*. 2015). The impact of CRD on cancer incidence in people with a corresponding lack of a circadian gene mutation has increased the probability that epigenetic factors provide a link (Masri, Kinouchi, and Sassone-Corsi 2015).

Clock gene expression is abnormal in the breast tumor tissues of women, where the expression of BMAL, PER1, and PER2 are down-regulated compared to normal tissues (Broadberry *et al*. 2018)(Winter *et al.* 2007). The loss of clock gene expression is correlated with prognosis for patients with cancer, with those women whose tumors express the lowest levels of clock gene expression doing poorly (Cadenas *et al.* 2014). All of the core clock genes are under-expressed in human pancreatic cancer tissue according to one study (Relles *et al.* 2013). PER2 is under-expressed in human non-small cell lung cancer tissue (Xiang *et al.* 2018). The clock genes PER1, PER2, and CRY2 are down-regulated in liver and ovarian tumors but CRY1 is up-regulated in cancerous ovarian tissue (Tokunaga *et al.* 2008)(Lin *et al.* 2008). Clock gene expression is disordered in a wide variety of human cancerous tissues.

Women with hormone-positive breast cancer have lower night time circulating melatonin levels (Tamarkin *et al.* 1982). Exposure to even low intensity light early in the night phase decreases plasma melatonin levels in women and men (Zeitzer *et al.* 2000). Observations similar to these, combined with epidemiological evidence, helped to generate the melatonin

hypothesis; this hypothesis states that the predisposition to carcinogenesis seen in shift workers is due to the disrupted melatonin levels (Stevens and Davis 1996). Plasma melatonin levels are lower in individuals who are awake during their night shift as compared to individuals who are asleep at night. Further, night work may increase oxidative stress damage to DNA (Bhatti *et al.* 2017). Since the development of the melatonin hypothesis, the interest in circadian biology has increased because, although the mechanistic links between human disease and CRD have not yet been established, there are suggestions that the tumor clock could be a viable therapeutic target (Kiessling and Cermakian 2017).

1.5 Circadian and cell cycles

The process by which the cells grow, divide, and replicate is called the cell cycle (Feillet *et al.* 2015). From a temporal perspective alone, it is tempting to view circadian and cell cycles as explicitly connected given that they have approximately the same 24 hour length at least in actively proliferating cells. Both cycles also display oscillating cycles and cancer cells display abnormalities in both the cell cycle (cell proliferation) and in the circadian cycle (clock gene expression) (Feillet *et al*. 2015). The cell cycle in divided into four phases: DNA replication occurs in the *S* phase; mitosis and cytokinesis occur in *M* phase; and, these are separated by two growth phases G_1 which proceeds *S;* and, G_2 which proceeds *M* (Duronio and Xiong 2013). Progression through the cell cycle is highly regulated and requires the coordinated activation of cyclin dependent kinases (CdK) and cyclins, of which there are several in mammalian cells. The levels of cyclin protein depend on the balance between transcriptional activity and degradation through the ubiquitin-dependent pathway (Satyanarayana and Kaldis 2009). Cyclin levels rise and fall throughout the cell cycle such that different subtypes and their CdK partners are associated with a particular phase of the cell cycle: for example Cyclin D and CDK 4/6 are

associated with the G_1 phase of the cell cycle and are involved in the transition to the *S* phase (Malumbres 2014). Cdks are regulated in part by CdK inhibitors (CKI) comprised of two families; the Cip/Kp branch which includes p21cip1 and the Ink4 group (Lim and Kaldis 2013). The Cdks are also inhibited by phosphorylation of a regulatory site by the Wee1 kinase which inactivates them while dephosphorylation by Cdc25 activates them (Malumbres 2014). Additionally there is oversight in the form of two cell cycle "check points", the first is more formally referred to as the G_1 restriction point because once the cell is past this, it is committed to entry to the *S* phase (Blagosklonny and Pardee 2002). The G_1 restriction point is controlled by the retinoblastoma protein (pRB) which exists in a hypophosphorylated form in quiescent cells and in this form suppresses the transcriptional activity of E2F genes, whose targets are required for progression into the *S* phase (Duronio and Xiong 2013). The second check point occurs in the late G_2/M transition and involves a number of factors including cell size and mitotic spindle readiness as well as a dynamic network of protein interactions (Barnum and O'Connell 2014). The tumor suppressor p53 also regulates the cell cycle particularly when stressors including DNA damage are present, through CKI gene transcription, including p21 (Duronio and Xiong 2013). A number of parallels can be observed when comparing the peak levels of mRNA transcripts for the clock genes and for the cyclins or p53 and it has been shown that silencing of the transcription factors BMAL or CLOCK, using small interfering RNAs (siRNA), lengthens the cell cycle (Farshadi *et al*. 2019). The Myc gene (c-Myc) has a number of influences on cell cycle progression as its expression causes the cells to exit quiescence and enter into the cell cycle, it inhibits the transcription of regulators such as the p21 and E2F transcriptions factors, and cyclins and Cdks are all targets of c-Myc (Bretones, Delgado, and León 2015). The Myc pathway signaling is over-expressed in a wide variety of human malignancies (Sanchez-Vega *et*

al. 2018). Increased c-Myc expression is observed in tumors which show down-regulated levels of PER2 (Papagiannakopoulos *et al.* 2016).

1.6 Research perspectives and aims

It is important to recognize the perspective of the circadian cycle that is derived from a molecular biology background. The primary and secondary control of clock gene expression at the cellular level and the hierarchal level of organization has largely been elucidated. The described circuit of transcriptional translation feedback loops of core clock genes (TTFL) drives the internal timing of the organism with extraordinary daily precision (Pilorz *et al.* 2020). Molecular science has derived the central model of cell signaling as the response to cell membrane receptor engagement by a ligand, intracellular signaling through primary and secondary messengers, with nuclear translocation and subsequent changes in gene expression by which the cell adapts to the environment or dies. It is important to appreciate that subtle changes in the cell's environment such as nutrient availability and ambient temperature can impact cell responses. Other components implicated in circadian regulation such as melatonin which has receptor and non-receptor pathways of influence and the subcellular organelle, mitochondria, which contributes to energetics and apoptosis may not fit the central dogma exactly. Finally, the secondary accessory TFFL involves nuclear receptors which themselves can influence expression and repression of transcription factors. Research interest in the area of circadian rhythm disruption has been increasing especially in the last decade and the field of publications are very diverse, ranging from molecular genetics, biochemistry, and biophysics, to metabolism, the nervous system, and behaviour. The relevance of such investigations cannot be disputed. The field contributes to the knowledge and understanding of chronotherapy, xenobiotic and pharmacological interactions, and pathophysiology (Robinson and Reddy 2014). One way to

organize the vast amount of information and investigation around the question, "how does circadian rhythm disruption lead to disease?", is to create a set of principles. Therefore, the aims of the project can broadly be thought of as:

Aim 1: To investigate the molecular changes that relate circadian disruption to diseases, such as cancer, by establishing a model that influences clock gene expression in peripheral (cancer) cells independent of central oscillators.

Aim 2: To investigate the molecular changes that relate circadian disruption to disease by examining the role of melatonin on clock gene expression and cell cycle kinetics.

Aim 3: To investigate the molecular changes that relate circadian disruption to disease by examining the role of mitochondria, reactive oxygen species (ROS) production, and cellular redox status.

Aim 4: To investigate the molecular changes that relate circadian disruption to disease by examining the role of perturbed energetics and cell metabolism on clock gene expression and cell cycle kinetics.

1.7 Research objectives

Four objectives are linked to the aims.

Objective 1: Explore the interconnection between the cell cycle and circadian cycle. This requires the interrogation of current protocols of cell synchronization including a temperature shift model in order to characterize a model where clock gene expression can be independent of cell cycle direction and has minimal dependence on pharmaceutical or hormone treatment.

Objective 2: Explore the impact of melatonin on clock gene expression and the regulation of the cell cycle independent of each other through use of the temperature shift model.

Objective 3: Determine the impact of drug and hormone exposure on cellular and mitochondrial ROS production using the temperature shift model.

Objective 4: Determine the impact of mitochondrial oxidative phosphorylation impairment on clock gene expression following development of an aberrant mitochondria cell line.

1.8 Overview of methodology and study limitations

The model selected for study has been exclusively performed in *in vitro* cell culture. The rationale is two- fold. There already exists an extensive body of animal work, however, the model is primarily in rodents which being nocturnal do not share equivalent human hormonal output patterns. Melatonin secretion occurs at night for both rodents and humans but for mice this represents the active period of their day. The second reason for *in vitro* work is that the focus here is on cellular and molecular mechanisms relating to clock gene expression and it is easier to control for the vast complexity of intracellular events in cell culture. Given that lifestyle, both in the choice of occupation, the social shift toward working and recreating past twilight, and the tendency to be connected to blue light-emitting technology at night, mean that the epigenetic contributions to circadian rhythm in theory could be substantial (Filipski *et al.* 2005). This is supported by the observations that CLOCK has histone acetyl transferase (HAT) action (Bellet and Sassone-Corsi 2010), and that there is differential hypermethylation of the promoter regions of the PER genes in breast cancer (Chen *et al.* 2005). While this study considers the contribution of oxidative stress and energetics on circadian gene expression, it does not include examination of other non -transcriptional factors such as cycling of the antioxidant system of peroxiredoxins

(Robinson and Reddy 2014). The main limitation of these experiments lies in the collection time limitation of 24 hours. This makes it difficult to define a circadian oscillation *per se* but the model is not limited in those terms and the time point collections have the potential to be carried out over longer periods of time, limited only by the researchers' endurance; whereas in other protocols, oscillation dampen out by 48 – 72 hours (Balsalobre *et al.* 1998)(Rossetti *et al.* 2012)(Lellupitiyage Don *et al.* 2019). As clock gene transcripts have been characterized in a large number of breast cancer and epithelial cell lines (Xiang *et al*. 2012)(Gutiérrez-Monreal *et al*. 2016)(Lellupitiyage Don *et al.* 2019), our study focuses on the gene expression by MCF-7 cells in response to exposure to the temperature shift model. While other cell lines have been incorporated into portions of this body of work, it is important to remember that the bulk of the results presented relate to the response of a particular cell line of human breast cancer. The characteristics of this cell line include: being an immortalized cell line derived from the pleural effusion of a woman with a breast adenocarcinoma (Lee, Oesterreich, and Davidson 2015), being estrogen receptor (ER) α positive, exhibiting anchorage-independent growth in a semi-solid medium, and in the presence of estradiol, being tumorigenic and invasive (Rossetti *et al.* 2012). The rationale for choosing the MCF-7 cell line is to build on recent evidence from investigations of circadian disruption and clock gene expression in breast cancer cell lines (Lellupitiyage Don *et al.* 2019)(Gutiérrez-Monreal *et al.* 2016)(Rossetti *et al.* 2012) and to involve a representative cell culture model that closely reflects the human epidemiological evidence. Although the results of some experiments using the non-neoplastic line of breast epithelial cells, HBL-100s, are presented and discussed, it would have been ideal to measure the effects of the temperature shift model in the non-neoplastic MCF-10A breast epithelial cell line in order to compare the results other studies (Gutiérrez-Monreal *et al.* 2016)(Rossetti *et al.* 2012). Another potential

limitation of the study is the ability to replicate some experiments given the technical expertise required such as fluorescent microscopy, RT-qPCR and the establishment of a *Rhø* cell line. Therefore, the variability of some results from a statistical point of view alone presented a challenge for analysis. At the end of the day, the emphasis has to be on the understanding that by their very nature, clock gene expression is temporally related and in the context of comparing results, it is also tissue-specific (Panda *et al.* 2002).

1.9 Thesis statement

One hypothesis about the etiology of the various diseases associated with circadian rhythm disruption is that there is a loss of synchronicity between the central and peripheral oscillators (Arble *et al*. 2009). The other hypothesis is related to the loss of melatonin regulation associated with light at night (Khan *et al.* 2019). The central pacemaker, the SCN, is primarily entrained by light: dark cycles but peripheral oscillators are impacted by a wide variety of stimuli including food, hormones, inflammation, hypoxia, oxidative stress, and temperature (Xie *et al.* 2019). Gene expression appears to be highly circadian-dependent (Lucassen *et al.* 2016). It is difficult to separate different variables related to peripheral oscillator regulation in an *in vivo* model, not only because of the SCN hierarchy but because behaviours, such as feeding, impact core body temperature and hormone secretion (Arble *et al.* 2009). The central question becomes, does circadian rhythm disruption directly lead to genomic instability, which predisposes to oncogenesis and what is the molecular mechanism? In order to address this question, an *in vitro* system using ERα-positive breast cancer cells are used partly because the model has been well characterized and partly due to the established relationship between breast cancer risk and night shift work. It is proposed that a novel temperature shift model be applied to the growth, cell cycle, gene expression, drug metabolism, and reactive oxygen species production aspects of

human ERα-positive breast cancer cells. The current body of research suggests that individuals with circadian gene mutations are not particularly cancer prone and that clock gene mutations within a wide variety of human tumors have been well characterized. Shift workers are predisposed to metabolic syndrome and mice fed at the wrong time of day, gain weight suggesting a relationship between clock regulation and metabolism (Garaulet and Gómez-Abellán 2014). A second novel approach is to utilize MCF-7 cells and impair their mitochondrial DNA (mtDNA) and study the effect on circadian gene expression. It is predicted that a temperature shift protocol will increase clock gene expression in MCF-7 cells and part of this mechanism is due to oxidative stress such that if oxidative phosphorylation is disrupted, circadian gene expression becomes dysregulated.

1.10 References

Arble, Deanna M., Joseph Bass, Aaron D. Laposky, Martha H. Vitaterna, and Fred W. Turek. 2009. "Circadian Timing of Food Intake Contributes to Weight Gain." *Obesity*. https://doi.org/10.1038/oby.2009.264.

Balsalobre, Aurélio, Francesca Damiola, and Ueli Schibler. 1998. "A Serum Shock Induces Circadian Gene Expression in Mammalian Tissue Culture Cells." *Cell*. https://doi.org/10.1016/S0092-8674(00)81199-X.

Barnum, Kevin J., and Matthew J. O'Connell. 2014. "Cell Cycle Regulation by Checkpoints." *Methods in Molecular Biology*. https://doi.org/10.1007/978-1-4939-888-2_2.

Bellet, Marina Maria, and Paolo Sassone-Corsi. 2010. "Mammalian Circadian Clock and Metabolism - The Epigenetic Link." *Journal of Cell Science*. https://doi.org/10.1242/jcs.051649.

Ben-Moshe, Zohar, Nicholas S. Foulkes, and Yoav Gothilf. 2014. "Functional Development of the Circadian Clock in the Zebrafish Pineal Gland." *BioMed Research International*. https://doi.org/10.1155/2014/235781.

Bhatti, Parveen, Dana K. Mirick, Timothy W. Randolph, Jicheng Gong, Diana Taibi Buchanan, Junfeng Zhang, and Scott Davis. 2017. "Oxidative DNA Damage during Night Shift Work." *Occupational and Environmental Medicine*. https://doi.org/10.1136/oemed-2017-104414.

Blagosklonny, Mikhail V., and Arthur B. Pardee. 2002. "The Restriction Point of the Cell Cycle." *Cell Cycle (Georgetown, Tex.)*. https://doi.org/10.4161/cc.1.2.108.

Bretones, Gabriel, M. Dolores Delgado, and Javier León. 2015. "Myc and Cell Cycle Control." *Biochimica et Biophysica Acta - Gene Regulatory Mechanisms*. https://doi.org/10.1016/j.bbagrm.2014.03.013.

Broadberry, Eleanor, James McConnell, Jack Williams, Nan Yang, Egor Zindy, Angela Leek, Rachel Waddington, et al. 2018. "Disrupted Circadian Clocks and Altered Tissue Mechanics in Primary Human Breast Tumours." *Breast Cancer Research*. https://doi.org/10.1186/s13058-018-1053-4.

Bunger, Maureen K., Lisa D.Wilsbacher, Susan M.Moran, Cynthia Clendenin, Laurel A.Radcliffe, John B.Hogenesch, M.CelesteSimon, Joseph S.Takahashi, Christopher A.Bradfield 2000. " *Mop3* Is an Essential Component of theMaster Circadian Pacemaker in Mammals". *Cell.* https://doi.org/10.1016/S0092-8674(00)00205-1

Cadenas, Cristina, Leonie Van De Sandt, Karolina Edlund, Miriam Lohr, Birte Hellwig, Rosemarie Marchan, Marcus Schmidt, Jörg Rahnenführer, Henrik Oster, and Jan G.

Hengstler. 2014. “Loss of Circadian Clock Gene Expression Is Associated with Tumor Progression in Breast Cancer.” *Cell Cycle*. https://doi.org/10.4161/15384101.2014.954454.

Chen, Shou Tung, Kong Bung Choo, Ming Feng Hou, Kun Tu Yeh, Shou Jen Kuo, and Jan Gowth Chang. 2005. “Deregulated Expression of the PER1, PER2 and PER3 Genes in Breast Cancers.” *Carcinogenesis*. https://doi.org/10.1093/carcin/bgi075.

Cuesta, Marc, Nicolas Cermakian, and Diane B. Boivin. 2015. “Glucocorticoids Entrain Molecular Clock Components in Human Peripheral Cells.” *FASEB Journal*. https://doi.org/10.1096/fj.14-265686.

Duronio, Robert J., and Yue Xiong. 2013. “Signaling Pathways That Control Cell Proliferation.” *Cold Spring Harbor Perspectives in Biology*. https://doi.org/10.1101/cshperspect.a008904.

Eclosion, Circadian. 2008. “Journal of Biological Rhythms.” *Journal of Biological Rhythms*. https://doi.org/10.1177/0748730405283418.

Farshadi, Elham, Jie Yan, Pierre Leclere, Albert Goldbeter, Inês Chaves, and Gijsbertus T.J. van der Horst. 2019. “The Positive Circadian Regulators CLOCK and BMAL1 Control G2/M Cell Cycle Transition through Cyclin B1.” *Cell Cycle*. https://doi.org/10.1080/15384101.2018.1558638.

Feillet, Celine, Gijsbertus T.J. van der Horst, Francis Levi, David A. Rand, and Franck Delaunay. 2015. “Coupling between the Circadian Clock and Cell Cycle Oscillators: Implication for Healthy Cells and Malignant Growth.” *Frontiers in Neurology*. https://doi.org/10.3389/fneur.2015.00096.

Filipski, E. 2002. “Host Circadian Clock as a Control Point in Tumor Progression.” *Cancer Spectrum Knowledge Environment*. https://doi.org/10.1093/jnci/94.9.690.

Filipski, Elisabeth, Pasquale F. Innominato, Ming-Wei Wu, Xiao-Mei Li, Stefano Iacobelli, Li-Jian Xian, Francis Levi. 2005. “Effects of Light and Food Schedules on Liver and Tumor Molecular Clocks in Mice.” *Journal of the National Cancer Institute.*

Fu, Loning, Helene Pelicano, Jinsong Liu, Peng Huang, and Cheng Chi Lee. 2002. “The Circadian Gene Period2 Plays an Important Role in Tumor Suppression and DNA Damage Response in Vivo.” *Cell*. https://doi.org/10.1016/S0092-8674(02)00961-3.

Gallego, Monica, and David M. Virshup. 2007. “Post-Translational Modifications Regulate the Ticking of the Circadian Clock.” *Nature Reviews Molecular Cell Biology*. https://doi.org/10.1038/nrm2106.

Garaulet, Marta, and Purificación Gómez-Abellán. 2014. “Timing of Food Intake and Obesity: A Novel Association.” *Physiology and Behavior*. https://doi.org/10.1016/j.physbeh.2014.01.001.

Grundy, Anne, Harriet Richardson, Igor Burstyn, Caroline Lohrisch, Sandip K. SenGupta, Agnes S. Lai, Derrick Lee, John J. Spinelli, and Kristan J. Aronson. 2013. "Increased Risk of Breast Cancer Associated with Long-Term Shift Work in Canada." *Occupational and Environmental Medicine*. https://doi.org/10.1136/oemed-2013-101482.

Gutiérrez-Monreal, Miguel A., Victor Treviño, Jorge E. Moreno-Cuevas, and Sean Patrick Scott. 2016. "Identification of Circadian-Related Gene Expression Profiles in Entrained Breast Cancer Cell Lines." *Chronobiology International*. https://doi.org/10.3109/07420528.2016.1152976.

Hansen, Johnni, and Richard G. Stevens. 2012. "Case-Control Study of Shift-Work and Breast Cancer Risk in Danish Nurses: Impact of Shift Systems." *European Journal of Cancer*. https://doi.org/10.1016/j.ejca.2011.07.005.

Hyuk, Wan Ko, Suzanne DiMassa, Young Kim Eun, Kiho Bae, and Isaac Edery. 2007. "Cis-Combination of the Classic PerS and PerL Mutations Results in Arrhythmic Drosophila with Ectopic Accumulation of Hyperphosphorylated PERIOD Protein." *Journal of Biological Rhythms*. https://doi.org/10.1177/0748730407306929.

Jones, Samuel E., Jacqueline M. Lane, Andrew R. Wood, Vincent T. van Hees, Jessica Tyrrell, Robin N. Beaumont, Aaron R. Jeffries, et al. 2019. "Genome-Wide Association Analyses of Chronotype in 697,828 Individuals Provides Insights into Circadian Rhythms." *Nature Communications*. https://doi.org/10.1038/s41467-018-08259-7.

Khan, Suliman, Yang Liu, Rabeea Siddique, Ghulam Nabi, Mengzhou Xue, and Hongwei Hou. 2019. "Impact of Chronically Alternating Light-Dark Cycles on Circadian Clock Mediated Expression of Cancer (Glioma)-Related Genes in the Brain." *International Journal of Biological Sciences*. https://doi.org/10.7150/ijbs.35520.

King, David P., Martha Hotz Vitaterna, Anne-Marie Chang, William F. Dove, Lawrence H. Pinto, Fred W. Turek, Joseph F. Takahaski 1997. "The Mouse *Clock* Mutation Behaves as an Antimorph and Maps Within in the W^{19H} Deletion Distal of *Kit.*" *Genetics.*

Kiessling, Silke, and Nicolas Cermakian. 2017. "The Tumor Circadian Clock: A New Target for Cancer Therapy?" *Future Oncology*. https://doi.org/10.2217/fon-2017-0456.

Lee, Adrian V., Steffi Oesterreich, and Nancy E. Davidson. 2015. "MCF-7 Cells - Changing the Course of Breast Cancer Research and Care for 45 Years." *Journal of the National Cancer Institute*. https://doi.org/10.1093/jnci/djv073.

Lellupitiyage Don, Sujeewa S., Hui Hsien Lin, Jessica J. Furtado, Maan Qraitem, Stephanie R. Taylor, and Michelle E. Farkas. 2019. "Circadian Oscillations Persist in Low Malignancy Breast Cancer Cells." *Cell Cycle*. https://doi.org/10.1080/15384101.2019.1648957.

Lim, Shuhui, and Philipp Kaldis. 2013. "Cdks, Cyclins and CKIs: Roles beyond Cell Cycle Regulation." *Development (Cambridge)*. https://doi.org/10.1242/dev.091744.

Loudon, A. S.I., Q. J. Meng, E. S. Maywood, D. A. Bechtold, R. P. Boot-Handford, and M. H. Hastings. 2007. "The Biology of the Circadian CK1ε Tau Mutation in Mice and Syrian Hamsters: A Tale of Two Species." In *Cold Spring Harbor Symposia on Quantitative Biology*. https://doi.org/10.1101/sqb.2007.72.073.

Lucassen, Eliane A., Claudia P. Coomans, Maaike van Putten, Suzanne R. de Kreij, Jasper H.L.T. van Genugten, Robbert P.M. Sutorius, Karien E. de Rooij. 2016. "Environmental 24-Hr Cycles Are Essential for Health." *Current Biology*. https://doi.org/10.1016/j.cub.2016.05.038.

Malumbres, Marcos. 2014. "Cyclin-Dependent Kinases." *Genome Biology*. https://doi.org/10.1186/gb4184.

Masri, Selma, Kenichiro Kinouchi, and Paolo Sassone-Corsi. 2015. "Circadian Clocks, Epigenetics, and Cancer." *Current Opinion in Oncology*. https://doi.org/10.1097/CCO.0000000000000153.

Mendoza, Jorge. 2007. "Circadian Clocks: Setting Time by Food." *Journal of Neuroendocrinology*. https://doi.org/10.1111/j.1365-2826.2006.01510.x.

Oliva-Ramírez, Jacqueline, María Maximina B. Moreno-Altamirano, Benjamín Pineda-Olvera, Patricia Cauich-Sánchez, and F. Javier Sánchez-García. 2014. "Crosstalk between Circadian Rhythmicity, Mitochondrial Dynamics and Macrophage Bactericidal Activity." *Immunology*. https://doi.org/10.1111/imm.12329.

Panda, Satchidananda, Marina P. Antoch, Brooke H. Miller, Andrew I. Su, Andrew B. Schook, Marty Straume, Peter G. Schultz, Steve A. Kay, Joseph S. Takahashi, and John B. Hogenesch. 2002. "Coordinated Transcription of Key Pathways in the Mouse by the Circadian Clock." *Cell*. https://doi.org/10.1016/S0092-8674(02)00722-5.

Papagiannakopoulos, Thales, Matthew R. Bauer, Shawn M. Davidson, Megan Heimann, Lakshmipriya Subbaraj, Arjun Bhutkar, Jordan Bartlebaugh, Matthew G. Vander Heiden, and Tyler Jacks. 2016. "Circadian Rhythm Disruption Promotes Lung Tumorigenesis." *Cell Metabolism*. https://doi.org/10.1016/j.cmet.2016.07.001.

Papantoniou, Kyriaki, Gemma Castaño-Vinyals, Ana Espinosa, Nuria Aragonés, Beatriz Pérez-Gõmez, Javier Burgos, Inés Gõmez-Acebo, et al. 2015. "Night Shift Work, Chronotype and Prostate Cancer Risk in the MCC-Spain Case-Control Study." *International Journal of Cancer*. https://doi.org/10.1002/ijc.29400.

Patke, Alina, Patricia J. Murphy, Onur Emre Onat, Ana C. Krieger, Tayfun Özçelik, Scott S. Campbell, and Michael W. Young. 2017. "Mutation of the Human Circadian Clock Gene CRY1 in Familial Delayed Sleep Phase Disorder." *Cell*. https://doi.org/10.1016/j.cell.2017.03.027.

Pilorz, Violetta, Mariana Astiz, Keno Ole Heinen, Oliver Rawashdeh, and Henrik Oster. 2020. "The Concept of Coupling in the Mammalian Circadian Clock Network." *Journal of Molecular Biology*. https://doi.org/10.1016/j.jmb.2019.12.037.

Potter, Gregory D.M., Debra J. Skene, Josephine Arendt, Janet E. Cade, Peter J. Grant, and Laura J. Hardie. 2016. "Circadian Rhythm and Sleep Disruption: Causes, Metabolic Consequences, and Countermeasures." *Endocrine Reviews*. https://doi.org/10.1210/er.2016-1083.

Preitner, Nicolas, Francesca Damiola, Luis-Lopez-Molina, Joszef Zakany, Denis Duboule, Urs Albrecht, and Ueli Schibler. 2002. "The Orphan Nuclear Receptor REV-ERBα Controls Circadian Transcription within the Positive Limb of the Mammalian Circadian Oscillator." *Cell*. https://doi.org/10.1016/S0092-8674(02)00825-5.

Preußner, Marco, and Florian Heyd. 2016. "Post-Transcriptional Control of the Mammalian Circadian Clock: Implications for Health and Disease." *Pflugers Archiv European Journal of Physiology*. https://doi.org/10.1007/s00424-016-1820-y.

Rijo-Ferreira, Filipa, and Joseph S. Takahashi. 2019. "Genomics of Circadian Rhythms in Health and Disease." *Genome Medicine*. https://doi.org/10.1186/s13073-019-0704-0.

Robinson, I., and A. B. Reddy. 2014. "Molecular Mechanisms of the Circadian Clockwork in Mammals." *FEBS Letters*. https://doi.org/10.1016/j.febslet.2014.06.005.

Rossetti, Stefano, Joseph Esposito, Francesca Corlazzoli, Alex Gregorski, and Nicoletta Sacchi. 2012. "Entrainment of Breast (Cancer) Epithelial Cells Detects Distinct Circadian Oscillation Patterns for Clock and Hormone Receptor Genes." *Cell Cycle*. https://doi.org/10.4161/cc.11.2.18792.

Salamanca-Fernández, E., Miguel Rodríguez-Barranco, M. Guevara, E. Ardanaz, A. Olry de Labry Lima, and M. J. Sánchez. 2018. "Night-Shift Work and Breast and Prostate Cancer Risk: Updating the Evidence from Epidemiological Studies." *Anales Del Sistema Sanitario de Navarra*. https://doi.org/10.23938/ASSN.0307.

Sanchez-Vega, Francisco, Marco Mina, Joshua Armenia, Walid K. Chatila, Augustin Luna, Konnor C. La, Sofia Dimitriadoy, et al. 2018. "Oncogenic Signaling Pathways in The Cancer Genome Atlas." *Cell*. https://doi.org/10.1016/j.cell.2018.03.035.

Satyanarayana, A., and P. Kaldis. 2009. "Mammalian Cell-Cycle Regulation: Several Cdks, Numerous Cyclins and Diverse Compensatory Mechanisms." *Oncogene*. https://doi.org/10.1038/onc.2009.170.

Savvidis, Christos, and Michael Koutsilieris. 2012. "Circadian Rhythm Disruption in Cancer Biology." *Molecular Medicine*. https://doi.org/10.2119/molmed.2012.00077.

Schernhammer, Eva S., Francine Laden, Frank E. Speizer, Walter C. Willett, David J. Hunter, Ichiro Kawachi, and Graham A. Colditz. 2001. "Rotating Night Shifts and Risk of Breast Cancer in Women Participating in the Nurses' Health Study." *Journal of the National Cancer Institute*. https://doi.org/10.1093/jnci/93.20.1563.

Shearman, L.P., M.J. Zylka, S.M. Reppert, D.R. Weaver. 1999. "Expression of Basic Helix-Loop-Helix/Pas Genes in the Mouse Suprachiasmatic Nucleus. *Neuroscience.* https://doi.org/10.1016/S0306-4522(98)00325-X

Stevens, Richard G., and Scott Davis. 1996. "The Melatonin Hypothesis: Electric Power and Breast Cancer." *Environmental Health Perspectives*. https://doi.org/10.2307/3432703.

Takahashi, Joseph S., Hee Kyung Hong, Caroline H. Ko, and Erin L. McDearmon. 2008. "The Genetics of Mammalian Circadian Order and Disorder: Implications for Physiology and Disease." *Nature Reviews Genetics*. https://doi.org/10.1038/nrg2430.

Takahashi, Joseph S. 2017. "Transcriptional Architecture of the Mammalian Circadian Clock." *Nature Reviews Genetics*. https://doi.org/10.1038/nrg.2016.150.

Tamarkin, Lawrence, Michael Cohen, Cheryl Reichert, Cheryl Reichert, Marc Lippman, and Bruce Chabner. 1981. "Melatonin Inhibition and Pinealectomy Enhancement of 7,12-Dimethylbenz(a)Anthracene-Induced Mammary Tumors in the Rat." *Cancer Research*.

Tamarkin, Lawrence, David Danforth, Alan Lichter, Ernest DeMoss, Michael Cohen, Bruce Chabner, and Marc Lippman. 1982. "Decreased Nocturnal Plasma Melatonin Peak in Patients with Estrogen Receptor Positive Breast Cancer." *Science*. https://doi.org/10.1126/science.7079745.

Tokunaga, Hideki, Yuji Takebayashi, Hiroki Utsunomiya, Jun Ichi Akahira, Masashi Higashimoto, Miyuki Mashiko, Kiyoshi Ito, Hitoshi Niikura, Sei Ichi Takenoshita, and Nobuo Yaegashi. 2008. "Clinicopathological Significance of Circadian Rhythm-Related Gene Expression Levels in Patients with Epithelial Ovarian Cancer." *Acta Obstetricia et Gynecologica Scandinavica*. https://doi.org/10.1080/00016340802348286.

Van Dycke, Kirsten C.G. Van, Wendy Rodenburg, Conny T.M. Van Oostrom, Linda W.M. Van Kerkhof, Jeroen L.A. Pennings, Till Roenneberg, Harry Van Steeg, and Gijsbertus T.J. Van Der Horst. 2015. "Chronically Alternating Light Cycles Increase Breast Cancer Risk in Mice." *Current Biology*. https://doi.org/10.1016/j.cub.2015.06.012.

Van Laake, Linda W., Thomas F. Luscher, Martin E. Yoing 2018. "The Circadian Clock in Cardiovascular Regulation and Disease: Lessons from the Nobel Prize in Physilogy and Medicine 2017. *European Heart Journal.* doi.org/10.1093/eurheartj/ehx775

Winter, Sherry L., Lucine Bosnoyan-Collins, Dushanthi Pinnaduwagez, and Irene L. Andrulis. 2007. "Expression of the Circadian Clock Genes Per1 and Per2 in Sporadic and Familial Breast Tumors." *Neoplasia*. https://doi.org/10.1593/neo.07595.

Wever, R. A. 1986. “Characteristics of Circadian Rhythms in Human Functions.” *Journal of Neural Transmission. Supplementum*.

Xiang, Run, Yue Cui, Yanping Wang, Tianpeng Xie, Xiaojun Yang, Zhu Wang, Juan Li, and Qiang Li. 2018. “Circadian Clock Gene Per2 Downregulation in Non-Small Cell Lung Cancer Is Associated with Tumour Progression and Metastasis.” *Oncology Reports*. https://doi.org/10.3892/or.2018.6704.

Xie, Yanling, Qingming Tang, Guangjin Chen, Mengru Xie, Shaoling Yu, Jiajia Zhao, and Lili Chen. 2019. “New Insights into the Circadian Rhythm and Its Related Diseases.” *Frontiers in Physiology*. https://doi.org/10.3389/fphys.2019.00682.

Yoo, Seung Hee, Shihoko Kojima, Kazuhiro Shimomura, Nobuya Koike, Ethan D. Buhr, Tadashi Furukawa, Caroline H. Ko, et al. 2017. “Period2 3′-UTR and MicroRNA-24 Regulate Circadian Rhythms by Repressing PERIOD2 Protein Accumulation.” *Proceedings of the National Academy of Sciences of the United States of America*. https://doi.org/10.1073/pnas.1706611114.

Zeitzer, Jamie M., Derk Jan Dijk, Richard E. Kronauer, Emery N. Brown, and Charles A. Czeisler. 2000. “Sensitivity of the Human Circadian Pacemaker to Nocturnal Light: Melatonin Phase Resetting and Suppression.” *Journal of Physiology*. https://doi.org/10.1111/j.1469-7793.2000.00695.x.

Zhang, Hirano A., Hsu P.-K., Jones C.R., Sakai N., Okuro M., McMahon T. 2016. “A PERIOD3 Variant Causes a Circadian Phenotype and Is Associated with a Seasonal Mood Trait.” *Proceedings of the National Academy of Sciences of the United States of America*. https://doi.org/10.1073/pnas.1600039113 LK

Zhang, Ray, Nicholas F. Lahens, Heather I. Ballance, Michael E. Hughes, and John B. Hogenesch. 2014. “A Circadian Gene Expression Atlas in Mammals: Implications for Biology and Medicine.” *Proceedings of the National Academy of Sciences of the United States of America*. https://doi.org/10.1073/pnas.1408886111.

Zhao, Xuan, Han Cho, Ruth T. Yu, Annette R. Atkins, Michael Downes, and Ronald M. Evans. 2014. “Nuclear Receptors Rock around the Clock.” *EMBO Reports*. https://doi.org/10.1002/embr.201338271.

Chapter 2

Chapter 2 A Temperature Shift Model to Study Clock Gene Expression in Cell Culture

2.1 Introduction

Cells in culture are assumed to be an unsynchronized population (Jackman and O'Connor 1998). Various protocols have been used to synchronize and manipulate cells in order to obtain sufficient quantities of products for reliable assays or to study various aspects of cell growth and metabolism. Many methodologies use drugs or chemicals such as hydroxyurea or thymidine to arrest cells at specific phases of the cell cycle (Rieder and Cole 2002) (Harper 2005). Cold shock, where cells are exposed to low temperature conditions (30° C) for several hours, results in cells progressing through the cell cycle but more slowly due to G_1/S arrest (Enninga *et al*. 1984). Different cell lines exhibit differing sensitivities and kinetics to cold shock (Rieder and Cole 2002). While the specific mechanisms involved in the impact of cold stress on cell growth and metabolism have not been fully elucidated, the pharmaceutical industry has exploited the fact that some cell lines have improved recombinant protein yields when cultured at sub-physiologic temperatures (Al-Fageeh *et al.* 2006). The use of more subtle temperature changes have also been demonstrated to act as a peripheral *zeitgeber* for circadian oscillators (Buhr, Yoo, and Takahashi 2010) (Brown *et al*. 2002). The intact SCN is not impacted by temperature change, perhaps due to specific aspects of their electrical physiology, whereas the mechanism for peripheral oscillators may be mediated through the heat shock factor 1 (HSF-1) pathway (Buhr, Yoo, and Takahashi 2010). Contact inhibition, centrifugal elutriation, and serum deprivation are

considered other drug- and chemical-free means of cell – cycle synchronization in mammalian cell culture (Davis, Ho, and Dowdy 2001).

The idea that peripheral clocks could be studied independently in a cell culture model was first described using a serum shock model where synchronization of circadian oscillation of clock genes was induced in rat fibroblasts and hepatoma cells (Balsalobre, Damiola, and Schibler 1998). In these experiments, the serum content of the media was changed from a low concentration (5% for 6-7 days) to 50% for a minimum of two hours which promoted almost synchronous entry into the circadian cycle and synchronous expression of many clock and clock-controlled genes (Balsalobre, Damiola, and Schibler 1998). Subsequent to this, it was demonstrated that various drugs or chemicals such as dexamethasone, calcimycin, phorbol 12-myristate 13- acetate (PMA), or forskolin could induce expression of PER1 but not PER2 (Balsalobre *et al.* 2000). Cell synchronization protocols have frequently been used in human breast cancer cell lines where the expression levels of the clock genes appear to be endogenously low but when the cells are synchronized in the circadian cycle the proportion of cells that express clock genes as measured by mRNA transcripts and/or protein expression is increased allowing detection by current methods (Lellupitiyage Don *et al*. 2019)(Gutiérrez-Monreal *et al.* 2016)(Rossetti *et al.* 2012). In addition, some cell lines such as the mouse melanoma B16, can be induced to express latent circadian rhythms using dexamethasone (Kiessling *et al.* 2017).

Clock genes are abnormally expressed in breast cancer tissues (Lesicka *et al.* 2019)(Lesicka *et al.* 2018)(Winter *et al.* 2007)(Chen *et al.* 2005). Although it can be challenging to demonstrate detectable levels of these transcripts in breast tumors, CLOCK is upregulated in tumor tissue as compared to adjacent non-neoplastic tissue and PER1, PER2, and CRY2 are down-regulated (Lesicka *et al*. 2018). PER1 and PER2 display altered gene expression in both

familial and sporadic breast cancers (Winter *et al*. 2007). Some evidence indicates that clock gene polymorphisms can be detected in breast cancer patients and that mutations in CRY2, PER1, and PER2 are associated with an increased cancer risk; notably mutations in PER2 are associated with cancer risk in hormone-positive patients (Lesicka *et al.* 2019). Other research has demonstrated abnormalities in the circadian expression of PER1 and PER2 in cancerous breast tissue that are the result of hypermethylation of their promoter regions; a change more associated with epigenetic influence on gene expression (Chen *et al.* 2005).

Occupational and life style choices, including shift work and the frequent passage across multiple time zones due to air travel, could contribute to the non-genetic factors that affect circadian regulation including glucocorticoid hormone influences (Kiessling, Eichele, and Oster 2010). Rodents that experience feeding restricted to their non-active period experience out of phase desynchrony between the peripheral circadian oscillators of the liver and the SCN (Damiola *et al*. 2000). It has been postulated that chronic dissociation of the peripheral oscillators from the central clock leads to disease (Robinson and Reddy 2014). In a mouse model of jet lag, desynchrony between the central and peripheral oscillators was demonstrated and while treatment with glucocorticoids can partially reset peripheral clocks, the response is highly tissue-specific (Kiessling, Eichele, and Oster 2010).

An increase in clock gene expression in response to serum shock synchronization has been demonstrated to decrease the proliferation of breast cancer cells in culture (Rossetti *et al*. 2012). Dexamethasone exposure increases circadian expression of clock genes in B16-BL6 mouse melanoma cells and decreases cell growth (Kiessling *et al.* 2017). These authors, (Kiessling *et al.* 2017) also demonstrated that the *S* phase of the cell cycle was shortened by dexamethasone treatment and that some of the genes that control cell cycle regulators were

expressed at increased levels. However, it is not clear whether this is an independent effect on the cell cycle mediated by glucocorticoid receptors or whether it is a consequence of the improved circadian gene expression.

Per2 mutant (m/m) mice are at risk of developing tumors before 6 months of age (Fu *et al*. 2002). Mice that lack a functional PER2 due to a mutation or to a knock-out of BMAL are at increased risk of lung cancer (Papagiannakopoulos *et al.* 2016). These findings, plus the *in vitro* experiments using MCF-7 cells where increased PER2 expression is associated with decreased cell proliferation, decreased anchorage-independent growth, and increased apoptosis, support the hypothesis that PER2 has tumor suppressor-like function (Xiang *et al.* 2008). This may be secondary to some regulatory feature that PER2 exerts on p53 by protein-protein interaction (Gotoh *et al.* 2016) or by having a stabilizing influence on its degradation (Gotoh *et al*. 2014). The relationship seems bidirectional because p53 regulates the expression of PER2 through competitive binding of the E-Box in the promoter region of PER2; the target of the CLOCK:BMAL transcriptional activators of the positive arm of the TFFL (Miki *et al.* 2013). In the canonical scheme of the core loop which drives the daily oscillations, it is the E-boxes of PER 1-3 and CRY 1/2 that are the targets of CLOCK:BMAL (Pilorz *et al.* 2020). A large percentage of the transcriptome oscillates in a circadian fashion (Li and Zhang 2015)(Zhang *et al.* 2014) with 5-20% of tissue-specific transcripts displaying temporal circadian oscillation (Takahashi 2017). The binding to E-box sites is thought to be one mechanism by which the core clock genes regulate the expression of other genes such as albumin D-site binding protein (DBP) which can also be regulated through binding to D-boxes and RORE elements (Ueda *et al.* 2005). HSF-1, an important component of the heat shock response, has also been identified as a circadian transcriptional activator (Reinke *et al.* 2008). Circadian regulation by transcriptome

control is only one element in a vast and complex network of clock-influenced pathways (Takahashi 2017).

Evidence of circadian influence on cell cycle kinetics has come from clock gene knock-out mice and from time lapse studies in cultured cells. Comparing DNA microarray data from wild type and CLOCK -/- mouse liver and skeletal tissue demonstrates that the CLOCK-/- tissue has altered gene expression profiles particularly in genes that control the cell cycle and that fibroblasts isolated from these mice exhibit slower cell proliferation rates (Miller *et al*. 2007). Cry1,2 -/- deficient mice experience slower liver regeneration after partial hepatectomy which seems to be due to the dysregulation of CLOCK:BMAL transcriptional control over the antagonistic regulators of the G_2/M checkpoint, WEE1 and Cdc25 (Matsuo *et al.* 2003). Per2 (m/m) mice demonstrate dysregulated cyclin D and cyclin A expression levels when compared to the control cells and thymocytes isolated from the mutant mice were resistant to apoptosis after γ irradiation due to decreased levels of intracellular p53 (Fu *et al.* 2002). In a genetically-engineered mouse model of lung adenocarcinoma, introducing additional Per2 (m/m) or BMAL -/- mutations in the mice increased lung tumor severity and increased tumor burden when the animals were placed on a L:D disrupted cycle while c-Myc expression was upregulated in their tumor cells (Papagiannakopoulos *et al.* 2016). More direct evidence linking the circadian and cell cycles is derived from *in vitro* experiments. Unsynchronized mouse fibroblasts (NIH 3T3 cells) were examined for both clock gene expression using a REV-ERBα:VENUS promoter-reporter and for ubiquitination using a fluorescence – based cell cycle indicator (FUCCI). The results of these studies demonstrated that the two cycles exhibited the same period length and are phased locked with the expression of the reporter peaking 5 hours after cell division (Feillet *et al.* 2014). The circadian cycle was affected by manipulating the cell cycle length and

synchronization following treatment with dexamethasone which resulted in two populations of cells; one still phase locked 1:1 and a second which demonstrated 3 cell cycles for every 2 circadian cycles (Feillet *et al.* 2014). Feillet *et al.* (2014) concluded that the connection between circadian and cell cycles was bidirectional however when the circadian cycle is lengthened in the same cell line using temperature differences, gene knock outs, or chemicals, the cell cycle becomes synchronized, leading others to conclude that the influence is unidirectional (Bieler *et al.* 2014). Synchronization of peripheral circadian oscillators as measured in liver cells by feeding (*in vivo* models) or serum shock synchronization (*in vitro)* presents a dilemma in adapting these models because hepatocytes are metabolically primed by food. For example, simply meal feeding versus *ad libitum* food availability, slows down tumor progression in mice. Therefore, increased cancer risk or risks of other diseases in response to night shift work, may not only be a case of light at night exposure but may also result from changes in daily eating/fasting habits indicating that feeding is a critical factor that must be controlled for in *in vivo* experiments that involve the whole organism which is constituted by a wide variety of cell types (Wu *et al.* 2004).

One of the body functions that shows changes that follow a daily rhythm are the fluctuations in body temperature, therefore the use of temperature as a synchronization method for mammalian has some theoretical basis (Albrecht and Eichele 2003). Cold shock has been described for cell cycle synchronization but not for clock gene oscillation (Enninga *et al.* 1994). The use of temperature pulses of 38.5° C applied to the tissues of $Per2^{Lucfierase}$ mice, otherwise maintained at 36° C, results in the resetting of peripheral clock genes (Buhr, Yoo, and Takahashi 2010). The circadian oscillation of body temperature has been validated in humans (Bailey and Heitkemper 2000) and described in a number of other species (as reviewed by Refinetti 2010).

The standard circadian laboratory reference for light: dark is described as intervals of 12-hour lights on and 12-hour lights off and core body temperature appears to be synchronized to the day: night cycle (as reviewed by Benstaali *et al.2001).* The purpose of the current study was to investigate whether repetitive temperature shifting spanning intervals of 12 hours to correspond to a circadian frequency, could result in the increased expression of clock genes in a cell culture model.

2.2 Materials and Methods

Cell culture

A human hormone responsive breast cancer cell line, MCF-7, a non-malignant human breast epithelial cell line, HBL-100, and a murine melanoma cell line, B16-BL6 , all originally obtained from the American Type Culture Collection (ATCC) were maintained in Hyclone Debucco's Modified Eagle Media (DMEM) with high glucose (GE Lifesciences®) and supplemented with 10% fetal bovine serum (FBS) and 1% antibiotic and anti-mycotic Solution® (A&A) (Fisher Scientific). The cells were maintained in a humidified environment at 37^{o} C and 5% CO_2.

Experimental protocols

A circadian rhythm in the cultured cells was induced by treatment with the temperature shift method. The temperature shift technique consisted of culturing cells for several days in an oscillating temperature environment: cells were kept in the 37^{o} C environment from 09:00 to 21:00 and transferred to a humidified incubator maintained at 34^{o} C also supplemented with 5% CO_2 from 21:00 to 09:00. The number of consecutive days of temperature shifts is presented in each aspect of the experiment. In addition, two other conditions were maintained for the duration of the experiment; a control condition where the cells were maintained at 37^{o} C with no shift, named control 37/37° C and a comparative condition where the cells were maintained at 34^{o} C continuously, named comparative 34/34° C; with each condition kept in separate humidified incubators and also supplemented with 5% CO_2. Cells were seeded in 100 mm tissue culture plates (100 mm diameter) at a dilution of 1:8 from a confluent parental plate on the first day of the shift experiment. For each experiment, 9 separate plates were created for each

condition, for a total of 27 plates. For most experiments, the cell cultures were shifted for 7 consecutive days and the cells harvested and collected on day 7 at nine different time points over 24 hours. Cells would typically reach confluence by day 4 and require reseeding (splitting). Experiments were performed in triplicate.

The effect of the experimental conditions on cell proliferations was determined by cell counting and viability assays. For cell counting, cells were seeded in 60 mm tissue culture plates initially at 50,000 cells/plate for the MCF-7 and HBL-100 cell lines and 25,000 cells/plate for the B16-BL6 line. Counts were done at approximately the same time of day for 5 consecutive days using a hemocytometer after adding trypan blue stain.

Cell viability was measured using the 3-(4,5-dimethylthiazol-2-yl) -2,5 – diphenyltetrazolium bromide assay (MTT). For each assay, 96 well plates were seeded at 2,000 cells/well in 200 µl media in triplicate and duplicate plates were allowed to grow under the indicated culture conditions. The MTT assay was performed daily for 10 days using the lab protocol; 10 µl of 5 mg/ml MTT was added to each well of the plate and then incubated at 37^{o} C for 3 hours. Then, the media was removed and replaced with 100 µl of Dimethyl sulfoxide (DMSO) to solubilize the produced formazan crystals. The plate wells were read at 540 nm wavelength on a Synergy® H4 Hybrid plate reader (Biotek) using Gen 5, version 2.00 software.

Serum Shock

A circadian rhythm was induced in cultured cells using the serum shock protocol. MCF-7 cells were grown in cell culture as previously outlined and seeded on to 100 mm tissue culture plates. After a minimum of 24 hours, the serum shock protocol, as previously described, was followed (Balsalobre, Damiola, and Schibler 1998). The cell cultures were serum deprived for

24 hours, and then serum shocked by treatment with 50% fetal bovine serum (FBS) for 2 hours. The cultures were then washed with PBS, pH 7.4, and maintained in media containing 10% FBS serum throughout the collection period. Cells were collected for flow cytometry analysis, protein assays, or RNA isolation at different time points over 24 hours, as indicated.

Protein extraction and Western Blotting

The levels of circadian control proteins were determined by western blot analysis of whole cell lysates. Cells were washed with ice cold PBS, pH 7.4, and the cells collected in 300 µl of ice cold radioimmunoprecipitation assay (RIPA) buffer containing 150 mM sodium chloride, 15 mM phosphate buffer, pH 7.4, 1% Triton-x 100, 0.5% sodium dodecyl sulfate (SDS), 0.5% sodium deoxycholate, 10 mM sodium fluoride (NaF), 10 mM sodium orthovanadate, and protease inhibitor cocktail (Thermo Scientific™ Pierce™ Protease Inhibitor Tablets). All reagents were obtained from Fisher Scientific unless otherwise indicated. The whole cell lysate was then collected using a plastic cell scraper. DNA and cellular cytoskeleton components in the cell lysates were sheared by passage through a 22 gauge needle several times and then stored at -80^0 C. Protein quantification was done using the bicinchoninic acid (BCA) assay (Thermo Scientific™ Pierce™ BCA Protein Assay Kit) versus a bovine serum albumin standard curve and read using a Synergy® H4 Hybrid plate reader (Biotek) using Gen 5, version 2.00 software. Electrophoresis was conducted using 25 µg of protein loaded onto 15 % polyacrylamide gels containing sodium dodecyl sulfate. After electrophoresis, the gels were transferred onto nitrocellulose membranes using a semi-dry protein transfer apparatus and the protein transfer was confirmed by Ponceau staining of the nitrocellulose membrane. The membranes were blocked by incubation in 5% low fat milk or 5% Bovine Serum Albumin (BSA) in Tris-buffered saline containing 0.1% Triton-20 (TBST), depending on the optimization protocol for the

antibody, overnight at 4^0 C. Primary antibodies were incubated with the membranes in 5% low fat milk or 1 % BSA in TBST at the dilutions listed below, overnight at 4^0 C. Secondary antibody-horseradish peroxidase conjugates were incubated at a dilution of 1:10,000 in TBST for 2 hours at room temperature. Chemiluminescent detection using the Thermo Scientific™ enhanced chemiluminescence (ECL) detection reagents was performed prior to membrane exposure to radiographic film or detection using a Gel documentation system.

All antibodies were obtained from SantaCruz Biotechnology. Primary antibodies against PER1 and PER2 were used at 1:500 dilutions in 5% low fat milk in TBST for blocking and for primary and secondary antibodies. Primary antibodies against p21, cyclin A, cyclin D_1 and cyclin E were used at a dilution of 1:200, cyclin B was used at a dilution of 1:100, and GAPDH was used at a dilution of 1:2000 using 5% BSA in TBST for blocking and in 1% BSA in TBST for the primary and secondary antibodies.

Flow cytometry for Cell Cycle Analysis

The DNA content of cells was determined by flow cytometry of propidium iodide-stained cells. Cells monolayers were washed with room temperature PBS, pH 7.4, and harvested with trypsin until detachment. The cells were collected by pipetting and placed in 1 ml Eppendorf vials and collected by centrifugation at 2000 rpm for 5 minutes. The supernatant was discarded and the cells resuspended in PBS, pH 7.4, and re-centrifuged. The remaining pellet was collected after decanting the supernatant and the cells resuspended in 70% ethanol and immediately stored at -20^0 C. Prior to analysis, the thawed samples were washed twice with PBS, pH 7.4, and centrifuged each time at 1000 rpm for 5 minutes. A propidium iodide (PI) stain solution, made up of 2 mg/ml propidium iodide and 100 μg/ml RNase, was added to a resuspended sample in 500 μl of PBS at a ratio of 1:1. The cells were incubated for 2 hours and

samples analyzed on a Cytomics FC 500 flow cytometer (Beckman Coulter). Images were analyzed using the cytomics software and then transferred to the Paint® program from the Beckman Coulter software.

Gene expression analysis using Reverse Transcriptase quantitative PCR (RT-qPCR)

The level of gene expression was determined using RT-qPCR of RNA purified from the cell cultures. RNA was prepared from cells in 100 mm culture plates lysed in a fixed volume of 500 µl of denaturing solution containing 4 M guanidinium thiocyanate, 25 mM sodium citrate, 0.1% N- laurosylsarcosine, and 0.1 M 2-β-mercaptoethanol as outlined (Chomczynski and Sacchi 2006). After immediate collection using a plastic cell scraper, the sample was stored at -80^0 C prior to RNA purification and solubilization using the phenol-chloroform extraction technique as described. RNA quantification based on an OD260 was determined using a spectrophotometer (Nanodrop®). A sample, corresponding to 100 ng of RNA was reverse transcribed using the protocol from the Superscript IV Vilo Master Mix without ezDNAse enzyme treatment as per Life Technologies®. Oligo-dT-primers were annealed at 25° C for 10 minutes and RNA reverse transcription allowed to proceed with incubation at 50° C for 10 minutes, and then the enzyme was inactivated for 5 minutes at 85° C using a thermocycler. Clock gene ID Taqman® assays were obtained from Life Technologies®. For some genes, these assays are inventoried and others were custom produced. The assay numbers are as listed: PER1, Hs00242988_m1; PER2, Hs01007553_m1; CLOCK, Hs00231857_m1; BMAL (ARNTL), Hs00154147_m1; CRY1, Hs00172734_m1; CRY2, HS00901393_m1; DBP, Hs00609747_m1; GAPDH, Hs02786624_g1; NR1 D1, Hs00253876_m1; PPIA, Hs04194521_s1; and, RPS17, Hs00734303_g1. Taqman® gene assays were performed using the Agilent Aria MX thermocycler using 80 ng of cDNA/sample. The Thermo Fisher protocol

for the TaqMan® Fast Advanced Master Mix was followed which consisted of UNG incubation for 1 cycle at 50° C for 2 minutes, enzyme activation for 1 cycle for 30 seconds at 95° C, and 40 cycles of alternating denaturing and annealing at 95° C for 1 second and 60° C for 20 seconds respectively. As per the Taqman ® technical bulletin the amplification efficiency is assumed to be 1 and a melting curve analysis is not completed due to regent consumption. Reference gene validation was determined as described below. Gene expression was measured using the 2^ΔΔCT method in accordance with the Minimum Information for Publication of RT-qPCR Experiments (MIQE) Guidelines (Bustin *et al*. 2009).

Reference Gene Selection and Validation

The Taqman® Human Endogenous Array Control Panel (Applied Biosystems®) was used to identify suitable housekeeping or reference genes against which to compare the genes of interest in both the experimental and control conditions. A 96 well plate is factory prepared with 32 previously identified reference genes. Samples of 3 different time points (0, 4, and 8 hours) of experimental samples derived from an independent shift experiment were loaded into the wells as described in the manufacturer's protocol. The replicates were compared across all 32 reference genes. Two genes, RPS17 and PPIA, were selected as reference genes based on the lowest coefficients of variation. These results are available in Appendix 1. The RPS17 gene encodes for a subunit of ribosomal proteins. Peptidylprolyl Isomerase A (PPIA) is a coding gene for a constituent cellular protein.

Relative ATP Luminescence

The level of adenosine triphosphate (ATP) present in the cells was detected using the Luminescent ATP Detection Assay Kit®. The kit was purchased from Abcam and the protocol

was followed as per the manufacturer's instructions. Cells were seeded onto 96 well plates which included three replicates for two different concentration of cells. Two plates were plated for each condition. The plate outlay was as per the protocol recommendations with the exception of two plates in the 34/34° C condition, where each plate had only 1 x 9 control replicates versus 2 replicates for the others. Temperature shift for the experimental plates commenced 48 hours prior to assay. Assays were started at 13:00 or 01:00 and after preparation. The level of luminescence following incubation of the lysed cells with luciferin and firefly luciferase where the light emitted corresponds with the level of ATP present versus an ATP standard, was measured using a Synergy® H4 Hybrid plate reader (Biotek) using Gen 5, version 2.00 software, set for luminescent detection.

Statistical Analysis

SPSS ® statistical software (IBM) or GraphPad Prism 5.0 was used for statistical analysis as indicated. The data was subjected to a normality test using the normality function within GraphPad, and if appropriate, $p<0.05$, a one analysis of variance (ANOVA) was used to compare groups with a post hoc Tukey test; otherwise Kruskal Wallis with a Dunn's comparison of groups as the post hoc was used. Unless otherwise stated, statistical significance was determined as $p<0.05$. Error bars within graphs indicate standard error of the mean (SEM), unless otherwise indicated.

2.3 Results

The total daily cell counts for MCF7 cultured using the temperature shift protocol over 5 days are displayed in Figure 2.1.

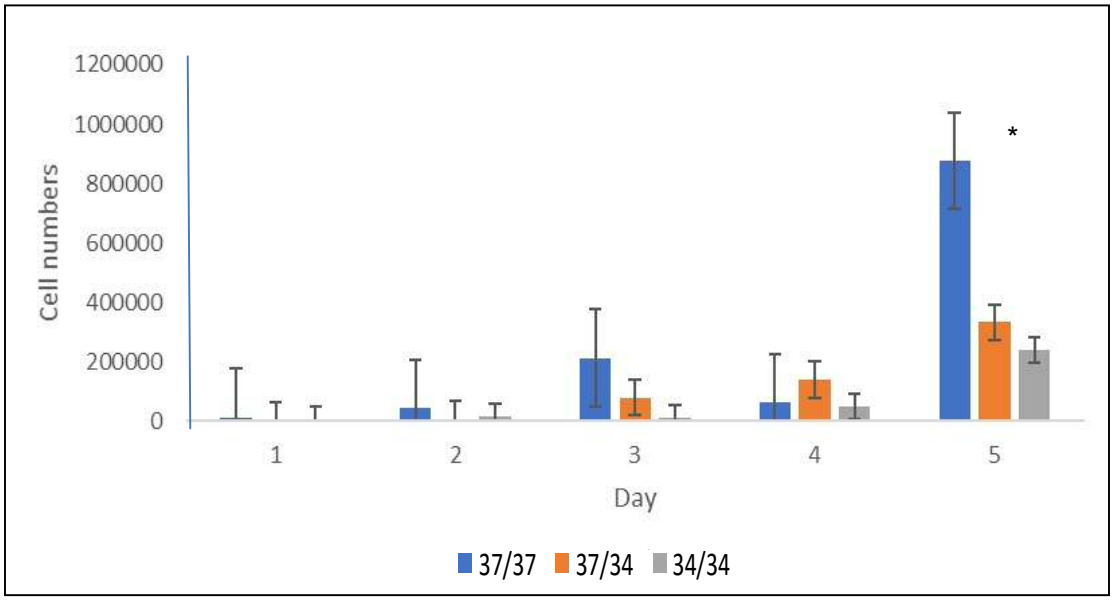

Figure 2.1. Comparison of daily cell counts of MCF-7 cells exposed to different temperature shift conditions. MCF-7 cells were cultured in media and incubated at 37° C for 24 h/day (blue), 37° C from 09:00 - 21:00 h and 34° C from 21:00-09:00 h (brown), or 34° C for 24 h/day (grey). Duplicate cultures were harvested each day for 5 days and trypan-blue stained cell suspensions counted in quadruplicate using a hemocytometer (n=6, $p<0.05$).

The only statistically significant difference in cell numbers for MCF-7 cells was shown for cells cultured at day 5 and between the control 37/37° C and the experimental 37/34° C conditions as the control numbers were much higher. This difference was also seen between the control and 34/34°C comparative condition but not between the 37/34° C and the 34/34° C sets. The results were repeated in parallel experiments with the HBL-100 and B16-BL6 cell lines with similar results with the exception that at day 5 all three conditions have significant differences

between them as displayed in Figure 2. 2. It appears that MCF-7 cell proliferation is less inhibited by culture at the 34/34°C condition than are the other cells lines.

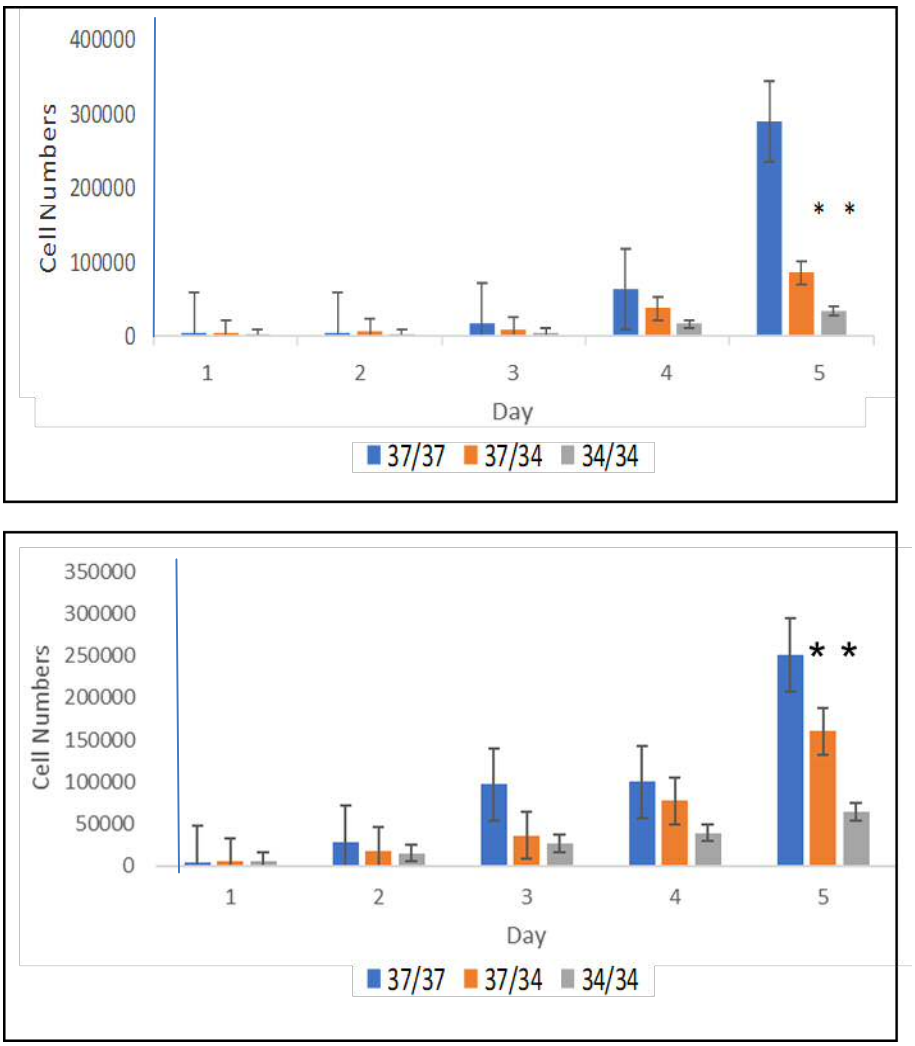

Figure 2.2 Comparison of cell counts of HBL-100 and B16-BL6 cells exposed to different temperature shift conditions. HBL-100 (top panel) and B16-BL6 cells (lower panel) were cultured in media and incubated at 37° C for 24 h/day (blue), 37° C from 9:00 - 21:00 h and 34° C from 21:00-9:00 h (brown), or 34° C for 24 h/day (grey). Duplicate cultures were harvested each day for 5 days and trypan-blue stained cell suspensions counted in quadruplicate using a hemocytometer (n=6, $p<0.05$)

The MTT assay was used for only two cell lines and the results for both the MCF-7 and B16-BL6 cells exposed to the temperature shift conditions are displayed in Figures 2.3 and 2.4, respectively. A two-way ANOVA (SPSS®) demonstrated statistical significance for the effect of temperature shift on viable cell number for both cell culture lines. The two-way ANOVA (SPSS®) are available in Appendix 2. The temperature shift resulted in a significant reduction in MTT absorbance at 7 days in both cell lines, after which point, the control cells have exhausted the media and don't survive. The MTT assay results parallel the cell count data.

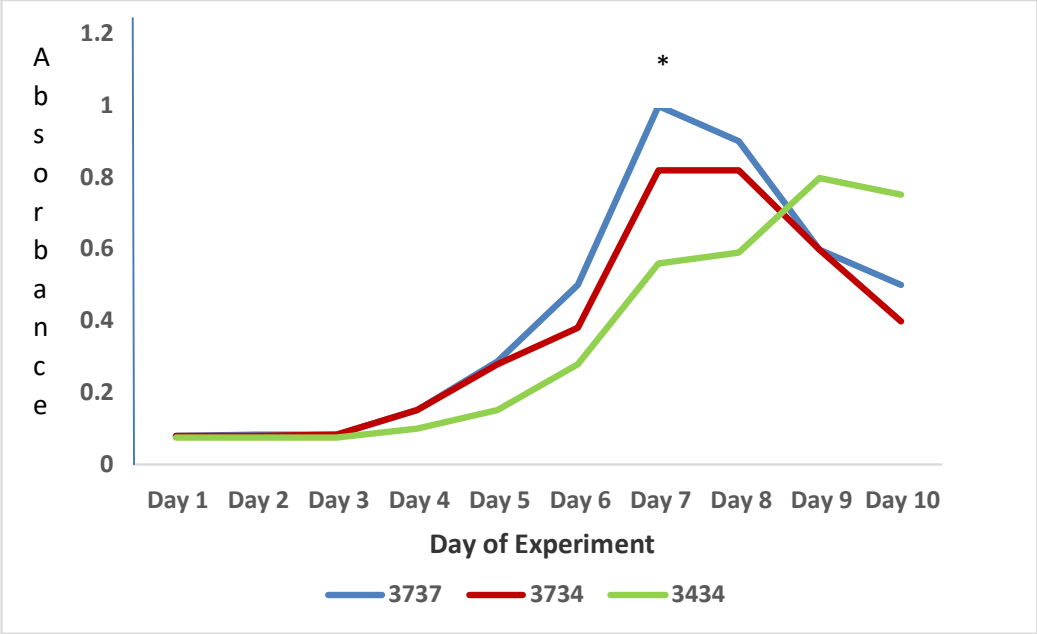

Figure 2.3. Daily results from the MTT assay for MCF-7 cells exposed to different temperature shift conditions. Cells were plated on 96 well plates and cultured at 37° C for 24 h/day (blue), 37° C from 9:00 - 21:00 h and 34° C from 21:00-9:00 h (brown), or 34° C for 24 h/day (green) and each day a replicate plate was assayed for MTT reducing activity. The MTT reagent (5 pg/well) was incubated with the cells for 3 h and the resulting brown precipitate, formazan, was solubilized in DMSO and absorbance read at OD540 which corresponds to the viable cells (n=3, $p<0.05$)

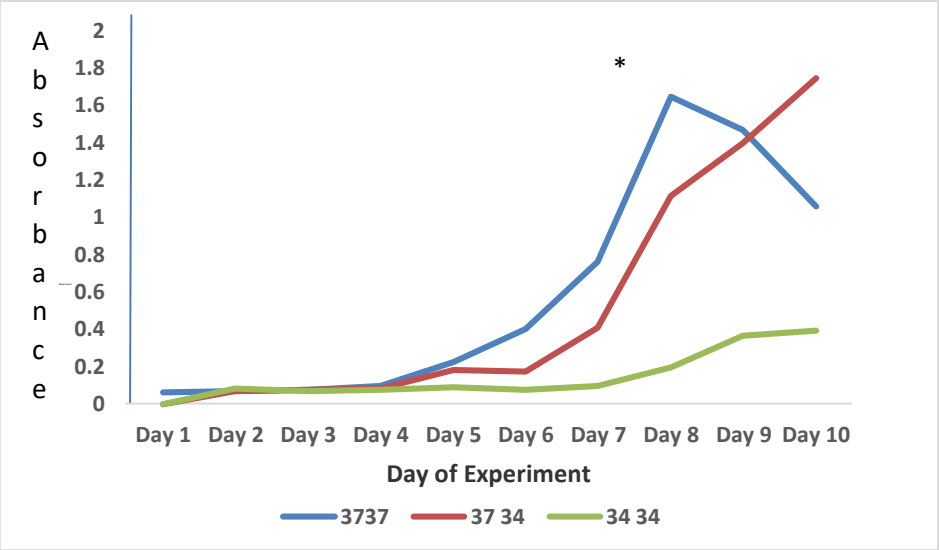

Figure 2.4. Daily results from the MTT assay for B16-BL6 cells exposed to the different temperature shift conditions. Cells were plated on 96 well plates and cultured at 37° C for 24 h/day (blue), 37° C from 09:00 - 21:00 h and 34° C from 21:00-09:00 h (brown), or 34° C for 24 h/day (green) and each day a replicate plate was assayed for MTT reducing activity. The MTT reagent (5 pg/well) was incubated with the cells for 3 h and the resulting brown precipitate, formazan, was solubilized in DMSO and absorbance read at OD540 which corresponds to the viable cells (n=3, $p<0.05$)

For the data on cell counts using trypan blue, after 5 days of culture the cells were shown to be confluent on the 60 mm culture plates resulting in inhibition of cell proliferation (contact-dependent inhibition) and the trypan blue stain uptake increased noticeably indicating reduced cell viability. The MTT assay, a colorimetric assay, measures differences in cell metabolism by correlating the amount of MTT absorbance with quantity of nicotinamide adenine dinucleotide phosphate (NADPH) present which reduces the MTT dye to formazan. MCF-7 cells displayed maximum absorbance for cells cultured under the 37/37^{o} C and the 37/34^{o} C conditions at day 7. The 34/34^{o}C condition-treated cells did not peak in absorbance until day 9. At day 10, B16-BL6 cells in both the 37/34^{o} C and 34/34^{o} C conditions did not appear to have peaked while the 37/37^{o}

C cells peaked at day 9. The MTT assay is essentially a test of metabolically active cells but is often used to imply relative differences in cell viability. These results comparing raw cell numbers and MTT relative absorbance, indicated that in this study using MCF-7 and B16-BL6 cells, the MTT accurately reflects viable cells.

Flow cytometry was performed to query if the reduction in cell numbers and the decrease in the MTT assay were due to differences in cell cycle dynamics. Lowering the ambient temperature to 34° C has been demonstrated to lengthen the cell cycle (Bieler *et al.* 2014). The 3 conditions did not demonstrate notable differences in the relative proportion of the cells in either the interphase (*G1* and *S* phases) or the mitosis phases over a 24 h period post-shift at 4 days. These data are demonstrated in Figure 2.5. The four-day duration of the experiment precludes the requirement to split or passage cells so that media changes and reseeding are not variables.

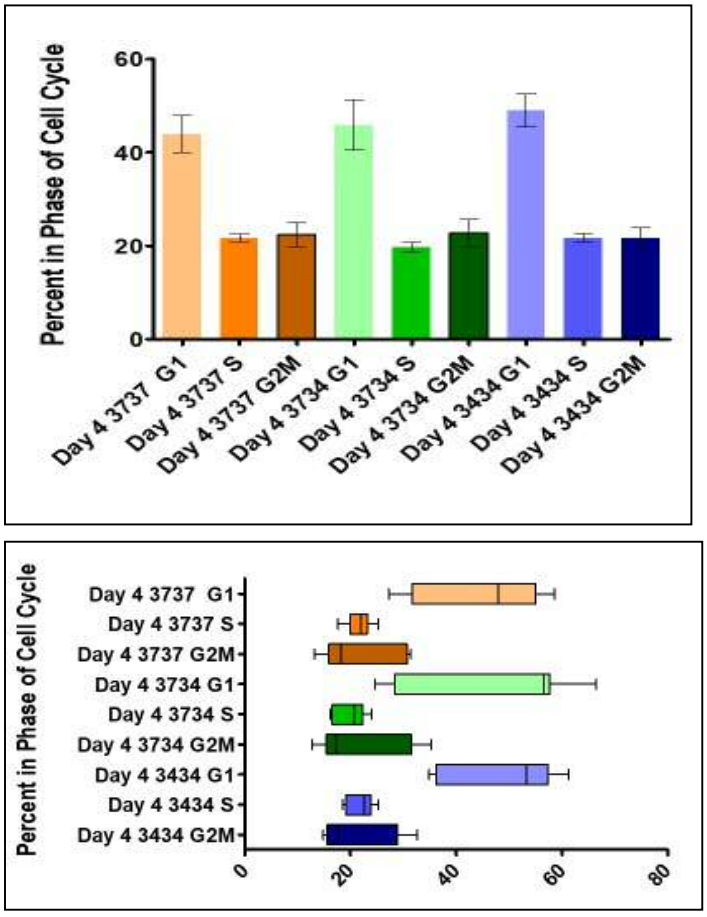

Figure 2.5. Graphical display comparing the proportion of cells in each cell cycle phase at day 4 of the temperature shift treatment. MCF-7 cells were cultured in media and incubated at 37° C for 24 h/day (brown), 37° C from 09:00 - 21:00 h and 34° C from 21:00-09:00 h (green), or 34° C for 24 h/day (blue) for 4 days. The cells were harvested, fixed in 70% methanol, stained with propidium iodide, and analyzed on a flow cytometer to determine the percentage of cells in each phase of the cell cycle (n=3, $p<0.05$)

After exposing the cells to seven days of the temperature shift protocol, no significant differences in cell cycle phases were detected between the control (37/37° C) and the experimental conditions (37/34° C), as presented in Figure 2.6. Statistical differences were shown when comparing the *S* phases between both the control and experimental conditions and the comparative 34/34° C condition such that a lower percentage of cells occurred in the *S* phase in the comparative 34/34° C condition.

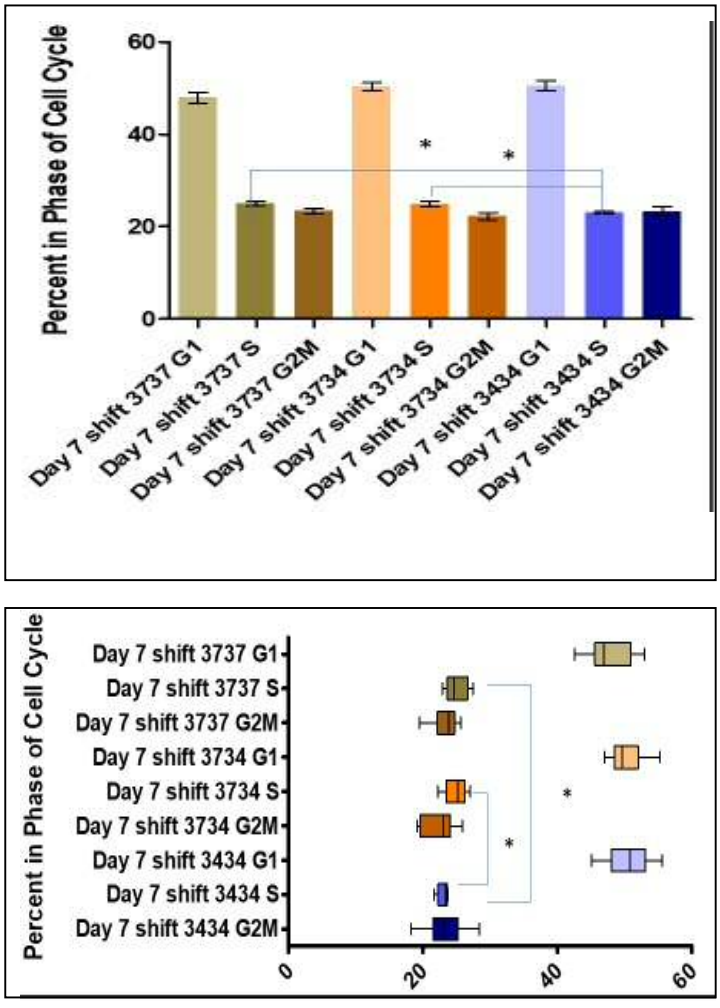

Figure 2.6. Graphical display comparing cell cycle phases at day 7 of shift. MCF-7 cells were cultured in media and incubated at 37° C for 24 h/day (brown), 37° C from 09:00 - 21:00 h and 34° C from 21:00-09:00 h (green), or 34° C for 24 h/day (blue) for 7 days. The cells were harvested, fixed in 70% methanol, stained with propidium iodide, and analyzed on a flow cytometer to determine the percentage of cells in each phase of the cell cycle (n=3, $p<0.05$)

However, after 14 days on the temperature shift cycle, the MCF-7 cells showed some changes in the cell cycle kinetics between the control and e: * imental conditions. The proportion of cells in the *S* phase was significantly higher in the experimental shift cells as presented in Figure 2.7. This became a consideration in selecting experimental duration.

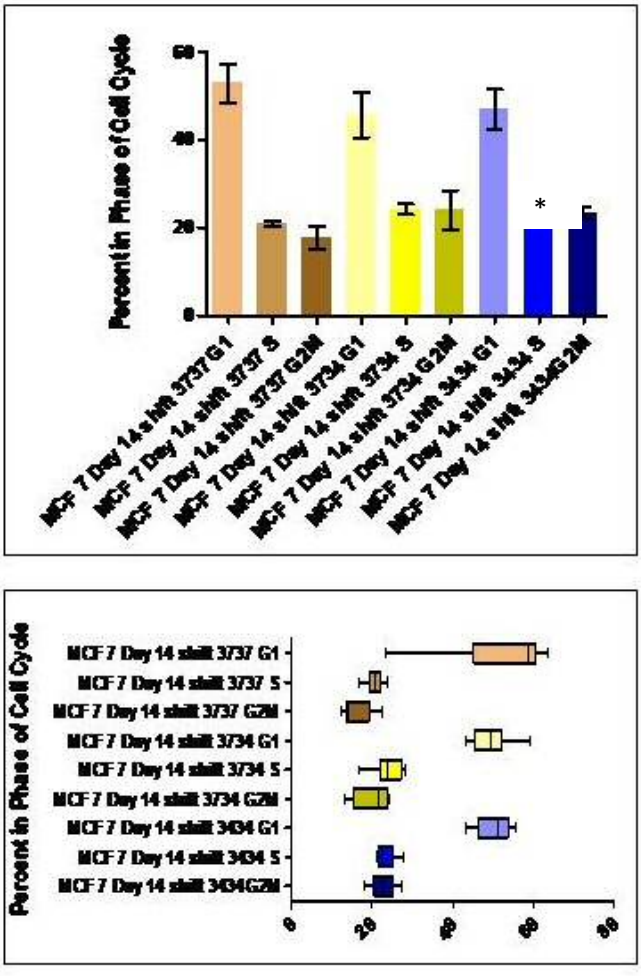

Figure 2.7. Graphical display comparing cell cycle phases at day 14 of temperature shift. MCF-7 cells were cultured in media and incubated at 37° C for 24 h/day (brown), 37° C from 09:00 - 21:00 h and 34° C from 21:00-09:00 h (green), or 34° C for 24 h/day (blue) for 14 days. The cells were harvested, fixed in 70% methanol, stained with propidium iodide, and analyzed on a flow cytometer to determine the percentage of cells in each phase of the cell cycle (n=3, $p<0.05$).

The histograms, as displayed in Figure 2.8, are typical of those derived from the cell cycle analysis between the control and experiential conditions and provide further evidence that when compared on a time by time point basis, there is little difference between the two conditions.

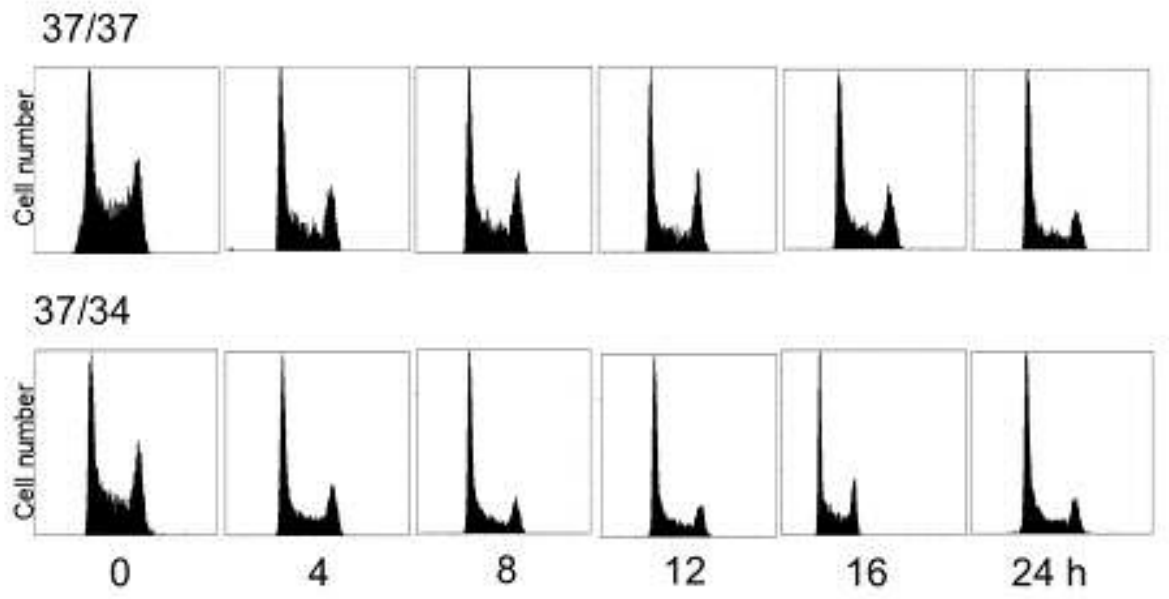

Figure 2.8. Histograms for flow cytometer of MCF-7 cells at 7 days of temperature shift. Images in the top row represent the histograms of cells exposed to the 37/37° C control condition harvested at time points 0, 4, 8 ,12 16 and 24 hour respectively with time 0 = 09:00. Images in the lower row represent the histogram of cells exposed to the 37/34° C experimental condition harvested at time points 0, 4, 8 ,12 16 and 24 hour, respectively with time 0 = 09:00(n=3).

These cell cycle results from MCF-7 cells subjected to the temperature shift protocol differed from the cell cycle flow results of cells induced by the serum shock method. Post-serum

shock, MCF-7 cells were synchronized in G_1 and remained there for approximately 4 hours before moving sequentially, and still synchronized in phase, through the S and G_2/M phases to achieve a bimodal peak within 12 hours and the population returning to principally G_1 by 24 hours post serum shock. This is displayed in the histograms obtained by flow cytometry analysis and are displayed in Figure 2.9.

Therefore, serum shock impacts the cell cycle through cell cycle synchronization while exposure of the cells to a temperature shift protocol for 4 - 7 days of experimental procedure does not cause changes in the cell cycle. Given that MCF-7 cells proliferate at a slower rate when treated with the temperature shift protocol, it is assumed that the duration of the cell cycle is longer. This cannot be attributed to arrest in any particular phase as measured by flow cytometry.

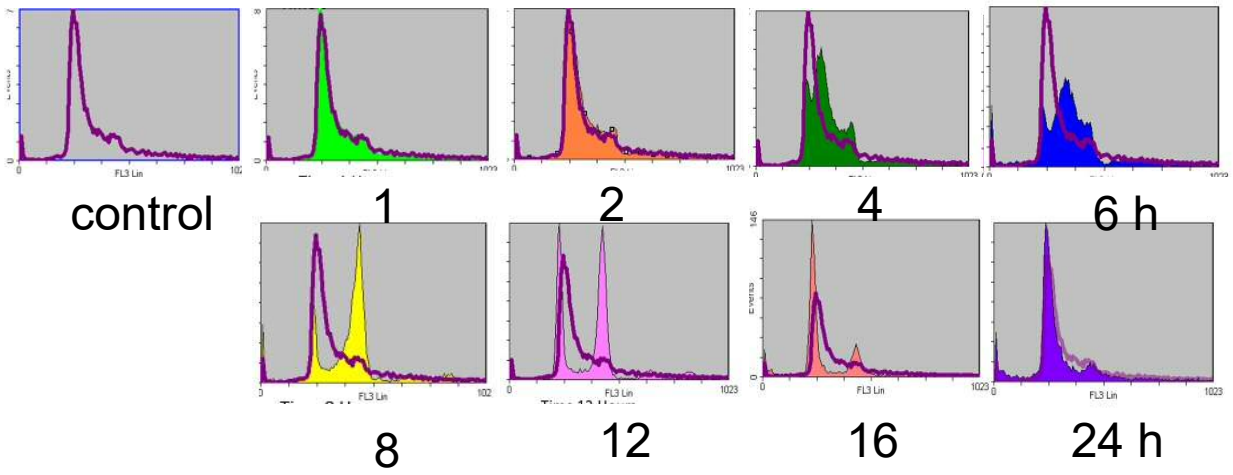

Figure 2.9. Cell cycle changes demonstrated in MCF-7 cells over 24 hours in response to treatment using a serum shock protocol. Cells were serum starved overnight and then treated with media containing 50% FBS for 2 h. The cells were then cultured in media containing 10% and collected at different times. The cells were fixed and stained in propidium iodide and analyzed by flow cytometry (n=3).

To explore differences in energy metabolism in temperature-shifted cells as suggested by the MTT assay, relative ATP production was measured using relative luminescence. ATP

production did differ between the control and experimental conditions as measured at midday and as demonstrated in Figure 2.10. The 37/34° C shifted cells had significantly lower ATP production at midday than cells treated with the 37/37° C control condition. This difference was not apparent at the 01:00 or during the night interval twelve hours later nor in the comparative 34/34°C condition. This suggests that there is a lower level of ATP production that occurs in 37/34° C temperature-shifted cells relative to the control cells that occurs sometime after 4 hours of introduction to the suboptimal temperature and that lasts for a minimum of 4 hours after shift back to the physiological temperature. Further, this change appears to apply only to the cells that experience the 3° C difference in temperature every 12 hours and not to cells continuously maintained at suboptimal temperatures which supports the idea that the temperature changes are able to disrupt energy metabolism.

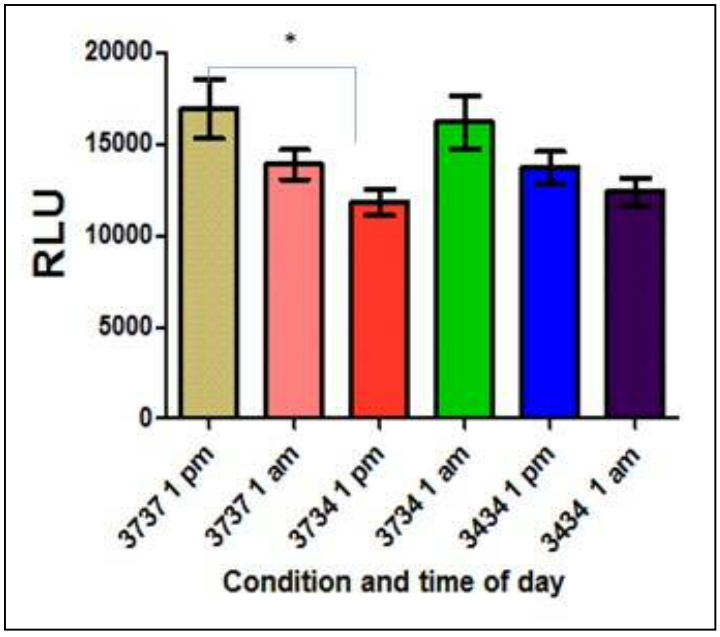

Figure 2.10. Relative differences in ATP production as measured by relative luminescence. Cells were exposed to the temperature shift protocol for 2 days and then collected at 01:00 or 13:00 for analysis of ATP levels using the luminex method to measure relative luminescence units (RLU) (n=3).

The relative expression of the composite clock genes as measured by RT-qPCR and quantified using the 2^ΔΔCq method is displayed in Figure 2.11. The reference gene selected for data normalization for this experiment was RPS 17 as described in the Materials and Methods section. The data presented in this figure are from the third replicate experiment which used 100 ng mRNA for reverse transcription. The results for the other replicates are available in Appendix 3. The first experiment used 25 ng mRNA and while gene expression could be detected with the shift condition at some time points, it was not detectable for the control condition (likely due to poor sensitivity) whereas differences were detected at 100 ng mRNA. Gene expression levels for PER1, PER2, CLOCK, BMAL, and NR1 D1 changed over the 24-hour experimental period after the cells were exposed to a seven-day shift and time 0=09:00. The temporal changes in gene expression were different for PER 1 as compared to PER 2. PER1 expression peaked at 6 hours post-shift while PER2 expression peaked at 1-hour post shift. CLOCK gene expression peaked at 12 – hours post shift and BMAL expression was relatively high, although peak BMAL expression was at one-hour post shift. All six genes exhibited an increase in gene expression at the 1-hour post shift time point and for all genes, except for PER2 and CLOCK, this presents the peak level of expression. It is possible that the return to physiological temperature resets the synchronization effect and even genes such as GAPDH, which was not used as a house keeping gene in this assay as the transcript levels were too variable over the 24-hour period, show this 1-hour post shift peak in expression. CLOCK was the only gene where this change in expression was not greater than two-fold at any time over the 24-hour period. The expression of NR1-D1, after the 1-hour post shift peak time point, has the next greatest fold change in expression at 6 hours post-shift, while BMAL expression is relatively low at this point. This is expected as NR1-D1 represses BMAL transcription. The temperature shift protocol does result in increased

gene expression in MCF-7 cells with PER2 demonstrating a cycle with a peak at 6 hours post shift in a 24-hour period.

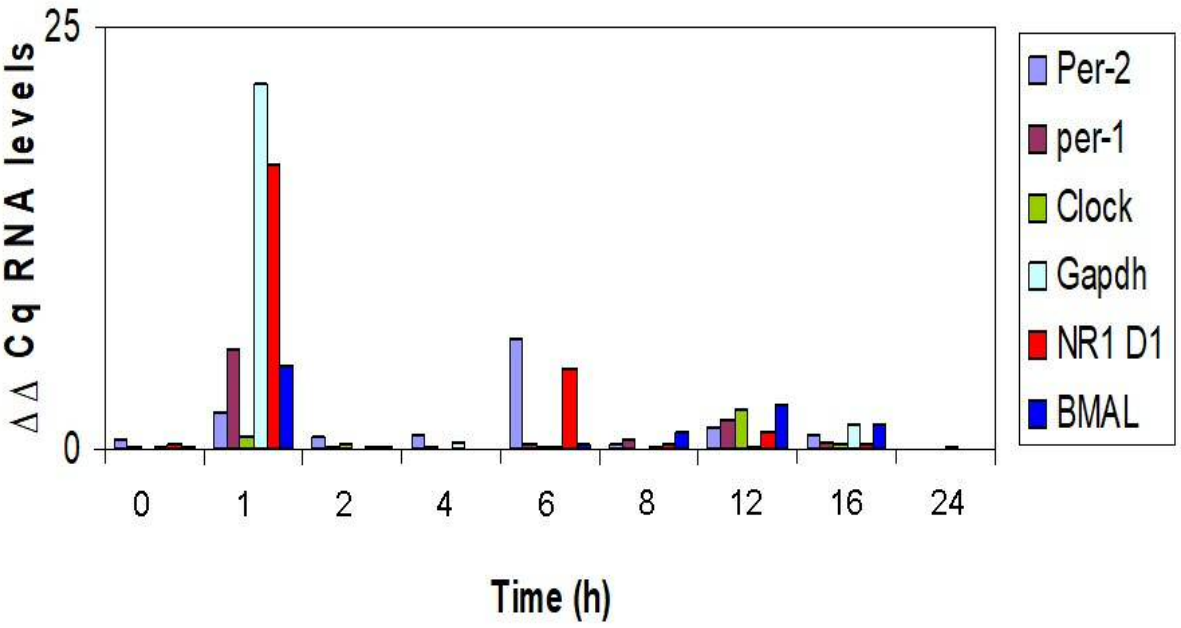

Figure 2.11. Comparative differences in clock gene expression over 24 hours using the shift model. Cells were exposed to the temperature shift protocol for 7 days and then RNA collected at different time points during the day. The RNA was subjected to RT-qPCR using TaqMan probes and relative gene expression was measured against the RPS17 reference gene using the 2^ΔΔCT method (n=2).

PER1and PER2 protein are demonstrated by western blot analysis shown in Figure 2.12. PER1 protein expression is different from PER2 and this mirrors the findings for mRNA. The PER1 protein levels appear relatively stable for the first 12 hours and this may reflect some alterations in post-translational modifications which differentially impacts the stability of the two proteins (Rossetti *et al* 2012).

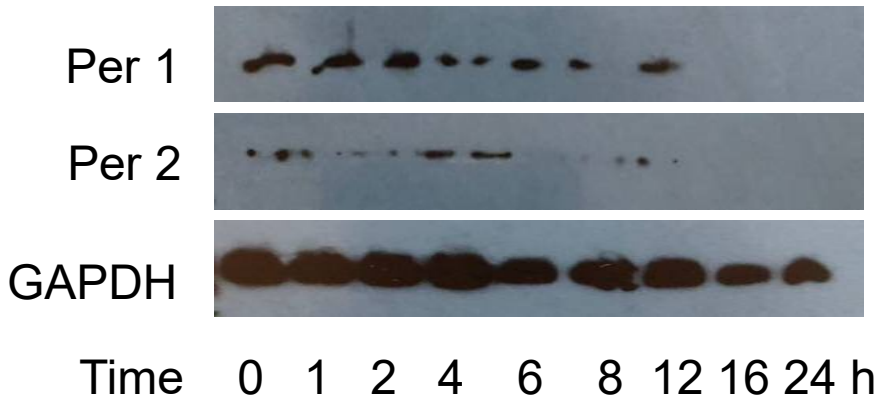

Figure 2.12. Western blot results from a seven-day shift experiment measuring PER1 and PER2. The 37/34° C experimental condition is displayed with time in hours and time 0 representing the time at 09:00 or when the cells are shifted back to 37° C from 34° C. GAPDH is the reference gene.

To further characterize any differences in cell cycle regulation between the temperature shift and control conditions, the protein levels of p21, part of a CKI family, and 4 cyclins were evaluated by western blot analysis as shown in Figure 2.13, at the same time points used for the gene expression analysis. Cyclin B expression (associated with entry into mitosis) was increased in cells exposed to both the 37/34° C and the 37/37° C conditions and no other cyclin expression was detected in either the control or the experimental conditions. Cyclin B is overexpressed in breast cancer cells (Aaltonen *et al*. 2009). The shift condition did demonstrate increased levels of p21 and although this did not result in any cell cycle phase arrest, it may explain the lower rate of cell proliferation as p21 is part of a family of CKIs (Xiong *et al.* 1993).

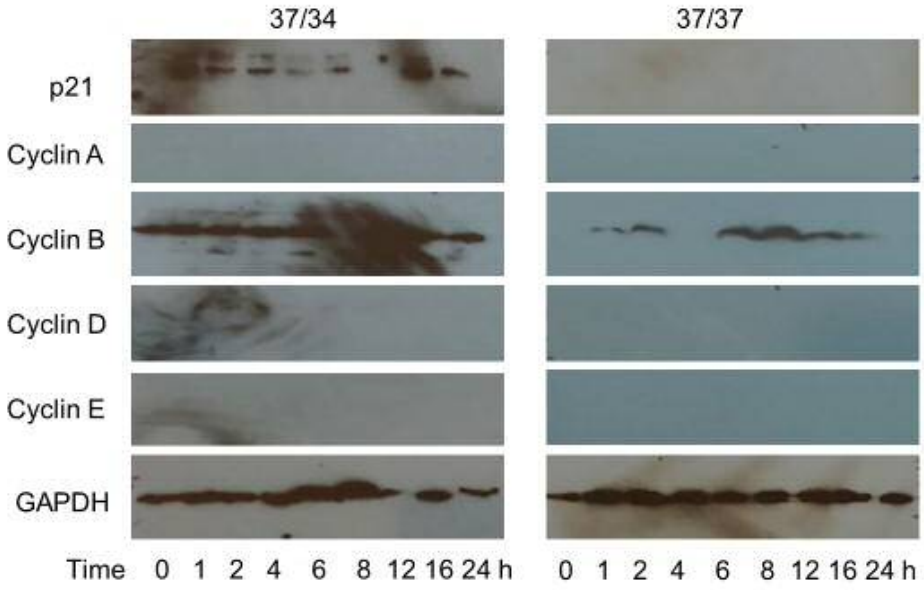

Figure 2.13. Western blot results from a seven-day shift experiment. The 37/34° C experimental condition experiment with time in hours and time 0 representing the time at 09:00 or when the cells are shift back to 37 °C from 34° C on the left hand side and the control condition of constant 37/37°C on the right hand side

Similar to the findings of Balsalobre *et al.* (1998), our experiments showed that the serum shock protocol synchronized gene expression in MCF-7 cells. In this series of experiments, there appeared to be two phases, the first and smaller synchronization of expression at one hour after shock and then the larger and second synchronization phase at 6 hours post-shock for all genes except Albumin D site-binding protein (DBP). DBP is not a core clock gene but is a target of the BMAL-CLOCK transcription factors and mediates the circadian transcription of key liver processes (Stratmann *et al*. 2010). The findings from this experiment are demonstrated in Figure 2.14.

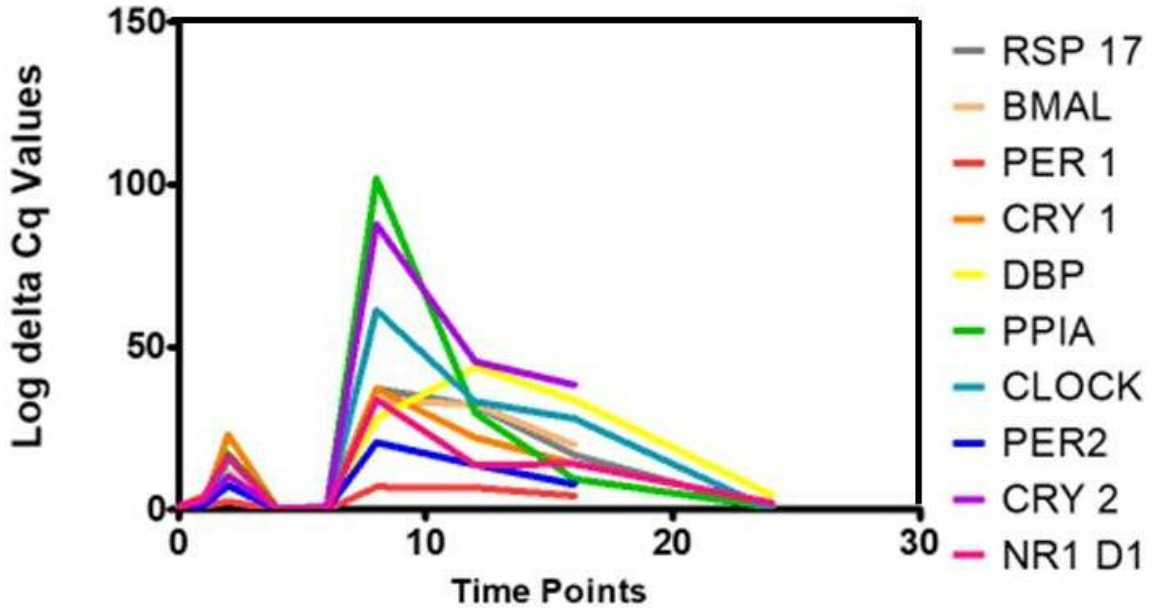

Figure 2.14. Synchronized gene expression in a serum shock experiment. MCF-7 cells were serum starved overnight and then treated with media containing 50% FBS for 2 h. The cells were then cultured in media containing 10% FCS and cells collected at various times during the day. The RNA was subjected to RT-qPCR using TaqMan probes and relative gene expression was measured against the RPS17 reference gene (n=3).

Western blot results from the serum shock experiment support the idea that both PER1 and PER2 are synchronized, as shown in Figure 2.15. Both PER1 and PER2 proteins appeared to be synchronized in tandem which was not consistent with the results from cells exposed to the temperature shift protocol. In this serum shock experiment, PER1 appeared to lose protein expression more quickly than PER2 and this may indicate post-translational changes related to that specific protocol that could be induced by other synchronized genes.

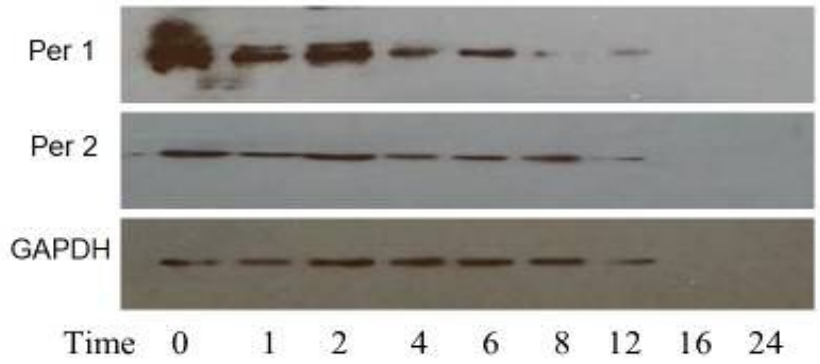

Figure 2.15. Western blot results from a serum shock experiment with time in hours and time 0 representing the time after cessation of 50% serum exposure (n=3).

The temperature shift protocol has been described and characterized using cell proliferation assays, flow cytometry of cell cycle, RT-qPCR to measure gene expression, and western blot analysis. Important differences exist between the cellular responses to the temperature shift and serum shock protocols however, both protocols result in increased clock gene expression in MCF-7 breast cancer cells.

2.4 Discussion

A serum shock protocol was used to demonstrate that circadian gene expression could be induced in rat fibroblasts and hepatoma cells (Balsalobre, Damiola, and Schibler 1998). While that publication demonstrated that the molecular mechanisms relating to clock gene expression identified in the SCN, were also present in peripheral cells, there was no explicit demonstration of cell cycle kinetics. However, based on the observations using the MCF-7 breast cancer cell line in this study, it would appear that clock gene expression in the serum shock model may be influenced by cell cycle kinetics. This is consistent with other results in which the cell cycle imparts control over circadian oscillators (Bieler *et al.* 2014). Other studies have failed to demonstrate any circadian oscillations in clock genes after serum shock (Rossetti *et al*. 2012). As demonstrated in Figure 2.14, gene expression may be synchronized when treated with the serum shock protocol although there was no anti-phase expression of any of the genes. While this may be advantageous in certain situations, the response of potential reference genes such as RPS 17 and PPIA in Figure 2.14, is not optimal. The potential confounding influence on reference gene expression in cells treated with the serum shock method has been identified in other studies (Schmittgen and Zakrajsek 2000). The fact that all researchers do not report variations in housekeeping genes may arise from slight differences in the serum shock protocol implementation or due to the use of MCF-7 cells with lineage-specific differences (Lee, Oesterreich, and Davidson 2015). Serum deprivation has been demonstrated to cause wild type mouse embryo cells and those deficient in *Rb*-/- or *Cyclin E*-/- to enter into G_0 with wild type cells entering into G_1 following serum addition while *Cyclin E*-/- cells are impaired at G_1 entry (Geng *et al.* 2003) and *Rb*-/- cells demonstrate an atypically early *Cyclin E* peak in G_1 (Herrera et *al.* 1996). Therefore, the serum shock protocol may induce cell cycle artifacts. The short-term

concentration of growth, mitogenic, or other factors could stimulate an artificial pan-response via underlying pathways that impact both the cell cycle and clock gene expression (Gutiérrez-Monreal *et al*. 2016). Further, the lack of any readily identifiable control condition in the standard serum shock protocol, except for comparison to Time 0, negates the use of the 2^ΔΔCq method for calculating RNA levels from qPCR data further hampering inter-experimental comparisons.

The results of this study indicate that cell growth and metabolism are impacted in the temperature shift protocol. Specifically, cell numbers are lower in the experimental condition (37/34° C shift) compared to the control condition (37/37° C) as daily counts progress but are higher than the cell counts for cells cultured at the constant suboptimal temperature (34/34° C) (Figure 2.1). This trend is statically significant for the MCF-7, HBL-100, and B16-BL6 cell lines studied except that for the MCF-7 cells significant differences existed at day 5 only between the control and experimental groups (Figures 2.1 and 2.2). It is advantageous to study the impact of a new protocol using multiple cell lines. MCF-7 cells are a human breast cancer epithelial cell line that are estrogen receptor (ER)α positive and progesterone receptor (PR) positive and demonstrate cell culture criterion for neoplasia in the presence of estrogen (Lee, Oesterreich, and Davidson 2015). In contrast, HBL-100 cells are a non-malignant human breast epithelial cell line that are thought to be immortalized via adenovirus SV 40 antigen but can transform over time to become tumorigenic in nude mice (de Fromentel *et al*. 1985). The murine melanoma B16-BL6 cell line has previously been demonstrated to have dysregulated clock gene function (Kiessling *et al.* 2017.) From analysis of the flow cytometry data of DNA content, the proliferation differences in response to different culture temperature conditions do not appear to be due to differences in cell cycle dynamics (Figures 2.5 and 2.6). The

experimental temperature-shifted cells progress through the cell cycle with no apparent phase arrest (Figures 2.5 and 2.6). It appears that the rate at which the cells grow and divide are slower. Metabolically, the temperature shifted experimental cells are significantly different. This is supported by both the MTT data and the ATP production assay (Figures 2.3 and 2.10) . While these metabolic changes may be expected in the cells maintained at suboptimal temperatures (Al-Fageeh *et al.* 2006), this is the first time, to our knowledge, that temperature shifted cells have been characterized in this way. This reinforces the concept that cellular metabolic changes and clock gene expression are related (Robinson and Reddy 2014).

While the temperature shift model also displays an ability to synchronize clock gene expression, it is clear that it is not cell cycle dependent. As displayed in Figure 2.11, all six genes studied demonstrated an increase in gene expression after one-hour of returning to the 37° C temperature. This trend is exhibited in the core clock genes as well as for glyceraldehyde – 3 phosphate dehydrogenase (GAPDH), a key enzyme in cell metabolism which is frequently used as a reference gene in RT-qPCR and as a loading control in western blots (Tristan *et al.* 2011). Based on the results of the reference gene validation portion of this study, it was apparent that GAPDH would not be suitable as a housekeeping gene. However, given that the shift experiment appears to have a metabolic impact and GAPDH is required for cell glycolysis among many other functions (Tristan *et al*. 2011), analysis of GAPDH was included in the study of gene expression. GAPDH showed a 21-fold change in expression at the one-hour post shift timepoint but returned to baseline until the 16-hour post shift timepoint when there was a small increase of 1.5-fold. There may be a metabolic shift that occurs in the cells within one hour after being returned to physiologic temperature that is related to the increase in GAPDH expression and to changes in the other core clock genes or this could be attributed to some other GAPDH

function which also influences clock gene expression or which is independent of them. Through the course of the day, the two transcription factors, CLOCK and BMAL, exhibit near parallel increases at one-hour post shift although they showed differences in magnitude and at 12 hours post-shift, they were both increased with very similar magnitude changes (2.3-fold for CLOCK and 2.7-fold for BMAL). More importantly, other than at one-hour post shift, the transcription factors are more closely in anti-phase with PER 1 and PER 2 expression, the protein arms of the transcription-translation – feedback loop (TTFL) which is the expected molecular relationship. This is in contrast to the gene expression results obtained with the serum shock method, where expression of PER1 and PER2 are in parallel with CLOCK and BMAL. In this study of the temperature shift model, PER 1 and PER 2 do not appear to have the same time sequence of expression, with PER 1 peaking at one hour post shift and PER 2 peaking at 6 hours post shift. The dynamic between the two period proteins including the post-transcriptional and post-translation differences and whether PER2 exerts hierarchical transcriptional influence is less well known than is the positive arm of the canonical TTFL (Chiou *et al.* 2016).

Recent studies have examined the circadian gene expression profiles in human breast cancer cell lines as compared to non-malignant breast epithelial lines (Rossetti *et al*. 2012) (Gutiérrez-Monreal *et al*. 2016) (Lellupitiyage Don *et al.* 2019). Table 2.1 presents a simple comparison of recent work.

Table 2.1. Contributions to the Current Understanding of Circadian Gene Expression in Human Breast Cancer Cell Lines

Authors and date of publication	S.Rossetti, J.Espostio, F. Corlazzoli, A. Gregoski, N. Sacchi 2012	M.A.Gutiérrez-Monreal, V.Treviño, J.E.Moreno-Cuevas, S.Scott 2016	S.S. Lellupitiyage Don, H.Lin, J.J.Furtado, M.Qraitem, S.R.Taylor, M.E.Farkas 2019
Title and journal	Entrainment of Breast (Cancer) Epithelial Cells Detects Distinct Circadian Oscillation Patterns for Clock and Hormone Receptor Genes Cell Cycle	Identification of Circadian-related Gene Expression Profiles in Entrained Breast Cancer Cell Lines Chronobiology International	Circadian Oscillations Persist in Low Malignancy Breast Cancer Cells Cell Cycle
Breast cancer lines used	All human derived: HME1- ERα +ve T47D - ERα +ve MCF-7 - ERα +ve MCF-10A - ERα -ve HS587T - ERα -ve MB-MDA-231 - ERα -ve	All human derived: MCF-7 – ERα +ve MCF-10A – noncancerous HCC 1954 – HER2/neu +ve MDA-MD -231 – triple -ve ZR-75-30 ERα +ve	All human derived: MCF-7 – ERα + ve and PR +ve MDA-MB-231 – triple -ve HEK 293 T (for transfections for luminometry)
Research question	To probe the possible co-regulation of hormone and circadian signaling	To probe the degree of dysfunction in the clock molecular mechanisms in breast cancer lines by looking at genome – wide expression profiles and to determine if breast cancer cell lines can be characterized in this way	To probe more sensitive methods to detect circadian oscillations (bioluminescence), Do circadian oscillations of clock genes occur in breast cancer cell lines and is the degree of dysregulation correlated with aggressiveness
Gene expression methodology – including synchronization protocol and quantity of mRNA used	Serum shock – 50% horse serum RT-qPCR – 1 μg mRNA – cDNA, 25 ng cDNA for qPCR,	Serum shock– 50% horse serum RT-qPCR – 500 ng mRNA to cDNA, 20 ng cDNA for q PCR Microarray	Serum shock – 50% FBS RT- qPCR – 100 ng cDNA – Used GAPDH as a control and used 2^ΔΔCq method Luminometry

Results	No circadian oscillation of any clock gene in MCF-7 cells CLOCK does not demonstrate circadian oscillation in any cell line Cell line specific differences with respect to response to serum shock and clock gene circadian oscillation No circadian oscillation of ERα receptor in ERα +ve cancer cell lines	Based on RT-qPCR data – no circadian oscillation of PER 2 or BMAL in the cancerous cell lines and BMAL expression disrupted as compared to MCF- 10 A and almost no expression of PER 2 in MCF-7 cell line Microarray data demonstrated that breast cancer cell can respond to serum shock with circadian oscillation of non - canonical genes	Based on RT-qPCR – BMAL and PER 2 transcripts detectable but no circadian oscillation in either cell line, with PER2 relative expression highest at 1 hour Luminometry – in MCF-7 cells – PER 2 and BMAL display circadian oscillation and are anti-phase to each other. No circadian oscillation of either found in MDA-MB-231
Conclusions	An ERα epithelial non-malignant cell line demonstrates a ER α receptor circadian oscillation in response to serum shock as well circadian oscillation in clock genes (HME1) and this is absent in ERα cancer cell lines, therefore circadian and hormone signaling may be linked	Breast cancer cell lines differ in their circadian oscillatory response to serum shock and receptor status does not appear to be a factor. Some cell lines respond with no synchronization in the core clock genes but do in clock-controlled genes so this may indicate that there is another mechanism to co -ordinate circadian oscillation (ie independent of transcription factors CLOCK/BMAL) and/ r there are factors in the serum shock protocol that can cause this synchronization	Luminometry allows for more frequent sampling and is a more sensitive method than RT- qPCR to detect low amplitude circadian oscillations. Loss of circadian oscillation is greater in triple -ve breast cancer cells and the ER-E2 pathway which is present in MCF-7 cells may contribute to circadian oscillations

Several factors can explain the differences in this study regarding the expression profile of all canonical clock genes including PER2 and BMAL in MCF-7 cells treated with the serum shock protocol. These encompass: modifications made experimentally to the serum shock

protocol, differences in the quantities of mRNA reverse transcribed and the amount of cDNA used for qPCR, and the use of different technologies including the use of the Taqman® Expression arrays, which incorporate a highly specific probe into the assay. In these experiments, the frequency of gene expression was only measured for 24 hours, therefore it is not possible to comment on the relative circadian oscillations except that there is no indication that the PER and CRY proteins are in anti-phase to their transcription factors as expected in the TTFL mechanism. In most other studies the oscillations in breast cancer cells induced by serum shock dampen out by 48-72 hours with the amplitude decreasing (Rossetti *et al*. 2012)(Gutiérrez-Monreal *et al*. 2016)(Lellupitiyage Don *et al*. 2019). The temperature shift model warrants further investigation over a longer period of time to determine if the oscillations observed are circadian and if the character of the wave pattern remains consistent. It would be very interesting to combine bioluminescence of promoter-reporter expression with this protocol.

A number of researchers have identified the role of PER 2 both as a potential tumor suppressor gene and as the clock gene most directly involved in breast tissue maintenance through estrogen receptor modulation (Yang *et al.* 2009)(Xiang *et al*. 2008)(Gery *et al.* 2007)(Fu *et al*. 2002). Overexpression of PER2 has been demonstrated to decrease cell proliferation *in vitro* (Xiang *et al*. 2008) (Gery *et al.* 2007) and its downregulation in mice increases tumor growth (Yang *et al*. 2009). Mice that are PER 2 (m/m) mutant have increased tumor susceptibility (Fu *et al.* 2002). Overexpression of PER2 does increase the proportion of cells in G_1 through a G_1/S block possibly by increasing p53 and simultaneously decreasing cyclin D_1 expression (Xiang *et al*. 2008) (Gery *et al.* 2007)(Fu *et al.* 2002). Decreased cyclin D_1 expression can result in G_1 phase arrest (Zhou *et al.* 2016). It is possible that the temperature shift model results in the induction of expression of clock genes whose inherent oscillations are

absent or below thresholds of detection in MCF-7 cells (Kiessling *et al.* 2017) rather than by inducing synchronization *per se*. The fold change increase of PER2 expression could be responsible for the decrease in cell proliferation in 37/34° C shifted and constant 34° C treated cells. However, this would not necessarily explain the differences in the MTT and ATP assays between the shift and control conditions.

In the Xiang *et al.* (2008) study, MCF-7 cells did not exhibit any PER2 expression on western blot analysis prior to transfection. However, there was no cell synchronization protocol used prior to protein extraction and the 10% polyacrylamide gels used may have been suboptimal for measuring the 140 kDa Per2 protein. In our experiments, a smaller size Per2 protein of approximately 45 kDa was identified in both control and experimental cells. It is thought that this smaller size represents the nuclear form of the period proteins (Yagita *et al.* 2000).

This study introduces temperature shift as an alternative experimental model to examine clock gene expression in cell culture. The protocol has been validated using RT-qPCR and western blots and has been characterized for its effect on proliferation and metabolic activity. While the protocol is labour intensive, this could be mitigated by the use of specialized incubators. The method described as the temperature shift model does not involve the use of nutrients or chemicals whose use could complicate results by activating signaling pathways that could induce changes in other non-circadian pathways. The model also allows for another layer of manipulation such as the addition of chemotherapeutic drugs or melatonin to study the impact on clock gene expression and the cell cycle. While it is not yet determined how deeply these two important aspects of cell regulation are related, a model with selective impact, could be helpful in making that determination. The use of the temperature shift protocol can also accommodate the requirements of the MIQE guidelines for evaluating changes in gene expression by qPCR. It

is highly recommended that the selection of any model involving synchronization include details on reference gene selection and validation and on cell cycle kinetics to allow for ease of comparison between studies. It may be worth noting that SCN cells can be synchronized by serum shock (Hurst, Mitchell, and Gillette 2002). However, SCN cells appear refractory to temperature pulses as a means of phase rest and entrainment (Buhr, Yoo, and Takahashi 2010). This supports the idea that the temperature shift model is a useful tool to study clock gene expression of peripheral oscillators.

2.5 References

Aaltonen, K., R. M. Amini, P. Heikkilä, K. Aittomäki, A. Tamminen, H. Nevanlinna, and C. Blomqvist. 2009. "High Cyclin B1 Expression Is Associated with Poor Survival in Breast Cancer." *British Journal of Cancer*. https://doi.org/10.1038/sj.bjc.6604874.

Al-Fageeh, Mohamed B., Rosalyn J. Marchant, Martin J. Carden, and C. Mark Smales. 2006. "The Cold-Shock Response in Cultured Mammalian Cells: Harnessing the Response for the Improvement of Recombinant Protein Production." *Biotechnology and Bioengineering*. https://doi.org/10.1002/bit.20789.

Albrecht, Urs, and Gregor Eichele. 2003. "The Mammalian Circadian Clock." *Current Opinion in Genetics and Development*. https://doi.org/10.1016/S0959-437X(03)00055-8.

Balsalobre, A., S. A. Brown, L. Marcacci, F. Tronche, C. Kellendonk, H. M. Reichardt, G. Schutz, and U. Schibler. 2000. "Resetting of Circadian Time in Peripheral Tissues by Glucocorticoid Signaling." *Science* 289 (5488): 2344–47. https://doi.org/10.1126/science.289.5488.2344.

Balsalobre, Aurélio, Francesca Damiola, and Ueli Schibler. 1998. "A Serum Shock Induces Circadian Gene Expression in Mammalian Tissue Culture Cells." *Cell*. https://doi.org/10.1016/S0092-8674(00)81199-X.

Bieler, Jonathan, Rosamaria Cannavo, Kyle Gustafson, Cedric Gobet, David Gatfield, and Felix Naef. 2014. "Robust Synchronization of Coupled Circadian and Cell Cycle Oscillators in Single Mammalian Cells." *Molecular Systems Biology*. https://doi.org/10.15252/msb.20145218.

Brown, Steven A., Gottlieb Zumbrunn, Fabienne Fleury-Olela, Nicolas Preitner, and Ueli Schibler. 2002. "Rhythms of Mammalian Body Temperature Can Sustain Peripheral Circadian Clocks." *Current Biology*. https://doi.org/10.1016/S0960-9822(02)01145-4.

Buhr, Ethan D., Seung Hee Yoo, and Joseph S. Takahashi. 2010. "Temperature as a Universal Resetting Cue for Mammalian Circadian Oscillators." *Science*. https://doi.org/10.1126/science.1195262.

Bustin, Stephen A., Vladimir Benes, Jeremy A. Garson, Jan Hellemans, Jim Huggett, Mikael Kubista, Reinhold Mueller. 2009. "The MIQE Guidelines: Minimum Information for Publication of Quantitative Real-Time PCR Experiments." *Clinical Chemistry*. https://doi.org/10.1373/clinchem.2008.112797.

Chen, Shou Tung, Kong Bung Choo, Ming Feng Hou, Kun Tu Yeh, Shou Jen Kuo, and Jan Gowth Chang. 2005. "Deregulated Expression of the PER1, PER2 and PER3 Genes in Breast Cancers." *Carcinogenesis*. https://doi.org/10.1093/carcin/bgi075.

Chiou, Yi Ying, Yanyan Yang, Naim Rashid, Rui Ye, Christopher P. Selby, and Aziz Sancar. 2016. “Mammalian Period Represses and De-Represses Transcription by Displacing CLOCK-BMAL1 from Promoters in a Cryptochrome-Dependent Manner.” *Proceedings of the National Academy of Sciences of the United States of America*. https://doi.org/10.1073/pnas.1612917113.

Chomczynski, Piotr, and Nicoletta Sacchi. 2006. “The Single-Step Method of RNA Isolation by Acid Guanidinium Thiocyanate-Phenol-Chloroform Extraction: Twenty-Something Years On.” *Nature Protocols*. https://doi.org/10.1038/nprot.2006.83.

Damiola, F., N. Le Minli, N. Preitner, B. Kornmann, F. Fleury-Olela, and U. Schibler. 2000. “Restricted Feeding Uncouples Circadian Oscillators in Peripheral Tissues from the Central Pacemaker in the Suprachiasmatic Nucleus.” *Genes and Development*. https://doi.org/10.1101/gad.183500.

Davis, P. K., A. Ho, and S. F. Dowdy. 2001. “Biological Methods for Cell-Cycle Synchronization of Mammalian Cells.” *BioTechniques*. https://doi.org/10.2144/01306rv01.

de Fromentel, C. Caron de, P. C. Nardeux, T. Soussi, C. Lavialle, S. Estrade, G. Carloni, K. Chandrasekaran, and R. Cassingena. 1985. “Epithelial HBL-100 Cell Line Derived from Milk of an Apparently Healthy Woman Harbours SV40 Genetic Information.” *Experimental Cell Research*. https://doi.org/10.1016/0014-4827(85)90238-1.

Enninga, Ilona C., R. T.L. Groenendijk, A. A. van Zeeland, and J. W.I.M. Simons. 1984. “Use of Low Temperature for Growth Arrest and Synchronization of Human Diploid Fibroblasts.” *Mutation Research/Environmental Mutagenesis and Related Subjects*. https://doi.org/10.1016/0165-1161(84)90020-7.

Feillet, Céline, Peter Krusche, Filippo Tamanini, Roel C. Janssens, Mike J. Downey, Patrick Martin, Michèle Teboul. 2014. “Phase Locking and Multiple Oscillating Attractors for the Coupled Mammalian Clock and Cell Cycle.” *Proceedings of the National Academy of Sciences of the United States of America*. https://doi.org/10.1073/pnas.1320474111.

Fu, Loning, Helene Pelicano, Jinsong Liu, Peng Huang, and Cheng Chi Lee. 2002. “The Circadian Gene Period2 Plays an Important Role in Tumor Suppression and DNA Damage Response in Vivo.” *Cell*. https://doi.org/10.1016/S0092-8674(02)00961-3.

Geng, Yan, Qunyan Yu, Ewa Sicinska, Manjusri Das, Jürgen E. Schneider, Shoumo Bhattacharya, William M. Rideout, Roderick T. Bronson, Humphrey Gardner, and Piotr Sicinski. 2003. “Cyclin E Ablation in the Mouse.” *Cell*. https://doi.org/10.1016/S0092-8674(03)00645-7.

Gery, S., R. K. Virk, K. Chumakov, A. Yu, and H. P. Koeffler. 2007. “The Clock Gene Per2 Links the Circadian System to the Estrogen Receptor.” *Oncogene*. https://doi.org/10.1038/sj.onc.1210585.

Gotoh, Tetsuya, Jae Kyoung Kim, Jingjing Liu, Marian Vila-Caballer, Philip E. Stauffer, John J. Tyson, and Carla V. Finkielstein. 2016. "Model-Driven Experimental Approach Reveals the Complex Regulatory Distribution of P53 by the Circadian Factor Period 2." *Proceedings of the National Academy of Sciences of the United States of America*. https://doi.org/10.1073/pnas.1607984113.

Gotoh, Tetsuya, Marian Vila-Caballer, Carlo S. Santos, Jingjing Liu, Jianhua Yang, and Carla V. Finkielstein. 2014. "The Circadian Factor Period 2 Modulates P53 Stability and Transcriptional Activity in Unstressed Cells." *Molecular Biology of the Cell*. https://doi.org/10.1091/mbc.E14-05-0993.

Gutiérrez-Monreal, Miguel A., Victor Treviño, Jorge E. Moreno-Cuevas, and Sean Patrick Scott. 2016. "Identification of Circadian-Related Gene Expression Profiles in Entrained Breast Cancer Cell Lines." *Chronobiology International*. https://doi.org/10.3109/07420528.2016.1152976.

Harper, Jane V. 2005. "Synchronization of Cell Populations in G1/S and G2/M Phases of the Cell Cycle." *Methods in Molecular Biology (Clifton, N.J.)*.

Herrera, R E, V P Sah, B O Williams, T P Mäkelä, R A Weinberg, and T Jacks. 1996. "Altered Cell Cycle Kinetics, Gene Expression, and G1 Restriction Point Regulation in Rb-Deficient Fibroblasts." *Molecular and Cellular Biology*. https://doi.org/10.1128/mcb.16.5.2402.

Hurst, William J., Jennifer W. Mitchell, and Martha U. Gillette. 2002. "Synchronization and Phase-Resetting by Glutamate of an Immortalized SCN Cell Line." *Biochemical and Biophysical Research Communications*. https://doi.org/10.1016/S0006-291X(02)02346-X.

Jackman, Joany, and Patrick M. O'Connor. 1998. "Methods for Synchronizing Cells at Specific Stages of the Cell Cycle." *Current Protocols in Cell Biology*. https://doi.org/10.1002/0471143030.cb0803s00.

Kiessling, Silke, Gregor Eichele, and Henrik Oster. 2010. "Adrenal Glucocorticoids Have a Key Role in Circadian Resynchronization in a Mouse Model of Jet Lag." *Journal of Clinical Investigation*. https://doi.org/10.1172/JCI41192.

Kiessling, Silke, Lou Beaulieu-Laroche, Ian D. Blum, Dominic Landgraf, David K. Welsh, Kai-Florian Storch, Nathalie Labrecque, Nicolas Cermakian. 2017. "Enhancing Circadian Clock Function in Cancer Cells Inhibits Tumor Growth". *BioMed central Biology.*

Lee, Adrian V., Steffi Oesterreich, and Nancy E. Davidson. 2015. "MCF-7 Cells - Changing the Course of Breast Cancer Research and Care for 45 Years." *Journal of the National Cancer Institute*. https://doi.org/10.1093/jnci/djv073.

Lellupitiyage Don, Sujeewa S., Hui Hsien Lin, Jessica J. Furtado, Maan Qraitem, Stephanie R. Taylor, and Michelle E. Farkas. 2019. "Circadian Oscillations Persist in Low Malignancy Breast Cancer Cells." *Cell Cycle*. https://doi.org/10.1080/15384101.2019.1648957.

Lesicka, Monika, Ewa Jabłońska, Edyta Wieczorek, Beata Pepłońska, Jolanta Gromadzińska, Barbara Seroczyńska, Leszek Kalinowski, Jarosław Skokowski, and Edyta Reszka. 2019. "Circadian Gene Polymorphisms Associated with Breast Cancer Susceptibility." *International Journal of Molecular Sciences*. https://doi.org/10.3390/ijms20225704.

Lesicka, Monika, Ewa Jabłońska, Edyta Wieczorek, Barbara Seroczyńska, Anna Siekierzycka, Jarosław Skokowski, Leszek Kalinowski, Wojciech Wąsowicz, and Edyta Reszka. 2018. "Altered Circadian Genes Expression in Breast Cancer Tissue According to the Clinical Characteristics." *PLoS ONE*. https://doi.org/10.1371/journal.pone.0199622.

Li, Shujing, and Luoying Zhang. 2015. "Circadian Control of Global Transcription." *BioMed Research International*. https://doi.org/10.1155/2015/187809.

Matsuo, Takuya, Shun Yamaguchi, Shigeru Mitsui, Aki Emi, Fukuko Shimoda, and Hitoshi Okamura. 2003. "Control Mechanism of the Circadian Clock for Timing of Cell Division in Vivo." *Science*. https://doi.org/10.1126/science.1086271.

Miki, Takao, Tomoko Matsumoto, Zhaoyang Zhao, and Cheng Chi Lee. 2013. "P53 Regulates Period2 Expression and the Circadian Clock." *Nature Communications*. https://doi.org/10.1038/ncomms3444.

Miller, Brooke H., Erin L. McDearmon, Satchidananda Panda, Kevin R. Hayes, Jie Zhang, Jessica L. Andrews, Marina P. Antoch. 2007. "Circadian and CLOCK-Controlled Regulation of the Mouse Transcriptome and Cell Proliferation." *Proceedings of the National Academy of Sciences of the United States of America*. https://doi.org/10.1073/pnas.0611724104.

Papagiannakopoulos, Thales, Matthew R. Bauer, Shawn M. Davidson, Megan Heimann, Lakshmipriya Subbaraj, Arjun Bhutkar, Jordan Bartlebaugh, Matthew G. Vander Heiden, and Tyler Jacks. 2016. "Circadian Rhythm Disruption Promotes Lung Tumorigenesis." *Cell Metabolism*. https://doi.org/10.1016/j.cmet.2016.07.001.

Pilorz, Violetta, Mariana Astiz, Keno Ole Heinen, Oliver Rawashdeh, and Henrik Oster. 2020. "The Concept of Coupling in the Mammalian Circadian Clock Network." *Journal of Molecular Biology*. https://doi.org/10.1016/j.jmb.2019.12.037.

Reinke, Hans, Camille Saini, Fabienne Fleury-Olela, Charna Dibner, Ivor J. Benjamin, and Ueli Schibler. 2008. "Differential Display of DNA-Binding Proteins Reveals Heat-Shock Factor 1 as a Circadian Transcription Factor." *Genes and Development*. https://doi.org/10.1101/gad.453808.

Rieder, Conly L., and Richard W. Cole. 2002. "Cold-Shock and the Mammalian Cell Cycle." *Cell Cycle*. https://doi.org/10.4161/cc.1.3.119.

Robinson, I., and A. B. Reddy. 2014. "Molecular Mechanisms of the Circadian Clockwork in Mammals." *FEBS Letters*. https://doi.org/10.1016/j.febslet.2014.06.005.

Rossetti, Stefano, Joseph Esposito, Francesca Corlazzoli, Alex Gregorski, and Nicoletta Sacchi. 2012. “Entrainment of Breast (Cancer) Epithelial Cells Detects Distinct Circadian Oscillation Patterns for Clock and Hormone Receptor Genes.” *Cell Cycle*. https://doi.org/10.4161/cc.11.2.18792.

Schmittgen, Thomas D., and Brian A. Zakrajsek. 2000. “Effect of Experimental Treatment on Housekeeping Gene Expression: Validation by Real-Time, Quantitative RT-PCR.” *Journal of Biochemical and Biophysical Methods*. https://doi.org/10.1016/S0165-022X(00)00129-9.

Stratmann, Markus, Frédéric Stadler, Filippo Tamanini, Gijsbertus T.J. Van Der Horst, and Jürgen A. Ripperger. 2010. “Flexible Phase Adjustment of Circadian Albumin D Site-Binding Protein (Dbp) Gene Expression by CRYPTOCHROME1.” *Genes and Development*. https://doi.org/10.1101/gad.578810.

Takahashi, Joseph S. 2017. “Transcriptional Architecture of the Mammalian Circadian Clock.” *Nature Reviews Genetics*. https://doi.org/10.1038/nrg.2016.150.

Tristan, Carlos, Neelam Shahani, Thomas W. Sedlak, and Akira Sawa. 2011. “The Diverse Functions of GAPDH: Views from Different Subcellular Compartments.” *Cellular Signalling*. https://doi.org/10.1016/j.cellsig.2010.08.003.

Ueda, Hiroki R., Satoko Hayashi, Wenbin Chen, Motoaki Sano, Masayuki Machida, Yasufumi Shigeyoshi, Masamitsu Iino, and Seiichi Hashimoto. 2005. “System-Level Identification of Transcriptional Circuits Underlying Mammalian Circadian Clocks.” *Nature Genetics*. https://doi.org/10.1038/ng1504.

Winter, Sherry L., Lucine Bosnoyan-Collins, Dushanthi Pinnaduwagez, and Irene L. Andrulis. 2007. “Expression of the Circadian Clock Genes Per1 and Per2 in Sporadic and Familial Breast Tumors.” *Neoplasia*. https://doi.org/10.1593/neo.07595.

Wu, M. W., X. M. Li, L. J. Xian, and F. Lévi. 2004. “Effects of Meal Timing on Tumor Progression in Mice.” *Life Sciences*. https://doi.org/10.1016/j.lfs.2004.02.014.

Xiang, Shulin, Seth B. Coffelt, Lulu Mao, Lin Yuan, Qi Cheng, and Steven M. Hill. 2008. “Period-2: A Tumor Suppressor Gene in Breast Cancer.” *Journal of Circadian Rhythms*. https://doi.org/10.1186/1740-3391-6-4.

Xiong, Yue, Gregory J. Hannon, Hui Zhang, David Casso, Ryuji Kobayashi, and David Beach. 1993. “P21 Is a Universal Inhibitor of Cyclin Kinases.” *Nature*. https://doi.org/10.1038/366701a0.

Yagita, Kazuhiro, Shun Yamaguchi, Filippo Tamanini, Gijsbertus T.J. Van Der Horst, Jan H.J. Hoeijmakers, Akira Yasui, Jennifer J. Loros, Jay C. Dunlap, and Hitoshi Okamura. 2000. “Dimerization and Nuclear Entry of MPER Proteins in Mammalian Cells.” *Genes and Development*. https://doi.org/10.1101/gad.14.11.1353.

Yang, Xiaoming, Patricia A. Wood, Eun Young Oh, Jovelyn Du-Quiton, Christine M. Ansell, and William J.M. Hrushesky. 2009. “Down Regulation of Circadian Clock Gene Period 2 Accelerates Breast Cancer Growth by Altering Its Daily Growth Rhythm.” *Breast Cancer Research and Treatment*. https://doi.org/10.1007/s10549-008-0133-z.

Zhang, Ray, Nicholas F. Lahens, Heather I. Ballance, Michael E. Hughes, and John B. Hogenesch. 2014. “A Circadian Gene Expression Atlas in Mammals: Implications for Biology and Medicine.” *Proceedings of the National Academy of Sciences of the United States of America*. https://doi.org/10.1073/pnas.1408886111.

Zhou, Jin, Lu Li, Li Fang, Hua Xie, Wenxiu Yao, Xiang Zhou, Zhujuan Xiong, Li Wang, Zhixi Li, and Feng Luo. 2016. “Quercetin Reduces Cyclin D1 Activity and Induces G1 Phase Arrest in HepG2 Cells.” *Oncology Letters*. https://doi.org/10.3892/ol.2016.4639.

Chapter 3

Chapter 3 Impact of Melatonin on the Cell Cycle and Clock Gene Expression

3.1 Introduction

The article describing the isolation and identification of melatonin from a bovine pineal gland was published in 1958 (Lerner *et al.* 1958). The hormone synthesis pathway, from tryptophan to serotonin to melatonin, results in a diurnal rhythm with a peak amplitude of melatonin concentration at night and whose rate is controlled by a series of enzymes that are under circadian control (Bernard *et al*. 1999). Melatonin is also produced in extra-pineal tissues including cerebral cortical cells and hepatocytes and exhibits different subcellular concentrations depending on the cell type and time of day (Venegas *et al.* 2012). Of the many interesting properties of melatonin, one is how evolutionarily conserved it is, being found in prokaryotes and among almost all of the phyla of eukaryotes (Venegas *et al.* 2012). The second unique feature of this hormone, is its chemical structure. *N*-acetyl-5-methoxytryptamine, which is classified as an indole compound possessing both benzene and pyrrole rings with the positions of the acetyl and methoxy groups affording the hormone with amphophilic properties: being both hydrophilic and lipophilic and hence able to cross cell membranes (Tan *et al.* 2005). The physical structure also enables melatonin to be a potent scavenger of free radicals and a powerful antioxidant (Shirinzadeh *et al.* 2010). In addition to acting as an antioxidant against both reactive oxygen species (ROS) and reactive nitrogen species (RNS), melatonin has been

described as having oncostatic, anti-inflammatory, immunomodulatory, and anti-aging effects mediated through receptor and non- receptor-based means (Hardeland 2009).

Within the scope of circadian hierarchical regulation, melatonin is considered one of the hormonal effector arms of the central SCN organization where the SCN exerts control via sympathetic nervous system innervation of the pineal gland (Chuffa *et al*. 2019). The nocturnal production of melatonin promotes central synchronization of peripheral oscillators and circadian genes, although the precise molecular mechanisms are not fully understood (Chuffa *et al*. 2019). Melatonin synthesis is rapidly decreased by exposure to blue light wavelengths (Tordjman *et al*. 2017). The nocturnal blood concentrations in people typically ranges from 80-120 pg/ml, being 5-8 times greater than the daytime levels (Karasek and Winczyk 2006). However, women with estrogen receptor positive (ER+) breast cancer have much lower nocturnal circulating melatonin levels as compared to healthy women (Tamarkin *et al.* 1982). The melatonin hypothesis postulates that exposure to light at night (LAN) causes chronic melatonin disruption, and therefore the loss of the protective effects of melatonin, which leads to tumorgenisis (Stevens and Davis 1996). A large study of nurses was published that showed that those nurses who worked rotating night and day shifts experienced an increased risk of breast cancer (Schernhammer *et al*. 2001). Other large epidemoligical studies involving shift work and animal studies, led to the International Agency for Cancer Research (IARC) to declare shift work a probable carcinogen, which was appended to *night* shift work in 2019 (Erren *et al.* 2019).

Melatonin has recently been shown to influence clock gene expression in cultures of MCF-7 cells (Xiang *et al.* 2012). The range of melatonin concentrations used in published *in vitro* experiments has varied widely. Melatonin decreased BMAL expression and increased PER2 expression in MCF-7 cells treated at a 1 nM concentration (Xiang *et al.* 2012). At a 100

nM concentration, melatonin can interfere with mitochondrial oxidative phosphorylation in the mitochondria of MCF-7 cells (Scott *et al*. 2001). Melatonin at 1-2 mM concentrations increases PER2 and CLOCK expression but down-regulates BMAL expression in prostate cancer cells (Jung-Hynes *et al*. 2010). Both the membrane receptor M_1 and the nuclear receptor RORα have been linked mechanistically to melatonin's influence on clock gene expression (Xiang *et al.* 2012)(Dai *et al.* 2001).

The purpose of this study was to examine the effects of physiological concentrations of melatonin on the growth of MCF-7 cells, and on cell cycle and clock gene expression in combination with the temperature shift model of circadian synchronization. Changes caused by treatment with melatonin that are different from those produced by the temperature shift alone, will be compared and further insights into the hormone's mechanism of action will be discussed.

3.2 Materials and Methods

Cell culture

A human hormone-responsive breast cancer cell line, MCF-7 cells, and a human breast epithelial cell line, HBL-100 cells, all originally obtained from the American Type Culture Collection (ATCC) were maintained in Hyclone Debucco's Modified Eagle Media (DMEM) with high glucose (GE Lifesciences) and supplemented with 10% fetal bovine serum (FBS) and 1% antibiotic and antimycotic solution® (A&A) (Fisher Sciences). They were maintained in a humidified environment at 37^{o} C and 5% CO_2.

Experimental protocols

The temperature shift technique consisted of MCF-7 cells being kept in a 37^{o} C environment from 09:00 to 21:00 and then transferred to a humidified 34^{o} C incubator supplemented with 5% CO_2 from 21:00 to 09:00. This was done for 7 consecutive days. In addition, two control conditions were maintained for the duration of the experiment; for the first control condition the cells were maintained at 37^{o} C continuously and for the second control condition the cells were maintained at 34^{o} C continuously, each in humidified incubators with 5% CO_2 supplementation. Cells were seeded in 100 mm tissue culture plates at a ratio of 1:8 on the first day of the shift experiment. At the 21:00 shift change, all three conditions received a media change with DMEM supplemented with melatonin (n- acetyl – 5 – methoxytryptamine, Santa Cruz Biotechnology) to a final concentration of 0.5 nM. At 9:00 the cells were again subjected to a media change, this time without melatonin. Experiments were performed in triplicate.

MTT Assay

For the 3-(4,5-dimethylthiazol-2-yl) -2,5 – diphenyltetrazolium bromide assay (MTT), 96 well plates were seeded with 2,000 cells/well for each cell type in 200 µl media containing either no melatonin as control or to a final concentration of 1 nM, 10 nM , 100 nM , 1 µM, or 1 mM melatonin and then the cells were incubated at 37° C for 4 days. Triplicates of each plate were prepared. The MTT assay was performed daily from days 2-4 days using the lab protocol where 5 pg/well MTT reagent was added to the wells on the day of the assay and the plate incubated at 37^{o} C for 3 hours. Then, the media was removed and replaced with 100 µl of dimethyl sulfoxide (DMSO) to solubilize the formazan crystals. The plate wells were read at 540 nm wavelength on a Synergy® H4 Hybrid plate reader (Biotek) using Gen 5, version 2.00 software. The average of the triplicate measures was reported along with the standard error of the mean (SEM).

Protein extraction and Western Blotting

Cells were washed with ice cold PBS pH 7.4 and then lysed in 300 µl of ice cold radioimmunoprecipitation assay (RIPA) buffer (150 mM sodium chloride, 15 mM phosphate buffer, pH 7.4, 1% Triton-X 100, 0.5% sodium dodecyl sulfate (SDS), 0.5% sodium deoxycholate, 10 mM sodium fluoride (NaF), 10 mM sodium orthovanadate, and protease inhibitor tablets (Thermo Scientific™ Pierce™ Protease Inhibitor Tablets). All reagents were obtained from Fisher Scientific unless otherwise indicated. The whole cell lysate was then collected from the plate using a plastic cell scraper. Cellular DNA and cytoskeletal proteins were sheared by passage through a 22 gauge needle several times and then stored at -80^{0} C. Protein quantification was done using the bicinchoninic acid (BCA) assay (Thermo Scientific™ Pierce™ BCA Protein Assay Kit) with a bovine serum albumin standard and read using a

Syngery® H4 Hybrid plate reader (Biotek) using Gen 5, version 2.00 software. Electrophoresis was performed using 25 μg of protein loaded per lane onto a 15% polyacrylamide gel containing SDS. After electrophoresis, the gels were transferred onto nitrocellulose membranes using a semidry transfer apparatus and 20% methanol, 192 mM glycine, and 25 mM Tris-HCl, pH 8, and protein transfer was confirmed by staining the membranes with 0.1% Ponceau S in 1% acetic acid. The membranes were blocked by incubation in 5% low fat milk or 5% Bovine Serum Albumin (BSA) in Tris-buffered saline, pH 7.4 and 0.05% Tween-20 (TBST), depending on the optimization protocol for the antibody, overnight at 4^0C. Primary antibodies were incubated in 5% low fat milk or 1% BSA in TBST at the dilutions listed below, overnight at 4^0 C. Secondary antibody-horseradish peroxidase (HRP) conjugates were incubated with the membrane at a dilution of 1:10,000 for 2 hours at room temperature. Chemiluminescent detection of HRP using the Thermo Scientific™ enhanced chemiluminescence (ECL) detection reagents was performed prior to membrane exposure to radiographic film.

All antibodies were obtained from SantaCruz Biotechnology. Primary antibodies that recognize Per1 and Per2 were used at 1:500 dilutions in 5% low fat milk in TBST for the block, primary antibody, and secondary antibody incubations. Primary antibodies that recognize HSP70, cyclin A, cyclin D_1, and cyclin E were used at a dilution 1:200, the antibody that recognizes cyclin B were used at a dilution of 1:100 and the antibody against β-actin was used at 1:1000 in 5% BSA in TBST for block and 1% BSA in TBST for the primary and secondary antibodies.

Flow cytometry for Cell Cycle Analysis

Cells were washed with PBS, pH 7.4, and harvested in 0.2% trypsin until detachment. The cells were collected and transferred to 1.5 ml microfuge tubes and centrifuged at 2000 rpm

for 5 minutes. The supernatant was discarded and the cells were washed with 1 ml PBS, pH 7.4, resuspended in 70% ethanol, and immediately stored at -20^0 C. Prior to analysis, the thawed samples were washed twice with PBS, pH 7.4, resuspended in 0.5 ml PBS, and 500 µl 100 µg/ml propidium iodide (PI) and 100 ng/ml RNase stain solution was added. The cells were incubated for 2 hours and samples analyzed on a Cytomics FC 500 flow cytometer (Beckman Coulter). Images were transferred to the Paint® program from the Beckman Coulter software.

Gene expression analysis using Reverse Transcriptase quantitative PCR (RT-qPCR)

Cell monolayers in 100 mm tissue culture plates were lysed in a fixed volume of 500 µl of denaturing solution containing 4 M guanidinium thiocyanate, 25 mM sodium citrate, 0.05% N- laurosylsarcosine, and 0.1 M 2-β- mercaptoethanol, as outlined (Chomczynski and Sacchi 2006). After immediate collection using a plastic cell scraper, the samples were stored at -80^0 C prior to RNA purification and solubilization using the phenol-chloroform technique, as described. RNA quantification was determined by measuring the OD260 using a spectrophotometer (Nanodrop®). 100 ng of RNA/sample was reverse transcribed using the protocol from the Superscript IV Vilo Master Mix without ezDNAse enzyme treatment as per the Life Technologies® instruction manual. The TaqMan® primers were annealed with the RNA at 25° C for 10 minutes, RNA reverse transcribed by incubation at 50° C for 10 minutes, and then the enzyme was inactivated for 5 minutes at 85° C using a thermocycler. The Clock gene ID Taqman® assays were obtained from Life Technologies®. For some genes, these assays are inventoried and for others they were custom produced. RPS-17 was used as the reference gene in this experiment. The assay numbers are as listed: PER1, Hs00242988_m1; PER2, Hs01007553_m1; CLOCK, Hs00231857_m1; BMAL (ARNTL), Hs00154147_m1; CRY1, Hs00172734_m1; CRY2, HS00901393_m1; TFAM, Hs00273372_s1; DBP, Hs00609747_m1;

and, RPS17, Hs00734303_g1. Taqman® gene assays were performed using 80 ng of cDNA and the Agilent Aria MX. The Thermo Fisher protocol for the TaqMan® Fast Advanced Master Mix was followed which consisted of UNG incubation for 1 cycle at 50° C for 2 minutes, 1 cycle of enzyme activation for 30 seconds at 95° C, and 40 cycles of alternating denaturing and annealing at 95° C for 1 second and 60° C for 20 seconds, respectively. As per the Taqman ® technical bulletin the amplification efficiency is assumed to be 1 and a melting cure analysis is not completed due to regent consumption. Gene expression was measured using the 2^ΔΔCT method in accordance with the Minimum Information for Publication of RT-qPCR Experiments (MIQE) Guidelines. (Bustin *et al*. 2009).

Statistical Analysis

SPSS ® statistical software (IBM) or GraphPad Prism 5.0 was used for statistical analysis as indicated. The data was subjected to a normality test using the normality function within GraphPad/Prism and if appropriate, $p<0.05$, the data was subject to a one analysis of variance (ANOVA) to compare groups which were then tested with a post hoc Tukey test; otherwise the groups were compared with a Kruskal Wallis test with a Dunn's comparison of groups as the post hoc. Unless otherwise stated, statistical significance was determined as $p<0.05$. Error bars within graphs indicate standard error of the mean (SEM), unless otherwise indicated.

3.3 Results

In order to examine the impact of different concentrations of melatonin on cell viability and metabolism of a breast cancer and a breast epithelial cell line, an MTT assay was performed. For this experiment, the cells were maintained continuously at 37°C and were not subjected to the temperature shift protocol. MCF-7 cell growth and viability were significantly inhibited when cultured in media supplemented with a concentration of 1 mM melatonin in that the relative absorbance was significantly lower compared to cells cultured in the absence of melatonin. This indicates lower metabolic activity in the culture and indirectly, less cell viability. This is presented in Figure 3.1. Treatment with lower concentrations of melatonin did not demonstrate a significant positive or negative effect on the viability of MCF-7 cells. Conversely HBL-100 cells treated with melatonin for 4 days had a significantly higher relative absorbance when treated at the 1 nM, 10 nM, and 100 nM concentrations when compared with the absence of melatonin or to the higher concentrations of melatonin of 1 μM or 1 mM. The viability of HBL-100 cells at day 4 of treatment with the 1 μM or 1 mM concentrations of melatonin was not significantly different from those cells that received no melatonin, indicating that even at high concentrations, melatonin did not appear to adversely affect non-cancerous cells. The lower concentrations of melatonin had a positive effect on HBL-100 cell viability with the MTT-dependent absorbance of cells treated at the physiological concentration of 1 nM being significantly higher than the cells treated with the 10 nM or 100 nM concentrations as measured at day four. The results are summarized in Figure 3.2. In this study, melatonin at high concentrations can negatively impact cancer cells but there is no negative impact on non-malignant breast epithelial cells and low melatonin concentrations confer a benefit to non-malignant cells.

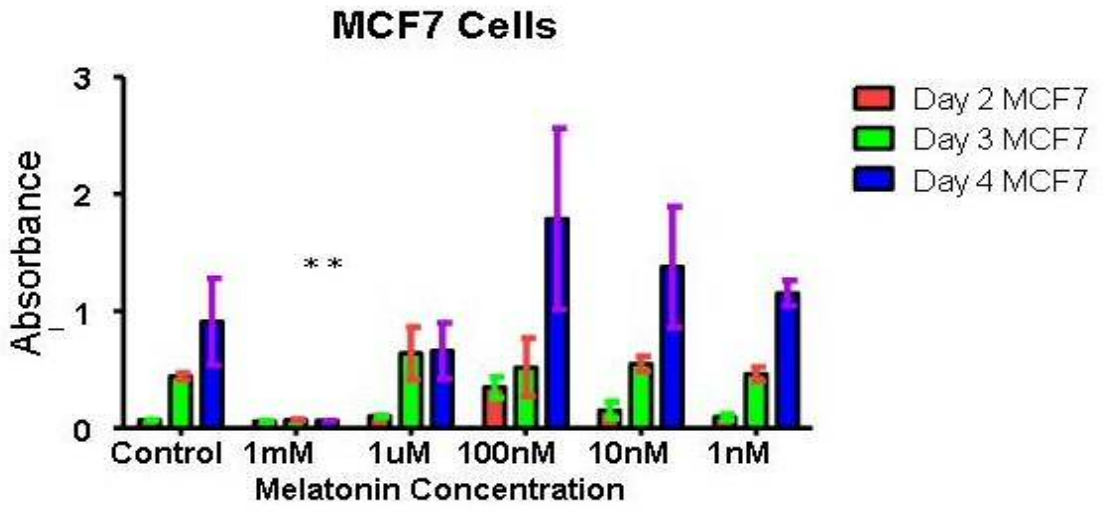

Figure 3.1 Viability of MCF-7 cells treated with different melatonin concentrations. Cultures of MCF-7 cells were treated with 1 nM, 10 nM, 100 nM, 1 μM, and 1 mM melatonin on day 1 and the viability of the cultures was measured for days 2 - 4 using an MTT assay. The Y axis denotes the relative absorbance of the active product, formazan (n=3, $p<0.05$).

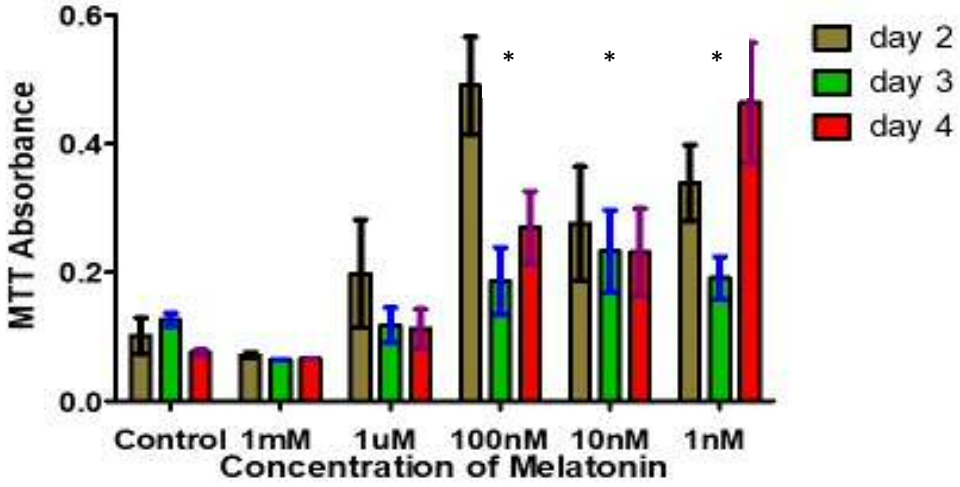

Figure 3.2 The viability of HBL-100 cells treated with different melatonin concentrations. Cultures of HBL-100 cells were treated with 1 nM, 10 nM, 100 nM, 1 μM, and 1 mM melatonin on day 1 and the viability of the cultures was measured for days 2 -4 using an MTT assay. The Y axis denotes the relative absorbance of the active product formazan which viable cells can convert from the 3-(4,5-dimethylthiazol-2-yl) -2,5 – diphenyltetrazolium bromide assay (MTT) (n=3, $p<0.05$).

To determine if the addition of melatonin for 12 hours/day had an impact on MCF-7 cell cycle kinetics, flow cytometry was performed using the nucleic acid stain, propidium iodide (PI). MCF-7 were subjected to temperature shift for 7 days prior to analysis and compared to a control group of MCF-7 cells that were kept continuously at 37°C. Melatonin was added each dram from 21:00 to 09:00 to a final concentration for 0.5nM. The histograms presented in Figure 3.3 represent a portion of the results where the X axis of the histogram indicates the relative intensity of the stain and therefore the amount of DNA present in the cells and the Y axis indicates the proportion of cells within each phase of the cell cycle: the first major peak represents cells in *Go/G1* containing the "normal" amount (2N) of DNA; the second major peak represents cells in the G_2/M phase containing a duplicated genome (4N); and, the cells between the two peaks represents cells in the S phase where they are actively undergoing DNA replication. All of these histograms indicate a higher proportion of cells in both the S and G_2/M phases for both the control and shift condition as compared to the histograms in Figure 2.8.

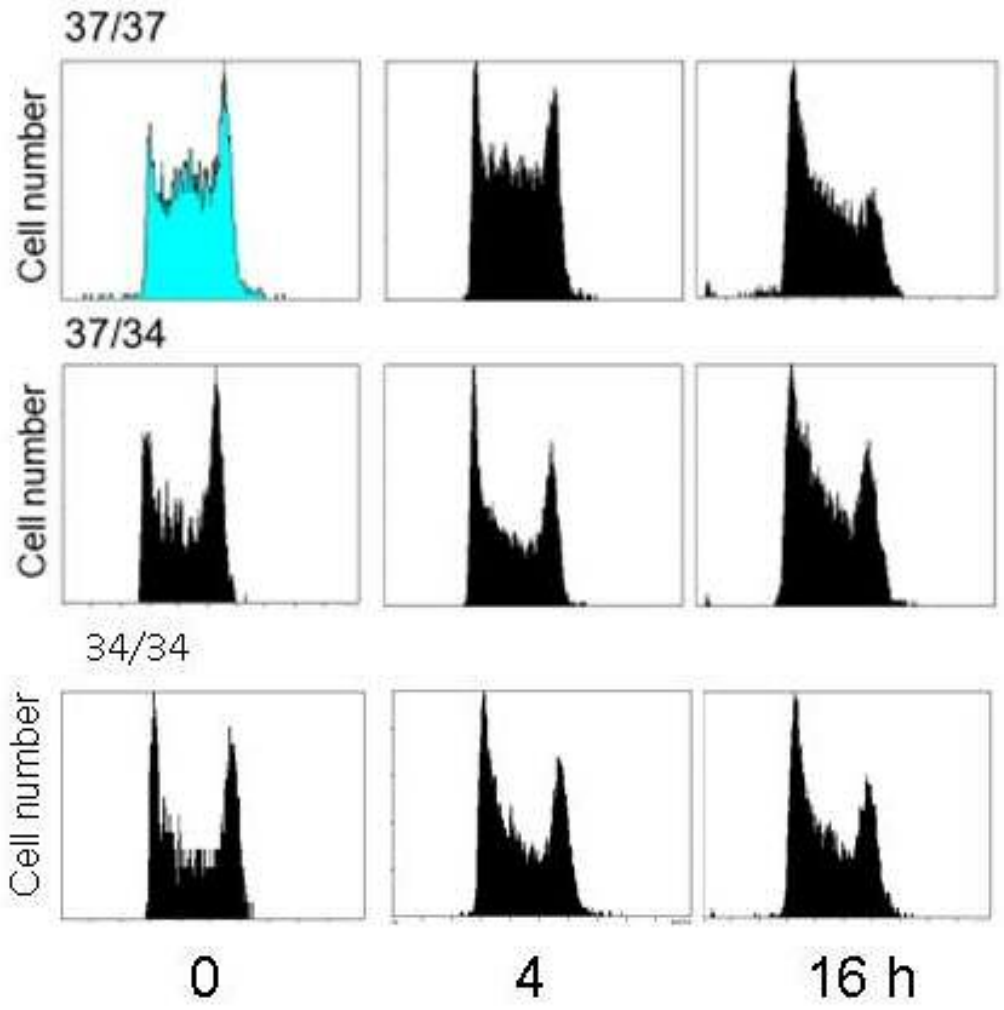

Figure 3.3 Histograms for flow cytometry of MCF-7 cells, representing a portion of the results, stained with propidium iodide after treatment with temperature shift and melatonin. MCF-7 were exposed to the temperature shift protocol with 0.5 nM melatonin added at 21:00 to 09:00 for 7 days. The cells were harvested, fixed in 70% ethanol, and stained with propidium iodide for analysis by flow cytometry. The top panels represent cells exposed to 37/37° C control condition, at time points 0, 4, and 16 hours post shift respectively with time 0 = 09:00. Images on the middle panels represent cells exposed to the 37/34° C experimental condition, at time points 0, 4, and 16 hours respectively with time 0 = 09 00. Images on the bottom panels represent cells exposed to the 34/34° C comparative condition, at time points 0, 4, and 16 hours respectively with time 0 = 09 00(n=3)

Significant differences in the cell cycle profiles are seen in cells treated with melatonin, where the proportion of cells in the G_1 phase for the shift condition is significantly greater than the proportion of control cells in the G_1 phase. It is of interest, that a significantly smaller proportion of cells were present in the *S* phase for the comparative 34/34° C condition as compared to the control condition. This is demonstrated in Figures 3.4 and 3.5. While the smaller proportion of cell in the *S* phase for the comparative condition also exists in the temperature shift condition, as demonstrated in Figure 2.6, there was no differences in the proportion of cells in the G_1 phase, indicating that melatonin has an effect on cell cycle kinetics in addition to the effects present in temperature-shifted cells.

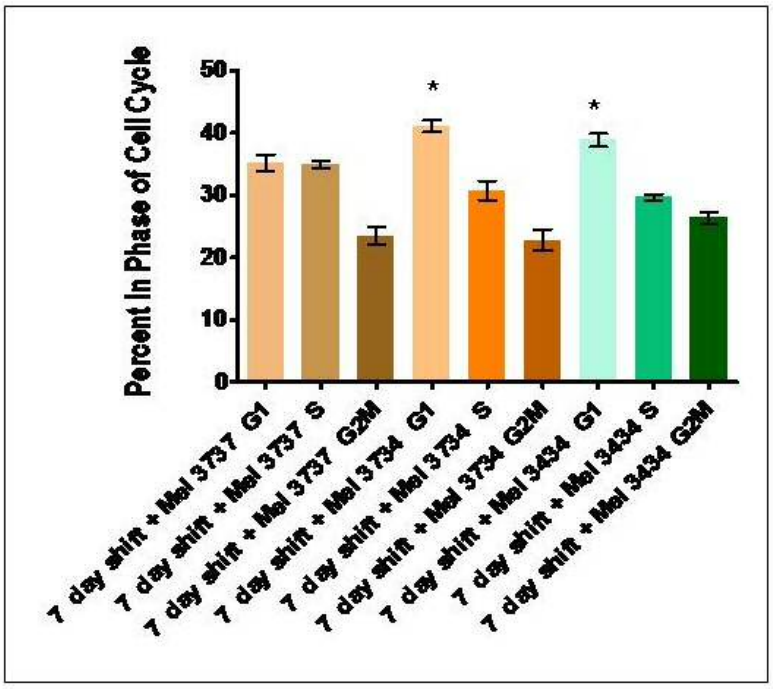

Figure 3.4 Graphical display comparing cell cycle phases at day 7 of shift plus melatonin. MCF-7 cells were cultured in media with the addition of 0.5 nM melatonin from 21:00 to 09:00. Cells were incubated at 37° C for 24 h/day (brown), 37° C from 9:00 - 21:00 h and 34° C from 21:00-9:00 h (orange), or 34° C for 24 h/day (green) for 7 days. The cells were harvested, fixed in 70% methanol, stained with propidium iodide, and analyzed on a flow cytometer to determine the percentage of cells in each phase of the cell cycle (n=3, $p<0.05$).

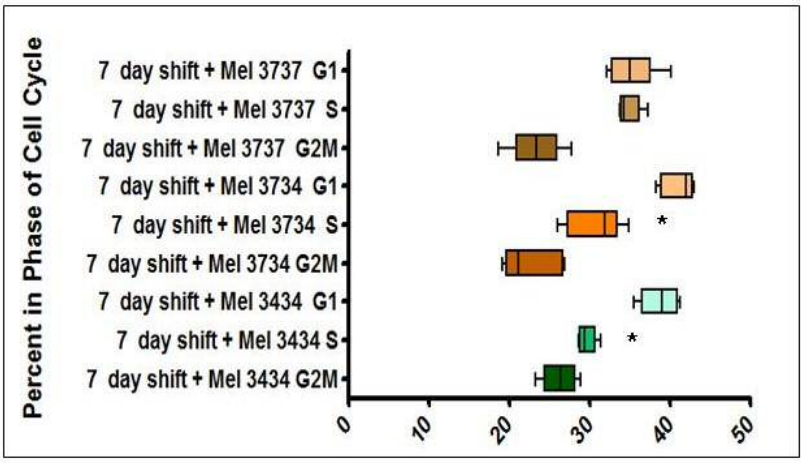

Figure 3.5 Graphical display comparing cell cycle phases at day 7 of shift plus melatonin. MCF-7 cells were cultured in media with the addition of 0.5 nM melatonin from 21:00 to 09:00. Cells were incubated at 37° C for 24 h/day (brown), 37° C from 9:00 - 21:00 h and 34° C from 21:00-9:00 h (orange), or 34° C for 24 h/day (green) for 7 days. The cells were harvested, fixed in 70% methanol, stained with propidium iodide, and analyzed on a flow cytometer to determine the percentage of cells in each phase of the cell cycle ($n=3$, $p<0.05$).

In order to further explore the differences in cell cycle kinetics, western blot analysis of cyclin expression was performed. The interrogation for heat shock protein (HSP) 70 expression was also included as it may be involved in the temperature shift pathway and explain some of the impact on cell regulation. Interestingly, cyclin A, associated with S-phase, exhibited increased expression in the control condition as compared to the experimental condition. There appears to be a much greater relative quantity at time 0 and 1 hours, relative to the time of melatonin removal and then a second peak of expression at 6 hours after melatonin removal. The comparisons are illustrated in Figure 3.6. Cyclin B is present in both the control and experimental samples; however, it was expressed at higher levels in the 37/37° C condition and did not appear to be inhibited by melatonin. Cyclin $D_{1,}$ associated with G_1-phase, was absent in the experimental condition but was detected in the control condition and the relative concentration appeared to increase after melatonin was removed, however the loading control β-

actin also exhibited this pattern, indicating either an artifact of protein quantification or the effect of melatonin on the expression of both proteins. Cyclin E, associated with the transition between G_1 and S phase, appeared to be the one exception whose expression appeared to be enhanced in the shift condition. In the control cells, the peak of cyclin E expression occurred at 12 hours after melatonin removal while for the experimental condition, the peak in cyclin E expression occurred earlier, at 2 hours after melatonin removal and was still detectable at 4 and 8 hours after. The expression of HSP70, part of the heat shock factor (HSF) pathway, was detectable in both conditions, and was expressed at higher levels in the shift condition which is expected due to the temperature fluctuations of the shift which requires an adaptive response by the cell.

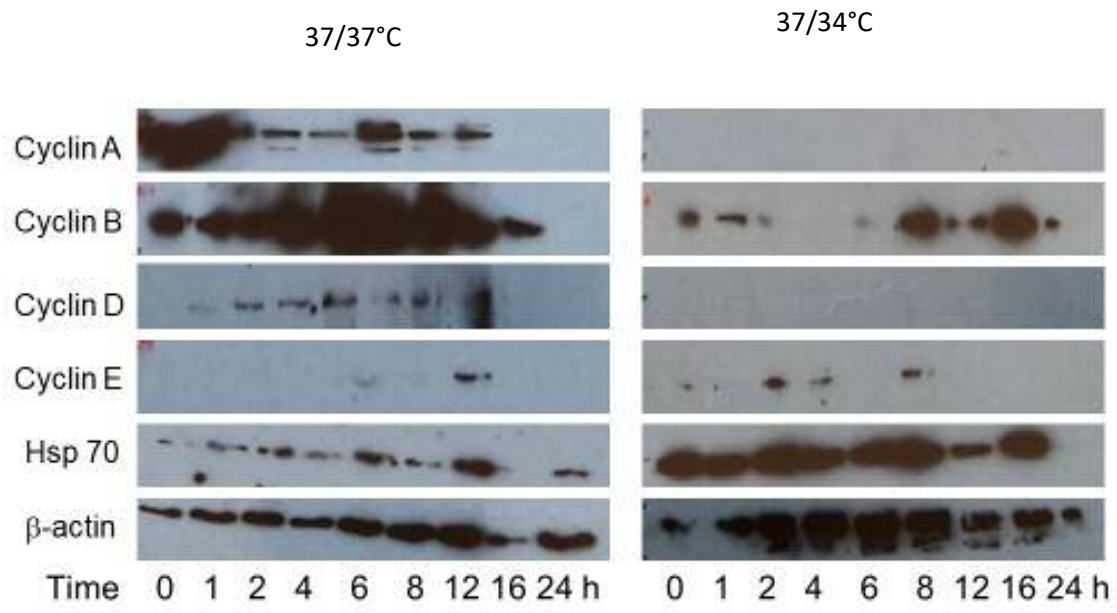

Figure 3.6 Western blot results from a seven-day shift plus 0.5 nM melatonin from 21:00 to 09:00 experiment. The 37/37° C control condition experiment with time in hours and time 0 representing 09:00 is displayed on the left-hand side. The experimental condition of 37/34° C is displayed on the right -hand side with time 0 = 09:00 when the cells are shifted back to 37° C from 34° C and the melatonin is removed.

To investigate the impact of melatonin on Clock gene expression, RT-qPCR was performed using RPS-17 as the reference gene. Six core clock genes, CLOCK, BMAL, PER1, PER2, CRY1, and CRY2 were selected as well as the clock-controlled gene DBP and a transcriptional activator of important mitochondrial genes, transcription factor A mitochondrial (TFAM). Figure 3.7 demonstrates the overall comparison in fold gene expression while Figure 3.8 illustrates the same data but compartmentalized to allow for ease of comparison. Peak expression for CLOCK, BMAL, and PER2 occurred at 24 hours, which is 12 hours after melatonin addition and shift to 34°C while peak PER1 expression occurred at 4 hours, mid-day, which is 4 hours after melatonin removal and shift to 37°C. CRY2 and TFAM expression peaked at 1 hour, while CRY1 expression peaked at 2 hours, and DBP expression peaked at 4 hours after melatonin removal and shift to 37°C.

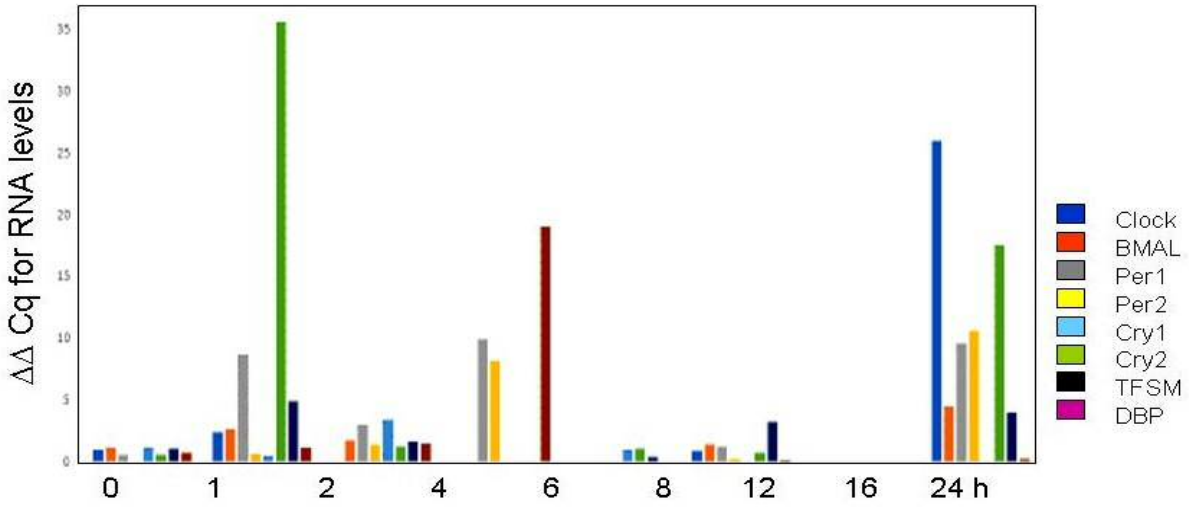

Figure 3.7 Overview of the relative gene expression of clock genes CLOCK, BMAL, PER1, PER2, CRY1, CRY2 and DBP and TFAM. Cells were exposed to the temperature shift protocol for 7 days and melatonin at a concentration of 0.5 nM from 21:00 to 09:00. RNA collected at different time points during the day. The RNA was subjected to RT-qPCR using TaqMan probes and relative gene expression was measured against the RPS17 reference gene using the 2^ΔΔCT method (n=3).

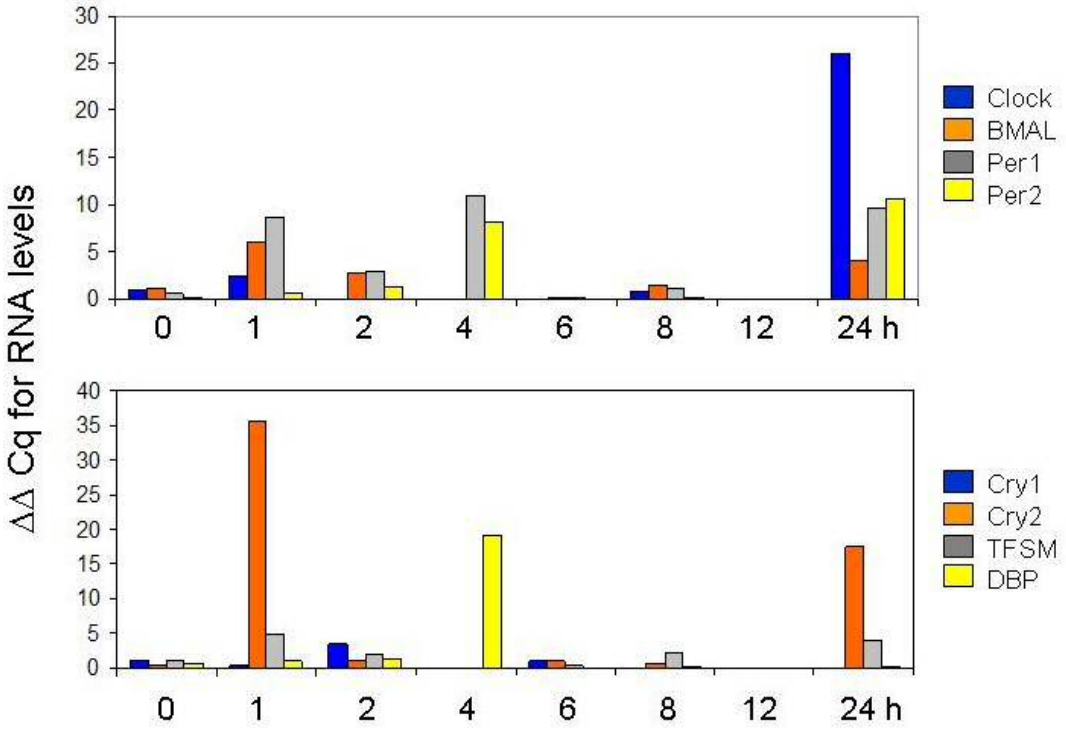

Figure 3.8 Relative gene expression of clock genes CLOCK, BMAL, PER1, PER2 in the top panel and CRY1, CRY2, DBP and TFAM in the bottom panel. Cells were exposed to the temperature shift protocol for 7 days and melatonin at a concentration of 0.5 nM from 21:00 to 09:00. RNA collected at different time points during the day. The RNA was subjected to RT-qPCR using TaqMan probes and relative gene expression was measured against the RPS17 reference gene using the 2^ΔΔCT method(n=3).

The Clock gene expression results are different when compared to the gene expression profiles for temperature shifted MCF-7 cells with no added melatonin as shown in Figure 3.9 (and presented in the last chapter). Table 3.1 shows the comparison between the two sets of experiments, however, since they were different experiments performed at different times, statistical significance was not computed. In addition to the observation that melatonin treatment shifts the time of peak gene expression for the core clock genes, there is a trend towards increasing the relative fold changes in gene expression as well.

Table 3.1 Core Clock Gene Upregulation in Response to Shift and Shift plus Melatonin in MCF7 Breast Cancer Cells

Gene	*Peak time - shift*	*Relative fold change at peak*	*Peak time – shift + melatonin*	*Relative fold change at peak*
CLOCK	12 hours	2.3	24 hours	26
BMAL	4 hours	4.9	24 hours	4.5
PER1	1 hour	6.1	4 hours	9.9
PER2	6 hours	6.6	24 hours	10.6

The only gene whose relative fold change was not increased when the temperature shift also included melatonin treatment, was BMAL.

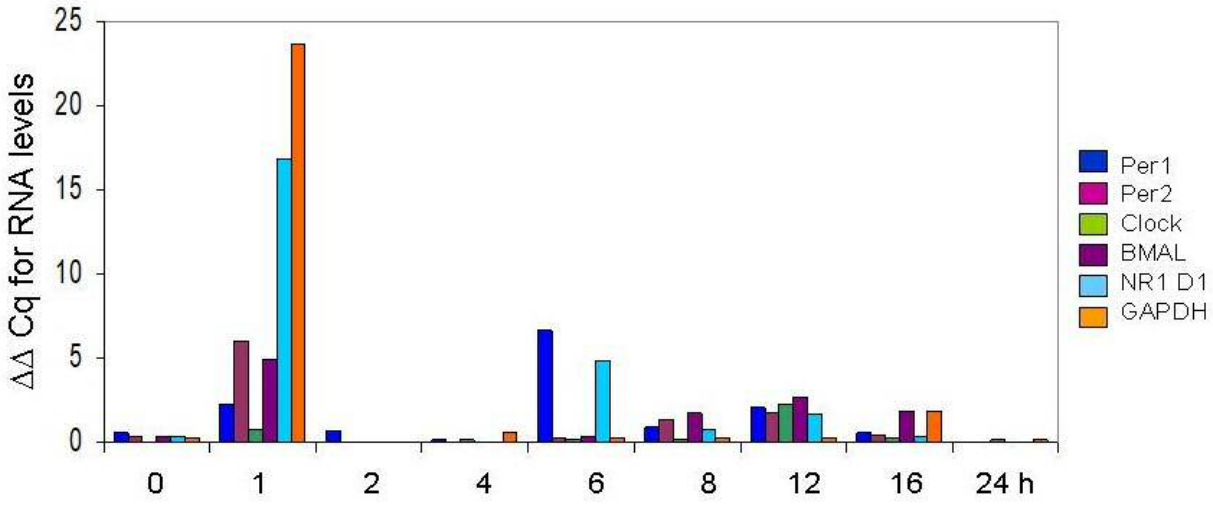

Figure 3.9 Comparative differences in clock gene expression over 24 hours using the shift model in the absence of added melatonin (From figure 2.11) (n=2).

A separate experiment was performed that directly compared exposure to the temperature shift to exposure to the temperature shift plus melatonin treatment through an identical seven-day period: in both groups the cells were subjected to media changes at 21:00 and 09:00 but with or without melatonin addition overnight. The log Cq values for the amount of gene expression are

presented in Figure 3.10. Statistical analysis did not indicate any significant differences between the overall means for CLOCK, BMAL, PER1, or PER2 expression between the temperature shift only and the temperature shift plus melatonin conditions. After 12 hours, CLOCK expression showed a marked increase in expression in the temperature shift plus melatonin condition as compared to shift only condition, however, the time point differences and the accompanying variation between replicates did not result in any significant differences between the two protocols in overall means.

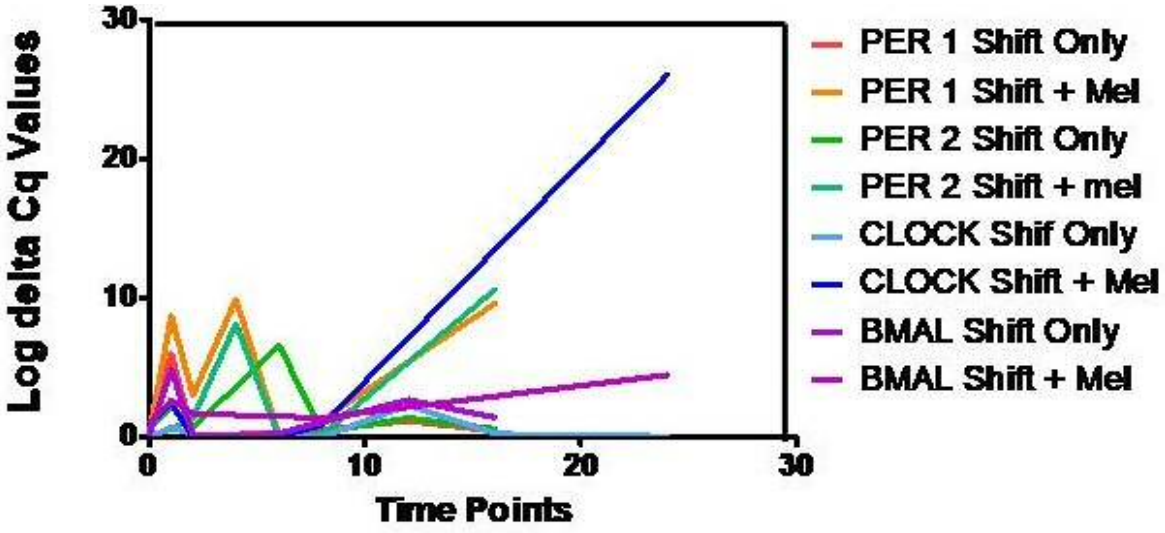

Figure 3.10 Relative gene expression of shift condition (37/34 °C) and shift plus 0.5 nM melatonin by the log values of their Cq values. Cells were exposed to the temperature shift protocol in the presence or absence of melatonin treatment for 7 days and then RNA collected at different time points during the day. The RNA was subjected to RT-qPCR using TaqMan probes and relative gene expression was measured against the RPS17 reference. Log Cq (2^{Δ}Cq) values are represented (n=2).

Western blot analysis results for PER1 and PER2 levels indicate that there is increased expression in the control cells versus cells exposed to the 37/34 °C experimental condition when melatonin is added from 21:00 to 09:00 daily during a seven-day shift protocol. This parallels the findings for the changes in expression for most of the cyclins. Therefore, melatonin may not

significantly change the temporal properties of gene expression but it may confer post transcriptional, translational, or post-translational modifications of the cyclins or of PER1/PER 2. There are differences in the expression of PER1 and PER2 between the control plus melatonin and the temperature shift plus melatonin conditions over the nine time points. In the control condition, melatonin appears to enhance the expression of both PER1 and PER2 and cells exposed to the temperature shift plus melatonin demonstrate different peaks from those exposed to temperature shift alone (Figure 2.13), a finding that is consistent with the RT-qPCR results as indicated in Table 3.1. While the trends are consistent, significant differences were not achieved.

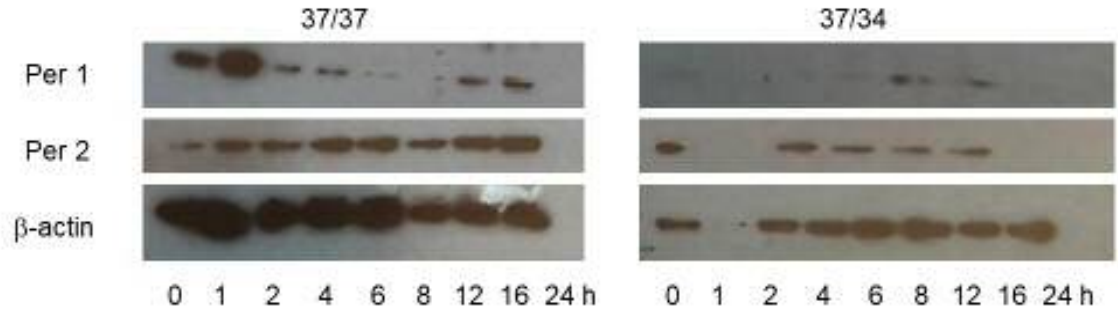

Figure 3.11 Western blot results from a seven-day shift plus 0.5 nM melatonin from 21:00 to 09:00 experiment. The 37/37 °C control condition experiment with time in hours and time 0 representing the time at 09:00. The experimental condition of 37/34°C is display on the righthand side with time 0 = 09:00 when the cells are shifted back to 37°C from 34°C and the melatonin is removed. These western blots represent results from experiments run parallel to Figure 3.8.

Melatonin can influence cancer cells differently from non-malignant cells *in vitro.* This study demonstrates that exposure to pharmacological (1 mM) concentrations of melatonin conferred a negative effect on the viability of MCF-7 breast cancer cells as measured by the MTT assay while having no significant impact on non-malignant breast epithelial cells Figures 3.1 and 3.2. Physiological (1 nM) concentrations of melatonin appeared to confer a significant

metabolic advantage to non-malignant cells, in that it promoted cell growth as measured by the MTT assay, which does not occur in cancer cells (Figures 3.1 and 3.2). The addition of melatonin for 12 hours per day plus exposure to the temperature shift condition did result in significant changes in cell cycle kinetics (Figures 3. And 3.5). While melatonin may cause some changes in the profiles of clock gene expression, it does not appear that the overall impact is significant.

3.4 Discussion

Melatonin, at a physiological concentration of 1 nM has previously been shown to have an anti-proliferative effect on MCF-7 cells and to significantly increase the expression of both the p53 and $p21^{WAF1}$ proteins (Mediavilla, Cos, and Sánchez-Barceló 1999). MCF-7 cell growth is activated by the presence of estrogen (Lee, Oesterreich, and Davidson 2015). Melatonin interferes with estrogen stimulation of MCF-7 cells (Gonzalez *et al.* 2008), in a manner not mediated by direct binding to the ER α but by preventing receptor binding to calmodulin, a secondary messenger in signal transduction that binds to intracellular calcium, as well as by disruption of ERα transcription (Del Río *et al.* 2004). It is quite likely that melatonin exerts its oncostatic effect through multiple pathways as previous studies have demonstrated that melatonin delays cell cycle progression, suppresses ERα mRNA transcript levels, and disrupts ERα activity in hormone positive breast cancers which is mediated through binding to the membrane-bound MT1 receptor, a G protein coupled receptor (Hill *et al.* 2011). In this study, treatment with physiological concentrations of melatonin (1 nM) did not show an impact on MCF-7 metabolism or affect cell proliferation, while pharmacologic concentrations (1 mM) did inhibit MCF-7 cell proliferation. The differences from published experiments may be due to the use of a longer duration of melatonin exposure in this experiment and/or because different MCF-7 cell sources or subtype were used. However, treatment of HBL-100 cells, a non-neoplastic breast epithelial cell line, with a pharmacological concentration of melatonin had no adverse effects while treatment with a physiological concentration was beneficial and promoted HBL-100 cell proliferation. This confirms previous work where treatment with melatonin exerted a differential impact on malignant versus non-malignant cells perhaps through down-regulating autophagy and promoting tumor cell death (Sagrillo-Fagundes, Bienvenue-Pariseault, and

Vaillancourt 2019). Melatonin's anti-proliferative effect is concentration dependent (Hill and Blask 1988).

Melatonin's anti-proliferative effect can also be due to its impact on cell cycle kinetics. The results of this study are consistent with previous results which demonstrate that melatonin causes a delay in the G_1/S transition and thus a higher proportion of melatonin-treated cells are present in the G_1 phase of the cell cycle (Cos *et al.* 1991). The results of this study are significant because they further validate the temperature shift model and show that cells exposed to a combination of melatonin and the temperature shift condition provides different results than cells exposed to the temperature shift condition alone with respect to cell cycle kinetics (Figures 2.5 and 2.6 versus Figures 3.4 and 3.5). The induction of p53 by melatonin may also result in G_1 arrest and this pathway is activated by DNA damage (Miki *et al.* 2013). MCF-7 cells do contain a functional p53 gene: although many cancer cells do not possess p53 activity, in MCF-7 cells p53 is not the functional pathway when apoptosis is triggered (Fan *et al.* 1995). Treatment with melatonin also significantly increases the cell cycle duration in MCF-7 cells (Cos, Recio, and Sánchez-Barceló 1996). The impact of melatonin on the expression levels of the cyclins, key components in the regulation of the cell cycle, were also examined. The expression levels of many cyclins are known to be dysregulated in cancer cells (Siu, Rosner, and Minella 2012) with the over-expression of cyclin B_1 being relatively common in breast cancer where its level of expression is reported to be linked to tumor aggressiveness (Aaltonen *et al.* 2009). This would explain our results that show a high level of cyclin B_1 expression as measured by western blot analysis in both the control and temperature shifted experimental cells even in the presence of melatonin (Figure 3.6). However, cyclin B_1 appears to be expressed at a lower level in the temperature shift plus melatonin-treated cells. In fact, all of the cyclins, with the exception of

cyclin E, appear to be decreased by exposure to the temperature shift condition rather than by treatment with melatonin alone (Figure 3.6). Cyclin E combines with Cdk -2 to promote entry of the cell into the *S* phase so its increased expression in the temperature shift plus melatonin condition is not consistent with our observation of an increased proportion of cells in G_1 (Siu, Rosner, and Minella 2012). However, decreased cyclin D_1 expression is consistent with a prolonged G_1 phase (Zhou *et al.* 2016), as is observed in the temperature shift plus melatonin condition, shown in Figure 3.6. Melatonin blocks the recruitment of the transcriptional coactivator p300 to the cyclin D1 promoter (Hill *et al.* 2011). MCF-7 cells have been identified as unique in that they are ERα positive and concomitantly over-express cyclin E (Gray-Bablin *et al.* 1996). It is possible that the results here are more reflective of an aberrant cell line where the cell cycle activity is complex and dysregulated such that exposure to both the temperature shift and melatonin conditions have a seemingly contradictory impact on cyclin expression. Clearly in this case the over-expression of cyclin E is not a factor in the observed delay into *S* phase entry. It was demonstrated in Figure 2.14 that p21 expression in MCF-7 cells is increased by the temperature shift and p21 is a potential inhibitor of all the CDK – cyclin complexes (Xiong *et al.* 1993). Melatonin has previously been shown to increase the expression of p21 in MCF-7 cells (Mediavilla, Cos, and Sánchez-Barceló 1999) so it is possible that the combined effect of temperature shift plus melatonin treatment resulted in the increased proportion of cells in G_1. The appearance of a high proportion of cells in the G_2/M phase as observed in the flow cytometry histograms in Figure 3.3 for both the control and experimental conditions in response to melatonin treatment could be due to an impact on cyclin B_1/CDK1 activity mediated by p53 (Aaltonen *et al.* 2009) (Mediavilla, Cos, and Sánchez-Barceló 1999) which would normally delay the transition to mitosis. Melatonin at physiological concentrations also decreases

telomerase activity, an enzyme which contributes to chromosomal lengthening and maintains cell immortalization in MCF-7 cells which could also decrease proliferation (Leon-Blanco *et al.* 2003).

As demonstrated in Figures 2.11 and 3.9, exposure of cells to the temperature shift protocol can increase the expression of clock genes in MCF-7 cells. While the addition of melatonin did not significantly increase the expression of these genes, there were differences between the peak expression time points for PER1, PER2, CLOCK, and BMAL. CLOCK expression was increased by10-fold in the temperature shift and melatonin condition compared to the temperature shift only condition, as summarized in Table 3.1. This was reproduced in a second experiment that compared the temperature shift to the temperature shift and melatonin condition although in this case the protocol also involving a media change for the shifted cells at both 21:00 and 09:00 in an effort to control for the potential impact of a media change on its own. The results in this study for MCF-7 cells exposed to the temperature shift model and melatonin are not consistent with the results reported by other investigators for exposure of MCF-7 cells to a serum shock synchronization followed by exposure to 1 nM melatonin (Xiang *et al.* 2012). In this case the serum shock plus melatonin had a differential effect on clock gene expression and the oscillation pattern and amplitude of the CLOCK gene was not impacted by the presence of melatonin (Xiang *et al.* 2012). This same paper demonstrated that melatonin plus or minus exposure to the serum shock condition upregulated PER 2 and down regulated BMAL and RORα1. RORα1 is a nuclear orphan receptor and treatment with melatonin decreases it transcriptional activity in MCF-7 cells (Dai *et al.* 2001). While BMAL expression was increased in response to exposure to the temperature shift plus melatonin condition in these experiments, the fold change in expression was less than exposure to the temperature shift alone

(Table 3.1). The data from this current study also indicated that melatonin plus temperature shift results in greater expression of PER1, PER2, and CRY2 (Table 3.1) and the results of western blot analysis indicate that melatonin on its own can increase the expression of the PER protein at least in the control condition (Figure 3.11). This is consistent with the results of Xiang *et al.* (2012) where exposure to a serum shock plus melatonin treatment increased PER1, PER2, and CRY 2 expression and treatment with melatonin on its own, with no prior serum shock, significantly increased PER2 expression compared to its normal baseline expression which is below the limit of detection in MCF-7 cells. Therefore, melatonin may impact PER2 expression independent of temperature shift or serum shock synchronization.

Melatonin may influence clock gene expression in MCF-7 cells directly through interaction with nuclear receptors (Dai *et al*. 2001), through the interruption of the estrogen signaling pathways (Menéndez-Menéndez and Martínez-Campa 2018), or through a combination of both. MCF-7 cells express the G-protein coupled membrane receptor, M_1 (Ram *et al.* 1998). Melatonin may impact clock gene expression through a membrane receptor pathway involving cAMP (Godson and Reppert 1997) or through a regulatory influence on protein degradation and its products (Vriend and Reiter 2015). Melatonin has many intracellular target proteins and while no direct binding to clock gene proteins has been identified to date (Liu *et al.* 2019), melatonin may influence clock gene expression through down-regulation of signaling pathways such as cAMP/PKA and Akt or through interaction with other targets (Hill *et al.* 2011). Oxidative stress also influences clock gene expression and because melatonin is a potent antioxidant, it may influence the cellular redox homeostasis, and thereby indirectly regulate circadian rhythm (Wilking *et al*. 2013). It is probable that all of these molecular mechanisms contribute to melatonin's influence at different times, in different tissues, and on different

circadian genes (Xiang *et al*. 2012). The temperature shift model plus the addition of melatonin has replicated work that indicates that melatonin influences the cell cycle kinetics of MCF-7 cells *in vitro* and has the potential to be useful in further mechanistic studies.

3.5 References

Aaltonen, K., R. M. Amini, P. Heikkilä, K. Aittomäki, A. Tamminen, H. Nevanlinna, and C. Blomqvist. 2009. "High Cyclin B1 Expression Is Associated with Poor Survival in Breast Cancer." *British Journal of Cancer*. https://doi.org/10.1038/sj.bjc.6604874.

Bailey, Sandra L., Margaret M. Heitkemper 2000. "Circadian Rhythmicity of Cortisol and Body Temperature: Morningness - Eveningness Effects". *Chronobiology International.* https://doi.org/10.1081/CBI-100103189

Benstaali C., A. Mailloux, A. Bogdan, A. Auzéby, Y. Touitou 2001. "Circadian rhythms of body temperature and motor activity in rodents Their relationships with the light-dark cycle". *Life Sciences*. https://doi-org./10.1016/S0024-3205(01)01081-5

Bernard, Marianne, Jérôme Guerlotté, Pierre Grève, Aline Gréchez-Cassiau, Michael P. Iuvone, Martin Zatz, Nelson W. Chong, David C. Klein, and Pierre Voisin. 1999. "Melatonin Synthesis Pathway: Circadian Regulation of the Genes Encoding the Key Enzymes in the Chicken Pineal Gland and Retina." In *Reproduction Nutrition Development*. https://doi.org/10.1051/rnd:19990305.

Bustin, Stephen A., Vladimir Benes, Jeremy A. Garson, Jan Hellemans, Jim Huggett, Mikael Kubista, Reinhold Mueller. 2009. "The MIQE Guidelines: Minimum Information for Publication of Quantitative Real-Time PCR Experiments." *Clinical Chemistry*. https://doi.org/10.1373/clinchem.2008.112797.

Chomczynski, Piotr, and Nicoletta Sacchi. 2006. "The Single-Step Method of RNA Isolation by Acid Guanidinium Thiocyanate-Phenol-Chloroform Extraction: Twenty-Something Years On." *Nature Protocols*. https://doi.org/10.1038/nprot.2006.83.

Chuffa, Luiz Gustavo de Almeida, Fábio Rodrigues Ferreira Seiva, Maira Smaniotto Cucielo, Henrique Spaulonci Silveira, Russel J Reiter, and Luiz Antonio Lupi. 2019. "Clock Genes and the Role of Melatonin in Cancer Cells: An Overview." *Melatonin Research*. https://doi.org/10.32794/mr11250026.

Cos, Samuel, David E. Blask, Athena Lemus-Wilson, and Anna B. Hill. 1991. "Effects of Melatonin on the Cell Cycle Kinetics and 'Estrogen-rescue' of MCF-7 Human Breast Cancer Cells in Culture." *Journal of Pineal Research*. https://doi.org/10.1111/j.1600-079X.1991.tb00007.x.

Cos, Samuel, J. Recio, and E. J. Sánchez-Barceló. 1996. "Modulation of the Length of the Cell Cycle Time of MCF-7 Human Breast Cancer Cells by Melatonin." *Life Sciences*. https://doi.org/10.1016/0024-3205(95)02359-3.

Dai, Jun, Prahiad T. Ram, Lin Yuan, Louaine L. Spriggs, and Steven M. Hill. 2001. "Transcriptional Repression of RORα Activity in Human Breast Cancer Cells by Melatonin." *Molecular and Cellular Endocrinology*. https://doi.org/10.1016/S0303-7207(01)00449-X.

Del Río, Beatriz, Juana M. Garćia Pedrero, Carlos Martínez-Campa, Pedro Zuazua, Pedro S. Lazo, and Sofía Ramos. 2004. "Melatonin, an Endogenous-Specific Inhibitor of Estrogen Receptor α via Calmodulin." *Journal of Biological Chemistry*. https://doi.org/10.1074/jbc.M403140200.

Erren, Thomas C., Peter Morfeld, J. Valérie Groß, Ursula Wild, and Philip Lewis. 2019. "IARC 2019: 'Night Shift Work' Is Probably Carcinogenic: What about Disturbed Chronobiology in All Walks of Life?" *Journal of Occupational Medicine and Toxicology*. https://doi.org/10.1186/s12995-019-0249-6.

Fan, Saijun, Martin L. Smith, Dennis J. Rivet, Diane Duba, Qimin Zhan, Kurt W. Kohn, Albert J. Fornace, and Patrick M. O'Connor. 1995. "Disruption of P53 Function Sensitizes Breast Cancer MCF-7 Cells to Cisplatin and Pentoxifylline." *Cancer Research*.

Godson, Catherine, and Steven M. Reppert. 1997. "The Mel(1a) Melatonin Receptor Is Coupled to Parallel Signal Transduction Pathways." *Endocrinology*. https://doi.org/10.1210/endo.138.1.4824.

Gonzalez, A., S. Cos, C. Martinez-Campa, C. Alonso-Gonzalez, S. Sanchez-Mateos, M. D. Mediavilla, and E. J. Sanchez-Barcelo. 2008. "Selective Estrogen Enzyme Modulator Actions of Melatonin in Human Breast Cancer Cells." *Journal of Pineal Research*. https://doi.org/10.1111/j.1600-079X.2008.00559.x.

Gray-Bablin, Julie, Juan Zalvide, M. Pat Fox, Chris J. Knickerbocker, James A. Decaprio, and Khandan Keyomarsi. 1996. "Cyclin E, a Redundant Cyclin in Breast Cancer." *Proceedings of the National Academy of Sciences of the United States of America*. https://doi.org/10.1073/pnas.93.26.15215.

Hardeland, Rüdigger. 2009. "Melatonin: Signaling Mechanisms of a Pleiotropic Agent." *BioFactors*. https://doi.org/10.1002/biof.23.

Hill, Steven M., and David E. Blask. 1988. "Effects of the Pineal Hormone Melatonin on the Proliferation and Morphological Characteristics of Human Breast Cancer Cells (MCF-7) in Culture." *Cancer Research*.

Hill, Steven M., David E. Blask, Shulin Xiang, Lin Yuan, Lulu Mao, Robert T. Dauchy, Erin M. Dauchy, Tripp Frasch, and Tamika Duplesis. 2011. "Melatonin and Associated Signaling Pathways That Control Normal Breast Epithelium and Breast Cancer." *Journal of Mammary Gland Biology and Neoplasia*. https://doi.org/10.1007/s10911-011-9222-4.

Jung-Hynes, Brittney, Wei Huang, Russel J. Reiter, and Nihal Ahmad. 2010. "Melatonin Resynchronizes Dysregulated Circadian Rhythm Circuitry in Human Prostate Cancer Cells." *Journal of Pineal Research*. https://doi.org/10.1111/j.1600-079X.2010.00767.x.

Karasek, Michal, and K. Winczyk. 2006. "Melatonin in Humans." In *Journal of Physiology and Pharmacology*. https://doi.org/10.1016/b0-12-341103-3/00197-2.

Lee, Adrian V., Steffi Oesterreich, and Nancy E. Davidson. 2015. "MCF-7 Cells - Changing the Course of Breast Cancer Research and Care for 45 Years." *Journal of the National Cancer Institute*. https://doi.org/10.1093/jnci/djv073.

Leon-Blanco, Mercedes M., Juan M. Guerrero, Russel J. Reiter, Juan R. Calvo, and David Pozo. 2003. "Melatonin Inhibits Telomerase Activity in the MCF-7 Tumor Cell Line Both in Vivo and in Vitro." *Journal of Pineal Research*. https://doi.org/10.1034/j.1600-079X.2003.00077.x.

Lerner, Aaron B., James D. Case, Yoshiyata Takahashi, Teh H. Lee, and Wataru Mori. 1958. "Isolation of Melatonin, the Pineal Gland Factor That Lightens Melanocytes." *Journal of the American Chemical Society*. https://doi.org/10.1021/ja01543a060.

Liu, Lei, Nedjma Labani, Erika Cecon, and Ralf Jockers. 2019. "Melatonin Target Proteins: Too Many or Not Enough?" *Frontiers in Endocrinology*. https://doi.org/10.3389/fendo.2019.00791.

Mediavilla, M. D., S. Cos, and E. J. Sánchez-Barceló. 1999. "Melatonin Increases P53 and P21WAF1 Expression in MCF-7 Human Breast Cancer Cells in Vitro." *Life Sciences*. https://doi.org/10.1016/S0024-3205(99)00262-3.

Menéndez-Menéndez, Javier, and Carlos Martínez-Campa. 2018. "Melatonin: An Anti-Tumor Agent in Hormone-Dependent Cancers." *International Journal of Endocrinology*. https://doi.org/10.1155/2018/3271948.

Miki, Takao, Tomoko Matsumoto, Zhaoyang Zhao, and Cheng Chi Lee. 2013. "P53 Regulates Period2 Expression and the Circadian Clock." *Nature Communications*. https://doi.org/10.1038/ncomms3444.

Ram, P. T., T. Kiefer, M. Silverman, Y. Song, G. M. Brown, and S. M. Hill. 1998. "Estrogen Receptor Transactivation in MCF-7 Breast Cancer Cells by Melatonin and Growth Factors." *Molecular and Cellular Endocrinology*. https://doi.org/10.1016/S0303-7207(98)00095-1.

Refinetti, Roberto 2010. "The Circadian Rhythm of Body Temperature." *Frontiers in Bioscience.* https://doi.org/10.1016/0031-9384(92)90188-8

Sagrillo-Fagundes, Lucas, Josianne Bienvenue-Pariseault, and Cathy Vaillancourt. 2019. "Melatonin: The Smart Molecule That Differentially Modulates Autophagy in Tumor and Normal Placental Cells." *PLoS ONE*. https://doi.org/10.1371/journal.pone.0202458.

Schernhammer, Eva S., Francine Laden, Frank E. Speizer, Walter C. Willett, David J. Hunter, Ichiro Kawachi, and Graham A. Colditz. 2001. "Rotating Night Shifts and Risk of Breast Cancer in Women Participating in the Nurses' Health Study." *Journal of the National Cancer Institute*. https://doi.org/10.1093/jnci/93.20.1563.

Scott, Aaron E., Gregory N. Cosma, Anthony A. Frank, Robert L. Wells, and Henry S. Gardner. 2001. "Disruption of Mitochondrial Respiration by Melatonin in MCF-7 Cells." *Toxicology and Applied Pharmacology*. https://doi.org/10.1006/taap.2000.9115.

Shirinzadeh, Hanif, Burcu Eren, Hande Gurer-Orhan, Sibel Suzen, and Seçkin Özden. 2010. "Novel Indole-Based Analogs of Melatonin: Synthesis and in Vitro Antioxidant Activity Studies." *Molecules*. https://doi.org/10.3390/molecules15042187.

Siu, Ka Tat, Marsha Rich Rosner, and Alex C. Minella. 2012. "An Integrated View of Cyclin E Function and Regulation." *Cell Cycle*. https://doi.org/10.4161/cc.11.1.18775.

Stevens, Richard G., and Scott Davis. 1996. "The Melatonin Hypothesis: Electric Power and Breast Cancer." *Environmental Health Perspectives*. https://doi.org/10.2307/3432703.

Tamarkin, Lawrence, David Danforth, Alan Lichter, Ernest DeMoss, Michael Cohen, Bruce Chabner, and Marc Lippman. 1982. "Decreased Nocturnal Plasma Melatonin Peak in Patients with Estrogen Receptor Positive Breast Cancer." *Science*. https://doi.org/10.1126/science.7079745.

Tan, Dun-xian, Russel Reiter, Lucien Manchester, Mei-ting Yan, Mamdouh El-Sawi, Rosa Sainz, Juan Mayo, Ron Kohen, Mario Allegra, and Rudiger Hardelan. 2005. "Chemical and Physical Properties and Potential Mechanisms: Melatonin as a Broad Spectrum Antioxidant and Free Radical Scavenger." *Current Topics in Medicinal Chemistry*. https://doi.org/10.2174/1568026023394443.

Tordjman, Sylvie, Sylvie Chokron, Richard Delorme, Annaelle Charrier, Eric Bellissant, Nemat Jaafari, and Claire Fougerou. 2017. "Melatonin: Pharmacology, Functions and Therapeutic Benefits." *Current Neuropharmacology*. https://doi.org/10.2174/1570159x14666161228122115.

Venegas, Carmen, José A. García, Germaine Escames, Francisco Ortiz, Ana López, Carolina Doerrier, Laura García-Corzo, Luis C. López, Russel J. Reiter, and Darío Acuña-Castroviejo. 2012. "Extrapineal Melatonin: Analysis of Its Subcellular Distribution and Daily Fluctuations." *Journal of Pineal Research*. https://doi.org/10.1111/j.1600-079X.2011.00931.x.

Vriend, Jerry, and Russel J. Reiter. 2015. "Melatonin Feedback on Clock Genes: A Theory Involving the Proteasome." *Journal of Pineal Research*. https://doi.org/10.1111/jpi.12189.

Wilking, Melissa, Mary Ndiaye, Hasan Mukhtar, and Nihal Ahmad. 2013. “Circadian Rhythm Connections to Oxidative Stress: Implications for Human Health.” *Antioxidants and Redox Signaling*. https://doi.org/10.1089/ars.2012.4889.

Xiang, S., L. Mao, T. Duplessis, L. Yuan, R. Dauchy, Ee Dauchy, D. Blask, T. Frasch, and S. M. Hhill. 2012. “Oscillation of Clock and Clock Controlled Genes Induced by Serum Shock in Human Breast Epithelial and Breast Cancer Cells: Regulation by Melatonin.” *Breast Cancer: Basic and Clinical Research*. https://doi.org/10.4137/BCBCR.S9673.

Xiong, Yue, Gregory J. Hannon, Hui Zhang, David Casso, Ryuji Kobayashi, and David Beach. 1993. “P21 Is a Universal Inhibitor of Cyclin Kinases.” *Nature*. https://doi.org/10.1038/366701a0.

Zhou, Jin, Lu Li, Li Fang, Hua Xie, Wenxiu Yao, Xiang Zhou, Zhujuan Xiong, Li Wang, Zhixi Li, and Feng Luo. 2016. “Quercetin Reduces Cyclin D1 Activity and Induces G1 Phase Arrest in HepG2 Cells.” *Oncology Letters*. https://doi.org/10.3892/ol.2016.4639.

Chapter 4

Chapter 4 Cellular Responses to Melatonin or Chemotherapeutic Drugs as Measured by Reactive Oxygen Species Production in a Temperature Shift Model

4.1 Introduction

Aerobic respiration provides for the energy requirements of the mammalian cell. The process of aerobic respiration uses oxygen to turn carbohydrates and fats into energy, in the form of adenosine triphosphate (ATP) and primarily involves the transfer of two electron pairs through a series of reduction-oxidative or redox reactions to oxygen, in the mitochondria (Turpaev 2002). Part of the normal processes of the electron transport chain (ETC) within the inner mitochondrial membrane involves the generation of reactive oxygen species (ROS) which include: hydrogen peroxide (H_2O_2), single oxygen ($^1O_2$), superoxide (O_2-), and the hydroxyl radical (-OH) (Siauciunaite *et al.* 2019). While small amounts of ROS serve useful cellular functions, including signal transduction, larger quantities are toxic to the cell since the presence of unstable free radicals can damage many macromolecules (Finkel 2011). The intracellular balance of ROS is tightly controlled by enzymatic and non-enzymatic mechanisms and a failure to effectively detoxify ROS results in oxidative stress for the cell, and if system-wide, for the organism (Yokoyama *et al*. 2017).

There are several non-enzymatic antioxidants that scavenge free radicals including β-carotene, vitamin C, vitamin E, glutathione (GSH), and melatonin (Milkovic *et al.* 2019) (Lobo *et al.* 2010). Melatonin is concentrated in the mitochondria, where the primary source of electron leakage and superoxide generation occurs (Reiter *et al.* 2018). Melatonin can act as a direct scavenger of ROS and can indirectly contribute to optimal redox balance by stimulating the production of other anti-oxidant enzymes (Reiter *et al.* 2016) (Manchester *et al*. 2015). While the primary source of intracellular ROS production is in mitochondria, reactions involving the cell membrane and those occurring in the cytosol contribute to total intracellular ROS generation (Finkel 2011). Extracellular sources of ROS can also accumulate in response to inflammation or drug and chemical exposure and metabolism (Snezhkina *et al*. 2020). Enzymatic degradation of ROS within the cell is compartmentalized; with NAD(P)H oxidases specific to the cell membrane, superoxide dismutase (SOD1) in the cytoplasm, and SOD2 containing manganese in the mitochondria (Turpaev 2002). This subcellular specialization helps to manage free radicals, to minimize the risks of free radical damage, and to facilitate the generated signaling processes, which drives a third feature of free radical regulation - the up-regulation of genes required for enzyme production (Liu et al. 2005). A group of antioxidants that function outside of the cytoplasmic peroxisomes or lysosomes, are called the peroxiredoxins and provide essential redox buffering as well (Finkel 2011).

ROS can damage macromolecules through the oxidation of proteins, including transcription factors, kinases, and phosphatases with the exposed cysteine residues being particularly vulnerable, through the peroxidation of lipids, and through DNA adduct formation (Milkovic *et al.* 2019). The ability of ROS to promote genomic instability through DNA damage has historically led to the idea that an excess of ROS is a key contributor to carcinogenesis

(Idelchik *et al*. 2017). However, the ability of ROS to activate the key cellular signaling pathways that activate cell growth and proliferation including NRF2/KEAP 1, NF-κβ, PI3K/AKT, and MAP kinase are now elucidated as contributing factors to carcinogenesis (Ray, Huang, and Tsuji 2012). Increased ROS levels are a feature of malignant cells (Weinberg and Chandel 2009). However, very high levels of ROS can induce cell senescence and apoptosis in malignant cells and malignant cells are as susceptible to damage by extracellular sources of ROS such as ionizing radiation, drugs, and ultraviolent light as are normal cells (Milkovic *et al.* 2019).

The circadian regulation of ROS and their generation is interrelated with the ability of ROS to impact clock genes (Stangherlin and Reddy 2013). The ratio of the oxidized and reduced forms NAD+/NADH and NADP+/NADPH influence the DNA binding efficiency of both CLOCK and BMAL (Stangherlin and Reddy 2013) (Liu et al. 2005). Mitochondrial respiration and mitochondrial number and dynamics are under circadian control (De Goede *et al.* 2018)(Ezagouri and Asher 2018) (Peek *et al.* 2013). Non-transcriptional control of clock rhythms have been demonstrated in response to the circadian redox cycling of the peroxiredoxins in human red blood cells; cells that have no nucleus or mitochondria (O'Neill and Reddy 2011). Mitochondria are the only mammalian subcellular organelle that contains DNA (mtDNA), which encodes for thirteen mitochondrial proteins, and mutations in mitochondrial number and DNA are common in cancer cells (Idelchik *et al*. 2017). Chemically-derived mitochondrial deficient *Rhø* cells are reported not to generate ROS (Kalghatgi *et al*. 2013) (Weinberg and Chandel 2009). Interestingly, mtDNA-depleted cells have a poor ability to form tumors in mice but this can be restored with transfer of donor mtDNA from malignant cells (Dong *et al*. 2017). ROS levels increase during cell cycle progression and dampening of ROS with a mitochondrial antioxidant, causes G_1 arrest (Weinberg and Chandel 2009). Therefore, mitochondria, ROS

production, and the management of redox homeostasis in the cell are important considerations in tumor initiation and progression. To investigate the impact of the temperature shift model on ROS production, MCF-7 breast cancer cells were exposed to an antioxidant (melatonin) or known ROS generators (chemotherapeutic drugs) and their cellular responses observed.

4.2 Materials and Method

Cell culture

A human hormone responsive breast cancer cell line, MCF-7 cells, originally obtained from the American Type Culture Collection (ATCC) were maintained in Hyclone Debucco's Modified Eagle Media (DMEM) with high glucose (GE Lifesciences) and supplemented with 10% fetal bovine serum (FBS) and 1% antibiotic and antimycotic solution® (A&A) (Fisher). The cells were maintained in a humidified environment at 37^{o} C and 5% CO_2.

Experimental protocols

Cell viability was measured using the 3-(4,5-dimethylthiazol-2-yl) -2,5 – diphenyltetrazolium bromide assay (MTT) assay. MCF-7 cells were seeded with 2,000 cells/well in a 96 well plate, and 100 µl media was added to each well on day 1 of the experiment. Triplicate plates were prepared. The cells were subjected to three conditions; a control condition of 37/37° C, 37/34° C (the experimental condition where the plates were shifted to a 34°C incubator at 21:00 and returned to 37°C at 09:00), and a 34/34° C comparative condition. On day 3 at 09:00, each well per plate received a further 100 µl of media containing drugs such that the final concentrations were as follows:

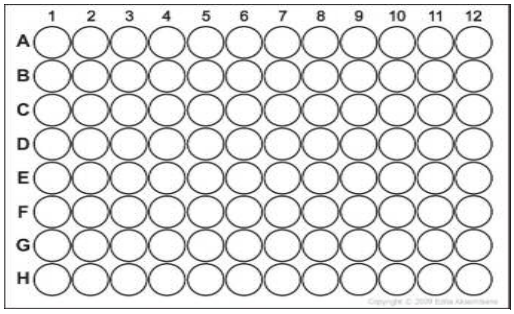

Column 1 – no melatonin or drug – control

Column 2 – melatonin (n- acetyl – 5 – methoxytryptamine, Santa-Cruz Biotechnology), 1nM

Column 3 – melatonin, 10 nM

Column 4 – melatonin, 100 nM

Column 5 – melatonin, 100 µM

Column 6 - docetaxel, 2.5 ng/ml

Column 7 - cisplatin, 22.9 µM

Column 8 – doxorubicin, 0.00984 µM

Column 9 – 0.5% ethanol (positive control)

The concentrations of docetaxel, cisplatin, and doxorubicin were selected based on published inhibitory concentration or IC_{50} values (Genomics of Drug Sensitivity in Cancer – Sanger Institute). After 24-hours of melatonin or drug exposure, an MTT assay was performed on day 4 using the lab protocol where 5 pg/well MTT was added each day of the assay and the replicate plate and incubated at 37^{o} C for 3 hours. Then the media was removed and replaced with 100 µl of dimethyl sulfoxide (DMSO) to solubilize the formazan product crystals. The plate wells were read at 540 nm wavelength on a Synergy® H4 Hybrid plate reader (Biotek) using Gen 5, version 2.00 software. The average absorbance of the triplicate experiments is reported along with the standard error of the mean (SEM).

Microscopy

MCF-7 cells were seeded onto 6 well plates and different plates were exposed to 3 separate conditions: 2 plates were exposed to the control condition of 37/37° C; 2 plates were exposed to an experimental condition of 37/34° C, where the plates were shifted to a 34° C incubator at 21:00 and returned to 37° C at 09:00; and, 2 plates were exposed to a comparative condition of 34/34° C. On day 4 at 09:00, 4/6 wells in each plate received either docetaxel at a final concentration of 2.5 ng/ml or 5.0 ng/ml or melatonin at a final concentration of 1 nM or 10 nM, for 24 hours and 1/6 wells in each plate remained as a control. On day 5 the remaining well received 12.5 μM of 30% hydrogen peroxide (H_2O_2) for 30 minutes as a positive control. After a 30-minute incubation, all of the wells were washed with 37° C PBS, pH 7.4, and 1 ml of phenol-free FluoroBrite® DMEM media (Gibco) was added per well. For each condition, one plate received 2 μl/ml CellROX® Orange reagent (Thermo Fisher Scientific) and was incubated at 37° C for 30 minutes, as per the manufacturer's protocol, with 2 drops/ml of NucBlu® Live Ready Probe® stain (Thermo Fisher Scientific) added for the last 10 minutes. The second, duplicate plate received 1μl/ml MitoSOX Red Mitochondrial Superoxide Indicator® (Thermo Fisher Scientific) and was incubated at 37° C for 15 minutes, as per the manufacturer's protocol, with 2 drops/ml of NucBlu® Live Ready Probe® stain (Thermo Fisher Scientific) added for the last 10 minutes. Images were captured using an Olympus fluorescence microscope model DP80 with the manufacturer's CellSens Dimension software. Final image capture used the TritC/ DAPI overlay filter set for detection of the fluorescence dyes.

In a second experiment, MCF-7 cells were seeded at 50,000 cells /well onto 6 well plates and the individual plates were exposed to 3 conditions: 2 plates were exposed to the control condition of 37/37° C; 2 plates were exposed to an experimental condition of 37/34° C, where the plates were shifted to a 34° C incubator at 21:00 and returned to 37° C at 09:00; and, 2 plates

were exposed to a comparative condition of 34/34° C. On day 4 at 09:00, 4/6 wells in each plate received melatonin at a final concentration of 1 nM or 100 μM or cisplatin or doxorubicin at a final concentration corresponding to their respective IC_{50} values and 1 well in each plate received 0.5% ethanol and one well remained as a negative control. On day 5, all the wells were washed with 37° C PBS, pH 7.4, and 1 ml of phenol-free FluoroBrite® DMEM media (Gibco) was added. For each condition, one plate received 2 μl/ml CellROX® Orange reagent (Thermo Fisher Scientific) and was incubated at 37° C for 30 minutes, as per the manufacturer's protocol, with 2 drops/ml of NucBlu® Live Ready Probe® stain (Thermo Fisher Scientific) added for the last 10 minutes. The second duplicate plate received 1μl/ml MitoSOX Red Mitochondrial Superoxide Indicator® (Thermo Fisher Scientific) and was incubated at 37° C for 15 minutes, as per the manufacturer's protocol, with 2 drops/ml of NucBlu® Live Ready Probe® stain (Thermo Fisher Scientific) added for the last 10 minutes. Images were captured using an Olympus fluorescence microscope model DP80 with the manufacturer's CellSens Dimension software. The final image capture separately recorded the TritC and DAPI filtered images, as the overlay made a comparison between the CellROX Orange and the MitoSOX Red images for each condition difficult.

Protein extraction and Western Blotting

Cell lysates were subjected to immunoblot analysis for the transcription factor for mitochondrial (TFAM). The proteins from MCF-7 cells were extracted from cells plated on to 100 mm tissue culture plates. The cells were subjected to three separate conditions which included: a control condition of cells at 37/37° C; the 37/34° C experimental condition where the plates were shifted to a 34° C incubator at 21:00 and returned to 37° C at 09:00; and, a 34/34° C comparative condition. After 3 days, the cells were exposed to 22.9 μM cisplatin for 24 hours

with control plates for each temperature condition treated in the absence of drug. Whole cell lysates were then collected. The cells were washed with ice cold PBS, pH 7.4, and whole cell lysates collected in 300 µl of ice cold radioimmunoprecipitation assay (RIPA) buffer containing 150 mM sodium chloride, 15 mM sodium phosphate, pH 7.4, 1% Triton X-100, 0.5% sodium dodecyl sulfate (SDS), 0.5% sodium deoxycholate, 10 mM sodium fluoride (NaF), 10 mM sodium orthovanadate, and protease inhibitors (Thermo Scientific™ Pierce™ Protease Inhibitor Tablets). All reagents were obtained from Fisher Scientific unless otherwise indicated. The cell lysates were collected using a plastic cell scraper and the DNA and cytoskeletal proteins sheared by passage through a 22 gauge needle several times and then stored at -80^0 C. Protein quantification was done using the bicinchoninic acid (BCA) assay (Thermo Scientific™ Pierce™ BCA Protein Assay Kit) with bovine serum albumin as the standard and read using a Synergy® H4 Hybrid plate reader (Biotek) using Gen 5, version 2.00 software. Electrophoresis was performed using 25 µg of protein loaded per lane onto a 15 % polyacrylamide gel containing SDS. After electrophoresis, the gels were transferred onto nitrocellulose membranes using a semi-dry transfer apparatus in 192 mM glycine, 25 mM Tris-HCl, pH 8, and 20% methanol, and protein transfer was confirmed by staining the blots with 0.1% Ponceau S in 1% acetic acid. The membranes were blocked by incubation in 5% low fat milk in TBST overnight at 4^0 C. Primary antibodies against TFAM at a dilution of 1:200 and GAPDH at a dilution of 1:2000 (Santa Cruz Biotechnology) were incubated in 5% low fat milk in TBST, overnight at 4^0 C. Secondary antibody-HRP conjugates were incubated with the blots at a dilution of 1:10,000 for 2 hours at room temperature. Chemiluminescent detection of the HRP was detected using the Thermo Scientific™ enhanced chemiluminescence (ECL) detection reagents and exposure to radiographic film.

4.3 Results

The MTT assay was used to investigate the effects of exposure to the temperature shift protocol and or the control condition on MCF-7 cells when challenged with a 24-hour exposure to chemotherapeutic drugs or an antioxidant (melatonin) on cellular metabolism and cell viability. Varying concentrations of melatonin were used for comparison. The results displayed in Figure 4.1. show two aspects to consider. The first is that there was a significant difference in cell viability between cells treated with the 37/37° C control condition versus the 37/34° C experimental condition: the temperature shift resulted in significantly less absorbance therefore inferring less cell viability or a decreased metabolic ability to convert MTT to formazan. The lower MTT value exists for the cells treated with the negative control (as in no melatonin or drug) condition, 10 nM melatonin, docetaxel, cisplatin, doxorubicin, and the positive (0.5% ethanol as detailed in the materials and methods) control. This is consistent with the data in Figures 2.1 and 2.3 where the temperature shift was shown to impact MCF-7 cell viability. It is interesting that for all of the chemotherapeutic and ethanol conditions, except docetaxel, the effect of the temperature shift was not significantly from the no treatment control (as in no melatonin or drug). This confirms that with the exception of docetaxel, this difference in cell viability is a temperature-shift effect. For each treatment with chemotherapeutic drug or ethanol, including the addition of docetaxel, the absorbance of cells treated with the 37/37° C condition was not significantly different from the negative control treatment (as in no drug or melatonin). The temperature shift condition plus docetaxel treatment results in increased MTT-dependent absorbance as compared to the no treatment 37/34°C and therefore presumably a metabolic advantage and increased cell number.

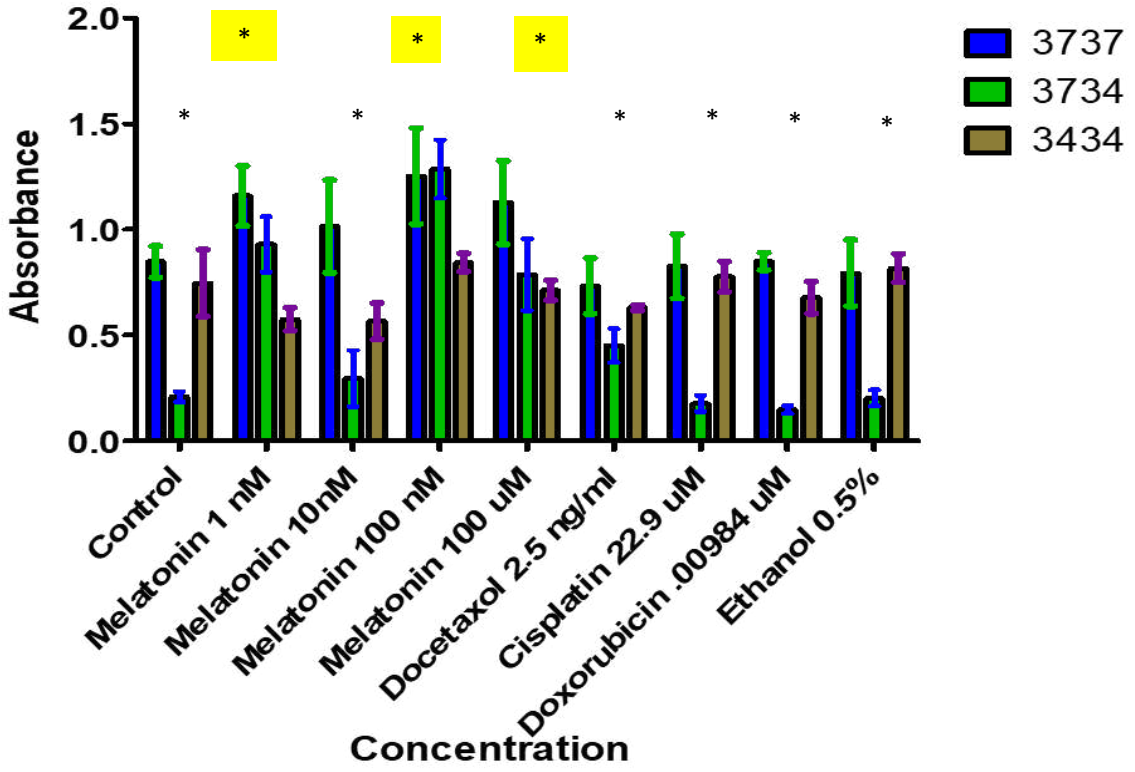

Figure 4.1 MCF-7 cells proliferation as measured by MTT assay on day of shift experiment and after 24 hours of melatonin or drug exposure. Cultures of MCF-7 cells were treated with 1 nM, 10 nM, 100 nM, or 100 µM melatonin or docetaxel, cisplatin, or doxorubicin on day 1 and the viability of the cultures was measured on day 2 using an MTT assay. The Y axis denotes the relative absorbance of the active product, formazan ($n=3$, $p<0.05$). The * where noted denotes statistical difference between the 37/37 and the 37/34 conditions the * surrounded by the yellow box denotes statistical difference between the 37/37 no treatment control and the 37/37 of that specific melatonin concentration results.

The second important aspect shown by the data is that treatment with melatonin has an effect on cell metabolism or cell viability. Treatment of cells with melatonin at concentrations of 1 nM, 100 nM, or 100 µM did not cause a significant difference in viability between cells exposed to the control 37/37°C condition, and the experimental 37/34° C condition. The addition of these concentrations of melatonin were sufficient to reverse the inhibition of MTT activity shown by cells exposed to the temperature shift condition. The MTT activity for cells

exposed to the control 37/37° C condition and treated with melatonin concentrations of 1 nM and 100 nM also exhibited significantly greater absorbance than cells exposed to the 37/37° C condition in the absence of melatonin, indicating that this is likely a melatonin effect rather than a temperature shift effect.

In order to examine for any differences in ROS production between the control and experimental temperature shift conditions, and to determine whether the production of the ROS showed any subcellular localization to the mitochondria after drug or melatonin treatment, a selection of fluorescent-based probes was used. The main source of the superoxide (O_2 -) molecule is mitochondrial due to electron leakage during oxidative phosphorylation. The MitoSOX Red Mitochondrial Superoxide Indicator® preferentially binds to O_2 - and is expected to stain mitochondria. CellROX Orange® binds to H_2O_2, -OH, and O_2 – and reflects total cellular ROS. Based on a qualitative comparison of images displayed in Figure 4.2, exposure of MCF-7 cells to the temperature shift condition (37/34°C) induced the production of total cellular ROS in the cytosol, cell membrane, and mitochondrial compartments. Exposure of MCF-7 cells to the 37/37° C control condition did not promote any significant ROS production. The comparative condition, 34/34° C, where cells are kept at suboptimal temperature conditions, also induced production of total ROS and part of this is a mitochondrial contribution. These findings are displayed in Figures 4.2 and 4.3. This demonstrates that part of the mechanism of action of the temperature shift may be due to ROS induction but this does not appear to be attributable to an impact on oxidative phosphorylation in the mitochondria as the superoxide molecule was not detected in the 37/34 °C shift condition (Figure 4.3).

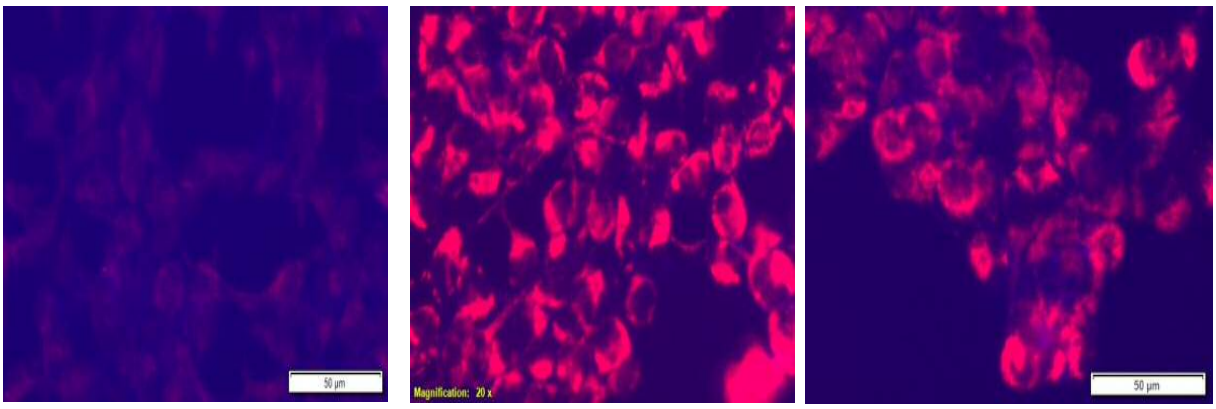

Figure 4.2 No treatment control of MCF-7 cells as imaged using CellROX Orange® and NucBlue® with the left panel representing the 37/37° C control condition, the middle panel representing the 37/34° C experimental condition, and the right panel image representing the 34/34° C comparative condition (n=3).

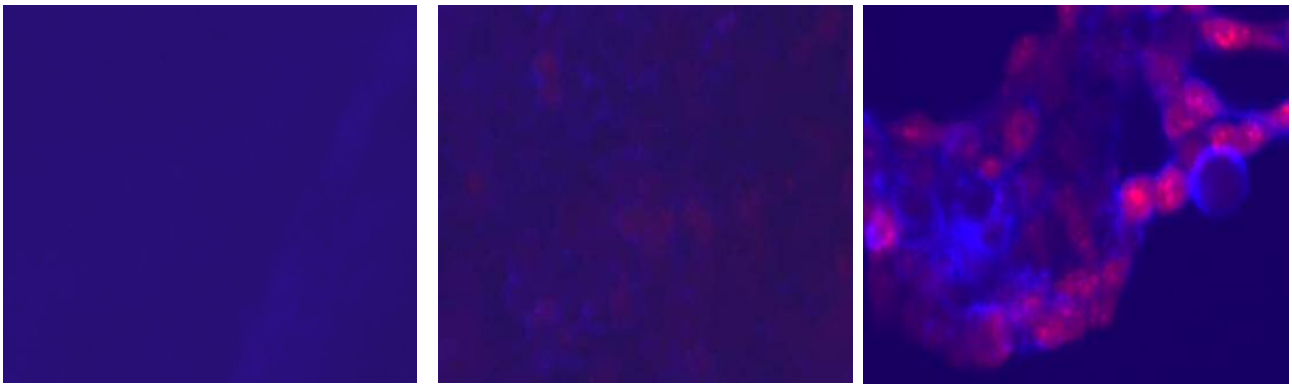

Figure 4.3 No treatment control of MCF-7 cells as imaged using MitoSOX Red Mitochondrial Superoxide Indicator® and NucBlue ® with the left panel representing the 37/37° C control condition, the middle panel representing the 37/34° C experimental condition, and the right panel image representing the 34/34° C comparative condition (n=3).

MCF-7 cells exposed to docetaxel for 24 h either at the IC_{50} concentration or at 2 times that concentration (5.0 ng/ml) produced cellular ROS at all three experimental temperature conditions. The source of the ROS production appeared to be primarily non-mitochondrial. The results are displayed in Figures 4.4, 4.5, 4.6, and 4.7.

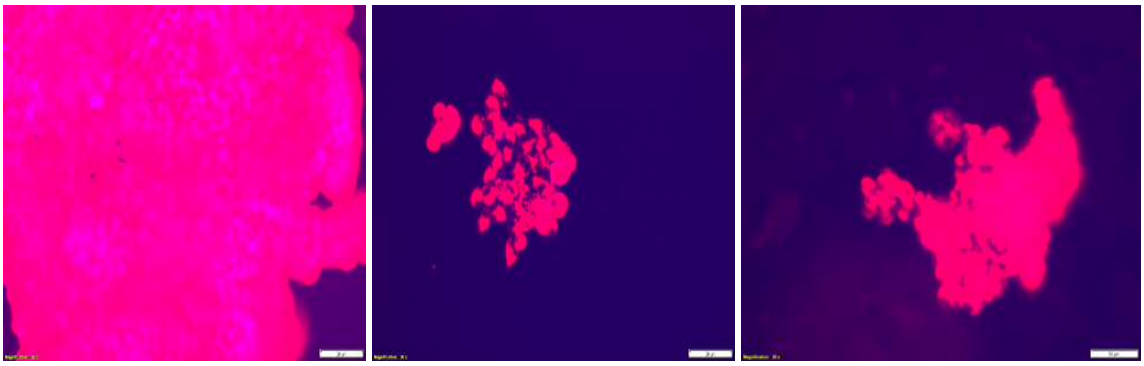

Figure 4.4 Treatment of MCF-7 cells after a 24 hour exposure to 2.5 ng/ml docetaxel as imaged using CellROX Orange® and NucBlue® with the left panel representing the 37/37° C control condition, the middle panel representing the 37/34° C experimental condition, and the right panel image representing the 34/34° C comparative condition (n=3).

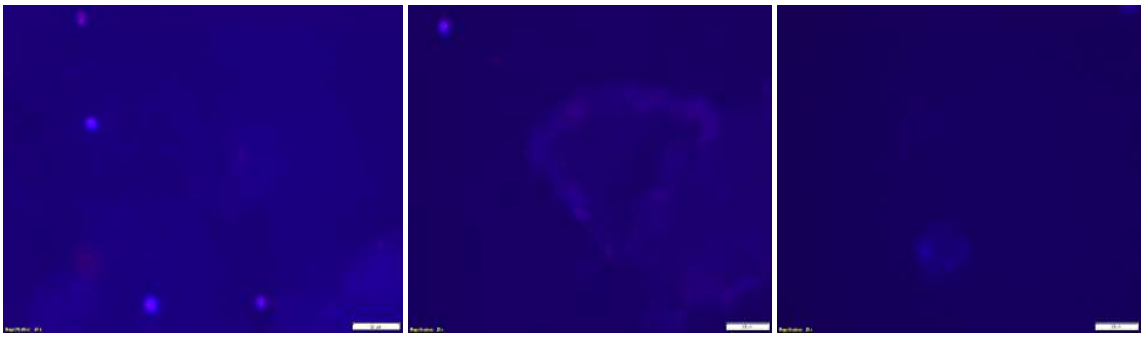

Figure 4.5 Treatment of MCF-7 cells after a 24 hour exposure to 2.5 ng/ml docetaxel as imaged using MitoSOX Red Mitochondrial Superoxide Indicator® and NucBlue® with the left panel representing the 37/37° C control condition, the middle panel representing the 37/34° C experimental condition, and the right panel image representing the 34/34° C comparative condition (n=3).

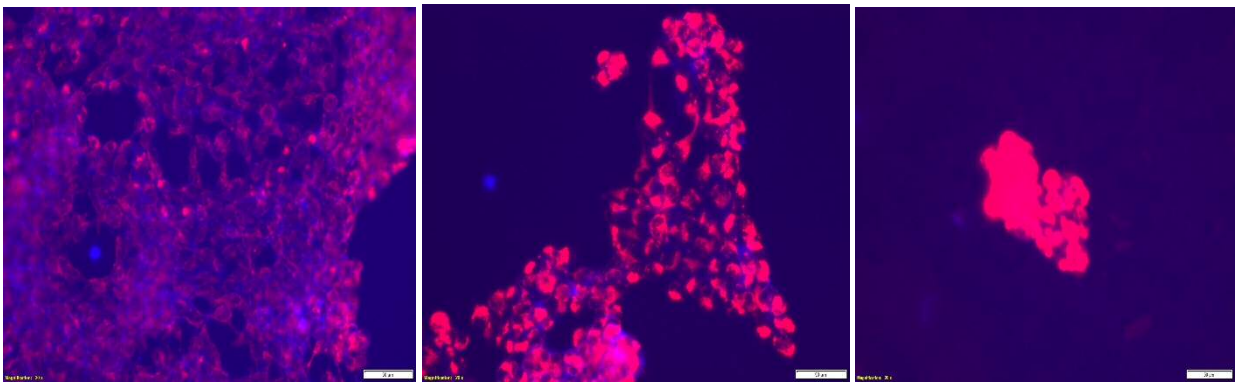

Figure 4.6 Treatment of MCF-7 cells after a 24 hour exposure to 5.0 ng/ml docetaxel as imaged using CellROX Orange® and NucBlue® with the left panel representing the 37/37° C control condition, the middle panel representing the 37/34° C experimental condition and the right panel image representing the 34/34° C comparative condition (n=3).

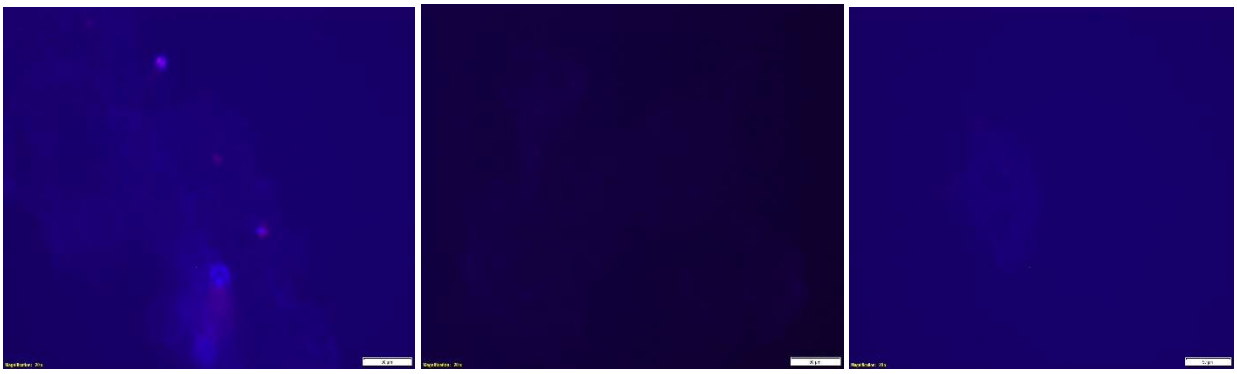

Figure 4.7 Treatment of MCF-7 cells after a 24 hour exposure to 5.0 ng/ml docetaxel as imaged using MitoSOX Red Mitochondrial Superoxide Indicator® and NucBlue® with the left panel representing the 37/37° C control condition, the middle panel representing the 37/34° C experimental condition, and the right panel image representing the 34/34° C comparative condition (n=3).

Therefore, exposure to the chemotherapeutic drug, docetaxel, increased total cellular ROS but not through mitochondrial sources. Exposure to physiological concentrations of melatonin (1 nM) caused MCF-7 cells to produce detectable levels of cellular ROS in all the temperature conditions as shown in Figure 4.8. However, there appeared to be a gradient of

response with the 34/34° C comparative condition demonstrating the greatest induction of ROS, then the temperature shift condition, followed by the control condition. The mitochondrial contribution to ROS production can be observed to be minimal except for the control condition of 37/37° C where the superoxide molecule is detectable. This is demonstrated in Figure 4.9. It appears that at a 1 nM concentration, melatonin is acting as a pro-oxidant in MCF-7 cells at all temperature conditions, however, at that concentration the amount of mitochondrial ROS produced by cells treated with the temperature shift condition or at the suboptimal temperature was very low. The MTT assay (Figure 4.1) results suggest that at 1 nM melatonin there is a benefit to the cell that is dependent on the presence of hormone but not on treatment with the temperature shift. Figure 4.9 suggests that this benefit could be related to decreased superoxide production in the mitochondria.

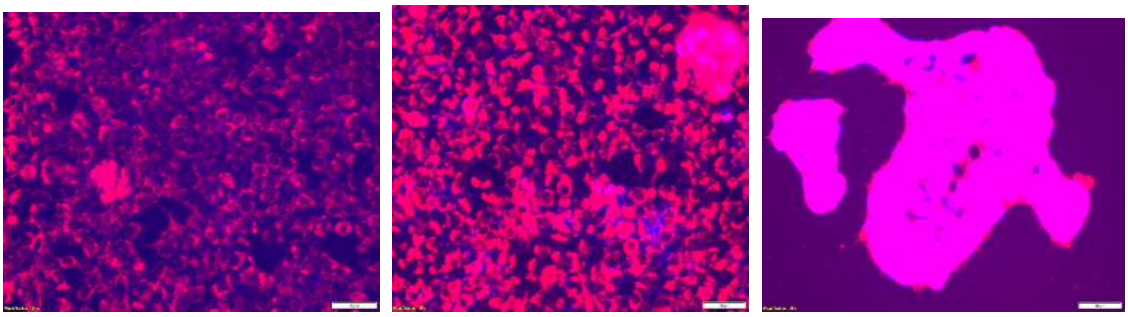

Figure 4.8 Treatment of MCF-7 cells after a 24 hour exposure to 1 nM melatonin as imaged using CellROX Orange® and NucBlue® with the left panel representing the 37/37° C control condition, the middle panel representing the 37/34° C experimental condition, and the right panel image representing the 34/34° C comparative condition (n=3).

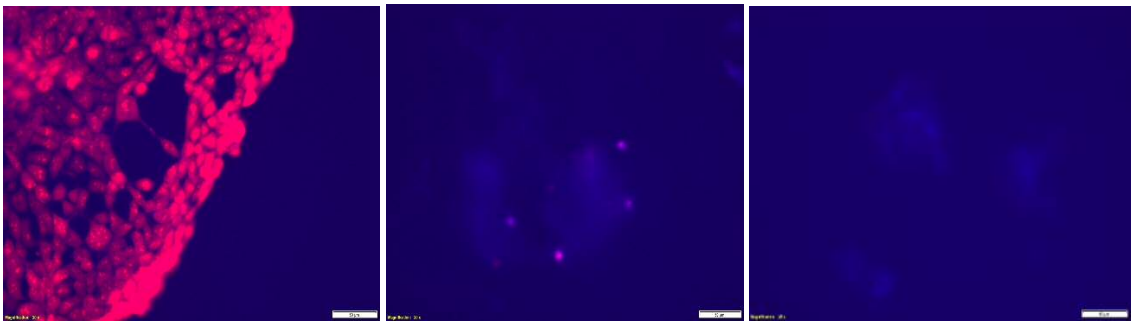

Figure 4.9 Treatment of MCF-7 cells after a 24 hour exposure to l nM melatonin as imaged using MitoSOX Red Mitochondrial Superoxide Indicator® and NucBlue® with the left panel representing the 37/37° C control condition, the middle panel representing the 37/34° C experimental condition, and the right panel image representing the 34/34° C comparative condition (n=3).

The response of the MCF-7 cells to 10 nM melatonin is different in two ways. First, although cells treated with 10 nM melatonin and subjected to all three temperature shift conditions demonstrated cellular ROS production, the gradient has shifted such that the greatest induction of ROS is in cells treated with the 34/34 °C condition and the cells maintained at the 37/37°C control condition had comparatively more ROS induction than cells treated with the temperature shift condition. This is displayed in Figure 4.10. At 10 nM, melatonin appeared to function as a pro-oxidant in MCF-7 cells.

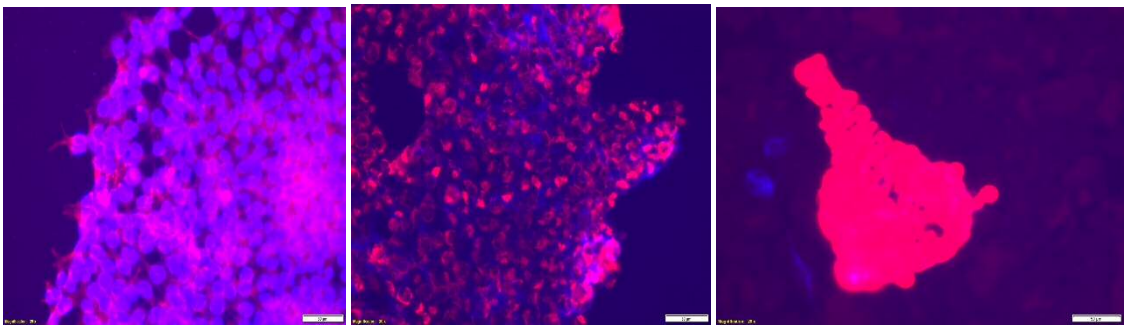

Figure 4.10 Treatment of MCF-7 cells after a 24 hour exposure to 10 nM melatonin as imaged using CellROX Orange® and NucBlue® with the left panel representing the 37/37° C control condition, the middle panel representing the 37/34° C experimental condition, and the right panel image representing the 34/34° C comparative condition (n=3).

When the cells were treated with 10 nM melatonin there appeared to be very little mitochondrial sourced ROS production in any of the conditions as shown in the images in Figure 4.11. Therefore, it appears that the pro-oxidant effect induced by treatment with 10 nM melatonin is generated from non-mitochondrial sources.

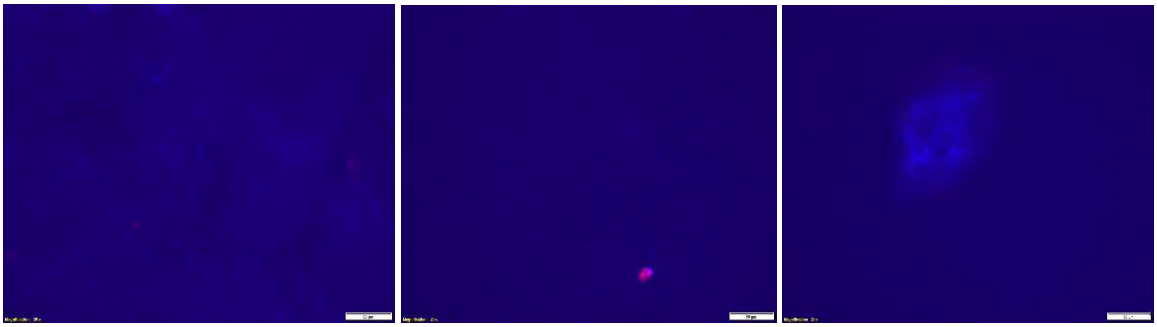

Figure 4.11 Treatment of MCF-7 cells after a 24 hour exposure to l0 nM melatonin as imaged using MitoSOX Red Mitochondrial Superoxide Indicator® and NucBlue® with the left panel representing the 37/37° C control condition, the middle panel representing the 37/34° C experimental condition, and the right panel image representing the 34/34° C comparative condition (n=3).

Hydrogen peroxide was used as a positive control in this experiment but had an impact on cell viability despite using referenced IC_{50} values (12.5µM) so that the total number of remaining cells was very low. The total cellular ROS response was positive despite the low number of surviving cells, with no mitochondrial source signal for the shift condition as seen in Figures 4.12 and 4.13.

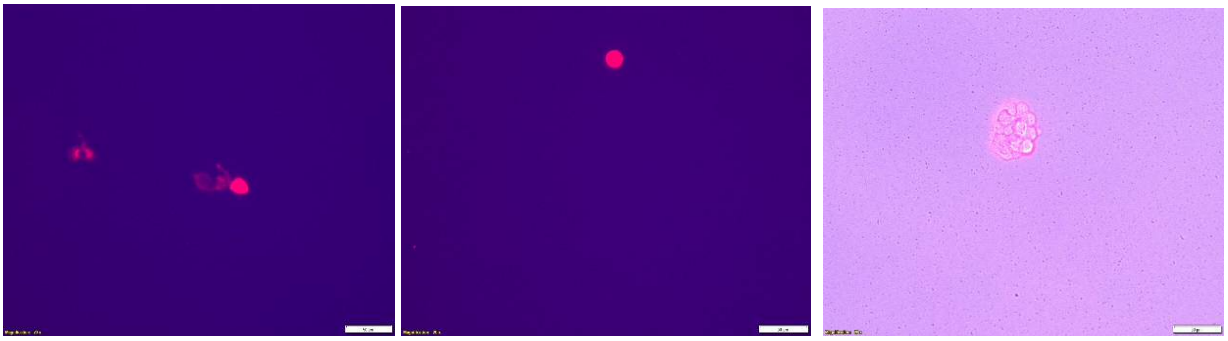

Figure 4.12 Treatment of MCF-7 cells after a 24 hour exposure to 12.5 µM H_2O_2 as a positive control as imaged using CellROX Orange® and NucBlue® with the left panel representing the 37/37° C control condition, the middle panel representing the 37/34° C experimental condition, and the right panel image representing the 34/34° C comparative condition but with no DAPI stain (n=3).

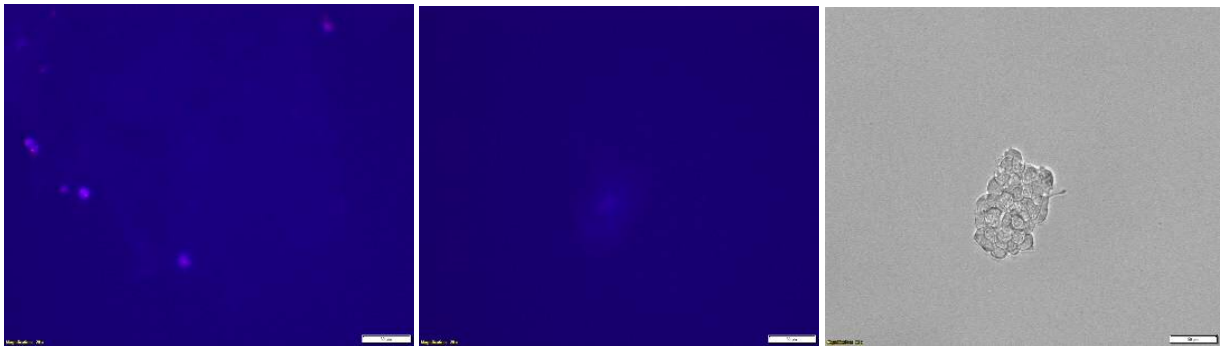

Figure 4.13 Treatment of MCF-7 cells after a 24 hour exposure to 12.5 µM H_2O_2 as a positive control as imaged using MitoSOX Red Mitochondrial Superoxide Indicator® and NucBlue® with the left panel representing the 37/37° C control condition, the middle panel representing the 37/34° C experimental condition, and the right panel image representing the 34/34° C comparative condition phase contrast only. No viable cells were imaged for the 37/37° C control condition(n=3).

The results of the MTT assays suggests that cells treated with the temperature shift plus chemotherapy drug or ethanol results in decreased cell metabolism and viability and that this effect is due to the temperature shift (Figure 4.1). From Figures 4.4- 4.7, it is shown that treatment of MCF-7 cells with docetaxel increases total cellular ROS under any condition. These results are expected as chemotherapeutic drugs are known to increase ROS production (Yokoyama *et al.* 2017).

Since the changes in cell viability in response to exposure to drug plus the temperature shift condition are primarily a response to the temperature shift, based on Figure 4.1, it was decided to compare intracellular sources of ROS in cells treated with a temperature shift in combination with either cisplatin or doxorubicin. Cisplatin treatment at IC_{50} concentration (22.9 μM), appears to induce mitochondrial ROS almost exclusively as shown in Figure 4.14. This result was anticipated as cisplatin preferentially binds to mtDNA and promotes adduct formation (Hu *et al.* 2016).

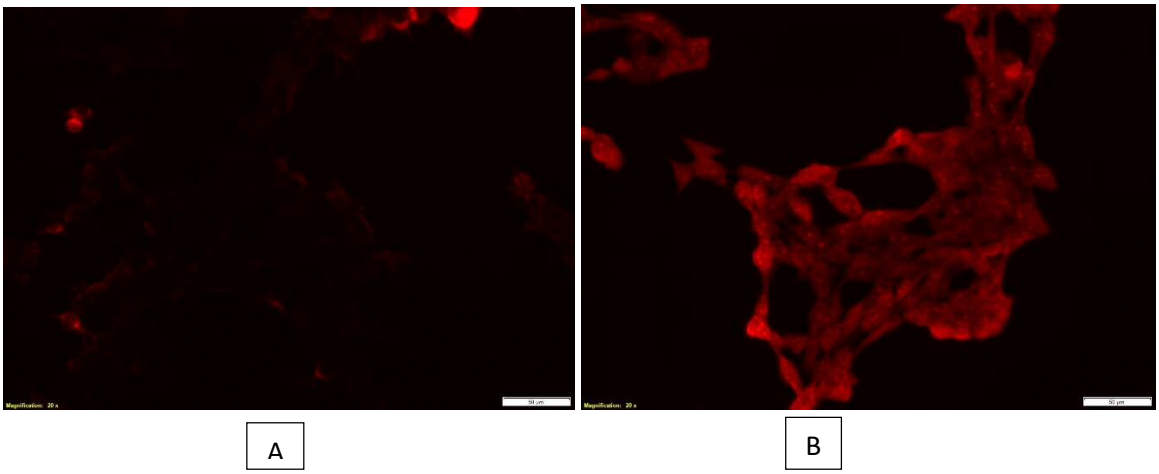

Figure 4.14 MCF-7 cells as imaged using A = CellROX Orange® at 37/34° C and B = MitoSOX Red Mitochondrial Superoxide Indicator® at 37/34° C after 24 exposure to 22.9 μM cisplatin (n=3).

Doxorubicin at the IC_{50} concentration (0.00984 μM) induced both total cellular and mitochondrial ROS in MCF-7 cells exposed to the temperature shift as seen in Figure 4.15.

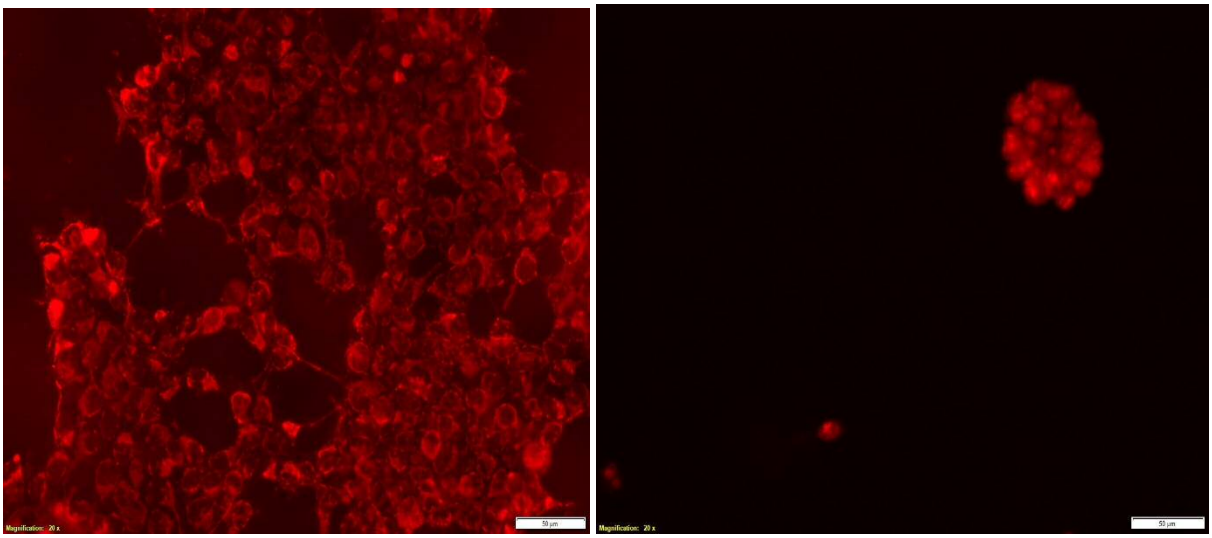

A B

Figure 4.15 MCF-7 cells as imaged using A = CellROX Orange® at 37/34° C and B = MitoSOX Red Mitochondrial Superoxide Indicator® at 37/34° C after 24 exposure to 0.00984 µM doxorubicin (n=3).

Ethanol, at a concentration of 0.5%, provided a more favorable positive control as compared to hydrogen peroxide for the shift condition as seen in Figure 4.16 as there is a fluorescence signal detected for total cellular and mitochondrial ROS and a larger proportion of viable cells. ROS production occurs as cells metabolize ethanol provided that the concentration of ethanol is sufficiently high to activate detoxification systems (Gonthier *et al.* 2004).

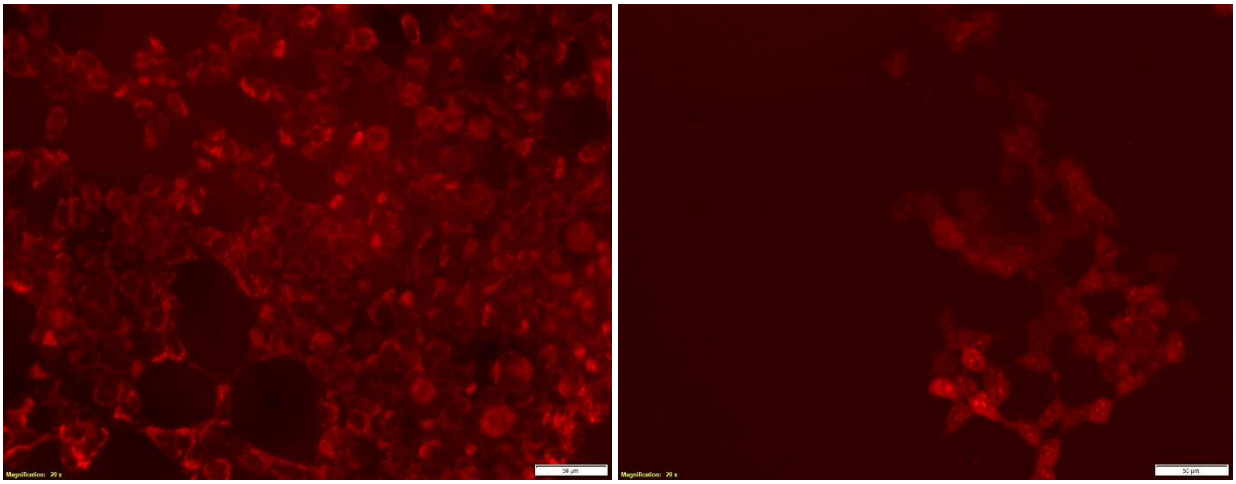

A B

Figure 4.16 MCF-7 cells as imaged using A = CellROX Orange® at 37/34° C and B = MitoSOX Red Mitochondrial Superoxide Indicator® at 37/34° C after 24 exposure to 0.5% ethanol as a positive control (n=3).

In order to further investigate if the apparent targeting of the mitochondria by cisplatin would be reflected in mitochondrial signaling to the nucleus, MCF-7 cells were exposed to the chemotherapeutic drug for 24 hours and then probed for the presence of the nuclear-located transcription factor for mitochondrial proteins (TFAM). The results are presented in Figure 4.17.

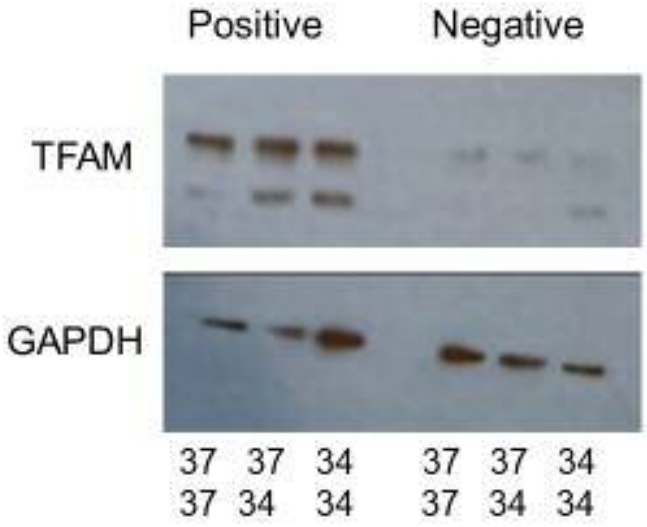

Figure 4.17 Western blot of MCF-7 cells after exposure to 24 hours of 22.9 μM cisplatin (positive) or no cisplatin (negative) with antibody detection for TFAM and GAPDH as a loading control.

Cisplatin-treated cells exposed to all three temperature shift conditions had increased levels of TFAM as compared to cells treated in the absence of cisplatin. The chemotherapeutic drug at the concentration used also increased the superoxide production to increase mitochondrial ROS. The increased ROS production and/or the mtDNA damage may signal to the nucleus to increase the transcription of TFAM which is the main nuclear encoded

transcription factor for mitochondrial proteins. It is possible that the superoxide molecule is part of the signaling pathway that regulates mitochondrial function.

Treatment with the temperature shift plus chemotherapeutic drugs impairs MCF-7 metabolism and this appears to be primarily a temperature shift effect (Figure 4.1). The response is similar for melatonin at 10 nM but not at the other concentrations. Melatonin at 10 nM is a pro-oxidant increasing H_2O_2 and -OH but not superoxide production (Figures 4.10 and 4.11). Different concentrations of melatonin appear to have different effects as while at 1 nM concentration melatonin is also pro-oxidant (Figure 4.8) it increases superoxide production in some conditions (Figure 4.9). Chemotherapeutic drugs increase intracellular ROS with different drugs having different intracellular effects. Cisplatin increases mitochondrial ROS and TFAM transcription and this relationship suggests that mitochondrial damage is relayed to the nucleus and may be mediated by ROS production.

4.4 Discussion

The paradigm for understanding the role of cellular reactive oxygen species (ROS) production and homeostasis has shifted. Previously, any positive contribution of ROS was underappreciated since ROS were largely considered to be mutagenic or toxic. Currently, the importance of low levels of ROS as signaling molecules in normal cells and the relative higher amounts maintained by cancer cells is garnering interest (Idelchik *et al.* 2017). Tumor cells utilize ROS as signaling molecules to maintain proliferation and tumorgenicity and to evade senescence and apoptosis (Weinberg and Chandel 2009). However, even cancer cells must maintain an optimal balance in the threshold levels of ROS production or face cell death (Porporato *et al.* 2018) (Turpaev 2002). There are limited reports on the ability of chemotherapeutic agents to induce ROS in malignant cells and it appears that compounds differ in this ability (Yokoyama *et al*. 2017).

In order to further study ROS induction by treatment of MCF-7 cells with chemotherapeutic agents and to determine if the temperature shift model impacted this effect, MTT assays and microscopy using fluorogenic probes that measure intracellular ROS production were used. The relative absorbance produced by cells assessed with the MTT assay reflects the viable cells' ability to metabolize formazan and so an increased absorbance is correlated with increased metabolism and therefore indirectly, an increase in cell viability. It appears that after 24 hours of drug treatment, the cells were still viable, as expected since cells typically die 48-72 hours after exposure to chemotherapeutic drugs at their IC_{50} concentrations. Exposure of cells to the temperature shift condition produced significantly less MTT-mediated absorption for cells treated with only media (the negative control), 10 nM melatonin, all of the chemotherapy drugs,

and the positive control (ethanol) conditions as compared to cells exposed to the 37/37° C control condition (Figure 4.1). This would suggest a reduction in cell metabolism or cell viability that is mediated by exposure to a temperature shift rather than by treatment with a chemotherapeutic drug or melatonin at the 10 nM concentration. The melatonin concentrations of 1 nM, 100 nM, or 100 μM did not display any significant differences in MTT absorbance between the 37/37° C and 37/34° C conditions. However, treatment of temperature-shifted cells with those concentrations of melatonin increased the amount of MTT activity compared to the negative control (no melatonin or drug) at 37/34° C, inferring some sort of beneficial impact of melatonin for those shifted cells. Docetaxel had the same significant effect for the temperature shift plus drug treatment as compared to the 37/34° C condition in the absence of drug which indicates that docetaxel appears to impart some metabolic benefit, at least in the short term (Figure 4.1). Figure 3.1 supports the result that differing concentrations of melatonin can produce different effects. In Figure 3.1, the relative absorbance of the MTT assay was measured after four days of melatonin exposure and for cells grown at a constant 37° C temperature, with no temperature shift. It is possible that the duration of treatment produces some differences in response as well as the concentration of melatonin. It is interesting that at some concentrations, melatonin seemed to have a beneficial effect on cell metabolism and viability for both the control and the temperature shift conditions as compared to the negative control in MCF-7 breast cancer cells. The conclusion is that for those concentrations, the change in viability is a melatonin effect. It is possible that the shift protocol imparts some metabolic stress on the cell which in the long-term decreases cell growth which can be rescued in the short-term by treatment with melatonin. Oxidative stress in MCF-7 cells, has been demonstrated to decrease cell proliferation (Weinberg and Chandel 2009) and melatonin could act as an antioxidant to ameliorate that stress

(Turpaev 2002). If exposure of cells to the temperature shift protocol induced ROS as suggested by Figure 4.2, then melatonin may add a protective effect which has important therapeutic implications. Anti-cancer therapies that depend on ROS production as a mechanism of action may be undermined by the concurrent use of antioxidants such as melatonin.

Fluorogenic probes can be used to detect and measure cellular ROS production (Yokoyama *et al.* 2017)(Kalghatgi *et al.* 2013)(Robinson *et al.* 2006). The principle by which these permeable probes can be used to image live cells is based on the reduced form of the dye being weakly fluorescent but upon entering the cell and being oxidized by ROS it will emit brighter, detectable signals (Yokoyama *et al.* 2017). Depending on the reagent used, the production of ROS can be localized to different subcellular localizations or be oxidized by specific ROS: for example, hydroethidine, the reagent in the MitoSOX^{TM} Red Mitochondrial Superoxide Indicator (ThermoFisher Scientific) is oxidized primarily by the superoxide radical and upon excitation will indicate ROS localized to the mitochondria (Robinson *et al.* 2006). CellROX^{TM} Orange measures whole cell ROS and reactive nitrogen species (RNS), as detailed in the manufacturer's insert. It is important to note some limitations with the use of fluorogenic probes. These two particular dyes have not been validated to be used concomitantly and therefore the protocol required two different populations of cells to compare whole cell ROS and mitochondrial sourced superoxide in the same experiment. Additionally, the filters required to optimize the CellROX orange dye are not standard on all models of fluorescent microscopes so some signal can be lost which was further impaired by using the DAPI filter. The MitoSOX Red manufacturer's protocol for excitation and emission have not been supported in the literature (Robinson *et al.* 2006), again making the detection technically challenging and requiring optimization. The images captured are representaive of the general trends in repeated

experiments. In addition, three images were captured per condition plate in order to acquire technical replicates. While the images are visually compelling, fluorecent microscopy is a qualitative technique and ideally ROS detection should be replicated by a quantitative methodology (Yokoyama *et al.* 2017)(Kalghatgi *et al.* 2013)(Robinson *et al.* 2006). Nevertheless, the results obtained relating to ROS induction by chemotherapeutic agents were consistent with other studies (Yokoyama *et al.* 2017). Further, when the images were obtained using the same microscope settings across the different experimental conditions, the differences in staining intensity were often very obvious on inspection.

The induction of whole cellular ROS following exposure to the temperature shift condition and the comparative (34/34°C) conditions in Figure 4.2 and the increase in mitochondrial superoxide detection following exposure to the 34/34 °C condition in Figure 4.3 provide some evidence as to the mechanism of action of the temperature shift protocol and its impact on cell metabolism. It is expected that exposure to the suboptimal temperature will induce a degree of oxidative stress. The greater duration of exposure to the 34/34°C comparative condition induced mitochondrial ROS, indicating that this temperature change, if sustained, can impact the mitochondria. One possible mechanism is related to a potential decrease in the expression of the inner mitochondrial membrane uncoupling proteins (UCPs) which normally serve to decrease ROS levels by uncoupling the electron transfer chain from ATP synthase (complex v) to generate heat and thus impact the mitochondrail membrane potential ($\Delta\psi m$). Since MCF-7 cell have been shown to express high levels of UCPs, if the UCPs are inhibited at suboptimal temperature, then superoxide radical generation should increase (Johar *et al*. 2015).

The taxane drug, docetaxel, generated the production of whole cellular ROS but not mitochondial O_2- when used at the IC_{50} or two times the IC_{50} as shown in Figure 4.4- 4.8. This

paralleles a finding which showed that treatment with another taxane, paclitaxel, increases the CellROX-dependent fluorescent signal in human colorectal cancer cells (Yokoyama *et al.* 2017). Yokoyama *et al.* (2017) utilized 10 μM paclitaxel, which is higher than the IC_{50} for paclitaxel , and documented apoptosis in some cells even after only 24 hours of exposure. Additionally, the CellROX® Green reagent used in those experiments only detects the hydroxyl and superoxide radicals whereas the CellROX® Orange reagent detects a broader range of ROS and RNS. Docetaxel, is a partially synthetic drug derived from the structure of paclitaxel with the precursor originally isolated from a species of yew tree, *Taxus baccata-L,* and while both are considered deterimental to cancer cell replication by interfering with microtubular degradation, docetaxel is both more potent and more water soluble compared to paclitaxel (Hill *et al.* 1994). While some of the negative side effects of chemotherapy have been attributed to ROS production (Mercuro *et al.* 2007), studies examing ROS production in cancer cells by different chemotherapeutic drugs are quite limited (Yokoyama *et al.* 2017).

Treatment with doxorubicin induced the production of whole cellular ROS and mitochondrial ROS as indicated in Figure 4.15. Doxorubicin is an anthracycline drug with an activity that includes being an inhibitor of topoisomerase II, a multifunctional enzyme with a role in DNA replication (Nitiss 2009). Since doxorubicin is serially reduced to its alkylating metabolites, it is expected to have an impact on the redox balance of the cell (Bartoszek 2002). Conversely, treatment with cisplatin selectively generated mitochondrial ROS but little CELLRox® Orange signal as shown in Figure 4.14. Cisplatin is a platinium-based compound used in a variety of chemotheraputic protocols and its primary method of action is the formation of adducts in DNA molecules with mtDNA being particularly sensitive due to the lack of nucleotide excision repair mechanisms (Hu *et al.* 2016) (Alexeyev *et al.* 2013). To further

explore if this would be supported by an increase in the expression of TFAM, a nuclear-encoded transcription factor of key mitochondrial enzymes, western blot analysis was performed which showed that cispaltin-treated MCF-7 cells displayed higher levels of TFAM 30 hours after drug exposure compared to untreated cells, as shown in Figure 4.17. The interpretation of this is that a combination of ROS production by mitochondria and/or mtDNA damage resulted in increased TFAM transcription. This response was present at all three temperature conditions which confirms that mitochondria-induced ROS may be an important factor in cisplatin's mode of action in malignant cells and which is a feature of the negative side effects of the drug. It also introduces the possibility that mitochonrial ROS generation results in signaling, directly or indirectly, to the nucleus. Neither carboplatin or oxaliplatin, two other platinium dervied anticancer drugs, used at a 10 μM concentration produced any CellROX signal in the Yokoyama *et al.* (2017) study. This may be due to the high concentrations of drugs used which induced some apoptosis and/or the difference in the fluorogenic probe used. Untreated cells in this study produced very little TFAM at any of the temperature condtions. Therefore, exposure to the temperature shift protocol or constant maintenance at 34° C did not produce enough mitochondrial stress to result in increased levels of TFAM in MCF-7 cells.

Melatonin at 1 nM and 10 nM concentrations resulted in production of whole cell ROS in cells exposed to all three temperature conditions (Figures 4.8 and 4.10) with exposure to the suboptimal temperature (34/34°C) inducing the greatest production. This is paradoxical as melatonin is classified as an antioxidant and these results suggest that it is acting as a pro-oxidant. Melatonin has been reported to uncouple oxidation phosphoryaltion in MCF-7 cells (Scott *et al.* 2001) which should decrease mitochondrial ROS. Exposure of cells to the temperature shift protocol increases whole cellular ROS as seen in Figure 4.2 and exposure to the

temperature shift plus treatment with melatonin produced a similar result. It is suggested that there is a gradient in ROS production in cells exposed to the different temperature shift exposures in the presence of 1 nM melatonin: exposure to the 34/34° C condition and 1 nM melatonin generated the most CELLRox® Orange signal; then exposure to the 37/34° C temperature shift and 1 nM melatonin; and, then exposure to normal physiological temperature and 1 nM melatonin generated the lowest level of ROS as shown in Figure 4.8. This suggests that ROS production and oxidative stress results from temperature changes but that the impact may be quite specific because exposure to the 37/37° C condition and treatment with 1 nM melatonin was still able to induce mitochondrial ROS. This was abolished at the 10 nM melatonin concentration and therefore melatonin at higher concentrations may disrupt mitochondrial respiration. Exposure to the temperature shift condition resulted in oxidative stress as evidenced by an increase in H_2O_2 and -OH detection. Further, melatonin can act as a pro-oxidant or an antioxidant in MCF-7 cells, depending on the concentration used.

It is important to note that mitochondrial number, function, and DNA are often abnormal in cancer cells (Porporato *et al*. 2018). Non-cancerous cells can contain mitochondria that have both non-mutated mtDNA and abberant mtDNA which is called heteroplasmy (Whitehall and Greaves 2019). Due to the proximity of mitochondria to intracellular ROS production, oxidative damage and mutation of mtDNA occurs, and mutations in mtDNA that code for the electron transport chain subunits, particularly subunits I and IV, are thought to contribute to the initiation of carcinogensis (Hertweck and Dasgupta 2017). Therefore the role of the mitochondria in the development and subsequent maintenance of the cancer phenotype is hugely important (Idelchik *et al*. 2017).

Circadian control of mitochondrial respiration is thought to be regulated by the nutrients available for oxidation and their respective metabolic pathways (De Goede *et al.* 2018). The vast majority of mitochondrial enzymes, whether they are involved in carbohydrate or fatty acid metabolism, such as components of the electron transport chain (ETC) or the tricarboxylic acid (TCA), oscillate in a circadian manner in mouse liver (Neufeld-Cohen *et al.* 2016). The relationship between circadian rhythm and mitochondria does not appear to be unidirectional especially given the role on the redox balance and clock gene regulation (Stangherlin and Reddy 2013). A link between circadian transcriptional activity and oxidative stress may be that the binding affinity of CLOCK/BMAL1 to DNA is influenced by the cellular NAD+/NADH or NADP/NADPH ratios (Liu *et al*. 2005).

Transcriptional regulation by ROS includes but is not limited to effects on the mitogen-activated protein kinases (MAP kinases) which can activate the c-Jun and the ASK1 cascades, through protein kinase Cα, or ATF2 via p38 kinase, both of which may influence cell proliferation (Martínez-Limón *et al.* 2020)(Turpaev 2002). Oxidative stress typically results in a transcriptional response by many key enzymes that contain antioxidant response elements (ARE) in their gene regulatory regions (Liu *et al*. 2005). A major event is thought to be the binding of Nrf2 to AREs. Nrf2 in its inactive form is bound to Keap1, an intracellular protein with a cysteine residue that once oxidized, frees Nrf2 for nuclear translocation and DNA-binding activty (Liu *et al*. 2005). Estrogen has been shown to increase ROS production in MCF-7 cells probably through signals mediated by ERα as higher ERα:ERβ ratios are correlated with higher ROS generation (Johar *et al.* 2015). ROS production in MCF-7 cells also activates the PI3K pathway, involving Akt, which modifies the activity of Nfr2 such that a typical ROS induction of apoptosis response is inhibited (Johar *et al.* 2015). These examples provide some further insight

into how complicated ROS signaling is and how specfic adaptions by ERα in breast tissues can be involved in cancer initiation and propagation.

In summary, this study has demonstrated that exposure of MCF-7 cells to the temperature shift condition, which is used to synchronize circadian rhythms *in vitro,* has an impact on mitochondrial metabolism as measured by the MTT assay and ROS response. The temperature shift increases total cellular ROS but does not appear to impact mitochondrial ROS production. Both of these effects may lead to a decrease in cell proliferation through intracellular signalling pathways. Different chemotherapeutic drugs can induce differences in ROS production and that ability may have important therapeutic implications both on the side effects experienced or on the use of antioxidants by patients. The role of circadian rhythm disturbance on mitochondrial function and malfunction, directly or through loss of a melatonin regulatory feature, may be at the crossroads of understanding the relationship between circadian disruption and disease.

4.5 References

Alexeyev, Mikhail, Inna Shokolenko, Glenn Wilson, and Susan LeDoux. 2013. "The Maintenance of Mitochondrial DNA Integrity - Critical Analysis and Update." *Cold Spring Harbor Perspectives in Biology*. https://doi.org/10.1101/cshperspect.a012641.

Bartoszek, Agnieszka. 2002. "Metabolic Activation of Adriamycin by NADPH-Cytochrome P450 Reductase; Overview of Its Biological and Biochemical Effects." *Acta Biochimica Polonica*. https://doi.org/10.18388/abp.2002_3790.

DeGoede, Paul De, Jakob Wefers, Eline Constance Brombacher, Patrick Schrauwen, and Andries Kalsbeek. 2018. "Circadian Rhythms in Mitochondrial Respiration." *Journal of Molecular Endocrinology*. https://doi.org/10.1530/JME-17-0196.

Dong, Lan Feng, Jaromira Kovarova, Martina Bajzikova, Ayenachew Bezawork-Geleta, David Svec, Berwini Endaya, Karishma Sachaphibulkij, et al. 2017. "Horizontal Transfer of Whole Mitochondria Restores Tumorigenic Potential in Mitochondrial DNA-Deficient Cancer Cells." *ELife*. https://doi.org/10.7554/eLife.22187.

Gonthier, B., N. Signorini-Allibe, A. Soubeyran, H. Eysseric, F. Lamarche, and L. Barret. 2004. "Ethanol Can Modify the Effects of Certain Free Radical-Generating Systems on Astrocytes." *Alcoholism: Clinical and Experimental Research*. https://doi.org/10.1097/01.ALC.0000122271.32522.A7.

Ezagouri, Saar, and Gad Asher. 2018. "Circadian Control of Mitochondrial Dynamics and Functions." *Current Opinion in Physiology*. https://doi.org/10.1016/j.cophys.2018.05.008.

Finkel, Toren. 2011. "Signal Transduction by Reactive Oxygen Species." *Journal of Cell Biology*. https://doi.org/10.1083/jcb.201102095.

Hertweck, Kate L., and Santanu Dasgupta. 2017. "The Landscape of MtDNA Modifications in Cancer: A Tale of Two Cities." *Frontiers in Oncology*. https://doi.org/10.3389/fonc.2017.00262.

Hill, Bridget T., Richard D.H. Whelan, Sharon A. Shellard, Siobhan McClean, and Louise K. Hosking. 1994. "Differential Cytotoxic Effects of Docetaxel in a Range of Mammalian Tumor Cell Lines and Certain Drug Resistant Sublines in Vitro." *Investigational New Drugs*. https://doi.org/10.1007/BF00873957.

Hu, Jinchuan, Jason D. Lieb, Aziz Sancar, and Sheera Adar. 2016. "Cisplatin DNA Damage and Repair Maps of the Human Genome at Single-Nucleotide Resolution." *Proceedings of the National Academy of Sciences of the United States of America*. https://doi.org/10.1073/pnas.1614430113.

Idelchik, María del Pilar Sosa, Ulrike Begley, Thomas J. Begley, and J. Andrés Melendez. 2017. "Mitochondrial ROS Control of Cancer." *Seminars in Cancer Biology*. https://doi.org/10.1016/j.semcancer.2017.04.005.

Johar, Ramesh, Rohit Sharma, Amanpreet Kaur, and Tapan K. Mukherjee. 2015. "Role of Reactive Oxygen Species in Estrogen Dependant Breast Cancer Complication." *Anti-Cancer Agents in Medicinal Chemistry*. https://doi.org/10.2174/1871520615666150518092315.

Kalghatgi, Sameer, Catherine S. Spina, James C. Costello, Marc Liesa, J. Ruben Morones-Ramirez, Shimyn Slomovic, Anthony Molina, Orian S. Shirihai, and James J. Collins. 2013. "Bactericidal Antibiotics Induce Mitochondrial Dysfunction and Oxidative Damage in Mammalian Cells." *Science Translational Medicine*. https://doi.org/10.1126/scitranslmed.3006055.

Liu, Hongjun, Renata Colavitti, Ilsa I. Rovira, and Toren Finkel. 2005. "Redox-Dependent Transcriptional Regulation." *Circulation Research*. https://doi.org/10.1161/01.RES.0000188210.72062.10.

Lobo, V., A. Patil, A. Phatak, and N. Chandra. 2010. "Free Radicals, Antioxidants and Functional Foods: Impact on Human Health." *Pharmacognosy Reviews*. https://doi.org/10.4103/0973-7847.70902.

Manchester, Lucien C., Ana Coto-Montes, Jose Antonio Boga, Lars Peter H. Andersen, Zhou Zhou, Annia Galano, Jerry Vriend, Dun Xian Tan, and Russel J. Reiter. 2015. "Melatonin: An Ancient Molecule That Makes Oxygen Metabolically Tolerable." *Journal of Pineal Research*. https://doi.org/10.1111/jpi.12267.

Martínez-Limón, Adrián, Manel Joaquin, María Caballero, Francesc Posas, and Eulàlia de Nadal. 2020. "The P38 Pathway: From Biology to Cancer Therapy." *International Journal of Molecular Sciences*. https://doi.org/10.3390/ijms21061913.

Mercuro, Giuseppe, Christian Cadeddu, Alessandra Piras, Mariele Dessì, Clelia Madeddu, Martino Deidda, Roberto Serpe, Elena Massa, and Giovanni Mantovani. 2007. "Early Epirubicin-Induced Myocardial Dysfunction Revealed by Serial Tissue Doppler Echocardiography: Correlation with Inflammatory and Oxidative Stress Markers." *The Oncologist*. https://doi.org/10.1634/theoncologist.12-9-1124.

Milkovic, Lidija, Ana Cipak Gasparovic, Marina Cindric, Pierre-Alexis Mouthuy, and Neven Zarkovic. 2019. "Short Overview of ROS as Cell Function Regulators and Their Implications in Therapy Concepts." *Cells*. https://doi.org/10.3390/cells8080793.

Neufeld-Cohen, Adi, Maria S. Robles, Rona Aviram, Gal Manella, Yaarit Adamovich, Benjamin Ladeuix, Dana Nir, et al. 2016. "Circadian Control of Oscillations in Mitochondrial Rate-Limiting Enzymes and Nutrient Utilization by PERIOD Proteins." *Proceedings of the*

National Academy of Sciences of the United States of America. https://doi.org/10.1073/pnas.1519650113.

Nitiss, John L. 2009. "Targeting DNA Topoisomerase II in Cancer Chemotherapy." *Nature Reviews Cancer*. https://doi.org/10.1038/nrc2607.

O'Neill, John S., and Akhilesh B. Reddy. 2011. "Circadian Clocks in Human Red Blood Cells." *Nature*. https://doi.org/10.1038/nature09702.

Peek, Clara Bien, Alison H. Affinati, Kathryn Moynihan Ramsey, Hsin Yu Kuo, Wei Yu, Laura A. Sena, Olga Ilkayeva, et al. 2013. "Circadian Clock NAD+ Cycle Drives Mitochondrial Oxidative Metabolism in Mice." *Science*. https://doi.org/10.1126/science.1243417.

Porporato, Paolo Ettore, Nicoletta Filigheddu, José Manuel Bravo San Pedro, Guido Kroemer, and Lorenzo Galluzzi. 2018. "Mitochondrial Metabolism and Cancer." *Cell Research*. https://doi.org/10.1038/cr.2017.155.

Ray, Paul D., Bo Wen Huang, and Yoshiaki Tsuji. 2012. "Reactive Oxygen Species (ROS) Homeostasis and Redox Regulation in Cellular Signaling." *Cellular Signalling*. https://doi.org/10.1016/j.cellsig.2012.01.008.

Reiter, Russel J., Juan C. Mayo, Dun Xian Tan, Rosa M. Sainz, Moises Alatorre-Jimenez, and Lilian Qin. 2016. "Melatonin as an Antioxidant: Under Promises but over Delivers." *Journal of Pineal Research*. https://doi.org/10.1111/jpi.12360.

Reiter, Russel J., DunXian Tan, Sergio Rosales-Corral, Annia Galono, XinJia Zhou, Bing Xu. 2018. "Mitochondria: Central Organelles for Melatonin's Antioxidant and Anti-aging Actions". *Molecules.* https://doi.org/10.3390/molecules.2302050.

Robinson, Kristine M., Michael S. Janes, Mariana Pehar, Jeffrey S. Monette, Meredith F. Ross, Tory M. Hagen, Michael P. Murphy, and Joseph S. Beckman. 2006. "Selective Fluorescent Imaging of Superoxide in Vivo Using Ethidium-Based Probes." *Proceedings of the National Academy of Sciences of the United States of America*. https://doi.org/10.1073/pnas.0601945103.

Scott, Aaron E., Gregory N. Cosma, Anthony A. Frank, Robert L. Wells, and Henry S. Gardner. 2001. "Disruption of Mitochondrial Respiration by Melatonin in MCF-7 Cells." *Toxicology and Applied Pharmacology*. https://doi.org/10.1006/taap.2000.9115.

Siauciunaite, Rima, Nicholas S. Foulkes, Viola Calabrò, and Daniela Vallone. 2019. "Evolution Shapes the Gene Expression Response to Oxidative Stress." *International Journal of Molecular Sciences*. https://doi.org/10.3390/ijms20123040.

Snezhkina, Anastasiya V., Anna V. Kudryavtseva, Olga L. Kardymon, Maria V. Savvateeva, Nataliya V. Melnikova, George S. Krasnov, and Alexey A. Dmitriev. 2020. "ROS

Generation and Antioxidant Defense Systems in Normal and Malignant Cells." *Oxidative Medicine and Cellular Longevity*. https://doi.org/10.1155/2019/6175804.

Stangherlin, Alessandra, and Akhilesh B. Reddy. 2013. "Regulation of Circadian Clocks by Redox Homeostasis." *Journal of Biological Chemistry*. https://doi.org/10.1074/jbc.R113.457564.

Turpaev, K. T. 2002. "Reactive Oxygen Species and Regulation of Gene Expression." *Biochemistry (Moscow)*. https://doi.org/10.1023/A:1014819832003.

Weinberg, Frank, and Navdeep S. Chandel. 2009. "Reactive Oxygen Species-Dependent Signaling Regulates Cancer." *Cellular and Molecular Life Sciences*. https://doi.org/10.1007/s00018-009-0099-y.

Whitehall, Julia C., and Laura C. Greaves. 2019. "Aberrant Mitochondrial Function in Ageing and Cancer." *Biogerontology*. https://doi.org/10.1007/s10522-019-09853-y.

Yokoyama, Chikako, Yuto Sueyoshi, Mika Ema, Yumi Mori, Kazuto Takaishi, and Hisashi Hisatomi. 2017. "Induction of Oxidative Stress by Anticancer Drugs in the Presence and Absence of Cells." *Oncology Letters*. https://doi.org/10.3892/ol.2017.6931.

Chapter 5

Chapter 5 Clock Gene Expression in a Human Breast Cancer Mitochondrial Impaired Cell Line

5.1 Introduction

Mitochondria are important membrane bound subcellular organelles that contain their own DNA (mtDNA) and are at the center of the endosymbiotic theory of eukaryote evolution (Gray 2012). The circular nature of mtDNA and its slight differences in genetic code are features emphasized by proponents that point to a mitochondrial origin as more Archean than eukaryotic but it seems most likely that there was a combination event (Friedman and Nunnari 2014). Structurally, mitochondria are ovoid in shape and contain an inner and an outer membrane, separated by an intermembrane space, with the inner membrane surrounding a matrix within a network of membrane cristae (Friedman and Nunnari 2014). Functionally, this organelle is not only the site of energy production within the cell but it also has roles in the generation of reactive oxygen species (ROS) secondary to its bioenergetic duty, as well as regulatory effects in apoptosis, modification of intracellular calcium signalling, and regulation of heme biosynthesis (Shokolenko and Alexeyev 2017). Oxidative phosphoryation is derived from the successive oxidation of metabolites where electrons pass through an electron transport chain (ETC) localized to the inner mitochondrial membrane which is coupled with the phosphorylation of adenosine diphosphate (ADP) to adenosine triphosphate (ATP); the major energy currency of

the cell (Mookerjee *et al.* 2010). Five protein complexes reside along the inner mitochondrial membrane and coordinate oxidative phosphorylation; complex I where NADH is oxidized to NAD+, complexes II, III (cytochrome *c* reductase), and IV (cytochrome *c* oxidase) where electrons are sequentially donated, and complex V, or ATP synthase, where ADP is phosphorylated (Demine, Renard, and Arnould 2019). Electron leakage, primarily at complexes I and III are key sources of ROS production, which can occur despite an electrochemical gradient that flows with a decreasing potential down the sequence of enzymes and which is maintained by the ability of ATP synthase to pump protons back into the matrix (Mookerjee *et al.* 2010).

The mitochondria genome is central to oxidative phosphorylation as mtDNA contains 37 genes, 13 of which code for proteins that include subunits of complex I, III, IV, and V and 22 tRNAs, and 2 rRNAs (Taanman 1999). Both transcription and translation occur in the organelle and transcription can be activated by and is therefore dependent on the nuclear mitochondral transctipion factor A (TFAM) (Kang and Hamasaki 2005). The other portions of complex I, III, IV, and V and all of the subunits of complex II are encoded in the nucleus (Mastroeni *et al*. 2017). The number of mitochondria in cells vary from a few hundred to thousands and the regulation of their dyanmics of fission and fusion is complex (Friedman and Nunnari 2014). Mutations in mtDNA have been shown to be linked to a number of diseases including cancer (Chatterjee, Mambo, and Sidransky 2006).

Cellular respiration in normal mammalian physiology is compartmentalized: glycolysis is the break down of glucose to pyruvate through a series of enzymatic steps that occurs in the cytosol and then pyruvate is translocated to the mitochondria and enters the tricarboxylic acid cycle (TCA) which produces a number of substrates for oxidative phosphylation on the inner mitochondrial membrane (Peek *et al.* 2015). The Warburg Effect is described as the preference

of malignant cells to produce ATP through the glycolytic pathway and satisfying their energy requirements by rapidly increasing the rate of these reactions (Liberti and Locasale 2016). Pyruvate is metabolized to lactate by lactate dehydrogenase (LDH) and NADH is simultaneously oxidized to NAD+ (Rogatzki *et al.* 2015). A second metabolic switch that cancer cells trigger is to use the pentose phospate pathway which shuttles glucose–6 phospate (G6P), one of the intermediates of glycolysis, through a series of enzymatic reactions with no ATP production but with restoration of cellular NADPH (Jin and Zhou 2019). Malignant cells may utilize multiple pathways to satisfy their energetic and substrate demand for rapid growth and proliferation, including oxidatve phosphorylation (Ashton *et al.* 2018). The generation of mtDNA-depleted, or *Rhø* cells, by culturing the cells in low concentrations of ethidium bromide (EtBr) for a prolonged period of time to damage the ability of mtDNA to produce subunits of oxidative phosphorylation, was initally developed to study mitochondrial disorders (Schubert *et al.* 2015). The use of EtBr or inhibitors of the enzyme complexes involved in oxidative phosphorylation, such as rotenone, antimycin A, or oligomycin, has enriched the field of study of cellular physiology including clock gene regulation (Peek *et al*. 2015).

It seems intuitve that circadian rhythms regulate metabolic pathways when the relationship between light/dark phases and feeding/fasting activites are considered. A large percentage of transcripts oscillate in a circadian manner in the mouse liver (Miller *et al.* 2007). Circadian control of the regulatory proteins involved in metabolic reactions dictates clock control of basal glycolytic rates (Thurley *et al.* 2017). Evidence of circadian regulation of metabolic processes is provided by three key examples: (I) the circadian oscillation of the rate limiting enzyme of NAD+ generation, nicotinamide phosphoribosyltransferase (NAMPT) (Peek *et al.* 2013); (II) the post-translational modifications to the complex I cycle proteins are under

circadian gene influence (Cela *et al*. 2016); and, (III) PER protein regulation of substrate and mitochondrial enzymes (Neufeld-Cohen *et al.* 2016). This is not to infer that these represent the only examples of circadian involvement or that the feedback is unidirectional (Scrima *et al.* 2016).

Oxidative phosphorylation requires both mitochondrial and nuclear programming for transcriptional activity and regulation of energy production (Friedman and Nunnari 2014). The uncoupling of the ETC and the phosphylation of ADP can be influenced experimentally by chemicals or through natural factors including melatonin (Demine, Renard, and Arnould 2019). Instrinsic regulation of oxidative phosphorylation occurs through the uncoupled proteins (UCPs) which function to protect mitochondria from excessive ROS accumulation (Mookerjee *et al.* 2010). *Rhø* cells, which lack functional oxidative phosphorylation, demonstrate decreased clock gene expression even after serum shock synchronization (Scrima *et al*. 2016). The purpose of this study was to examine the impact of the temperature shift model on circadian gene expression in *Rhø* cells.

5.2 Materials and Methods

Cell culture and The Propagation of a mtDNA free Cell Line (Rhø cell)

A human hormone responsive breast cancer cell line, MCF-7, originally obtained from the American Type Culture Collection (ATCC) was maintained in Hyclone Debucco's Modified Eagle Media (DMEM) with high glucose and pyruvate (GE Lifesciences) and supplemented with 10% fetal bovine serum (FBS) and 1% antibiotic and antimycotic solution® (A&A) (Fisher) and grown on 100 mm tissue culture plates. The protocol for generation of a mtDNA free or *Rhø* cell was adapted (King and Attardi 1996) such that ethidium bromide (Sigma-Aldrich) was added at a final concentration of 50 ng/ml and uridine (Sigma-Aldrich) was added at a final concentration of 50 μg/ml to the culture media and the cells were passaged as required for a minimum of 6 weeks. For comparison, to ensure that the cells cultured with ethidium bromide and uridine were mtDNA deficient, control plates with no addition of uridine were also prepared (King and Attardi 1996). Cell cultures were maintained in a humidified environment at 37^{o} C and 5% CO_2.

Experimental protocols

A temperature shift technique was used to induce a circadian rhythm in cell cultures. The temperature shift technique consisted of cells being kept in a humidified 37^{o} C environment, supplemented with CO_2 from 09:00 to 21:00 and then transferred to a humidified 34^{o} C incubator supplemented with 5% CO_2 from 21:00 to 09:00. Cells were subjected to the shift protocol is as described for seven days prior to sample collection. In addition, the cells were subjected to two control conditions that were maintained for the duration of the experiment; cells were cultured at 37^{o} C continuously and a second set were cultured at 34^{o} C continuously. Cells were seeded in 100 mm tissue culture plates at a ratio of 1:8 on the first day of the shift experiment.

Microscopy

Images of control MCF-7 cells that were not cultivated with ethidium bromide and the *Rhø* cells were captured using an Olympus fluorescence microscope model DP80 with the manufacturer's CellSens Dimension software. Phase contrast and MitoTracker™ Red CMXRos® (Thermo Fisher Scientific) protocols were used to compare the two cell lines. The MitoTracker™ Red CMXRos® (Thermo Fisher Scientific) protocol was performed as per the manufacturer's recommendations. The MitoTracker™ Red powder was resuspended in DMSO to a final concentration of 1 mM and 5 µl of this stock solution was added to 5 ml of culture media and incubated with the cells at 37° C for 30 minutes before imaging.

Protein extraction and Western Blotting for MCF-7 Rho Cell Characterization

Cells were washed with ice cold PBS, pH 7.4, and then lysed in 300 µl of ice cold radioimmunoprecipitation assay (RIPA) buffer (150 mM sodium chloride, 15 mM phosphate buffer, pH 7.4, 1% Triton-X 100, 0.5% sodium dodecyl sulfate (SDS), 0.5% sodium deoxycholate, 10 mM sodium fluoride (NaF), 10 mM sodium orthovanadate), and protease inhibitor tablets (Thermo Scientific™ Pierce™ Protease Inhibitor Tablets). All reagents were obtained from Fisher Scientific unless otherwise indicated. The whole cell lysate was then collected from the plate using a plastic cell scraper. Cellular DNA and cytoskeletal proteins were sheared by passage through a 22 gauge needle several times and then stored at -80^0 C. Protein quantification was done using the bicinchoninic acid (BCA) assay (Thermo Scientific™ Pierce™ BCA Protein Assay Kit) with a bovine serum albumin standard and read using a Synergy® H4 Hybrid plate reader (Biotek) using Gen 5, version 2.00 software. Electrophoresis was performed using 30 µg of protein loaded per lane onto a 15 % polyacrylamide gel containing SDS. After electrophoresis, the gels were transferred onto nitrocellulose membranes using a

semidry transfer apparatus and 20% methanol, 192 mM glycine, and 25 mM Tris-HCl, pH 8, and protein transfer was confirmed by staining with 0.1% Ponceau S in 1% acetic acid. The membranes were blocked by incubation in 5% low fat milk in TBST overnight at 4^0 C. The Total OXPHOS Human WB Antibody Cocktail ® (Abcam) was incubated with the membrane at a dilution of 1:200 in 5% low fat milk in TBST overnight at 4^0 C. The secondary antibody, an HRP-conjugated anti-mouse IgG (Santa Cruz Biotechnology), was incubated with the membrane at a dilution of 1:500 for 2 hours at room temperature. Chemiluminescent detection of HRP was performed using the Thermo Scientific ECL detection reagents prior to membrane exposure to radiographic film or exposure using a GelDoc image analyzer.

Relative ATP Luminescence

The level of ATP in the cell lines was measured using the Luminescent ATP Detection Assay Kit® purchased from Abcam using the protocol described in the manufacturer's instructions. Cells were seeded onto 96 well plates at two concentrations of 25,000 cells/well and 12,500 cells/well, each in triplicate. Three plates were prepared: plate 1 contained *Rhø* cell groups 1, 1B, and 2; plate 2 had groups 3, 4, and A; and, plate 3 had groups B and C. The different groups refer to the dates at which *Rhø* cell cultivation commenced using ethidium bromide at a final concentration of 50 ng/ml and uridine at a final concentration of 50 µg/ml in pyruvate enriched media. The level of luminescence following incubation of the lysed cells with luciferin and firefly luciferase where the light emitted corresponds with the level of ATP present versus an ATP standard, was measured using a Synergy® H4 Hybrid plate reader (Biotek) using Gen 5, version 2.00 software, set for luminescent detection.

Flow cytometry for Cell Cycle Analysis

Cell DNA content was measured using flow cytometry of propidium iodide-labelled cells. Cells were washed with room temperature PBS, pH 7.4, and treated with trypsin. The cells were collected and placed in 1.5 ml microfuge tubes and centrifuged at 2000 rpm for 5 minutes. The supernatant was discarded and the cells washed with PBS, pH 7.4, and then resuspended in 70% ethanol and immediately stored at -20^0 C. Prior to analysis, the thawed samples were washed twice with PBS, pH 7.4, and suspended in 0.5 ml PBS, pH 7.4, and 0.5 ml of a 2 mg/ml propidium iodide (PI) stain solution containing 100 ng/ml RNase was added. The cells were incubated for 2 hours and then the samples were analyzed on a Cytomics FC 500 flow cytometer (Beckman Coulter). Images generated from the flow cytometer software were transferred unto the Paint® program for figure creation.

Gene expression analysis using Reverse Transcriptase quantitative PCR (RT-qPCR)

The experimental condition was those where the cells culture in 100 mm plates in complete media were shifted from 37° C to 34° C at 21:00 and then shifted back to 37° C at 09:00 each day for the duration of the shift experiment. The control condition was selected to be cell cultures maintained at 37° C for 24 hours/day during the duration of the shift experiment. Cell monolayers were lysed in a fixed volume of 500 µl of denaturing solution containing 4 M guanidinium thiocyanate, 25 mM sodium citrate, 0.05% N- laurosylsarcosine, and 0.1 M 2- β-mercaptoethanol (Chomczynski and Sacchi 2006). After collection, the sample was stored at -80^0 C prior to RNA purification and solubilization using the phenol-chloroform technique as described. RNA was quantified by measuring the OD260 using a spectrophotometer (Nanodrop®). 100 ng RNA was reverse transcribed using the protocol from the Superscript IV Vilo Master Mix without ezDNAse enzyme treatment as per Life Technologies®. Oligo-dT-primers were annealed at 25° C for 10 minutes, the RNA reverse transcribed by incubation at 50°

C for 10 minutes, and then the enzyme inactivated for 5 minutes at 85° C using a thermocycler. Clock gene ID Taqman® assays were obtained from Life Technologies®. For some genes, these assays are inventoried and others they were custom produced. The assay numbers are as listed: PER1, Hs00242988_m1; PER2, Hs01007553_m1; CLOCK, Hs00231857_m1; BMAL, (ARNTL); TFAM, Hs00273372_s1; GAPDH, Hs02786624_g1; MT-ATP6, Hs02596862_g1; PPIA, Hs04194521_s1; and, RPS17, Hs00734303_g1. Taqman® gene assays were performed using the Agilent Aria MX and 80 ng of cDNA. The Thermo Fisher protocol for the TaqMan® Fast Advanced Master Mix was followed which consisted of UNG incubation for 1 cycle at 50° C for 2 minutes, 1 cycle of enzyme activation for 30 seconds at 95° C, and 40 cycles of alternating denaturing and annealing at 95° C for 1 second and 60°C for 20 seconds, respectively. As per the Taqman ® technical bulletin the amplification efficiency is assumed to be 1 and a melting curve analysis is not completed due to regent consumption. Gene expression was measured using the 2^ΔΔCT method in accordance with the MIQE Guidelines. (Bustin *et al*. 2009).

Statistical Analysis

SPSS ® or GraphPad Prism 5.0 was used for statistical analysis as indicated. The data was subjected to a normality test using the normality function within GraphPad, and if appropriate, $p<0.05$, a one analysis of variance (ANOVA) was used to compared the groups with a post hoc Tukey test; otherwise a Kruskal Wallis test to discern differences with a Dunn's comparison of groups as the post hoc was used. Unless otherwise stated, statistical significance was determined as $p<.05$. Error bars within graphs indicate standard error of the mean (SEM), unless otherwise indicated.

5.3 Results

The development of a MCF-7 cell line that exhibits mitochondrial impairment would assist in evaluating the relationship between mitochondrial metabolism, circadian rhythm, and whether mtDNA has any regulatory role in clock gene expression. The addition of low concentrations of ethidium bromide (EtBr) to the cultures over time has been used to create a cell line lacking in mitochondrial DNA, also called a *Rhø* cell line (King and Attardi 1996). *Rhø* cells acquire changes in morphology in response to the EtBr incubation as shown in Figure 5.1. The cells continue to group together but the individual cell membranes become less distinct. The cells grow more slowly in culture and require fewer passages, but more frequent media replacement. While the MCF-7 *Rhø* cells were able to survive for prolonged periods of time, other cell lines such as HBL-100s, and T98G human glioblastoma cells, were not successfully cultivated in low levels of EtBr.

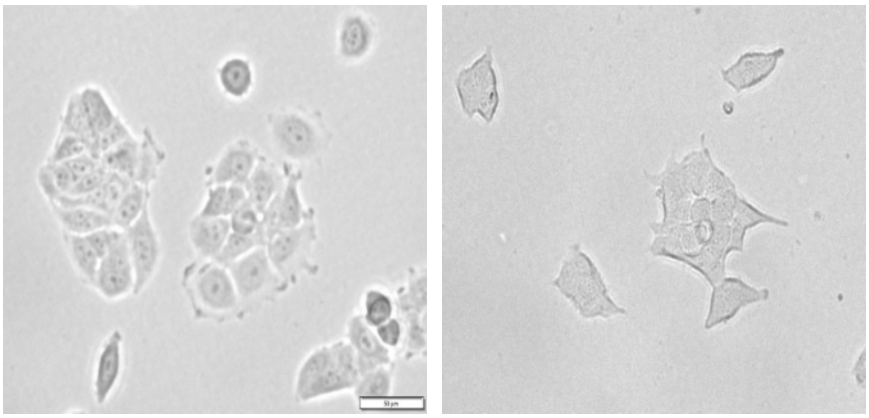

Figure 5.1 Comparison of untreated MCF-7 cells on the left with MCF-7 cells that have had ethidium bromide added to the media for the previous 28 days on the right as captured by phase contrast microscopy (magnification 20X).

To determine if the *Rhø* cells still had mitochondria, they were stained with MitoTracker™ Red CMXRos (Thermo Fisher Scientific) according to the manufacturer's protocol and imaged using a fluorescent microscope. The MitoTracker™ stain is localized to the

mitochondria as shown in Figure 5.2. The *Rhø* cells still acquire stain indicating there are mitochondria present although they are fewer in number, have abnormal morphology, and show much more variability in the stain uptake pattern in individual cells.

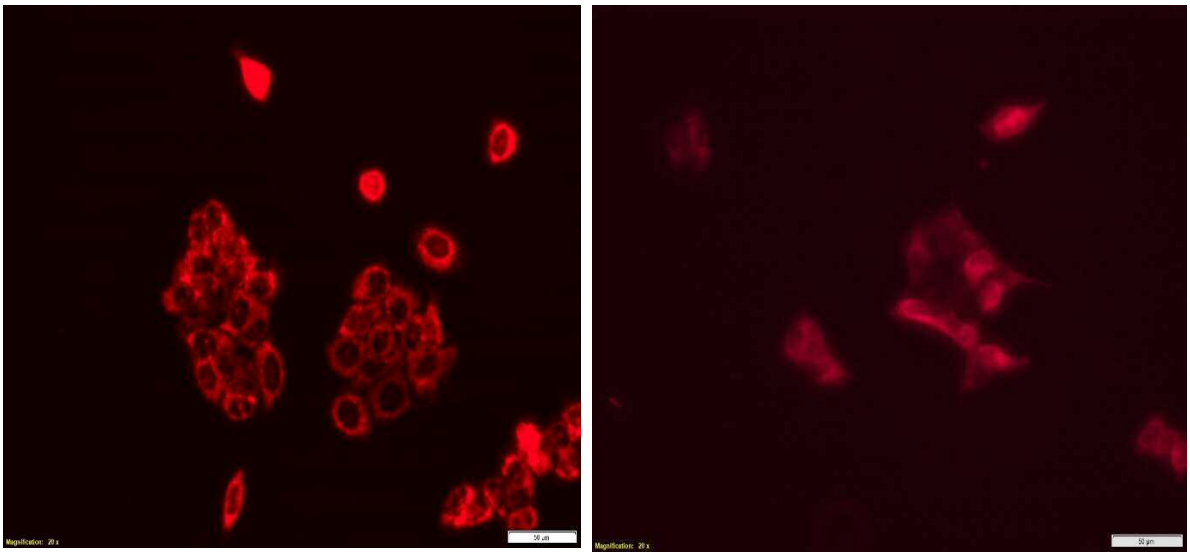

Figure 5.2 Comparison of untreated MCF-7 cells on the left with MCF-7 that have had ethidium bromide added to the media for the previous 28 days on the right as captured after staining with MitoTracker™ Red fluorescent dye (magnification 20X).

In order to further characterize the mtDNA-depleted *Rhø* MCF-7 cell lines prior to examining the effect of applying the temperature shift protocol, two separate procedures were performed to confirm mitochondrial dysfunction. The first was to use western blot analysis of the cells with a Total OXPHOS Human WB Antibody Cocktail ® (Abcam) to characterize the expression of the various mitochondrial proteins. The results are displayed in Figure 5.3.

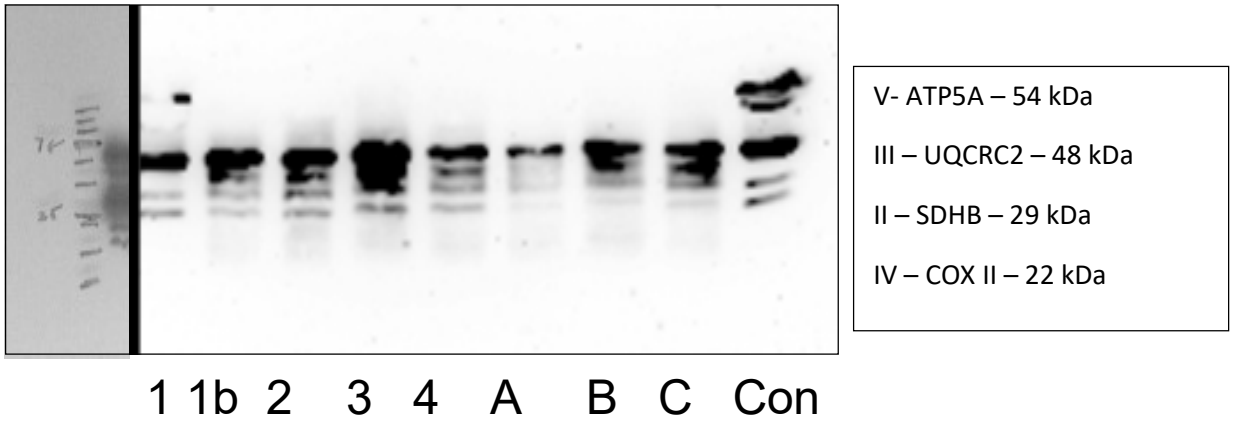

Figure 5.3 MCF-7 *Rhø* cells as characterized by antibody staining by western blot analysis. Extracts from eight groups of *Rhø* cells labelled as 1, 1b, 2, 3, 4, A, B, C, and the control group, untreated MCF-7 cells on the far right (con) were subjected to western blot analysis. The blots were probed with the total OXPHOS antibody cocktail that contained antibodies that recognized components of each of the 5 mitochondrial enzyme complexes.

All of the *Rhø* cells contained a positive signal that corresponds to the protein subunit of complex II of oxidative phosphorylation which is expected because this is the one subunit of the five where the proteins are all encoded in the nucleus and post-translationally targeted to the mitochondria. The control group appeared to be positive for all five subunits as expected for untreated functional MCF-7 cells. The *Rhø* subgroups do not contain components of subunits III or V but all except group A appear to have some expression of subunits I and IV. This indicates that the mtDNA is not able to functionally transcribe and/or the mitochondria translate these protein subunits. The second method employed to characterize the *Rhø* cells was a functional assay examining ATP production. Since oxidative phosphorylation produces an abundance of cellular ATP and the mtDNA encode for components of 4/5 subunits required for oxidative phosphorylation, the treatment of cells with EtBr is anticipated to cause a reduction in ATP production relative to intact cells. The ATP production was measured at a single interval of thirty minutes using the Luminescent ATP Detection Assay Kit® (Abcam) and the total

compared via relative luminescence produced by each of the different cell lines. The results are displayed in Figure 5.4

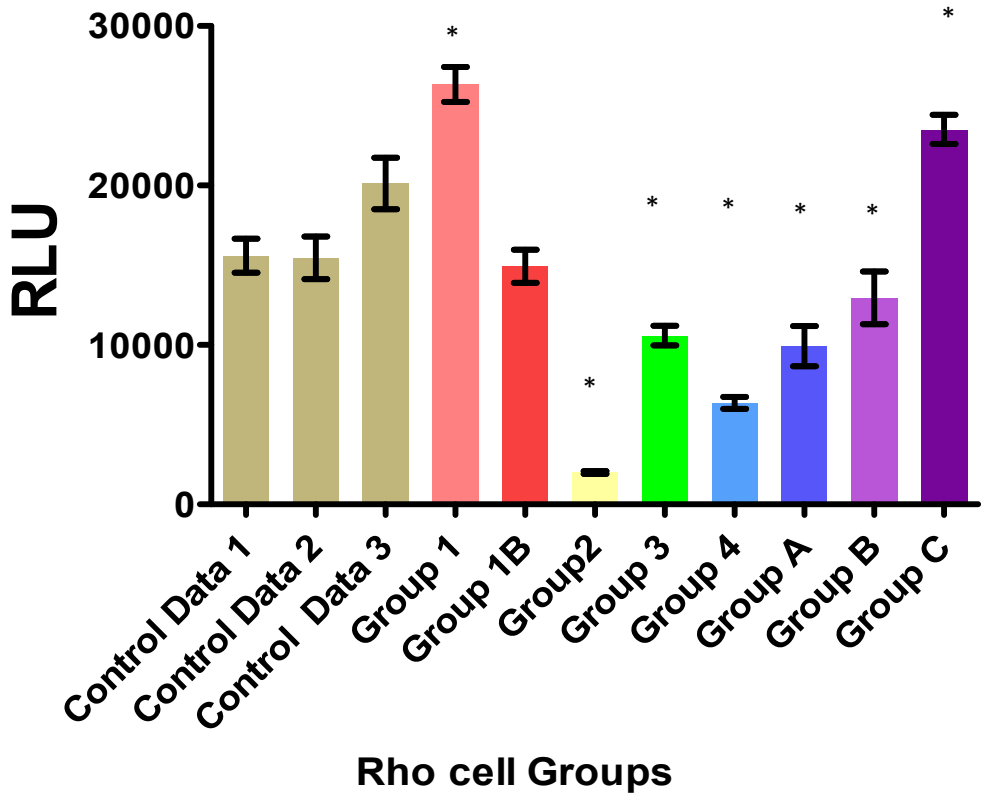

Figure 5.4 ATP Production of groups of *Rhø* cells and controls. The level of ATP was determined using the Luminex ATP assay in triplicate in three 96 well plates each with an MCF-7 control: plate 1 contained control 1 and *Rhø* cells from groups 1, 1B, and 2; plate 2 contained control 2 and *Rhø* cells from groups 3, 4 , and A; and, plate 3 contained control 3, and *Rhø* cells from groups B and C (n=3, $p<0.05$).

Rhø cells from groups 2, 3, 4, A, and B demonstrate the expected results of having significantly lower ATP production due to impaired oxidative phosphorylation as compared to their controls. *Rhø* cells from groups 1 and C appear to have significantly greater total ATP production during this time interval as compared to their controls while the level of ATP

produced by cells from group 1B are the same as for control cells. Cancer cells acquire their energy sources using multiple pathways and MCF-7 cells have been demonstrated to use oxidative phosphorylation after exposure to radiation, indicating the cell line retains typical cell aerobic respiration competency (Lu *et al.* 2015) which is disrupted in at least some of the EtBr-treated cells.

To examine the impact of exposure to the temperature shift protocol on mtDNA-deficient cells, flow cytometry and RT-qPCR analysis of clock genes was performed after *Rhø* cells derived from MCF-7 breast cancer cells were subjected to a 7-day experimental temperature shift protocol. Flow cytometry analysis using the propidium iodide staining protocol with cells exposed to three different temperature conditions, the 37/37° C condition, the 37/34° C temperature shift condition, and the 34/34° C condition was conducted to investigate the impact of long-term EtBr treatment on cell cycle progression and queried what impact the shift condition may elicit. Cells exposed to all three temperature conditions showed that a large proportion of the EtBr-treated cells were in the sub G_1 peak as is evident on the histograms in Figure 5.5 and graphical displays of Figure 5.6 and 5.7. The presence of a sub-G1 peak is an indication of cellular apoptosis and nuclear fragmentation. There was a significantly greater proportion of cells in sub G_1 for the comparative 34/34 °C condition as compared to the shift condition. There was also a significantly greater proportion of cells in *S* phase in the control 37/37 °C condition as compared to the comparative 34/34°C condition. The most significant difference between the control and the experiment condition was the proportion of cells in the G_2M phase which was significantly greater for the shifted cells. These results are demonstrated in Figures 5.6 and 5.7. This is different from the data shown in Figure 2.7 where MCF-7 cells not treated with EtBr and exposed to the temperature shift condition for 7 days did not

demonstrate any significant differences between the control and the experimental conditions. The histograms in Figure 5.5 which includes several time points between the control and the experimental groups demonstrated an increased G_2M peak in the temperature-shifted cells. Therefore, the *Rhø* cells demonstrated reduced viability as supported by the presence of a large sub G_1 proportions in all three exposure condition conditions. While the sub G_1 is assumed to be comprised of apoptotic bodies, no investigation was performed to confirm this. Additionally, the temperature shift protocol induced a relative G_2M block.

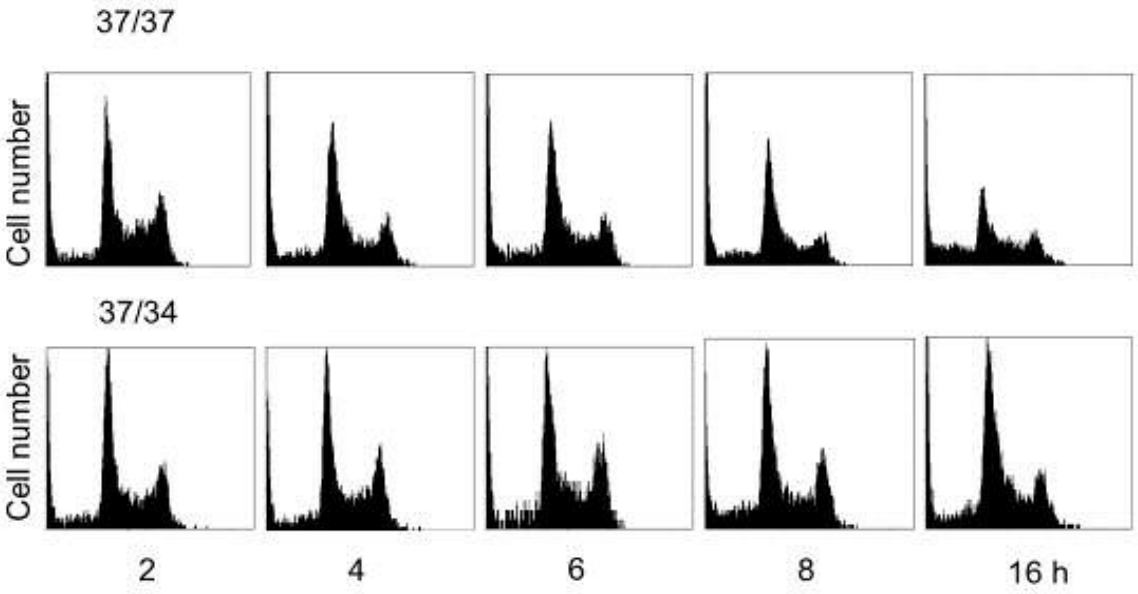

Figure 5.5 Histograms for flow cytometry of MCF-7 *Rho* cells at 7 day shift. Images on the top panels represent 37/37° C control condition, time points 2, 4, 6, 8, and 16 hours respectively with time 0 = 09:00. Images on the bottom panels represent 37/34° C experimental condition, time points 2, 4, 6, 8, and 16 hours respectively with time 0 = 09:00 (n=2).

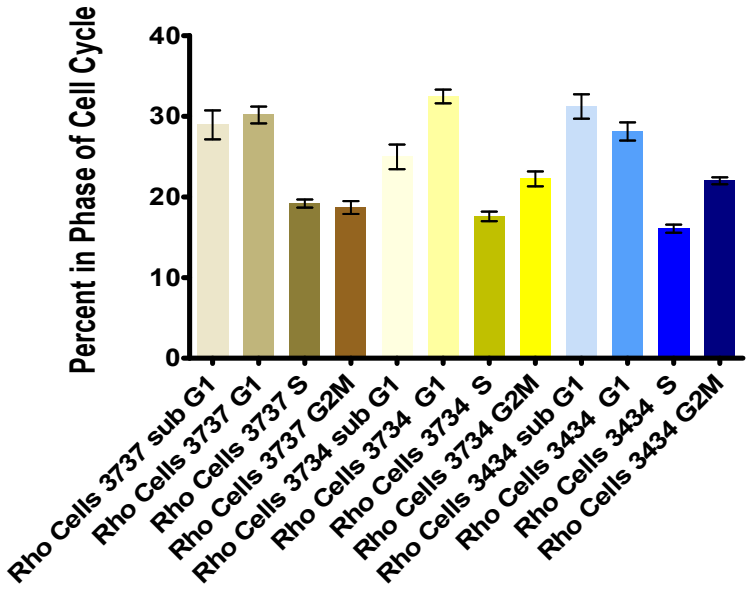

Figure 5.6 Graphical display comparing cell cycle phases at day 7 of shift in MCF-7 *Rhø* cells. (n=2, p<0.05)

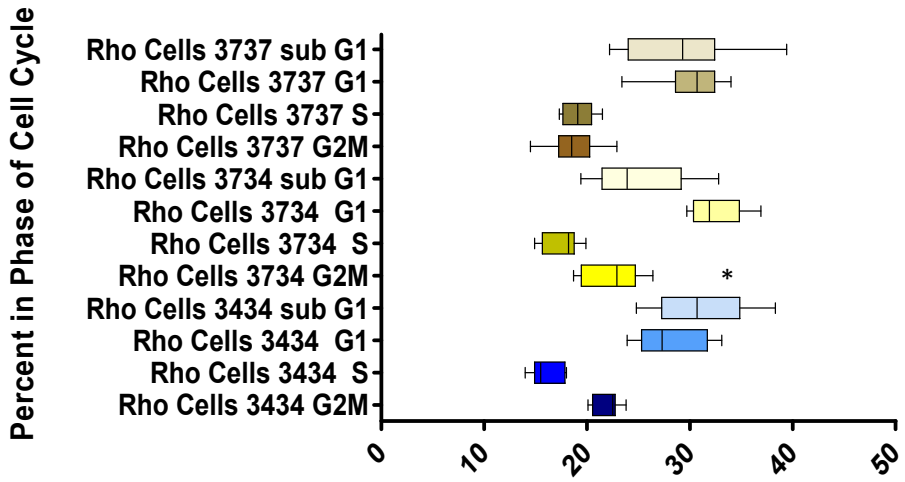

Figure 5.7 Graphical display comparing cell cycle phases at day 7 of shift in MCF-7 *Rhø* cells (n=2, p<0,05).

Gene expression for the MCF-7 *Rhø* cells was measured using RT-qPCR with RPS-17 as the reference gene. Several clock genes were selected including PER1, PER2, CLOCK, and

BMAL. Other genes including GAPDH, TFAM, and MT-ATP6 were also assayed. Table 5.1 demonstrates that gene expression levels, as evidenced by higher raw Ct (Cq) values, were low for CLOCK exposed at the 37/34 °C condition but still measurable across most time points. PER1 expression was detectable at most time points and had lower Ct (Cq) values than CLOCK indicating a higher degree of gene expression. The reference gene, RPS 17 could be detected across all time points except at 24 hours. Only MT-ATP 6 had lower Ct (Cq) values indicating the greatest relative expression. MT-ATP6 is a mitochondrial gene encoding a subunit of complex V and mutation of this gene is linked to several human diseases (Ganetzky *et al.* 2019). It was not expected to detect mRNA transcripts from the mitochondria in the EtBr disrupted cells, however, given the mRNA collection procedure contamination with mitochondrial DNA cannot be ruled out and the MT-ATP-6 product might be the result of amplifying the mtDNA. Therefore, it isn't possible to determine if the MT-ATP6 detected was functional.

Table 5.1 mRNA Mean Ct Values as Measured by RT-qPCR for Two Housekeeping Genes, RPS 17 and PPIA, Two Clock Genes PER1 and CLOCK and TFAM, GAPDH and MT- ATP for the Shift *Rhø* Cells for Several Time Points over 24 Hours

Time Point	**RPS 17**	**PPIA**	**GAPDH**	**MT-ATP6**	**TFAM**	**PER1**	**CLOCK**
0	35	36	35	21	40	28	34
1	36	-	-	26	-	-	27
2	31	32	34	22	39	34	-
4	28	32	30	24	38	35	-
6	35	-	32	24	-	35	35
8	31	30	-	34	-	24	34
12	21	-	-	33	-	27	32
16	34	-	23	20	-	35	40
24	21	28	-	-	34	22	28

Unfortunately, the *Rhø* cells exposed to the 37/37° C condition had no raw Cq values below the threshold of 40 cycles for any of the clock genes across all time points. These results are available in Appendix 4. This made it impossible to calculate 2^ΔΔCq values for those genes. The reference gene, RPS-17, was detectable above the threshold as were other genes including TFAM and GAPDH and the relative gene expression could be calculated for those candidates. The results are presented in Figure 5.8. This suggests that cells require intact mitochondria, specifically functional mtDNA and oxidative phosphorylation to generate detectable clock gene expression. It would be expected that TFAM expression would be increased given the level of mtDNA damage and this has already been demonstrated in cisplatin-treated cells (Figure 4.17). Since GAPDH is an enzyme involved in the steps of glycolysis, it is expected that its expression would be upregulated in MCF-7 who have lost their oxidative phosphorylation ability.

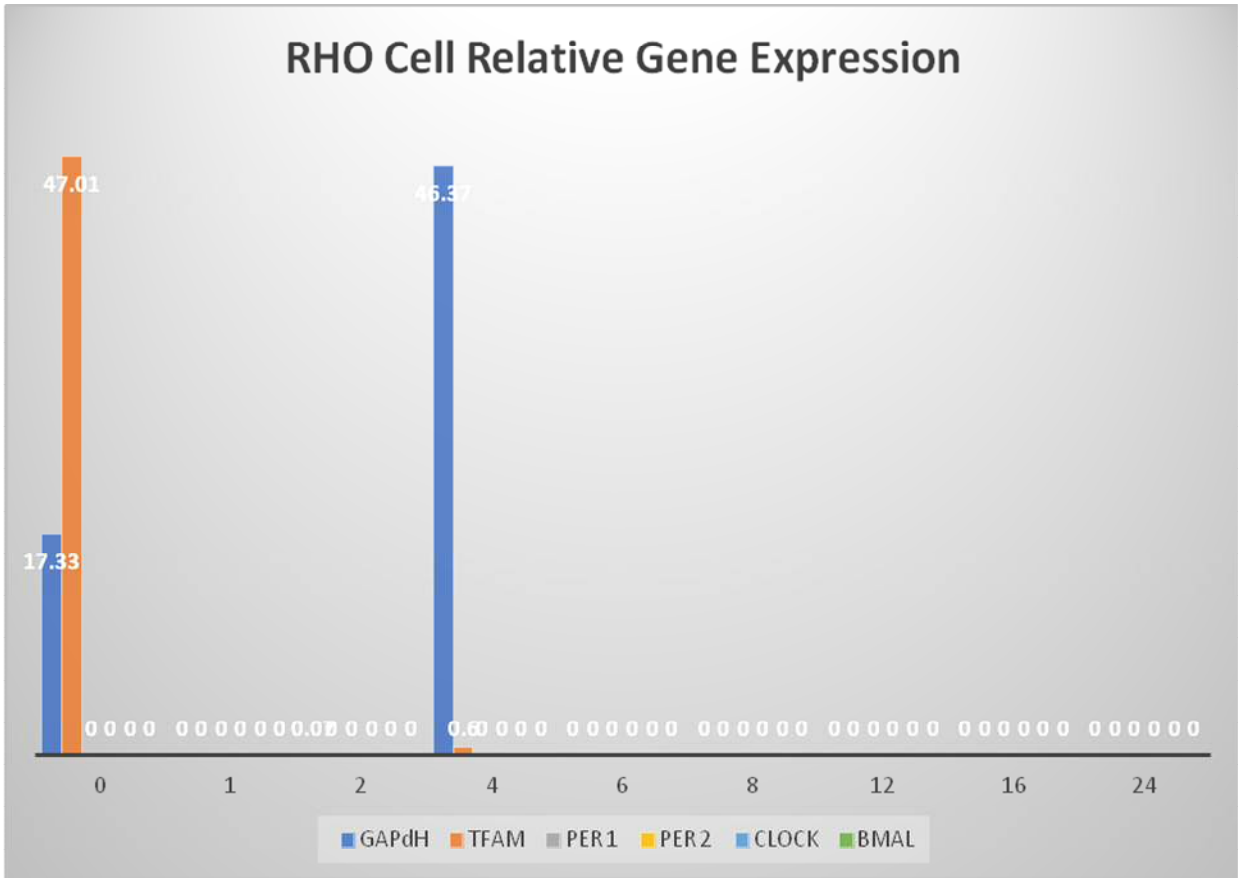

Figure 5.8 Relative gene expression using the 2^ΔΔCq method for MCF-7 *Rhø* cells for several time points over 24 hours (n=3).

TFAM exhibited its greatest increase in fold expression at 0 hours, when the shifted cells had been at suboptimal temperatures for 12 hours (21:00 to 09:00) and GAPDH experienced its peak in expression at 4 hours post shift. Damage to nuclear DNA has been demonstrated in response to long term EtBr treatment (Spadafora *et al*. 2016). It is possible that this has occurred in this study however the detection of housekeeping genes and other nuclear encoded genes including some of the core clock genes suggests that any mutation created had minimal impact.

5.4 Discussion

Current research has been directed to looking for the link between circadian disruption and cancer as well as between metabolic syndrome and rhythm disorders (Touitou, Reinberg, and Touitou 2017). These investigations support the idea that there is a leading role played by mitochondria in the pathogenesis of these diseases and that mtDNA-deficient cell lines provide a novel means to further study these relationships (Scrima *et al.* 2016). Consistent with the findings of this study, the long term addition of a low concentration of EtBr, that preferentially damages the mtDNA, causes functional and significant gross morphological changes in the cells that include modifications to the subcellular mitochondrial network (Gilkerson *et al.* 2000). Although many fluorescent dyes can be used to measure changes in the mitochondrial membrane potential ($\Delta\psi_m$), MitoTracker ^{TM} Red has been used to identify mitochondria in *Rhø* cells (Schubert *et al.* 2015) (Perry *et al.* 2011). Figure 5.2 does illustrate that in this study the mitochondria are present in *Rhø* cells, however the numbers and/or the structure appear to differ significantly from that of control cells.

King and Attardi (1996) outline that the best experimental control for identifying the *Rhø* cell is the inability of mitochondria-deficient cells to survive in the absence of uridine supplementation and argues that the use of RT-qPCR must be carefully interpreted as the nuclear genome is frequently contaminated with fragments of mtDNA (Ju *et al.* 2015). Uridine supplementation is mandatory as uridine synthesis requires a functional electron transport chain (King and Attardi 1996). The current study also included characterizing the loss of the mtDNA-encoded subunits of the ETC complexes I, III, IV, and V and a reduction in overall ATP production. While all of the isolated mitochondria-deficient MCF7 *Rhø* cell lines in the study

were shown to express the nuclear-encoded subunit of complex II and were shown to express diminished levels of the ETC complex III and V subunits as expected, some subline groups did express complex I and IV subunits as illustrated by Figure 5.3. These results are consistent with the findings of other groups as *Rhø* cell cultivation doesn't necessarily completely eliminate all of the ETC subunits but rather reduces their abundance and functionality (Ma *et al.* 2010).

MCF-7 *Rhø* cell sublines 2, 3, 4, A, and B did demonstrate lower levels of ATP production (Figure 5.4) despite having evidence to show that the complex I and IV subunits were still expressed, which indicates that oxidative phosphorylation is not functioning properly. MCF-7 *Rhø* cell sublines1 and 1B had been established for the longest time and it is likely that *Rhø* cells over time can compensate for the loss of oxidative phosphorylation by upregulating other ATP production pathways (Scrima et *al.* 2016). The Warburg Effect describes how cancer cells preferentially shift to glycolysis to manufacture their ATP and although glycolysis produces markedly lower levels of ATP than oxidative phosphorylation, the rate of production can be increased and therefore over time comparable amounts can be produced (Liberti and Locasale 2016). Glyceraldehyde 3-phosphate dehydrogenase (GAPDH) is a key glycolytic enzyme in the pathway from glucose to pyruvate and it is frequently overexpressed in cancer cells (Colell, Green, and Ricci 2009). Pyruvate is fermented to lactate by lactate dehydrogenase (LDH) which simultaneously oxidizes NAPH to NAD+ and therefore impacts the redox balance of the cell (Valvona *et al*. 2016). The other metabolic shift that cancer cells utilize is the activation of the pentose phosphate pathway and although this pathway does not directly produce ATP, NADPH is generated, imposing further redox changes on the cell (Lucarelli *et al.* 2015). It is not entirely clear what the benefits of these metabolic shifts are to cancer cells, however the

concomitant generation of ROS and redox fluxes, and their impact on cell signaling are becoming increasingly appreciated (Liberti and Locasale 2016).

ROS levels increase as the cell cycle progresses and since cancer cells are highly proliferative this may be another source of ROS accumulation (Weinberg and Chandel 2009). *Rhø* cells generate markedly reduced ROS levels due to the nonfunctional ETC (Chandel and Schumacker 1999). It is not surprising that cell cycle kinetics would also be impacted in *Rhø* cells due to the presence of fewer and morphologically- and functionally- impaired mitochondria. Experiments using *Rhø* cells generated from human lung carcinoma and osteosarcoma cell lines were able to show a cell cycle delay (Mineri *et al*. 2009). The mtDNA depletion from MCF-7 cells in this study also resulted in changes in the cell cycle as illustrated in Figures 5.5, 5.6, and 5.7. In addition, the *Rhø* cells were exposed to the temperature shift protocol for 7 days to look at the relationship between circadian rhythms and cellular metabolism. In Figure 2.7, normal MCF-7 cells exposed to the temperature shift condition did not demonstrate any significant differences in cell cycle kinetics between the shifted cells and the control condition. However, when the MCF-7 *Rhø* cells were subjected to the temperature shift protocol they had a significantly greater proportion of cells in G_2M. It is realistic to expect that mitochondrial abnormalities, especially lower energetic availability could contribute to a G_2M block but previous studies had shown that a HeLa *Rhø* cell line failed to demonstrate delayed cell cycle progression attributable to any specific phase arrest (Schauen *et al*. 2006). Schauen *et al.* (2006) found that the energy differences between *Rhø* and wild type cells were minimal but did demonstrate the down regulation of several cell cycle modulators in *Rhø* cells and went on to speculate that this may be due to the overall low ROS level. In this study, the ROS level of the MCF-7 *Rhø* cells was not measured as it was assumed to be low based on other studies given the

removal of the ETC, the largest generator of intracellular ROS. Exposure of normal MCF-7 cells to the temperature shift protocol does result in an increase in intracellular ROS levels but this is apparently not due to the superoxide molecule (Figures 4.2 and 4.3). This would be an interesting area to quantify. Melatonin treatment plus exposure to the temperature shift protocol induces a G_2M delay (Figure 3.5) and this may be due to the influence of CKIs and/or a reduction in cyclin expression. Melatonin has been shown to uncouple oxidative phosphorylation in MCF-7 cells (Scott *et al*. 2001). The uncoupling response in mitochondria is a regulatory feature which prevents excess ROS accumulation and also leads to thermogenesis in certain tissues while disrupting the activity of ATP synthase and resulting in a marked loss of ATP generation (Xu, Pagadala, and Mueller 2015). Both the ETC and ADP phosphorylation are impaired in *Rhø* cells and it is interesting to speculate on the effects that melatonin might have on their viability and cell cycle kinetics. It is possible that the MCF-7 *Rhø* cell responses to the temperature shift protocol corresponding to a G_2M block is due to something intrinsic to human breast cancer cells (Ma *et al*. 2010). MCF-7 cells respond to oxidative stress induced by hydrogen peroxide in a dose-dependent manner with a G_2M delay (Mahalingaiah and Singh 2014) and the mechanism involved in the *Rhø* cell response to exposure to a temperature shift may be related to H_2O_2 production. The increased sub G_1 populations across all three temperature conditions is an interesting finding (Figures 5.5, 5.6 and 5.7). *In vitro* derived *Rhø* cells have been shown to be more resistant to apoptosis (Chen *et al.* 2016). It was not specifically determined in this study if the sub G_1 populations shown in flow cytometry studies are apoptotic bodies, however the use of PI and/or 70 % ethyl alcohol in the flow preparation may have sensitized the cells and led to programmed cell death. The significantly increased

proportion of MCF-7 *Rhø* cells in *S* phase in the comparative 34/34° C condition is consistent with the findings for the normal MCF-7 cells shown in Figure 2.7.

The delay in cell cycle progression found in this study is consistent with the findings of other investigations with the unique aspect of this study being the specific G_2M phase block associated with exposure of the MCF-7 *Rhø* cells to the temperature shift. A second difference with the MCF-7 *Rhø* cells being exposed to the temperature shift condition is the change in gene expression. The temperature shift model results in increased clock gene expression at specific times in normal MCF-7 cells as measured by the 2^ΔΔCq method and as shown in Figures 2.10 and 2.11. The MCF-7 *Rhø* cells exposed to the temperature shift model do not show this increase in the relative expression of clock genes at any timepoint after temperature shift for seven days but this is not the case with all genes since the expression of the mitochondrial transcription factor A (TFAM) and GAPDH as well as the housekeeping gene RPS-17 can be easily measured as shown in Figure 5.8. TFAM is a nuclear encoded transcription factor responsible for the maintenance of mtDNA which will bind with high affinity to damaged mtDNA and is expressed at relatively high levels in *Rhø* cells as supported by Figure 4.17 (Kang and Hamasaki 2005). TFAM can be over-expressed in cancer cells and increased levels have been correlated to a loss of mtDNA (Qiao *et al.* 2017). Therefore, the result of this study is consistent with previous results. The expression of GAPDH was also expected as it has been previously used as an internal control for gene expression studies of *Rhø* cells (Lee *et al*. 2008). Therefore, it appears that clock gene expression is specifically unresponsive in MCF-7 *Rhø* cells subjected to circadian rhythm manipulation (by temperature shifting for 7 days) and does not show the synchronization-dependent upregulation detected in wild-type MCF-7 cells. This is consistent with the findings reported in a study that used human liver tumor mtDNA-depleted

cells and found significantly reduced BMAL expression in the *Rhø* cells after circadian synchronization in response to treatment with the serum shock protocol (Scrima *et al*. 2016). The current study supports the conclusions of those authors which stated that impairment of mitochondrial oxidative phosphorylation contributes to clock gene dysregulation and this could be the keystone of the relationship between circadian disruption and metabolism: active oxidative phosphorylation may be an important component in maintaining circadian rhythms (Scrima *et al*. 2016).

5.5 References

Ashton, Thomas M., W. Gillies McKenna, Leoni A. Kunz-Schughart, and Geoff S. Higgins. 2018. "Oxidative Phosphorylation as an Emerging Target in Cancer Therapy." *Clinical Cancer Research*. https://doi.org/10.1158/1078-0432.CCR-17-3070.

Cela, Olga, Rosella Scrima, Valerio Pazienza, Giuseppe Merla, Giorgia Benegiamo, Bartolomeo Augello, Sabino Fugetto. 2016. "Clock Genes-Dependent Acetylation of Complex I Sets Rhythmic Activity of Mitochondrial OxPhos." *Biochimica et Biophysica Acta - Molecular Cell Research*. https://doi.org/10.1016/j.bbamcr.2015.12.018.

Chandel, Navdeep S., and Paul T. Schumacker. 1999. "Cells Depleted of Mitochondrial DNA (P0) Yield Insight into Physiological Mechanisms." *FEBS Letters*. https://doi.org/10.1016/S0014-5793(99)00783-8.

Chatterjee, A., E. Mambo, and D. Sidransky. 2006. "Mitochondrial DNA Mutations in Human Cancer." *Oncogene*. https://doi.org/10.1038/sj.onc.1209604.

Chen, Hulin, Junling Wang, Zhongrong Liu, Huilan Yang, Yingjie Zhu, Minling Zhao, Yan Liu, and Miaomiao Yan. 2016. "Mitochondrial DNA Depletion Causes Decreased ROS Production and Resistance to Apoptosis." *International Journal of Molecular Medicine*. https://doi.org/10.3892/ijmm.2016.2697.

Chomczynski, Piotr, and Nicoletta Sacchi. 2006. "The Single-Step Method of RNA Isolation by Acid Guanidinium Thiocyanate-Phenol-Chloroform Extraction: Twenty-Something Years On." *Nature Protocols*. https://doi.org/10.1038/nprot.2006.83.

Colell, A., D. R. Green, and J. E. Ricci. 2009. "Novel Roles for GAPDH in Cell Death and Carcinogenesis." *Cell Death and Differentiation*. https://doi.org/10.1038/cdd.2009.137.

Demine, Renard, and Arnould. 2019. "Mitochondrial Uncoupling: A Key Controller of Biological Processes in Physiology and Diseases." *Cells*. https://doi.org/10.3390/cells8080795.

Friedman, Jonathan R., and Jodi Nunnari. 2014. "Mitochondrial Form and Function." *Nature*. https://doi.org/10.1038/nature12985.

Ganetzky, Rebecca D., Claudia Stendel, Elizabeth M. McCormick, Zarazuela Zolkipli-Cunningham, Amy C. Goldstein, Thomas Klopstock, and Marni J. Falk. 2019. "MT-ATP6 Mitochondrial Disease Variants: Phenotypic and Biochemical Features Analysis in 218 Published Cases and Cohort of 14 New Cases." *Human Mutation*. https://doi.org/10.1002/humu.23723.

Gilkerson, Robert W., Daciana H. Margineantu, Roderick A. Capaldi, and Jeanne M.L. Selker. 2000. “Mitochondrial DNA Depletion Causes Morphological Changes in the Mitochondrial Reticulum of Cultured Human Cells.” *FEBS Letters*. https://doi.org/10.1016/S0014-5793(00)01527-1.

Gray, Michael W. 2012. “Mitochondrial Evolution.” *Cold Spring Harbor Perspectives in Biology*. https://doi.org/10.1101/cshperspect.a011403.

Jin, Lin, and Yanhong Zhou. 2019. “Crucial Role of the Pentose Phosphate Pathway in Malignant Tumors (Review).” *Oncology Letters*. https://doi.org/10.3892/ol.2019.10112.

Ju, Young Seok, Jose M.C. Tubio, William Mifsud, Beiyuan Fu, Helen R. Davies, Manasa Ramakrishna, Yilong Li. 2015. “Frequent Somatic Transfer of Mitochondrial DNA into the Nuclear Genome of Human Cancer Cells.” *Genome Research*. https://doi.org/10.1101/gr.190470.115.

Kang, Dongchon, and Naotaka Hamasaki. 2005. “Mitochondrial Transcription Factor A in the Maintenance of Mitochondrial DNA: Overview of Its Multiple Roles.” In *Annals of the New York Academy of Sciences*. https://doi.org/10.1196/annals.1338.010.

King, Michael P., and Giuseppe Attardi. 1996. “[27] Isolation of Human Cell Lines Lacking Mitochondrial DNA.” *Methods in Enzymology*. https://doi.org/10.1016/s0076-6879(96)64029-4.

Lee, Wan, Hyo Im Choi, Mi Jin Kim, and Seung Yoon Park. 2008. “Depletion of Mitochondrial DNA Up-Regulates the Expression of MDR1 Gene via an Increase in MRNA Stability.” *Experimental and Molecular Medicine*. https://doi.org/10.3858/emm.2008.40.1.109.

Liberti, Maria V., and Jason W. Locasale. 2016. “The Warburg Effect: How Does It Benefit Cancer Cells?” *Trends in Biochemical Sciences*. https://doi.org/10.1016/j.tibs.2015.12.001.

Lu, Chung Ling, Lili Qin, Hsin Chen Liu, Demet Candas, Ming Fan, and Jian Jian Li. 2015. “Tumor Cells Switch to Mitochondrial Oxidative Phosphorylation under Radiation via MTOR-Mediated Hexokinase II Inhibition - A Warburg-Reversing Effect.” *PLoS ONE*. https://doi.org/10.1371/journal.pone.0121046.

Lucarelli, Giuseppe, Vanessa Galleggiante, Monica Rutigliano, Francesca Sanguedolce, Simona Cagiano, Pantaleo Bufo, Gaetano Lastilla. 2015. “Metabolomic Profile of Glycolysis and the Pentose Phosphate Pathway Identifies the Central Role of Glucose-6-Phosphate Dehydrogenase in Clear Cell-Renal Cell Carcinoma.” *Oncotarget*. https://doi.org/10.18632/oncotarget.3823.

Ma, Yewei, Ren Kui Bai, Robert Trieu, and Lee Jun C. Wong. 2010. “Mitochondrial Dysfunction in Human Breast Cancer Cells and Their Transmitochondrial Cybrids.” *Biochimica et Biophysica Acta - Bioenergetics*. https://doi.org/10.1016/j.bbabio.2009.07.008.

Mahalingaiah, Prathap Kumar S., and Kamaleshwar P. Singh. 2014. “Chronic Oxidative Stress Increases Growth and Tumorigenic Potential of MCF-7 Breast Cancer Cells.” *PLoS ONE*. https://doi.org/10.1371/journal.pone.0087371.

Mastroeni, Diego, Omar M. Khdour, Elaine Delvaux, Jennifer Nolz, Gary Olsen, Nicole Berchtold, Carl Cotman, Sidney M. Hecht, and Paul D. Coleman. 2017. “Nuclear but Not Mitochondrial-Encoded Oxidative Phosphorylation Genes Are Altered in Aging, Mild Cognitive Impairment, and Alzheimer’s Disease.” *Alzheimer’s and Dementia*. https://doi.org/10.1016/j.jalz.2016.09.003.

Miller, Brooke H., Erin L. McDearmon, Satchidananda Panda, Kevin R. Hayes, Jie Zhang, Jessica L. Andrews, Marina P. Antoch. 2007. “Circadian and CLOCK-Controlled Regulation of the Mouse Transcriptome and Cell Proliferation.” *Proceedings of the National Academy of Sciences of the United States of America*. https://doi.org/10.1073/pnas.0611724104.

Mineri, Rossana, Norman Pavelka, Erika Fernandez-Vizarra, Paola Ricciardi-Castagnoli, Massimo Zeviani, and Valeria Tiranti. 2009. “How Do Human Cells React to the Absence of Mitochondrial DNA?” *PLoS ONE*. https://doi.org/10.1371/journal.pone.0005713.

Mookerjee, Shona A., Ajit S. Divakaruni, Martin Jastroch, and Martin D. Brand. 2010. “Mitochondrial Uncoupling and Lifespan.” *Mechanisms of Ageing and Development*. https://doi.org/10.1016/j.mad.2010.03.010.

Neufeld-Cohen, Adi, Maria S. Robles, Rona Aviram, Gal Manella, Yaarit Adamovich, Benjamin Ladeuix, Dana Nir. 2016. “Circadian Control of Oscillations in Mitochondrial Rate-Limiting Enzymes and Nutrient Utilization by PERIOD Proteins.” *Proceedings of the National Academy of Sciences of the United States of America*. https://doi.org/10.1073/pnas.1519650113.

Peek, C. B., K. M. Ramsey, D. C. Levine, B. Marcheva, M. Perelis, and J. Bass. 2015. “Circadian Regulation of Cellular Physiology.” In *Methods in Enzymology*. https://doi.org/10.1016/bs.mie.2014.10.006.

Qiao, Lihua, Guoqing Ru, Zhuochao Mao, Chenghui Wang, Zhipeng Nie, Qiang Li, Yiyi Huang-yang. 2017. “Mitochondrial DNA Depletion, Mitochondrial Mutations and High TFAM Expression in Hepatocellular Carcinoma.” *Oncotarget*. https://doi.org/10.18632/oncotarget.21033.

Rogatzki, Matthew J., Brian S. Ferguson, Matthew L. Goodwin, and L. Bruce Gladden. 2015. “Lactate Is Always the End Product of Glycolysis.” *Frontiers in Neuroscience*. https://doi.org/10.3389/fnins.2015.00022.

Schauen, Matthias, Dimitry Spitkovsky, Jens Schubert, Jürgen H. Fischer, Jun Ichi Hayashi, and Rudolf J. Wiesner. 2006. “Respiratory Chain Deficiency Slows down Cell-Cycle

Progression via Reduced ROS Generation and Is Associated with a Reduction of P21CIP1/WAF1." *Journal of Cellular Physiology*. https://doi.org/10.1002/jcp.20711.

Schubert, Susanna, Sandra Heller, Birgit Löffler, Ingo Schäfer, Martina Seibel, Gaetano Villani, and Peter Seibel. 2015. "Generation of Rho Zero Cells: Visualization and Quantification of the MtDNA Depletion Process." *International Journal of Molecular Sciences*. https://doi.org/10.3390/ijms16059850.

Scott, Aaron E., Gregory N. Cosma, Anthony A. Frank, Robert L. Wells, and Henry S. Gardner. 2001. "Disruption of Mitochondrial Respiration by Melatonin in MCF-7 Cells." *Toxicology and Applied Pharmacology*. https://doi.org/10.1006/taap.2000.9115.

Scrima, Rosella, Olga Cela, Giuseppe Merla, Bartolomeo Augello, Rosa Rubino, Giovanni Quarato, Sabino Fuget. 2016. "Clock-Genes and Mitochondrial Respiratory Activity: Evidence of a Reciprocal Interplay." *Biochimica et Biophysica Acta - Bioenergetics*. https://doi.org/10.1016/j.bbabio.2016.03.035.

Shokolenko, Inna N., and Mikhail F. Alexeyev. 2017. "Mitochondrial Transcription in Mammalian Cells." *Frontiers in Bioscience - Landmark*. https://doi.org/10.2741/4520.

Spadafora, Domenico, Nataliya Kozhukhar, Vladimir N. Chouljenko, Konstantin G. Kousoulas, and Mikhail F. Alexeyev. 2016. "Methods for Efficient Elimination of Mitochondrial DNA from Cultured Cells." *PLoS ONE*. https://doi.org/10.1371/journal.pone.0154684.

Taanman, Jan Willem. 1999. "The Mitochondrial Genome: Structure, Transcription, Translation and Replication." *Biochimica et Biophysica Acta - Bioenergetics*. https://doi.org/10.1016/S0005-2728(98)00161-3.

Thurley, Kevin, Christopher Herbst, Felix Wesener, Barbara Koller, Thomas Wallach, Bert Maier, Achim Kramer, and Pål O. Westermark. 2017. "Principles for Circadian Orchestration of Metabolic Pathways." *Proceedings of the National Academy of Sciences of the United States of America*. https://doi.org/10.1073/pnas.1613103114.

Touitou, Yvan, Alain Reinberg, and David Touitou. 2017. "Association between Light at Night, Melatonin Secretion, Sleep Deprivation, and the Internal Clock: Health Impacts and Mechanisms of Circadian Disruption." *Life Sciences*. https://doi.org/10.1016/j.lfs.2017.02.008.

Valvona, Cara J., Helen L. Fillmore, Peter B. Nunn, and Geoffrey J. Pilkington. 2016. "The Regulation and Function of Lactate Dehydrogenase A: Therapeutic Potential in Brain Tumor." *Brain Pathology*. https://doi.org/10.1111/bpa.12299.

Weinberg, Frank, and Navdeep S. Chandel. 2009. "Reactive Oxygen Species-Dependent Signaling Regulates Cancer." *Cellular and Molecular Life Sciences*. https://doi.org/10.1007/s00018-009-0099-y.

Xu, Ting, Vijayakanth Pagadala, and David M. Mueller. 2015. “Understanding Structure, Function, and Mutations in the Mitochondrial ATP Synthase.” *Microbial Cell*. https://doi.org/10.15698/mic2015.04.197.

Chapter 6

Chapter 6 Conclusions and Implications

Hanahan and Weinburg introduced a framework to understand the primary characteristics of malignancy and to show how these are features are interrelated in immortalized cell lines (Hanahan and Weinberg 2000). When this framework was updated a decade later, the authors stressed how genomic instability underpinned the six original features and added two additional features of malignant cells; evasion from immune system detection and destruction and cellular reprogramming of energy metabolism (Hanahan and Weinberg 2011). Hall, Rosbash and Young discovered that the foundation of our current understanding of the complexity of clock gene expression is the ability to co-ordinate various homeostatic and behavioural rhythms in an organism during the day (Huang 2018). Epidemiological evidence and a large volume of *in vivo* and *in vitro* research has increased our understanding of the complex relationship between circadian rhythm disruption and disease. The core motivation of the current study was to examine the underlying principles relating cancer to clock gene expression at the molecular level and to contribute to the knowledge of this interaction in the hopes that one day individuals will understand how important occupational and lifestyle choices are.

6.1 Summary of major findings

A synopsis of results by chapter includes:

Chapter 2

The temperature shift model resulted in a decrease in cell proliferation in MCF-7 human breast cancer cells, HBL-100 human breast epithelial cells, and murine melanoma BL6-B16 cells. This decrease appeared to be related to changes brought about in cell metabolism. MCF-7 cells, which typically have low levels of clock gene expression, responded to exposure to a temperature shift with an increase in clock gene expression, especially in PER2 levels over multiple time points and showed that PER1 expression is different from PER2 expression. The period protein gene expression profiles also differed from the transcription factors CLOCK: BMAL and this is the expected timing based on their physiological relationship. Exposure of cells to a serum shock protocol can also synchronize clock genes and was able to influence cell cycle kinetics whereas exposure to the temperature shift model for 7 days does not appear to affect cell cycle regulation.

Chapter 3

Treatment with melatonin can differently impact cancer cells and non-malignant cells. Treatment with high concentrations of melatonin can negatively impact the viability of MCF-7 cells as measured by the ability to reduce the MTT reagent to formazan in the MTT assay but did not affect HBL-100 cells. Treatment with low concentrations of melatonin conferred a proliferative advantage to non-malignant cells. Melatonin treatment of malignant cells impacted cell cycle kinetics by increasing the proportion of cells in the G_1 phase and while treatment with melatonin may change the expression profiles of clock genes there was no significant impact on overall transcript expression.

Chapter 4

Exposure of cells to the temperature shift condition plus treatment with chemotherapeutic drugs impaired MCF-7 cell metabolism in a manner that appears to be primarily be due to the temperature shift. This response was similar to treatment with 10 nM melatonin, however cells responded differently to other concentrations of melatonin. For example, treatment with 1 nM and 10 nM melatonin was pro-oxidant increasing H_2O_2 and -OH production, but not superoxide. Treatment with chemotherapeutic drugs can increase intracellular ROS production with different drugs having different intracellular effects. Treatment with cisplatin increased mitochondrial ROS production and TFAM transcription and this relationship suggests that mitochondrial damage is relayed to the nucleus and may be mediated by ROS. Exposure to the temperature shift protocol increased intracellular ROS levels and since intracellular ROS levels can decrease cell proliferation, this may be one mechanism of action to explain the anti-proliferative effects of the temperature shift model. Treatment of MCF-7 cells with melatonin at a physiological concentration of 1 nM or with 100 nM and greater can induce a protective effect on cells impacted by the temperature shift protocol. This may have important therapeutic implications if patients are receiving an anti-cancer treatment which includes ROS generation as a mechanism of action and thus they should discuss the concurrent use of antioxidants with their oncologist.

Chapter 5

Rhø, mitochondrial defective, cells can be generated from MCF-7 human breast cancer cells but this is not a universal ability inherent to all cancer cells. MCF-7 *Rhø* cells were characterized by the loss of mtDNA-derived protein subunits using the Total OXPHOS Human WB Antibody Cocktail ® (Abcam) and by a reduction in ATP production using a Luminescent

ATP Detection Assay Kit® (Abcam). The long-term culture with media containing EtBr did impact cell growth and viability. Exposure to the temperature shift protocol induced a G_2M block in MCF-7 *Rhø* cells and this may be a response to oxidative stress or mitochondrial changes or both. MCF-7 *Rhø* cells exhibited impaired clock gene expression when exposed to the temperature shift model and this parallels the results using other cell synchronization procedures with *Rhø* cells. This suggests that impaired oxidative phosphorylation has a role in circadian disruption.

6.2 Fulfillment of aims and objectives

Aim 1: To investigate the molecular changes that relate circadian disruption to disease by establishing a model that influences clock gene expression in peripheral cells independent of central oscillators.

The temperature shift protocol increased clock gene expression in MCF-7 breast cancer cells as shown in Figure 2.10 and 2.11. Exposure to the temperature shift model does not appear to impact the expression of circadian cycle clock genes in SCN cells (Buhr, Yoo, and Takahashi 2010). Conversely, exposure to a serum shock protocol appears to synchronize circadian gene expression in SCN cells (Hurst, Mitchell, and Gillette 2002). Understanding how peripheral oscillators may be differentially affected could assist in understanding the mechanisms related to central and peripheral uncoupling.

Aim 2: To investigate the molecular changes that relate circadian disruption to disease by examining the role of melatonin on clock gene expression and cell cycle kinetics.

Treatment with melatonin in cells exposed to the temperature shift condition caused a change in cell cycle kinetics that exposure to the temperature shift alone did not as shown in

Figure 3.4 and 3.5. This is consistent with other findings. There was no significant difference in clock gene expression imposed by melatonin when melatonin is paired with a temperature shift as shown in Figure 3.10

Aim 3: To investigate the molecular changes that relate circadian disruption to disease by examining the role of mitochondria, reactive oxygen species (ROS) production, and cellular redox status.

Exposure of MCF-7 cells to the temperature shift model increased intracellular ROS but not from the mitochondria. Differences in the metabolism of MCF-7 cells exposed to chemotherapeutic drugs plus exposure to the temperature shift are related primarily to the effect of the temperature shift. This is a different response than what was generated by treatment with melatonin where melatonin concentration and not the temperature shift contributed the most significant differences. Melatonin can increase intracellular ROS levels in MCF-7 cells and can exhibit anti-oxidant effects when those cells are exposed to a temperature shift condition. Different chemotherapeutic drugs can generate different profiles of ROS generation. The figures in Chapter 4 support these conclusions.

Aim 4: To investigate the molecular changes that relate circadian disruption to disease by examining the role of perturbed energetics and cell metabolism on clock gene expression and cell cycle kinetics.

Impaired oxidative phosphorylation negatively impacts clock gene expression in MCF-7 breast cancer cells as evidenced by Figure 5.8.

Objective 1: Explore the interconnection between the cell and circadian cycles. This requires the interrogation of current protocols of cell synchronization including the temperature shift model

in order to characterize a model where clock gene expression is independent of the cell cycle and has minimal dependence on pharmaceutical or hormone interactions.

Exposure to the temperature shift did not change cell cycle kinetics in terms of phase delays but did impact overall duration as evidenced by decreased cell proliferation. This suggests that increased clock gene expression impacts the cell cycle duration but does not impart a cell cycle phase delay or advance. Exposure of cells to the serum shock protocol synchronizes cell cycle and clock gene expression and therefore it may be difficult to draw conclusions about how clock gene expression is related to the cell cycle in experiments where a serum shock protocol is used to increase clock gene expression.

Objective 2: Explore the impact of treatment with melatonin on clock gene expression and on cell cycle regulation independent of each other through use of the temperature shift model.

This is addressed under Aim 2.

Objective 3: Determine the impact of drug and hormone exposure on cellular and mitochondrial ROS production in cells exposed to the temperature shift model.

This is addressed under Aim 3.

Objective 4: Determine the impact of mitochondrial oxidative phosphorylation impairment on clock gene expression by developing an aberrant mitochondria cell line.

This is addressed under Aim 4.

The aims and objectives for this study have been met and addressed.

6.3 Research question and hypothesis

The central question becomes, does circadian rhythm disruption directly lead to the genomic instability which predisposes to oncogenesis and what is the molecular mechanism?

This study did not directly answer the central question. However, the results suggest that oxidative stress and ROS production, as it relates to mitochondrial impairment, could be a tumor initiation factor resulting from impaired circadian gene expression in tissues. Research indicates that shift work causes oxidative stress (Bhatti *et al.* 2017). An increase in ROS production changes clock gene expression in MCF-7 cells (Johar et al. 2015)(Stangherlin and Reddy 2013).

It is predicted that a temperature shift protocol will increase clock gene expression in MCF-7 cells and part of this mechanism is due to oxidative stress such that if oxidative phosphorylation is disrupted, circadian gene expression becomes dysregulated.

The cumulative results from this study support the conclusion that the hypothesis is correct.

6.4 Contributions of the project to the advancement of knowledge

This project has described and characterized a model to study clock gene expression in cell culture as an alternative to serum shock synchronization and has verified the differential impact of melatonin on cells and on the cell cycle using the temperature shift model. Further, the results confirmed that MCF7-derived *Rhø* cells are viable and can withstand manipulation by temperature shift. Exposure to the temperature shift model increased clock gene expression in a human breast cancer cell line that typically has very low levels of circadian gene expression and

this is an accomplishment in itself. Exposure to the temperature shift condition can increase ROS production in cells and to our knowledge, this has not been investigated previously. When oxidative phosphorylation is impaired, the clock gene expression that was induced by the temperature shift was negated, suggesting a possible mechanism for circadian rhythm disruption impact on peripheral cell oscillators.

6.5 Next steps

The next phase of this work would be repeating the temperature shift experiments with a luciferase reporter construct of PER2 and a second with either CLOCK or BMAL using MCF-7 cells. BMAL expression has been reported in the literature and it would be a logical next step to involve a transcription factor and a clock effector protein. The luciferase system is reported to be more sensitive and would allow monitoring over a greater number of time points. It is recommended that the collection period be extended to 72 hours and the appropriate statistical methods to determine if there are oscillating waves of gene expression representative of a circadian cycle would also need to be employed. The luciferase paradigm may also assist in deducing whether the temperature shift model is synchronizing clock gene expression or inducing latent gene expression in a low frequency transcript cell line such as MCF-7 cells. It would be very informative to use MCF-10A cells as well to represent a non-cancerous breast epithelial cell line and/or an ERα positive breast epithelial cell line. Ideally the temperature shift model is characterized in those cell lines which have been characterized with the cell proliferation, cell cycle, and expression of housekeeping genes by RT-qPCR assays first. It is important to repeat the ROS experiments in response to exposure to the temperature shift condition for MCF-7 cells and the other cell lines and include a quantitative measurement

method for the superoxide radical to measure the mitochondrial contribution as well total cellular ROS production.

It would also be informative to selectively impair the subunits of oxidative phosphorylation through the serial addition of drugs and chemicals that are knows to impair specific subunit function and examine ROS production and clock gene expression. This might elucidate if a particular mtDNA mutation had an effect on clock gene expression or its relative contribution.

Another important aspect with using the MCF-7 *Rhø* cell line of inquiry would be to specifically examine apoptosis markers and proliferation markers during the cell cycle in response to exposure to the temperature shift protocol. It would be very interesting to combine melatonin addition and the temperature shift model in treating MCF-7 *Rhø* cells and examine the effect on cell cycle kinetics and clock gene expression to determine how these factors might be interrelated.

The temperature shift model requires study in a larger variety of cell lines *in vitro.* Testing the model with human lymphocytes *ex vivo* and examining clock gene expression may be the first step to examining night shift worker lymphocyte circadian gene expression as compared to controls in an attempt to get better answers to the central question of how chronic circadian disruption is involved in oncogenesis.

6.6 References

Bhatti, Parveen, Dana K. Mirick, Timothy W. Randolph, Jicheng Gong, Diana Taibi Buchanan, Junfeng Zhang, and Scott Davis. 2017. "Oxidative DNA Damage during Night Shift Work." *Occupational and Environmental Medicine*. https://doi.org/10.1136/oemed-2017-104414.

Buhr, Ethan D., Seung Hee Yoo, and Joseph S. Takahashi. 2010. "Temperature as a Universal Resetting Cue for Mammalian Circadian Oscillators." *Science*. https://doi.org/10.1126/science.1195262.

Hanahan, Douglas, and Robert A. Weinberg. 2000. "The Hallmarks of Cancer." *Cell*. https://doi.org/10.1016/S0092-8674(00)81683-9.

Hanahan, Douglas, and Robert A. Weinberg. 2011. "Hallmarks of Cancer: The next Generation." *Cell*. https://doi.org/10.1016/j.cell.2011.02.013.

Huang, Rong Chi. 2018. "The Discoveries of Molecular Mechanisms for the Circadian Rhythm: The 2017 Nobel Prize in Physiology or Medicine." *Biomedical Journal*. https://doi.org/10.1016/j.bj.2018.02.003.

Hurst, William J., Jennifer W. Mitchell, and Martha U. Gillette. 2002. "Synchronization and Phase-Resetting by Glutamate of an Immortalized SCN Cell Line." *Biochemical and Biophysical Research Communications*. https://doi.org/10.1016/S0006-291X(02)02346-X.

Johar, Ramesh, Rohit Sharma, Amanpreet Kaur, and Tapan K. Mukherjee. 2015. "Role of Reactive Oxygen Species in Estrogen Dependant Breast Cancer Complication." *Anti-Cancer Agents in Medicinal Chemistry*. https://doi.org/10.2174/1871520615666150518092315.

Stangherlin, Alessandra, and Akhilesh B. Reddy. 2013. "Regulation of Circadian Clocks by Redox Homeostasis." *Journal of Biological Chemistry*. https://doi.org/10.1074/jbc.R113.457564.

Appendix 1.

Co-efficient of variation for housekeeping gene selection, RPS 17 and PPIA

	G	H	I	J	K	L	M	N	O
	HMBS	IPO8	PGK1	RPLP0	TBP	TFRC	UBC	YWHAZ	PPIA
	Y	Y	Y	Y	Y	Y	Y	Y	Y
1	3	3	3	3	3	3	3	3	3
2									
3	29.58	33.02	25.54	22.23	31.02	27.21	22.96	30.08	23.53
4	31.44	33.22	25.95	25.83	33.00	28.33	26.61	32.18	24.60
5	31.96	36.86	28.01	27.04	34.83	34.32	31.13	37.67	24.66
6									
7	30.99	34.37	26.50	25.03	32.95	29.95	26.90	33.31	24.26
8	1.251	2.162	1.324	2.502	1.905	3.823	4.093	3.919	0.6358
9	0.7224	1.248	0.7642	1.445	1.100	2.207	2.363	2.263	0.3671
10									
11									
12	4.04%	6.29%	4.99%	9.99%	5.78%	12.76%	15.21%	11.77%	2.62%
13									
14	30.98	34.32	26.48	24.95	32.91	29.80	26.69	33.16	24.26
15	27.99	29.43	23.42	19.34	28.50	21.90	18.29	24.89	22.72
16	34.28	40.02	29.93	32.18	38.01	40.55	38.96	44.18	25.90
17									
18	92.98	103.1	79.50	75.10	98.85	89.86	80.70	99.93	72.79

	Y	Z	AA	AB	AC	AD	AE	AF
	ABL1	ELF1	MT-ATP6	MRPL-19	POP4	RPL37A	RPL30	RPS17
	Y	Y	Y	Y	Y	Y	Y	Y
1	3	3	3	3	3	3	3	3
2								
3	28.62	33.42	23.68	32.68	31.95	26.32	26.55	24.57
4	30.03	34.44	23.90	33.19	32.99	27.74	28.07	26.08
5	34.78	38.01	26.10	35.55	34.53	28.22	28.71	26.46
6								
7	31.14	35.29	24.56	33.81	33.16	27.43	27.78	25.70
8	3.227	2.410	1.338	1.531	1.298	0.9880	1.109	0.9997
9	1.863	1.392	0.7726	0.8840	0.7494	0.5704	0.6406	0.5772
10								
11								
12	10.36%	6.83%	5.45%	4.53%	3.91%	3.60%	3.99%	3.89%
13								
14	31.03	35.24	24.54	33.78	33.14	27.41	27.76	25.69
15	24.11	29.81	21.47	30.23	30.08	25.05	25.12	23.30
16	39.94	41.65	28.04	37.76	36.51	30.00	30.68	28.32
17								
18	93.43	105.9	73.68	101.4	99.47	82.28	83.33	77.11

Appendix 2.

Two-way ANOVA results for MTT assay

```
ANOVA MTT by temperature (1,3) day (1,12)/METHOD=EXPERIMENTAL/STATISTICS all.
```

ANOVA

Case Processing Summary[a]

Cases					
Included		Excluded		Total	
N	Percent	N	Percent	N	Percent
288	100.0%	0	0.0%	288	100.0%

a. MTT by temperature, day

Cell Means[a]

		MTT	
temperature	day	Mean	N
1	1	.06038	8
	2	.06888	8
	3	.07762	8
	4	.09637	8
	5	.22462	8
	6	.39937	8
	7	.76400	8
	8	1.64263	8
	9	1.46737	8
	10	1.05925	8
	11	.41900	8
	12	1.26037	8
	Total	.62832	96
2	1	.05750	8
	2	.06775	8
	3	.07825	8
	4	.08163	8
	5	.18113	8
	6	.17187	8
	7	.40600	8
	8	1.11525	8
	9	1.39525	8
	10	1.74213	8
	11	1.07762	8
	12	1.55088	8
	Total	.66044	96

ANOVA[a]

			Experimental Method			
			Sum of Squares	df	Mean Square	F
MTT	Main Effects	(Combined)	64.840	13	4.988	44.167
		temperature	9.954	2	4.977	44.072
		day	54.886	11	4.990	44.185
	2-Way Interactions	temperature * day	21.374	22	.972	8.603
	Model		86.214	35	2.463	21.813
	Residual		28.458	252	.113	
	Total		114.672	287	.400	

ANOVA[a]

			Experiment.
			Sig.
MTT	Main Effects	(Combined)	.000
		temperature	.000
		day	.000
	2-Way Interactions	temperature * day	.000
	Model		.000
	Residual		
	Total		

a. MTT by temperature, day

MCA[a]

			N	Predicted Mean		Deviation	
				Unadjusted	Adjusted for Factors	Unadjusted	Adjusted for Factors
MTT	temperature	1	96	.62832	.62832	.115073	.115073
		2	96	.66044	.66044	.147187	.147187
		3	96	.25099	.25099	-.262260	-.262260
	day	1	24	.06021	.06021	-.453042	-.453042
		2	24	.07367	.07367	-.439583	-.439583
		3	24	.07500	.07500	-.438250	-.438250
		4	24	.08358	.08358	-.429667	-.429667
		5	24	.16417	.16417	-.349083	-.349083
		6	24	.21525	.21525	-.298000	-.298000
		7	24	.42146	.42146	-.091792	-.091792
		8	24	.98525	.98525	.472000	.472000
		9	24	1.07517	1.07517	.561917	.561917
		10	24	1.06567	1.06567	.552417	.552417
		11	24	.84304	.84304	.329792	.329792
		12	24	1.09654	1.09654	.583292	.583292

a. MTT by temperature, day

Factor Summary[a]

		Eta	Beta
			Adjusted for Factors
MTT	temperature	.295	.295
	day	.692	.692

a. MTT by temperature, day

Model Goodness of Fit

	R	R Squared
MTT by temperature, day	.752	.565

```
ANOVA temperature MTT by day (1,12)/STATISTICS ALL.
```

ANOVA

Warnings

Unique sums of squares is now the default method in ANOVA.
MCA is not available with the unique sums of squares method.
MEAN statistic is not available with the unique sums of squares method.

Case Processing Summary[a]

Cases					
Included		Excluded		Total	
N	Percent	N	Percent	N	Percent
36	100.0%	0	0.0%	36	100.0%

a. temperature, MTT by day

ANOVA[a,b]

			Unique Method				
			Sum of Squares	df	Mean Square	F	Sig.
temperature	Main Effects	day	.000	11	.000	.000	1.000
	Model		.000	11	.000	.000	1.000
	Residual		24.000	24	1.000		
	Total		24.000	35	.686		
MTT	Main Effects	day	6.862	11	.624	3.823	.003
	Model		6.862	11	.624	3.823	.003
	Residual		3.916	24	.163		
	Total		10.779	35	.308		

a. temperature, MTT by day

b. All effects entered simultaneously

Appendix 3.

Replicates for RT-qPCR for seven-day shift experiment

MCF7 Seven day shift experiment # 1
3737 & 3734
2 reference genes: RSP 17 and PPIA
PER 1, PER 2, CLOCK, BMAL, CRY 1, CRY 2, NR1 D 1, DBP

Col. stats		A	B	C	D	E	F
		RSP 17 3737	RSP 17 3734	PPIA 3737	PPIA 37 34	PER 1 3737	PER1 3734
		Y	Y	Y	Y	Y	Y
1	Number of values	9	9	9	9	9	9
2							
3	Minimum	21	21	23	21	41	31
4	25% Percentile	28	22	27	24	41	34
5	Median	33	31	30	28	41	41
6	75% Percentile	34	35	33	31	41	41
7	Maximum	35	36	35	34	41	41
8							
9	Mean	31	29	30	28	41	38
10	Std. Deviation	4.5	6.2	3.9	4.2	0.0	4.2
11	Std. Error	1.5	2.1	1.3	1.4	0.0	1.4
12							
13	Lower 95% CI of mean	27	24	27	25	41	35
14	Upper 95% CI of mean	34	34	33	31	41	41
15							
16	Coefficient of variation	14.50%	21.29%	13.05%	15.24%	0.00%	11.20%
17							
18	Geometric mean	31	28	29	27	41	38
19	Lower 95% CI of geo. mean	27	24	26	24	41	34
20	Upper 95% CI of geo. mean	35	34	33	31	41	41
21							
22	Sum	278	261	266	250	369	340

	O	P	Q	R	S	T
	CRY 2 3737	CRY 2 3734	NR1 D1 3737	NR1 D1 3734	DBP 3737	DBP 3734
	Y	Y	Y	Y	Y	Y
1	9	9	9	9	9	9
2						
3	38	29	41	30	41	28
4	41	34	41	35	41	33
5	41	36	41	41	41	36
6	41	41	41	41	41	41
7	41	41	41	41	41	41
8						
9	41	37	41	38	41	37
10	1.1	4.1	0.0	4.3	0.0	4.9
11	0.37	1.4	0.0	1.4	0.0	1.6
12						
13	40	34	41	35	41	33
14	41	40	41	42	41	40
15						
16	2.76%	11.24%	0.00%	11.28%	0.00%	13.29%
17						
18	41	37	41	38	41	36
19	40	33	41	35	41	33
20	42	40	41	42	41	40
21						
22	366	331	369	346	369	329

Table format: Grouped		A		B		C		D	
		RSP 17 3737		RSP 17 3734		PPIA 3737		PPIA 37 34	
		A:Y1	A:Y2	B:Y1	B:Y2	C:Y1	C:Y2	D:Y1	D:Y2
1	Title	34.19	33.49	32.88	32.45	35.23	33.87	30.24	29.60
2	Title	29.28	29.61	35.71	35.71	30.77	29.59	33.07	32.28
3	Title	33.38	32.83	31.72	30.99	30.52	30.57	28.14	28.36
4	Title	34.54	35.11	20.72	21.08	32.91	33.37	22.92	20.07
5	Title	20.63	21.44	32.94	34.75	22.72	22.62	29.60	29.60
6	Title	35.69	34.03	36.23	36.00	32.48	31.94	32.72	35.01
7	Title	33.59	32.34	22.75	23.10	30.14	29.63	24.63	24.98
8	Title	29.84	31.41	26.61	26.25	27.30	29.66	26.36	25.99
9	Title	27.42	27.40	21.79	20.93	25.52	23.72	23.98	21.99

	I	J		K		L		M	
	< 3737	CLOCK 3734		BMAL 3737		BMAL 3734		CRY 1 3737	
	I:Y2	J:Y1	J:Y2	K:Y1	K:Y2	L:Y1	L:Y2	M:Y1	M:Y2
1	41	29.78	29.21	34.87	34.87	34.66	32.57	41	41
2	41	32.38	32.38	41.00	41.00	41.00	41.00	41	41
3	41	41.00	41.00	41.00	41.00	41.00	41.00	41	41
4	41	26.90	26.87	41.00	41.00	29.15	29.85	41	41
5	41	34.23	34.43	41.00	41.00	34.71	34.71	41	41
6	41	41.00	41.00	41.00	41.00	41.00	41.00	41	41
7	41	36.04	36.05	41.00	41.00	36.36	36.36	41	41
8	41	35.20	35.20	41.00	41.00	41.00	41.00	41	41
9	41	31.45	31.45	41.00	41.00	31.15	31.35	41	41

	R	S		T	
	1 3734	DBP 3737		DBP 3734	
	R:Y2	S:Y1	S:Y2	T:Y1	T:Y2
1	38.74	41	41	33.85	38.63
2	41.00	41	41	41.00	41.00
3	41.00	41	41	41.00	41.00
4	30.15	41	41	27.22	27.97
5	41.00	41	41	34.35	34.35
6	41.00	41	41	41.00	41.00
7	41.00	41	41	41.00	41.00
8	41.00	41	41	34.15	34.15
9	31.75	41	41	32.03	32.53

RSP

3737		3734		3434	
34.19	33.49	32.88	32.45	22.65	23
29.28	29.61	No Cq	35.71	22.24	22.96
33.38	32.83	31.72	30.99	21.61	22.38
34.54	35.11	20.72	21.08	32.94	33.59
20.63	21.44	32.94	34.75	31.96	31.97
35.69	34.03	36.23	36	31.66	32.96
33.59	32.34	22.75	23.1		
29.84	31.41	26.61	26.25	33.27	34.08
27.42	27.4	21.79	20.93	30.59	31.22

NO amplification on this one replicate except PPIA + MT-ATP6

PP1A

3737	
35.23	33.87
30.77	29.59
30.52	30.57
32.91	33.37
22.72	22.62
32.48	31.94
30.14	29.63
27.3	29.66
25.52	23.72

3734	
30.24	29.6
33.07	32.28
28.14	28.36
22.92	20.97
No Cq	29.6
32.72	35.01
24.63	24.98
26.36	25.99
23.98	21.99

3434	
22.76	22.36
24.5	24.85
25.3	33.9
34.45	32.33
29.23	30.58
31.23	32.91
32.89	32.7
No Cq	31.5

PER 1

3737		3734		3434	
0	0	36.69	34.78	0	0
0	0	0	0	0	0
0	0	0	0	32.2	35.73
0	0	29.63	33.3	0	0
0	0	0	0	32.08	31.25
0	0	0	0	0	0
0	0	0	0	0	
0	0	0	37.38	0	0
0	0	30.85	30.9	0	0

3737		3734		3434	
0	0	32.92	32.13	0	0
0	0	0	0	0	0
0	0	0	0	30.66	30.27
0	0	28.65	27.89	36.8	0
0	0	36.02	0	28.48	31.79
0	0	0	0	0	0
36.03	0	0	0		
0	0	0	0	0	35.45
38.22	0	31.47	30.68	0	0

CLOCK

3737		3734		3434	
0	0	29.78	29.21	0	0
0	0	0	32.38	0	0
0	0	0	0	28.56	28.92
0	0	26.9	26.87	0	0
0	0	34.23	34.43	29.57	29.3
0	0	0	0	0	0
0	0	36.04	36.05		
0	0	35.2	0	0	35.65
0	0	31.45	0	0	0

BMH

3737	
34.87	0
0	0
0	0
0	0
0	0
0	0
0	0
0	0
0	0

	3734	
0	34.66	32.57
1	0	0
2	0	0
4	29.15	29.85
6	0	34.71
8	0	0
12	0	36.36
16	0	0
24	31.15	31.35

3434	
0	0
0	0
31.69	32.43
0	0
32.08	32.79
0	0
37.34	0
0	0

NO Cg = 41

0
Same values

37/34 to 37/37
BMH to RSP 17

0	- 3.15	8.85
1	~~- 8.27~~	~~111~~ 76.96
2	1.75	0.29736
4	2.43	.18621
6	- 19.16	561917.0
8	- 1.26	2.3866718
12	5.40	.02368
16	4.20	.054598
24	- 3.70	12.9560

CRY1

3737		3734		3434		
0	0	30.78	30.67	0	0	CRY1
0	0	0	35.69	0	0	
0	0	0	36.46	29.07	29.05	
0	0	26.62	27.04	0	0	
0	0	33.12	0	28.49	30.37	
0	0	0	0	0	0	
0	0	36.72	34.94	0		
0	0	0	0	0	0	
0	0	27.77	27.63	0	0	

CRM 2

3737		3734		3434	
0	0	35.56	36.72	0	0
0	0	0	36.35	0	0
0	0	0	0	34.53	32.38
0	0	29.65	29.21	0	0
0	0	0	36.44	30.05	31.49
0	0	0	0	37.47	0
0	37.64	37.76	0		
0	0	0	0	35.1	0
0	0	31.49	31.63	0	0

NR1 D 1

3737		3734		3434	
0	0	36.85	38.74	0	0
0	0	0	0	0	0
0	0	0	0	30.88	34.95
0	0	30.11	30.15	0	0
0	0	0	0	31.17	31.64
0	0	0	0	0	0
0	0	0	0		
0	0	0	0	37.7	0
0	0	32.24	31.75	0	0

DBP

3737		3734		3434	
0	0	33.85	38.63	0	0
0	0	0	0	0	0
0	0	0	0	30.65	30.24
0	0	27.22	27.97	0	0
0	0	34.35	0	29.82	28.81
0	0	0	0	0	0
0	0	0	0		
0	0	0	34.15	0	0
0	0	32.03	32.53	0	0

MT-PT 6

3737		3734		3434	
25.8	23.87	24.62	20.46	27.1	14.72
22.92	21.74	23.86	22.13	17	16.55
25.76	23.58	18.67	18.16	19.52	17.35
25.59	24.77	15.02	16.64	24.81	31.09
16.96	16.35	22.72	23.81	19.08	19.96
22.47	22.19	23.48	22.92	20.99	24.11
22.24	20.47	19.49	18.11		
20.67	21.68	20.53	19.94	20.81	19.57
18.71	17.99	18.7	17.46	20.93	21.7

MCF7 Seven day Shift 3737 & 3734
Five time points
Reference Gene : RSP 17
PER1, PER 2, NR1 D1, CRY 1, CRY 2,
BMAL, CLOCK,

	I	J		K		L		M	
	3737	CRY 1 3734		CRY 2 37337		CRY 2 3734		BMAL 3737	
	I:Y2	J:Y1	J:Y2	K:Y1	K:Y2	L:Y1	L:Y2	M:Y1	M:Y2
1	28.93	32.13	29.91	29.22	28.73	29.27	29.96	32.21	32.74
2	31.09	31.00	29.41	30.55	29.89	28.67	28.68	31.31	31.15
3		33.82	31.35		32.66		32.58	34.40	35.05
4	31.81		34.59	32.00	29.91			32.13	33.04
5	33.97	30.83	32.53	34.34	32.53	30.50	30.85	34.56	

	E		F		G		H		
	PER 2 3737		PER 2 3734		NR1 D1 3737		NR1 D1 3734		CRY 1
	E:Y1	E:Y2	F:Y1	F:Y2	G:Y1	G:Y2	H:Y1	H:Y2	I:Y1
1	29.18	28.71	30.06	29.78	29.42	29.30	31.08	30.61	29.05
2	30.46	30.36	28.99	29.08	29.89	30.38	30.37	30.53	30.32
3	35.81		31.72	32.16	35.13		33.58		34.25
4	31.72	31.29		35.85	32.38	31.05			31.06
5		35.19	32.37	33.94	34.21		34.30	33.08	36.10

Table format: Grouped		A		B		C		D	
		RSP 17 3737		RSP 17 3734		PER1 3737		PER 1 3734	
		A:Y1	A:Y2	B:Y1	B:Y2	C:Y1	C:Y2	D:Y1	D:Y2
1	0	21.21	21.09	21.50	21.49	30.25	29.80	31.07	30.90
2	1	22.28	21.98	21.91	21.61	31.29	31.81	30.41	30.87
3	6	28.64	23.18	23.42	23.21			32.29	33.10
4	8	23.58	23.03	28.85	28.59	32.03	31.92		
5	24	24.66	24.95	23.81	24.08			31.69	31.49

	I	J		K		L		M	
	3737	CRY 1 3734		CRY 2 37337		CRY 2 3734		BMAL 3737	
	I:Y2	J:Y1	J:Y2	K:Y1	K:Y2	L:Y1	L:Y2	M:Y1	M:Y2
1	28.93	32.13	29.91	29.22	28.73	29.27	29.96	32.21	32.74
2	31.09	31.00	29.41	30.55	29.89	28.67	28.68	31.31	31.15
3		33.82	31.35		32.66		32.58	34.40	35.05
4	31.81		34.59	32.00	29.91			32.13	33.04
5	33.97	30.83	32.53	34.34	32.53	30.50	30.85	34.56	

	3737		3734		3434	
6	21.21	21.09	21.5	21.49	24.79	26.78
1	22.28	21.98	21.91	21.61	24.02	24.37
2	22.52	25.98	No Cq	No Cq	26.04	25.22
4	25.02	23.52	No Cq	No Cq	23.18	22.07
6	28.64	23.18	23.42	23.21	30.12	30.32
8	23.58	23.03	28.85	28.59	23.61	23.27
	No Cq	No Cq	24.23	26.89	25.11	23.89
	No Cq	No Cq	25.97	22.88	32.92	34.29
24	24.66	24.95	23.81	24.08	24.85	25.06

RSP 17

NO amplification at any time points for any target

NO amplification at any target except NR1D1 on one replicate at 16 hrs

	3737			3734			3434	
	30.25	29.8	0	31.07	30.9		No Cq	No Cq
	31.29	31.81	1	30.41	30.87		33.35	34.97
	34.13	36.6	2	No Cq	No Cq		No Cq	No Cq
	No Cq	36.31	4	No Cq	No Cq		31.34	31.53
	No Cq	No Cq	6	32.29	33.1		No Cq	No Cq
	32.03	31.92	8	No Cq	No Cq		28.96	31.58
	No Cq	No Cq	12	34.85	35.74		35.53	33.75
	No Cq	No Cq	16	31.33	31.77		No Cq	No Cq
	No Cq	No Cq	24	31.69	31.49		No Cq	No Cq

PER1

3737			3734		3434	
29.18	28.71	0	30.06	29.78	No Cq	35.33
30.46	30.36	1	28.99	29.08	33.24	33.24
32.96	31.95	2	No Cq	No Cq	No Cq	No Cq
33.89	34.2	4	No Cq	No Cq	30.26	30.61
35.81	No Cq	6	31.72	32.16	No Cq	No Cq
31.72	31.29	8	No Cq	35.85	30.37	30.63
No Cq	No Cq	12	34.34	33.73	34.2	35.52
No Cq	No Cq	16	30.2	30.83	No Cq	No Cq
No Cq	35.19	24	32.37	33.94	No Cq	35.68

PER2

3737		3734		3434	
29.42	29.3	31.08	30.61	No Cq	No Cq
29.89	30.38	30.37	30.53	34.48	No Cq
32.23	31.77	No Cq	No Cq	No Cq	No Cq
35.86	34.87	No Cq	No Cq	31.07	31.38
35.13	No Cq	33.58	No Cq	No Cq	No Cq
32.38	31.05	No Cq	No Cq	32.87	31.12
No Cq	No Cq	No Cq	No Cq	35.43	No Cq
No Cq	33.83	31.04	No Cq	No Cq	35.13
34.21	No Cq	34.3	33.08	No Cq	36.54

NR1 D1

3737			3734			3434	
29.05	28.93	0	32.13	29.91		34.03	No Cq
30.32	31.09	1	31	29.41		32.47	33.27
32.87	32.7	2	No Cq	No Cq		No Cq	No Cq
33.64	34.01	4	No Cq	No Cq		30.38	30.8
34.25	No Cq	6	33.82	31.36		No Cq	36.7
31.06	31.81	8	No Cq	34.59		32.42	30.59
No Cq	No Cq	12	35.46	32.91		34.04	33.18
No Cq	No Cq	14	30.22	30.77		No Cq	No Cq
36.1	33.97	24	30.83	32.53		36.47	No Cq

MCF7 shift only CRY 1

3737			3734		3434	
29.22	28.73	0	29.27	29.96	34.37	35.42
30.55	29.89	1	28.67	28.68	32.09	32.24
31.06	33.94	2	No Cq	No Cq	35.08	33.81
31.87	34.31	4	No Cq	No Cq	32.28	29.88
No Cq	32.66	6	No Cq	32.58	No Cq	No Cq
32	29.91	8	No Cq	No Cq	30.61	30.34
No Cq	No Cq	12	33.93	33.53	32.28	32.94
No Cq	No Cq	16	30.01	30.21	No Cq	No Cq
34.34	32.53	24	30.5	30.85	32.52	32.6

shift only MCF7 cells C CRY 2

3737			3734		3434	
32.21	32.74	0	31.54	32.95	No Cq	37.38
31.31	31.15	1	32	31.24	No Cq	35.63
32.96	36.08	2	No Cq	No Cq	34.93	No Cq
No Cq	33.95	3	No Cq	No Cq	33.68	33.99
34.4	35.05	6	34.47	33.84	No Cq	No Cq
32.13	33.04	8	36.1	No Cq	32.65	32.67
No Cq	No Cq	12	No Cq	35.75	35.3	34.59
No Cq	No Cq	14	32.91	32.53	No Cq	No Cq
34.56	No Cq	24	33.03	33.68	No Cq	No Cq

BMAL

3737			3734		3434	
26.63	27.19	0	27.04	28.99	33.41	No Cq
27.34	27.58	1	28.59	26.41	30.13	30.23
29.6	32.35	2	No Cq	No Cq	32.46	33.94
31.53	30.3	4	No Cq	No Cq	27.98	28.8
31.27	No Cq	6	30.03	29.44	No Cq	34.27
31.64	29.15	8	33.84	33.75	28.26	28.33
No Cq	No Cq	12	31.9	31.61	30.11	31.17
No Cq	No Cq	16	29	28.15	34.79	No Cq
31.05	31.26	24	28.67	28.7	31.76	33.7

CLOCK

Appendix 4.

Raw Cq data for *Rhø* cells

MCF7 Rho Cells Seven Day Shift
9 Time Points
Housekeeping gene: RSP 17
GAPdH, MT-ATP 6, NR1 D1, PER 2, TFAM, BMAL, * PER 1, * CLOCK

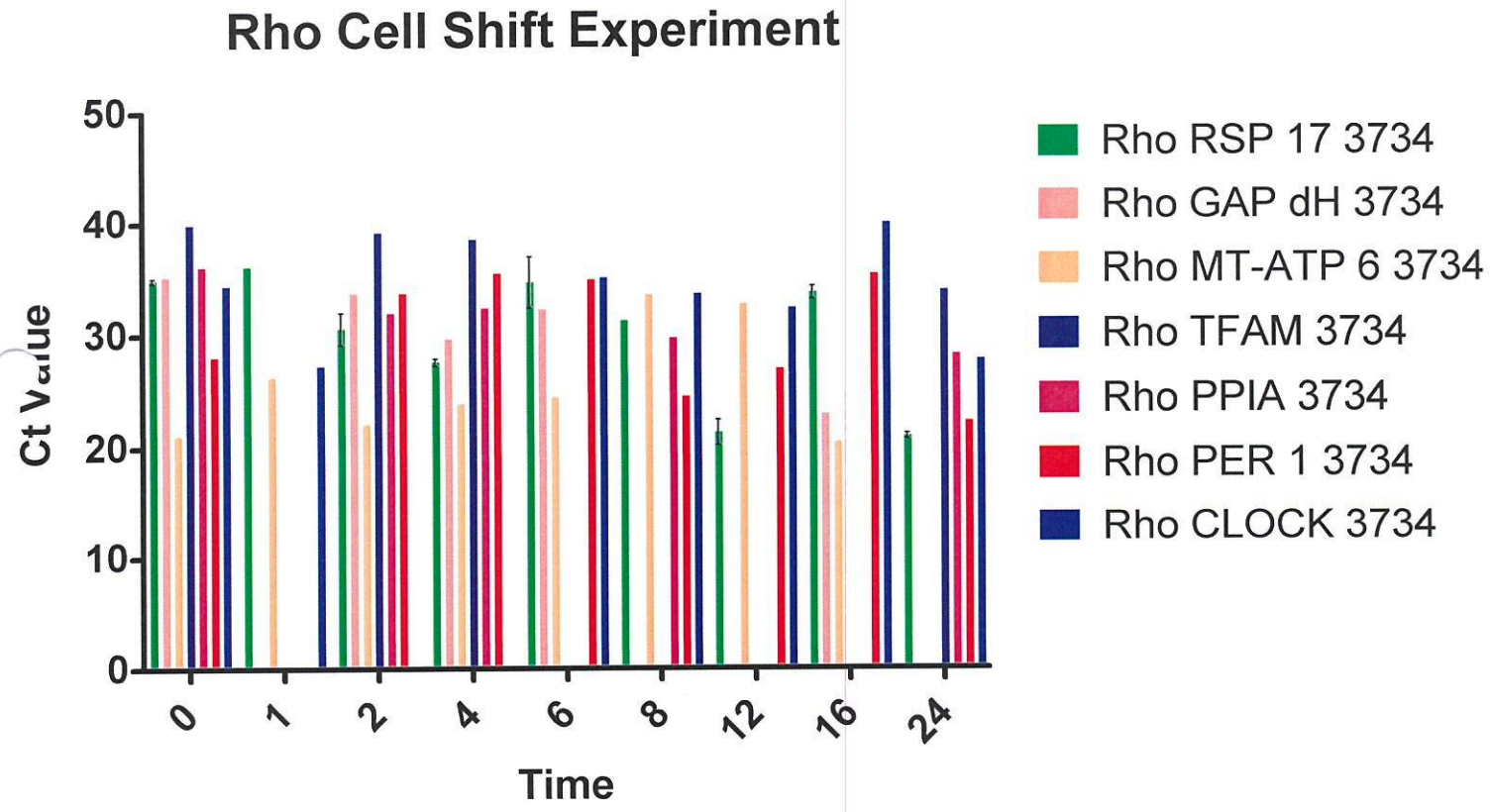
Rho Cell Shift Experiment
Ct Value
50
40
30
20
10
0
0
1
2
4
6
8
12
16
24
Time
Rho RSP 17 3734
Rho GAP dH 3734
Rho MT-ATP 6 3734
Rho TFAM 3734
Rho PPIA 3734
Rho PER 1 3734
Rho CLOCK 3734

	1way ANOVA Tabular results				
1	Table Analyzed	Data 1			
2					
3	Kruskal-Wallis test				
4	P value	0.6581			
5	Exact or approximate P value?	Gaussian Approximation			
6	P value summary	ns			
7	Do the medians vary signif. (P < 0.05)	No			
8	Number of groups	3			
9	Kruskal-Wallis statistic	0.8			
10					
11	Dunn's Multiple Comparison Test	Difference in rank sum	Significant? P < 0.05?	Summary	
12	Rho RSP 17 3737 vs Rho RSP 17 3734	3	No	ns	
13	Rho RSP 17 3737 vs Rho RSP 17 3434	3	No	ns	
14	Rho RSP 17 3734 vs Rho RSP 17 3434	0.8	No	ns	

	1way ANOVA Tabular results				
1	Table Analyzed	Data 1			
2					
3	Kruskal-Wallis test				
4	P value	0.0633			
5	Exact or approximate P value?	Gaussian Approximation			
6	P value summary	ns			
7	Do the medians vary signif. (P < 0.05)	No			
8	Number of groups	10			
9	Kruskal-Wallis statistic	16			
10					
11	Dunn's Multiple Comparison Test	Difference in rank sum	Significant? P < 0.05?	Summary	
12	Rho RSP 17 3734 vs Rho GAP dH 3734	-0.6	No	ns	
13	Rho RSP 17 3734 vs Rho MT-ATP 6 3734	13	No	ns	
14	Rho RSP 17 3734 vs Rho NR1 D1 3734	-6	No	ns	
15	Rho RSP 17 3734 vs Rho PER 2 3734	-17	No	ns	
16	Rho RSP 17 3734 vs Rho TFAM 3734	-21	No	ns	
17	Rho RSP 17 3734 vs Rho BMAL 3734	1	No	ns	
18	Rho RSP 17 3734 vs Rho PPIA 3734	-2	No	ns	
19	Rho RSP 17 3734 vs Rho PER 1 3734	-1	No	ns	
20	Rho RSP 17 3734 vs Rho CLOCK 3734	-6	No	ns	
21	Rho GAP dH 3734 vs Rho MT-ATP 6 3734	13	No	ns	
22	Rho GAP dH 3734 vs Rho NR1 D1 3734	-6	No	ns	
23	Rho GAP dH 3734 vs Rho PER 2 3734	-16	No	ns	
24	Rho GAP dH 3734 vs Rho TFAM 3734	-20	No	ns	
25	Rho GAP dH 3734 vs Rho BMAL 3734	2	No	ns	
26	Rho GAP dH 3734 vs Rho PPIA 3734	-2	No	ns	
27	Rho GAP dH 3734 vs Rho PER 1 3734	-0.6	No	ns	
28	Rho GAP dH 3734 vs Rho CLOCK 3734	-5	No	ns	
29	Rho MT-ATP 6 3734 vs Rho NR1 D1 3734	-19	No	ns	
30	Rho MT-ATP 6 3734 vs Rho PER 2 3734	-29	No	ns	
31	Rho MT-ATP 6 3734 vs Rho TFAM 3734	-34	Yes	*	
32	Rho MT-ATP 6 3734 vs Rho BMAL 3734	-11	No	ns	
33	Rho MT-ATP 6 3734 vs Rho PPIA 3734	-15	No	ns	
34	Rho MT-ATP 6 3734 vs Rho PER 1 3734	-14	No	ns	
35	Rho MT-ATP 6 3734 vs Rho CLOCK 3734	-19	No	ns	
36	Rho NR1 D1 3734 vs Rho PER 2 3734	-10	No	ns	
37	Rho NR1 D1 3734 vs Rho TFAM 3734	-15	No	ns	
38	Rho NR1 D1 3734 vs Rho BMAL 3734	8	No	ns	
39	Rho NR1 D1 3734 vs Rho PPIA 3734	4	No	ns	
40	Rho NR1 D1 3734 vs Rho PER 1 3734	5	No	ns	
41	Rho NR1 D1 3734 vs Rho CLOCK 3734	0.2	No	ns	
42	Rho PER 2 3734 vs Rho TFAM 3734	-4	No	ns	
43	Rho PER 2 3734 vs Rho BMAL 3734	18	No	ns	
44	Rho PER 2 3734 vs Rho PPIA 3734	14	No	ns	
45	Rho PER 2 3734 vs Rho PER 1 3734	15	No	ns	
46	Rho PER 2 3734 vs Rho CLOCK 3734	11	No	ns	
47	Rho TFAM 3734 vs Rho BMAL 3734	22	No	ns	

Table format: Grouped		A		B		C		D	
		Rho RSP 17 3737		Rho RSP 17 3734		Rho RSP 17 3434		Rho GAP dH 3737	
		A:Y1	A:Y2	B:Y1	B:Y2	C:Y1	C:Y2	D:Y1	D:Y2
1	0	27.75		34.69	35.08	29.55	34.40	32.27	32.01
2	1	22.89	22.61		36.08	33.74	28.61	24.34	24.93
3	2	36.06	34.77	29.15	31.96	33.27	34.90	34.73	
4	4	30.00	29.31	27.30	27.90		27.14		37.20
5	6			32.39	36.93	20.39	20.89		
6	8	32.08	32.32		31.25	20.05	20.15	24.27	23.54
7	12	36.39		22.46	20.22	28.83	29.52	33.70	
8	16	36.57	35.28	33.15	34.28		36.18		
9	24	34.60	32.90	21.22	20.73		36.04		

	I	J		K		L		M	
	TP 6 3434	Rho NR1 D1 3737		Rho NR1 D1 3734		Rho NR1 D1 3434		Rho PER 2 3737	
	I:Y2	J:Y1	J:Y2	K:Y1	K:Y2	L:Y1	L:Y2	M:Y1	M:Y2
1	22.08						36.49		
2	23.67	33.3	32.2						33.83
3	21.24								
4	22.69				34.61		36.36		
5	22.22					28.45	31.09		
6	30.36					27.58	27.70		
7	27.46				34.80				
8	31.78								
9				29.33	29.38				

	R	S		T		U		V	
	M 3434	Rho BMAL 3737		Rho BMAL 3734		Rho BMAL 3434		Rho PPIA 3737	
	R:Y2	S:Y1	S:Y2	T:Y1	T:Y2	U:Y1	U:Y2	V:Y1	V:Y2
1								32.63	36.13
2			33.43					25.65	25.95
3									
4								33.93	34.67
5						31.02	31.07		
6						30.42	30.17		
7									
8									
9				31.85	31.54				

Row stats		A			B			C	
		Rho RSP 17 3737			Rho RSP 17 3734			Rho RSP 17 343	
		Mean	**SEM**	**N**	**Mean**	**SEM**	**N**	**Mean**	**SEM**
1	0	27.750	0.000	1	34.885	0.195	2	31.975	2.425
2	1	22.750	0.140	2	36.080	0.000	1	31.175	2.565
3	2	35.415	0.645	2	30.555	1.405	2	34.085	0.815
4	4	29.655	0.345	2	27.600	0.300	2	27.140	0.000
5	6				34.660	2.270	2	20.640	0.250
6	8	32.200	0.120	2	31.250	0.000	1	20.100	0.050
7	12	36.390	0.000	1	21.340	1.120	2	29.175	0.345
8	16	35.925	0.645	2	33.715	0.565	2	36.180	0.000
9	24	33.750	0.850	2	20.975	0.245	2	36.040	0.000

		G			H			I	
	34	Rho MT-ATP 6 3737			Rho MT-ATP 6 3734			Rho MT-ATP 6 34	
	N	Mean	SEM	N	Mean	SEM	N	Mean	SEM
1	2	26.280	0.890	2	21.080	0.240	2	22.040	0.040
2	1	21.160	0.080	2	26.210	0.470	2	23.445	0.225
3	2	29.905	0.215	2	22.070	0.090	2	20.875	0.365
4	2	22.425	0.255	2	23.870	0.090	2	22.800	0.110
5	2				24.430	0.000	1	21.710	0.510
6	1	29.585	0.175	2	33.540	0.000	1	30.745	0.385
7	1	30.960	0.000	2	32.680	0.380	2	28.245	0.785
8		31.100	0.280	2	20.420	0.210	2	33.080	1.300
9									

		M			N			O	
	4	Rho PER 2 3737			Rho PER 2 3734			Rho PER 2 343	
	N	Mean	SEM	N	Mean	SEM	N	Mean	SEM
1	1								
2		33.830	0.000	1					
3									
4	1								
5	2							28.915	0.225
6	2							28.220	0.090
7									
8									
9					34.990	0.900	2		

		S			T			U	
		Rho BMAL 3737			Rho BMAL 3734			Rho BMAL 343	
	N	Mean	SEM	N	Mean	SEM	N	Mean	SEM
1									
2		33.430	0.000	1					
3	1								
4									
5	1							31.045	0.025
6								30.295	0.125
7									
8									
9					31.695	0.155	2		

		Y			Z		
		Rho PER 1 3734			Rho CLOCK 3734		
	N	Mean	SEM	N	Mean	SEM	N
1	2	28.010	0.040	2	34.355	0.365	2
2	1				27.240	0.390	2
3	1	33.680	1.680	2			
4	2	35.420	2.060	2			
5	2	34.885	0.475	2	35.050	0.000	1
6	2	24.495	0.295	2	33.620	0.000	1
7		26.940	1.020	2	32.340	0.630	2
8		35.335	1.805	2	39.960	0.000	1
9		22.270	0.190	2	27.760	0.000	1

	1way ANOVA Tabular results				
1	Table Analyzed	Data 1			
2					
3	Kruskal-Wallis test				
4	P value	0.0633			
5	Exact or approximate P value?	Gaussian Approximation			
6	P value summary	ns			
7	Do the medians vary signif. (P < 0.05)	No			
8	Number of groups	10			
9	Kruskal-Wallis statistic	16			
10					
11	Dunn's Multiple Comparison Test	Difference in rank sum	Significant? P < 0.05?	Summary	
12	Rho RSP 17 3734 vs Rho GAP dH 3734	-0.6	No	ns	
13	Rho RSP 17 3734 vs Rho MT-ATP 6 3734	13	No	ns	
14	Rho RSP 17 3734 vs Rho NR1 D1 3734	-6	No	ns	
15	Rho RSP 17 3734 vs Rho PER 2 3734	-17	No	ns	
16	Rho RSP 17 3734 vs Rho TFAM 3734	-21	No	ns	
17	Rho RSP 17 3734 vs Rho BMAL 3734	1	No	ns	
18	Rho RSP 17 3734 vs Rho PPIA 3734	-2	No	ns	
19	Rho RSP 17 3734 vs Rho PER 1 3734	-1	No	ns	
20	Rho RSP 17 3734 vs Rho CLOCK 3734	-6	No	ns	
21	Rho GAP dH 3734 vs Rho MT-ATP 6 3734	13	No	ns	
22	Rho GAP dH 3734 vs Rho NR1 D1 3734	-6	No	ns	
23	Rho GAP dH 3734 vs Rho PER 2 3734	-16	No	ns	
24	Rho GAP dH 3734 vs Rho TFAM 3734	-20	No	ns	
25	Rho GAP dH 3734 vs Rho BMAL 3734	2	No	ns	
26	Rho GAP dH 3734 vs Rho PPIA 3734	-2	No	ns	
27	Rho GAP dH 3734 vs Rho PER 1 3734	-0.6	No	ns	
28	Rho GAP dH 3734 vs Rho CLOCK 3734	-5	No	ns	
29	Rho MT-ATP 6 3734 vs Rho NR1 D1 3734	-19	No	ns	
30	Rho MT-ATP 6 3734 vs Rho PER 2 3734	-29	No	ns	
31	Rho MT-ATP 6 3734 vs Rho TFAM 3734	-34	Yes	*	
32	Rho MT-ATP 6 3734 vs Rho BMAL 3734	-11	No	ns	
33	Rho MT-ATP 6 3734 vs Rho PPIA 3734	-15	No	ns	
34	Rho MT-ATP 6 3734 vs Rho PER 1 3734	-14	No	ns	
35	Rho MT-ATP 6 3734 vs Rho CLOCK 3734	-19	No	ns	
36	Rho NR1 D1 3734 vs Rho PER 2 3734	-10	No	ns	
37	Rho NR1 D1 3734 vs Rho TFAM 3734	-15	No	ns	
38	Rho NR1 D1 3734 vs Rho BMAL 3734	8	No	ns	
39	Rho NR1 D1 3734 vs Rho PPIA 3734	4	No	ns	
40	Rho NR1 D1 3734 vs Rho PER 1 3734	5	No	ns	
41	Rho NR1 D1 3734 vs Rho CLOCK 3734	0.2	No	ns	
42	Rho PER 2 3734 vs Rho TFAM 3734	-4	No	ns	
43	Rho PER 2 3734 vs Rho BMAL 3734	18	No	ns	
44	Rho PER 2 3734 vs Rho PPIA 3734	14	No	ns	
45	Rho PER 2 3734 vs Rho PER 1 3734	15	No	ns	
46	Rho PER 2 3734 vs Rho CLOCK 3734	11	No	ns	
47	Rho TFAM 3734 vs Rho BMAL 3734	22	No	ns	

3737		3734		3434	
27.75	No Cq	34.69	35.08	29.55	34.4
22.89	22.61	No Cq	36.08	33.74	28.61
36.06	34.77	29.15	31.96	33.27	34.9
30	29.31	27.3	27.9	No Cq	27.14
		32.39	36.93	20.39	20.89
32.08	32.32	No Cq	31.25	20.05	20.15
36.39	No Cq	22.46	20.22	28.83	29.52
36.57	35.28	33.15	34.28	No Cq	36.18
34.6	32.9	21.22	20.73	No Cq	36.04

RSP 17 Rho

No amplification plate

except GAPdH TPPIA for time 0 & 2 replicate + MT-ATP6 for Neith

No amplification plate except MT-ATP6 for Neith

No amplification except GAPdH + MT-ATP6 TPPIA

3737		3734		3434	
32.27	32.01	No Cq	35.16	29.44	30.13
24.34	24.93	No Cq	No Cq	35.34	No Cq
34.73	No Cq	34.73	32.58	28.83	29.34
No Cq	37.2	29.64	29.58	22.55	28.35
		31.46	32.97	21.38	21.37
24.27	23.54	No Cq	No Cq	34.58	No Cq
33.7	No Cq	No Cq	No Cq	No Cq	38.64
No Cq	No Cq	23.06	22.77	No Cq	No Cq
No Cq	No Cq	No Cq	No Cq	No Cq	No Cq

GAP DH Rho

3737	
27.17	25.39
21.24	21.08
30.12	29.69
22.68	22.17
29.76	29.41
30.96	30.96
30.82	31.38
No Cq	No Cq

3734	
20.84	21.32
26.68	25.74
21.98	22.16
23.78	23.96
No Cq	24.43
33.54	No Cq
33.06	32.3
20.63	20.21
No Cq	No Cq

3434	
22	22.08
23.22	23.67
20.51	21.24
22.91	22.69
21.2	22.22
31.13	30.36
29.03	27.46
34.38	31.78
No Cq	No Cq

MT- ATP 6 Rho

3737	
No Cq	No Cq
33.3	32.2
No Cq	No Cq
No Cq	No Cq
No Cq	No Cq
No Cq	No Cq
No Cq	No Cq
No Cq	No Cq

3734	
No Cq	No Cq
No Cq	No Cq
No Cq	No Cq
No Cq	34.61
No Cq	No Cq
No Cq	No Cq
No Cq	34.8
No Cq	No Cq
29.33	29.38

3434	
No Cq	36.49
No Cq	No Cq
No Cq	No Cq
No Cq	36.36
28.45	31.09
27.58	27.7
No Cq	No Cq
No Cq	No Cq
No Cq	No Cq

Rho NR1 D1

note for CLOCK Rho cells - Threshold fluorecence error

3737		3734		3434	
No Cq	No Cq	No Cq	No Cq	No Cq	No Cq
No Cq	No Cq	No Cq	No Cq	No Cq	No Cq
No Cq	No Cq	No Cq	No Cq	No Cq	No Cq
No Cq	No Cq	No Cq	No Cq	No Cq	No Cq
		No Cq	No Cq	No Cq	No Cq
No Cq	No Cq	No Cq	No Cq	No Cq	No Cq
No Cq	No Cq	No Cq	No Cq	No Cq	No Cq
No Cq	No Cq	No Cq	No Cq	No Cq	No Cq
No Cq	No Cq	No Cq	No Cq	No Cq	No Cq

PER 1 Rho

amplification plots abnormal

3737	
No Cq	No Cq
No Cq	33.83
No Cq	No Cq
No Cq	No Cq
No Cq	No Cq
No Cq	No Cq
No Cq	No Cq
No Cq	No Cq

3734	
No Cq	No Cq
No Cq	No Cq
No Cq	No Cq
No Cq	No Cq
No Cq	No Cq
No Cq	No Cq
No Cq	No Cq
No Cq	No Cq
34.09	35.89

3434	
No Cq	No Cq
No Cq	No Cq
No Cq	No Cq
No Cq	No Cq
28.69	29.14
28.13	28.31
No Cq	No Cq
No Cq	No Cq
No Cq	No Cq

PER 2 Rho

38.27	No Cq	39.85	No Cq	No Cq
36.76	34.38	No Cq	No Cq	No Cq
No Cq	No Cq	39.85	38.41	39.61
39.82	No Cq	38.92	37.08	No Cq
		No Cq	No Cq	33.98
No Cq	No Cq	No Cq	No Cq	
No Cq	No Cq	No Cq	No Cq	
No Cq	No Cq	No Cq	No Cq	
No Cq	No Cq	34.45	33.33	

TFAM rho cells

3737	
No Cq	No Cq
No Cq	33.43
No Cq	No Cq
No Cq	No Cq
No Cq	No Cq
No Cq	No Cq
No Cq	No Cq
No Cq	No Cq

3734	
No Cq	No Cq
No Cq	No Cq
No Cq	No Cq
No Cq	No Cq
No Cq	No Cq
No Cq	No Cq
No Cq	No Cq
No Cq	No Cq
31.85	31.54

3434	
No Cq	No Cq
No Cq	No Cq
No Cq	No Cq
No Cq	No Cq
31.02	31.07
30.42	30.17
No Cq	No Cq
No Cq	No Cq
No Cq	No Cq

BMAL Rho

3737	
32.63	36.13
25.65	25.95
No Cq	No Cq
33.93	34.67
No Cq	No Cq
No Cq	No Cq
No Cq	No Cq
No Cq	No Cq

3734	
36.05	No Cq
No Cq	No Cq
32.49	31.36
32.55	32.12
No Cq	No Cq
No Cq	29.7
No Cq	No Cq
No Cq	No Cq
27.83	28.62

3434	
37.67	34.24
31.86	No Cq
34.1	No Cq
31.26	31.5
24	25
23.62	23.4
No Cq	No Cq
No Cq	No Cq
No Cq	No Cq

PPIA Rho

PER 1

Well	Well Type	Well Name	Dye	Target	Replicate	R Last	ΔR Last	Rn Last
A1	Unknown	3734 0	FAM	FAM	---	4636.389312	1079.775218	No Reference
A3	Unknown	3734 2	FAM	FAM	---	3838.043199	16.65992593	No Reference
A4	Unknown	3734 4	FAM	FAM	---	3521.464574	6.322661808	No Reference
A5	Unknown	3734 6	FAM	FAM	---	4036.616345	10.33334369	No Reference
A6	Unknown	3734 8	FAM	FAM	---	5275.570643	1963.92453	No Reference
A7	Unknown	3734 12	FAM	FAM	---	5985.102501	2428.830769	No Reference
A8	Unknown	3734 16	FAM	FAM	---	3351.972692	10.93036106	No Reference
A9	Unknown	3734 24	FAM	FAM	---	7881.250368	4500.139096	No Reference
A11	NTC	---	FAM	FAM	---	3241.15553	18.09580814	No Reference
B1	Unknown	3734 0	FAM	FAM	---	6027.4117	1982.448659	No Reference
B3	Unknown	3734 2	FAM	FAM	---	4154.197081	7.429415818	No Reference
B4	Unknown	3734 4	FAM	FAM	---	4359.079344	11.5072904	No Reference
B5	Unknown	3734 6	FAM	FAM	---	4593.630456	16.7063293	No Reference
B6	Unknown	3734 8	FAM	FAM	---	6387.229739	2327.124316	No Reference
B7	Unknown	3734 12	FAM	FAM	---	5967.835836	1359.696211	No Reference
B8	Unknown	3734 16	FAM	FAM	---	4210.655478	26.13252899	No Reference
B9	Unknown	3734 24	FAM	FAM	---	9274.883359	5461.223785	No Reference
B11	NTC	---	FAM	FAM	---	3834.454333	24.76261327	No Reference
C1	No RT	3734 0	FAM	FAM	---	3934.272576	25.19784436	No Reference
C3	No RT	3734 12	FAM	FAM	---	4556.14717	14.54205557	No Reference
C4	No RT	3734 24	FAM	FAM	---	4651.208706	13.21010257	No Reference
C11	NTC	---	FAM	FAM	---	3371.815069	26.52142883	No Reference
D11	NTC	---	FAM	FAM	---	4001.678866	7.603562803	No Reference

Final Call (ΔR)	Quantity (nanograms)	Quantity Avg. (nanograms)	Quantity SD (nanograms)
+	No Cq for FAM Standards	N/A	N/A
+	No Cq for FAM Standards	N/A	N/A
+	No Cq for FAM Standards	N/A	N/A
+	No Cq for FAM Standards	N/A	N/A
+	No Cq for FAM Standards	N/A	N/A
+	No Cq for FAM Standards	N/A	N/A
+	No Cq for FAM Standards	N/A	N/A
+	No Cq for FAM Standards	N/A	N/A
+	No Cq for FAM Standards	N/A	N/A
+	No Cq for FAM Standards	N/A	N/A
+	No Cq for FAM Standards	N/A	N/A
+	No Cq for FAM Standards	N/A	N/A
+	No Cq for FAM Standards	N/A	N/A
+	No Cq for FAM Standards	N/A	N/A
+	No Cq for FAM Standards	N/A	N/A
+	No Cq for FAM Standards	N/A	N/A
+	No Cq for FAM Standards	N/A	N/A
+	No Cq for FAM Standards	N/A	N/A
+	No Cq for FAM Standards	N/A	N/A
+	No Cq for FAM Standards	N/A	N/A
+	No Cq for FAM Standards	N/A	N/A
+	No Cq for FAM Standards	N/A	N/A
+	No Cq for FAM Standards	N/A	N/A

Cq Avg. Treated Ind. (ΔR)	Cq SD Treated Ind. (ΔR)	Melt Smoothing #	Melt Norm.
3734 O 27.97102176	No Cq	N/A	N/A
Z 35.35926321	No Cq	N/A	N/A
4 37.48381023	No Cq	N/A	N/A
6 35.35631785	No Cq	N/A	N/A
8 24.20347741	No Cq	N/A	N/A
12 25.92364206	No Cq	N/A	N/A
16 37.14288665	No Cq	N/A	N/A
22 22.46460397	No Cq	N/A	N/A
NTC 33.3720731	No Cq	N/A	N/A
3734 O 28.05363779	No Cq	N/A	N/A
Z 31.99648877	No Cq	N/A	N/A
4 33.36348993	No Cq	N/A	N/A
6 34.40750184	No Cq	N/A	N/A
8 24.79188433	No Cq	N/A	N/A
12 27.96363809	No Cq	N/A	N/A
16 33.52663447	No Cq	N/A	N/A
22 22.08468154	No Cq	N/A	N/A
NTC 34.07926285	No Cq	N/A	N/A
21.1057308	No Cq	N/A	N/A
37.23383045	No Cq	N/A	N/A
35.39636254	No Cq	N/A	N/A
33.7982992	No Cq	N/A	N/A
34.91669342	No Cq	N/A	N/A

Tm Product 5 (-R'(T))	Tm Product 6 (-R'(T))
N/A	N/A
N/A	N/A
N/A	N/A
N/A	N/A
N/A	N/A
N/A	N/A
N/A	N/A
N/A	N/A
N/A	N/A
N/A	N/A
N/A	N/A
N/A	N/A
N/A	N/A
N/A	N/A
N/A	N/A
N/A	N/A
N/A	N/A
N/A	N/A
N/A	N/A
N/A	N/A
N/A	N/A
N/A	N/A
N/A	N/A
N/A	N/A
N/A	N/A

CLDRC

Well	Well Type	Well Name	Dye	Target	Replicate	R Last	ΔR Last	Rn Last
A1	Unknown	3734 0	FAM	FAM	---	8622.253994	1751.152578	No Reference
A2	Unknown	3734 1	FAM	FAM	---	26486.6174	18655.87066	No Reference
A3	Unknown	3734 2	FAM	FAM	---	7170.870135	60.32643778	No Reference
A4	Unknown	3734 4	FAM	FAM	---	8304.322363	26.90790975	No Reference
A5	Unknown	3734 6	FAM	FAM	---	10309.79079	1980.17671	No Reference
A6	Unknown	3734 8	FAM	FAM	---	10844.89324	3749.524024	No Reference
A7	Unknown	3734 12	FAM	FAM	---	16018.04534	8459.873684	No Reference
A8	Unknown	3734 16	FAM	FAM	---	7037.436941	41.69872164	No Reference
A9	Unknown	3734 24	FAM	FAM	---	21912.80508	14883.18402	No Reference
A11	NTC	---	FAM	FAM	---	5881.058894	44.91291239	No Reference
B1	Unknown	3734 0	FAM	FAM	---	11242.21192	3077.757678	No Reference
B2	Unknown	3734 1	FAM	FAM	---	28928.38381	19953.73715	No Reference
B3	Unknown	3734 2	FAM	FAM	---	9546.034438	46.6928263	No Reference
B4	Unknown	3734 4	FAM	FAM	---	9611.38866	27.86271578	No Reference
B5	Unknown	3734 6	FAM	FAM	---	10090.50133	40.50986264	No Reference
B6	Unknown	3734 8	FAM	FAM	---	9584.317729	46.26282489	No Reference
B7	Unknown	3734 12	FAM	FAM	---	13914.09113	5669.21949	No Reference
B8	Unknown	3734 16	FAM	FAM	---	11292.37188	124.0413429	No Reference
B9	Unknown	3734 24	FAM	FAM	---	779.0027283	8.481859174	No Reference
B11	NTC	---	FAM	FAM	---	8623.751637	88.11938068	No Reference
C1	No RT	3734 0	FAM	FAM	---	8400.83685	71.28030937	No Reference
C2	No RT	3734 6	FAM	FAM	---	9118.4724	51.98462758	No Reference
C3	No RT	3734 12	FAM	FAM	---	9420.907809	94.04669496	No Reference
C4	No RT	3734 24	FAM	FAM	---	10432.26384	20.1154892	No Reference
C11	NTC	---	FAM	FAM	---	7877.789211	107.1372331	No Reference
D11	NTC	---	FAM	FAM	---	8755.137603	111.4116063	No Reference

Final Call (ΔR)	Quantity (nanograms)	Quantity Avg. (nanograms)	Quantity SD (nanograms)
+	No Cq for FAM Standards	N/A	N/A
+	No Cq for FAM Standards	N/A	N/A
-	No Cq for FAM Standards	No Cq	No Cq
-	No Cq for FAM Standards	No Cq	No Cq
+	No Cq for FAM Standards	N/A	N/A
+	No Cq for FAM Standards	N/A	N/A
+	No Cq for FAM Standards	N/A	N/A
-	No Cq for FAM Standards	No Cq	No Cq
+	No Cq for FAM Standards	N/A	N/A
-	No Cq for FAM Standards	No Cq	No Cq
+	No Cq for FAM Standards	N/A	N/A
+	No Cq for FAM Standards	N/A	N/A
-	No Cq for FAM Standards	No Cq	No Cq
-	No Cq for FAM Standards	No Cq	No Cq
-	No Cq for FAM Standards	No Cq	No Cq
-	No Cq for FAM Standards	No Cq	No Cq
+	No Cq for FAM Standards	N/A	N/A
+	No Cq for FAM Standards	N/A	N/A
-	No Cq for FAM Standards	No Cq	No Cq
-	No Cq for FAM Standards	No Cq	No Cq
-	No Cq for FAM Standards	No Cq	No Cq
-	No Cq for FAM Standards	No Cq	No Cq
-	No Cq for FAM Standards	No Cq	No Cq
-	No Cq for FAM Standards	No Cq	No Cq
-	No Cq for FAM Standards	No Cq	No Cq
-	No Cq for FAM Standards	No Cq	No Cq

Cq Avg. Treated Ind. (ΔR)	Cq SD Treated Ind. (ΔR)	Melt Smoothing #	Melt Norm.
34.72123066	No Cq	N/A	N/A
26.86441184	No Cq	N/A	N/A
No Cq	No Cq	N/A	N/A
No Cq	No Cq	N/A	N/A
35.05400695	No Cq	N/A	N/A
33.6156551	No Cq	N/A	N/A
31.70593065	No Cq	N/A	N/A
No Cq	No Cq	N/A	N/A
27.75861758	No Cq	N/A	N/A
No Cq	No Cq	N/A	N/A
33.9882561	No Cq	N/A	N/A
27.62737372	No Cq	N/A	N/A
No Cq	No Cq	N/A	N/A
No Cq	No Cq	N/A	N/A
No Cq	No Cq	N/A	N/A
No Cq	No Cq	N/A	N/A
32.96619102	No Cq	N/A	N/A
39.9624139	No Cq	N/A	N/A
No Cq	No Cq	N/A	N/A
No Cq	No Cq	N/A	N/A
No Cq	No Cq	N/A	N/A
No Cq	No Cq	N/A	N/A
No Cq	No Cq	N/A	N/A
No Cq	No Cq	N/A	N/A
No Cq	No Cq	N/A	N/A
No Cq	No Cq	N/A	N/A

Tm Product 5 (-R'(T))	Tm Product 6 (-R'(T))
N/A	N/A
N/A	N/A
N/A	N/A
N/A	N/A
N/A	N/A
N/A	N/A
N/A	N/A
N/A	N/A
N/A	N/A
N/A	N/A
N/A	N/A
N/A	N/A
N/A	N/A
N/A	N/A
N/A	N/A
N/A	N/A
N/A	N/A
N/A	N/A
N/A	N/A
N/A	N/A
N/A	N/A
N/A	N/A
N/A	N/A
N/A	N/A
N/A	N/A
N/A	N/A